

**Trichloramine in swimming pool water: analysis methods,  
factors influencing its fate and effects of UV treatment**

A thesis submitted to attain the degree of  
DOCTOR OF SCIENCE of ETH Zurich  
(Dr. sc. ETH Zurich)

presented by

FABIAN SOLTERMANN

MSc ETH Environ. Sc. ETH Zurich

born on November 24, 1981

citizen of Vechigen (BE), Switzerland

accepted on the recommendation of

Prof. Dr. Urs von Gunten, examiner

Dr. Silvio Canonica, co-examiner

Prof. Dr. Kristopher McNeill, co-examiner

Dr. Gérard Donzé, co-examiner

Dr. Nicolas Cimetiere, co-examiner









---

## Danksagung

Was für mich ein grosses und langes Projekt gewesen ist, mag für andere nur ein kleiner Abstecher auf ihrem Weg gewesen sein. Die Unterstützung all dieser Weggefährten war für mich jedoch enorm wertvoll und hat sehr zum Gelingen der Arbeit beigetragen. Meine Begleiter haben geschaut, dass ich nicht von meinem Weg abgekommen bin und haben mich immer wieder auf interessante Umwege geführt. Sie haben mir manches Hindernis aus dem Weg geräumt und mich motiviert und unterstützt, wenn es einmal nicht wie gewünscht vorwärts ging. Andere Weggefährten haben mir auch einfach das Leben an der EAWAG angenehm gestaltet, sei es mit der richtigen Musikwahl im Labor, mit gemeinsamen Kaffee- und Glacepausen oder mit Diskussionen im Büro. Nun ist es an der Zeit, all diesen Leuten herzlich zu danken.

Der grösste Dank gebührt sicher meinen beiden Betreuern Urs von Gunten und Silvio Canonica. Während meiner Doktorarbeit konnte ich jederzeit auf Urs und sein Metamorphosezimmer zählen, in welches man von Laborversuchen frustriert, verwirrt und enttäuscht eintritt und motiviert, voller Ideen und Enthusiasmus austritt. Dabei haben mir nebst den fachlichen Diskussionen auch immer wieder persönliche Gespräche und Anregungen geholfen. Für diese Unterstützung auf allen Ebenen möchte ich mich ganz herzlich bedanken! Silvio hat die Doktorarbeit initiiert und war mir mit seiner ruhigen und exakten Art sowie mit seinem fachlich ausgezeichneten Wissen stets eine grosse Hilfe.

Dem Bundesamt für Gesundheit (BAG) möchte ich einerseits für die Finanzierung der Doktorarbeit danken. Andererseits bedanke ich mich bei Gérard Donzé (BAG) für die fachliche Unterstützung und das mir entgegengebrachte Vertrauen. Er hat mich auf seine warme und freundliche Art während der ganzen Zeit begleitet.

Ebenfalls praktisch bis zum Schluss war Matthias Rudolf von Rohr mit mir unterwegs. Obwohl er treuer HC Lugano Fan ist, hätte ich mir keinen besseren Bürokollegen vorstellen können! Seine ausgeglichene und fröhliche Art sowie die gemeinsame Freude an der Musik hat es ermöglicht, dass es ab und zu einen Johnny-day gab und auch im Sommer noch Afro-Pfingsten waren.

Natürlich möchte ich die Bürokollegen auf der anderen Seite der Türe nicht vergessen! Nicht selten ging die Tür auf und Jannis Wenk, Sabrina Bahn Müller und Frank Leresche haben mit Gesprächen über Fachliches und Privates den Arbeitstrott durchbrochen. Insbesondere Frank wusste einem die Teepausen zu versüssen. Vielen Dank euch allen!

---

Tüchtig unter die Arme gegriffen hat mir Tobias Widler, indem er seine Masterarbeit über die UV-Bestrahlung von Chloraminen geschrieben und mich anschliessend 4 Monate als wissenschaftlicher Mitarbeiter unterstützt hat. Trotz dem MIMS, welches einem an den Rand der Verzweiflung bringen konnte, hat er den Mut nie verloren! Vielen Dank für die Unterstützung in unwirtlichem Gelände (Hallenbadkeller) und in den Wortgefechten mit Amisha.

Speziell danken möchte ich auch meinen drei Laborkollegen im B61.1. Minju Lee hat mich in der Nitrosaminstudie unterstützt und mich immer wieder mit seinen Abenteuern unterhalten. Justine Criquet ist mir stets mit fachlichem Rat zur Seite gestanden und hat mit französischer Musik und interessanten Gesprächen das Laborleben aufgelockert. Amisha Shah hat mit ihrer lebensfrohen und temperamentvollen Art keinen Alltag aufkommen lassen. Die Diskussionen mit ihr über Fachliches und Privates waren gleichermassen spannend.

Im Labor wurde ich zusätzlich von Elisabeth Sahli, Hansueli Laubscher und Jacqueline Traber unterstützt. Insbesondere Lisa gebührt ein grosses Dankschön für ihre stete, kompetente und praktische Hilfe.

Ohne die Hilfe von Philippe Périsset hätte meine Doktorarbeit wohl 8 statt 4 Jahre gedauert. Seine Hilfe bei der Automatisierung der Auswertung von MIMS-Daten haben mir etliche Stunden mühsamer Arbeit erspart. Die Zusammenarbeit mit Philippe bei der Programmentwicklung war mir eine grosse Freude. Auch Frants Lauritsen (University of Southern Denmark) und Oliver Aschwanden (Pfeiffer) haben sich immer wieder mit Rat und Tat um das Sorgenkind MIMS gekümmert. Besonders Oliver Aschwanden verdient dabei ein grosses Lob, da er sich nie entmutigen liess und stets auf kulante Art und Weise eine Lösung zu finden wusste.

Bei den Feldstudien wurde ich vom Kantonalen Labor unterstützt. René Schittli und Andreas Peter waren mit ihrer zuverlässigen, unkomplizierten, effizienten und kompetenten Art die perfekten Projektpartner. Vielen Dank. Für die Chlor und gebundene Chlor Messung konnten wir auf die hilfsbereite und unkomplizierte Unterstützung von Philippe Trösch und Bruno von Ballmoss (SWAN AG) zählen. Moritz Gabriel (Rhenovision) stand uns im Bereich UV Lampen mit Rat zur Seite. Ein besonderes Dankeschön möchte ich zudem Ruedi Spengler und seinem Team vom Water World Wallisellen aussprechen, welches mich während der Messkampagne bestens unterstützt und aufgenommen hat.

Natürlich möchte ich mich auch bei vielen weiteren Leuten in der „Urs von Gunten“-Gruppe bedanken: Yunho Lee, Saskia Zimmermann-Steffens, Hana Mestankova, Paul Borer, Kangmin

---

Chon, Yael Schindler, Michèle Heeb, Mélissa Huguet, Nadine Czekalski, Zhengqian Liu, Ursula Schönenberger, Ina Kristiana, Ana Sanchez-Polo und Chao Liu. Jede/r hat auf ihre/seine Art und Weise meine Zeit an der EAWAG mitgeprägt und bereichert. Besonders geschätzt habe ich, dass der Neo-Unihockey-Spieler und -Ambri-Fan Tony immer wieder einmal an die Glastür meines Büros geklopft hat.

Nicht genug danken kann ich meinen Eltern Nadia und Christian sowie meiner Schwester Daniela. Sie haben mich nicht nur auf diesem Weg, sondern schon mein ganzes Leben lang mit viel Liebe unterstützt und ich weiss, dass dies immer so sein wird.

Sämtliche Hochs und Tiefs in aller Nähe miterlebt hat Eliane Tresch. Danke dafür, dass du immer für mich da gewesen bist! Und ich freue mich auf Alles, was noch kommen wird...



---

# Table of contents

Danksagung	i
Table of contents	v
List of frequently used abbreviations	vii
Summary	ix
Zusammenfassung	xiii
<b>1 General Introduction</b>	<b>1</b>
1.1 History of swimming in pools	2
1.2 Water disinfection and pool water treatment	3
1.3 Disinfection by-products	10
1.4 Disinfection by-product mitigation strategies	20
1.5 Trichloramine in pool water and its mitigation by UV treatment	24
1.6 Thesis outline	25
References	27
<b>2 Trichloramine reactions with nitrogenous and carbonaceous compounds: kinetics, products and chloroform formation</b>	<b>35</b>
2.1 Introduction	37
2.2 Materials and Methods	39
2.3 Results and Discussion	42
2.4 Conclusions	58
References	61
<b>Supporting Information for Chapter 2</b>	<b>65</b>
<b>3 Software for the valve control of a membrane introduction mass spectrometer (MIMS 2000) and for MIMS data analysis: MIMS-VICI Driver and MIMS-VICI Analysis</b>	<b>87</b>
3.1 Introduction	89
3.2 Materials and Methods	94
3.3 Results and Discussion	96
3.4 Conclusions	101
References	103
<b>Supporting Information for Chapter 3</b>	<b>105</b>

---

<b>4</b>	<b>Comparison of a novel extraction-based colorimetric (ABTS) method with membrane introduction mass spectrometry (MIMS): trichloramine dynamics in pool water</b>	<b>113</b>
4.1	Introduction	115
4.2	Materials and Methods	119
4.3	Results and Discussion	124
4.4	Conclusions	135
	References	137
	<b>Supporting Information for Chapter 4</b>	<b>141</b>
<b>5</b>	<b>Photolysis of inorganic chloramines and efficiency of trichloramine abatement by UV treatment of swimming pool water</b>	<b>163</b>
5.1	Introduction	165
5.2	Materials and Methods	167
5.3	Results and Discussion	173
5.4	Conclusions	187
	References	189
	<b>Supporting Information for Chapter 5</b>	<b>193</b>
<b>6</b>	<b>Enhanced N-nitrosamine formation in pool water by UV irradiation of chlorinated secondary amines in the presence of monochloramine</b>	<b>213</b>
6.1	Introduction	215
6.2	Materials and Methods	219
6.3	Results and Discussion	222
6.4	Conclusions	236
	References	239
	<b>Supporting Information for Chapter 6</b>	<b>243</b>
<b>7</b>	<b>General Conclusions</b>	<b>261</b>

Curriculum vitae

---

## List of frequently used abbreviations

ABTS	2,2-azino-bis(3-ethylbenzothiazoline-6-sulfonic acid) diammonium salt
BFA	body fluid analog
CDMA	chlorinated dimethylamine
EDC	electron donating capacity
DBP	disinfection by-product
DMNA	dimethylnitramine
DOC	dissolved organic carbon
DPD	<i>N,N</i> -dipropyl- <i>p</i> -phenylene-diamine
GC-MS	gas chromatography-mass spectrometer
HPLC	high-performance liquid chromatography
$k_{app}$	apparent rate constant
$k_{eff}$	effective rate constant
LP	low-pressure
MIMS	membrane introduction mass spectrometer
MP	medium-pressure
Mor	morpholine
NDMA	nitrosodimethylamine
PLFA	Pony Lake fulvic acid
SRFA	Swanee River fulvic acid
THM	trihalomethane
TOC	total organic carbon
t-BuOH	<i>tert</i> -butanol
UDMH	unsymmetrical dimethylhydrazine
UV	ultraviolet
QY	quantum yield





---

## Summary

Trichloramine is a disinfection by-product of concern in indoor swimming pools due to its adverse health effects. The goals of this doctoral thesis were to develop an analytical method for the measurement of trichloramine in swimming pool water, to quantify its concentrations in Swiss pool water and to investigate the factors influencing its formation and degradation. Furthermore, ultraviolet light (UV) treatment of pool water was studied not only as a mitigation strategy to reduce trichloramine concentrations, but also as a possible source of further disinfection by-products.

The use of swimming pools for sport and recreation is popular worldwide for every age class. Swimmers/bathers introduce human substances such as hair, skin particles, urine, sweat and personal care products but also viruses and bacteria into the pools. Therefore, pool water must be treated, disinfected and replaced regularly. In public swimming pools, pool water is commonly filtered and chlorinated continuously. This practice guarantees a proper disinfection of the pool water but results in the formation of numerous disinfection by-products, which can be carcinogenic and genotoxic in extreme cases. A volatile disinfection by-product of concern is trichloramine, which irritates the skin, the eyes and the respiratory tract and is suspected to cause asthma. Trichloramine belongs to the inorganic chloramines (mono-, di- and trichloramine) and is assumed to be formed by the reaction of free chlorine with nitrogenous precursors such as urea. It has been rarely measured in pool water due to the lack of an adequate analytical method. Therefore, little is known about its concentration in pool water, its formation and possible mitigation strategies.

An extraction-based, colorimetric method for trichloramine analysis was developed in this thesis (chapter 4). This low-cost and easy-applicable method was validated by measurements of pool water samples with the more sophisticated technique of membrane introduction mass spectrometry (MIMS). The measurements further showed that trichloramine concentration in Swiss pool water reached up to 0.5  $\mu\text{M}$  and was strongly correlated with the free chlorine and HOCl concentration ( $R^2 = 0.64$  and  $0.79$ , respectively). A correlation with pH and the total inorganic chloramine concentration was much less pronounced and no correlation was observed with the urea concentration. Continuous on-site measurements over several days with a high time-resolution ( $< 40$  min) confirmed that the trichloramine was strongly influenced by the residual free chlorine concentration.

The on-site measurements with MIMS were facilitated by a software, which was engineered in this thesis (chapter 3). This software supports the automated sample collection for continuous,

---

long-term sampling. It further assists the analysis of large data sets from sampling campaigns by assisting steady-state, flow-injection and continuous measurements. Thanks to the software, manual time-consuming work such as peak recognition and mean determination is minimized, thereby also reducing the arbitrariness of the operator.

The MIMS was also used to investigate the reactivity of trichloramine with model compounds such as primary and secondary amines, amides, hydroxylated phenolic compounds and fulvic acids (chapter 2). At pH 7 the second-order reaction rate constant with trichloramine were found to be low for amides ( $k_{\text{app}} = 10^{-2} - 10^{-1} \text{ M}^{-1} \text{ s}^{-1}$ ), slightly higher for primary amines ( $k_{\text{app}} = 10^{-1} - 10^0 \text{ M}^{-1} \text{ s}^{-1}$ ) and significant for secondary amines ( $k_{\text{app}} = 5 \times 10^1 - 5 \times 10^2 \text{ M}^{-1} \text{ s}^{-1}$ ). Measurements of the reaction products revealed that trichloramine mainly induces a chlorine addition but is also able to undergo an electron transfer reaction. Typically, free chlorine has a higher reactivity with most substances than trichloramine. Chlorination of many substances leads to a lower reactivity of trichloramine with these substances (e.g. secondary amines, fulvic acids and uric acid). UV irradiation of pool water, which breaks the nitrogen-chlorine bond of pool water compounds, increases the overall reactivity of trichloramine with the pool water matrix (chapter 5). Hence, residual free chlorine competes with trichloramine for the same substances in pool water and its presence hampers trichloramine degradation. Therefore, as long as free chlorine is present in pool water, the decay of trichloramine is close to the self-decay of trichloramine in pure water at the same pH.

A reduction of disinfection by-products, including trichloramine, in pool water may be achieved by lowering chlorine dosage. However, such a reduction is limited by the prescribed free chlorine concentration, which is needed to guarantee disinfection. A common technique to further mitigate trichloramine and the other inorganic chloramines is UV treatment. UV treatment in Swiss pool facilities is mainly performed with medium-pressure mercury lamps and less frequently with low-pressure mercury lamps. This thesis confirmed that trichloramine is degraded by 30–50 % with a UV irradiation of a medium-pressure lamp under similar conditions as in pool water treatment. This corresponded nicely to the UV-induced trichloramine degradation in two UV reactors during on-site measurements in a pool facility. However, the trichloramine degradation of about 50 % in the UV reactor resulted in a decrease of the trichloramine concentration in pool water of only about 10 and 20 % in a competition and a wading pool, respectively. This little effect of the UV treatment might be explained by a fast trichloramine formation in the pool water, which leads to almost the same steady-state concentration as without UV treatment in the competition pool (long residence time of 4–5 h before treatment) and to a slightly lower concentration in the wading pool (shorter residence

---

time of about 1 h). Hence, UV treatment does only effectively reduce trichloramine concentration in swimming pools with a short residence time and even in these pools, its effect is limited by the trichloramine formation in pool water.

The results described in chapter 5 also indicate that the other inorganic chloramines might be mitigated by UV treatment. However, to confirm these results, further long-term measurements would be necessary. This is also the case for the effect of UV irradiation on trihalomethanes. The results only show that trihalomethane concentrations remain unchanged after treatment in the UV reactor. The effect of UV irradiation on nitrosamines, a carcinogenic disinfection by-product, was investigated in chapter 6. Previous studies showed that nitrosamines, such as *N*-nitrosodimethylamine (NDMA), are photodegraded by UV irradiation from low- and medium-pressure mercury lamps. However, it could be shown in the present investigation that UV irradiation of swimming pool water also enhances NDMA formation. This enhancement was ascribed to the formation of reactive NDMA precursors (e.g. nitric oxide) from the phototransformation of chlorinated substrates, as it could be shown for monochloramine and chlorinated dimethylamine. Whether UV irradiation decreases the NDMA concentration in pool water depends on the initial NDMA concentration and the concentration of its precursors as well as on the applied UV dose. It is shown in chapter 6 that this formation pathway is also valid for other nitrosamines. Hence, whether UV treatment of pool water results in an increase or a decrease of the nitrosamine concentration depends on the specific conditions of the pool water and the treatment.

In conclusion, a low-cost and easy-applicable trichloramine measurement method was established. Pool water measurements showed that trichloramine concentrations are commonly below 0.5  $\mu\text{M}$  in Switzerland and depend strongly on the residual free chlorine concentration. Lowering free chlorine concentration in pool water might be a more effective trichloramine mitigation strategy than implementing a UV treatment. The overall effect of UV irradiation on pool water quality is difficult to assess since this thesis reveals positive and negative aspects of UV treatment in accordance with literature.



---

## Zusammenfassung

Trichloramin ist ein Desinfektionsnebenprodukt im Badewasser, welches die Gesundheit der Badegäste und des Personals in Hallenbädern gefährden kann. Im Rahmen dieser Doktorarbeit wurde eine Methode zur Trichloraminmessung in Badewasser entwickelt. Mit Hilfe dieser Messmethode wurden die Trichloraminkonzentration in verschiedenen Wasserproben von Hallenbädern bestimmt und Faktoren, welche die Bildung und den Abbau von Trichloramin beeinflussen, erruiert. Des Weiteren wurde der Trichloraminabbau in Badewasser mittels UV-Behandlung sowie der Einfluss der UV-Behandlung auf andere Desinfektionsnebenprodukte untersucht.

Schwimmbäder sind weltweit bei jeder Altersklasse beliebt, sei es um sportliche Aktivitäten auszuüben oder die Freizeit zu verbringen. Dabei geniessen die Badegäste nicht nur das Wasser, sondern geben auch körpereigene Substanzen wie Haare, Hautpartikel, Urin oder Schweiss ins Wasser ab. Zusätzlich gelangen auch Viren und Bakterien durch Badegäste ins Badewasser. Aus diesem Grund muss das Badewasser behandelt, desinfiziert und regelmässig ersetzt werden. In öffentlichen Schwimmbädern wird das Badewasser normalerweise kontinuierlich filtriert und gechlort, um eine stete Desinfektion zu gewährleisten. Allerdings entstehen dadurch gesundheitsgefährdende Desinfektionsnebenprodukte, welche sogar kanzerogen oder gentoxisch sein können. Eines dieser problematischen Nebenprodukte ist das flüchtige Trichloramin. Trichloramin reizt die Augen und die Haut, kann zur Entzündung der Atemwege führen und steht im Verdacht, Asthma zu verursachen. Trichloramin gehört zu den anorganischen Chloraminen (Mono-, Di- und Trichloramin, ebenfalls bekannt als gebundenes Chlor) und entsteht bei der Reaktion von freiem Chlor mit stickstoffhaltigen Vorläufersubstanzen wie zum Beispiel Harnstoff. Da bisher eine geeignete Methode zur Messung von Trichloramin in Wasser fehlte, wurden selten Trichloraminmessungen im Badewasser durchgeführt. So ist wenig bekannt über Trichloramin im Badewasser, über dessen Entstehung und die Möglichkeiten, die Trichloraminkonzentration im Badewasser zu verringern.

Im Kapitel 4 dieser Doktorarbeit wird eine auf Extraktion basierende, kolorimetrische Trichloramin-Messmethode vorgestellt, welche im Rahmen dieser Doktorarbeit entwickelt wurde. Die Messmethode ist kostengünstig und einfach anwendbar. Sie wurde mittels Vergleichsmessungen mit einem kommerziellen „Membran Introduction Mass Spectrometer (MIMS)“ validiert. Diese Messungen zeigten, dass Trichloramin in Schweizer Badewasser Konzentrationen von bis zu 0.5  $\mu\text{M}$  erreichen kann und dass dessen Konzentration stark mit der

---

Konzentration von freiem Chlor und der unterchlorigen Säure (HOCl) korreliert ist ( $R^2 = 0.64$  beziehungsweise 0.79). Die Korrelation der Trichloraminkonzentration mit dem pH oder dem gebundenen Chlor ist hingegen nur sehr schwach. Keinen Zusammenhang konnte zwischen der Harnstoff- und der Trichloraminkonzentration festgestellt werden. Kontinuierliche Trichloraminmessungen in einem Hallenbad über mehrere Tage mit einer hohen Auflösung (< 40 Min.) bestätigten, dass die Trichloraminkonzentration stark von der freien Chlorkonzentration beeinflusst wird.

Die Trichloramin-Messungen im Hallenbad mit dem MIMS wurden durch eine Software ermöglicht, dessen Entwicklung Bestandteil dieser Doktorarbeit war (Kapitel 3). Die Software unterstützt die automatische Probenahme bei kontinuierlichen Langzeitmessungen. Des Weiteren vereinfacht sie die Auswertung von grossen Datensätzen für verschiedene Messmethoden (steady-state, flow-injection und kontinuierliche Messungen). Dabei wird die zeitaufwendige Handarbeit sowie der Einfluss der auswertenden Person minimiert.

Das MIMS wurde auch verwendet, um die Reaktivität von Trichloramin mit Modellsubstanzen (Aminen, Amiden, hydroxylierten Phenolen und Fulvinsäuren) zu untersuchen (Kapitel 2). Trichloramin hat bei pH 7 eine tiefe Reaktionsrate zweiter Ordnung mit Amiden ( $k_{app} = 10^{-2} - 10^{-1} \text{ M}^{-1} \text{ s}^{-1}$ ), eine etwas höhere mit primären Aminen ( $k_{app} = 10^{-1} - 10^0 \text{ M}^{-1} \text{ s}^{-1}$ ) und eine deutlich höhere mit sekundären Aminen ( $k_{app} = 5 \times 10^1 - 5 \times 10^2 \text{ M}^{-1} \text{ s}^{-1}$ ). Die Messung von Reaktionsprodukten zeigte, dass Trichloramin hauptsächlich mittels einer Chloraddition reagiert, aber auch zu einem Elektronentransfer fähig ist. Für die meisten der untersuchten Substanzen ist die Reaktionsrate zweiter Ordnung von freiem Chlor höher als jene von Trichloramin. Die Reaktionsprodukte der Chlorung zeigten immer eine tiefere Reaktivität mit Trichloramin als die Ausgangssubstanzen (z.B. sekundäre Amine, Fulvinsäuren und Harnsäure). Dagegen erhöhte die UV-Bestrahlung von Hallenbadwasser dessen Reaktivität mit Trichloramin, vermutlich weil die UV-Bestrahlung die Stickstoff-Chlor-Bindungen von Substanzen in der Hallenbadmatrix spaltet (Kapitel 5). Folglich konkurrenziert Trichloramin im Badewasser mit dem freien Chlor um dieselben Reaktionspartner und die Präsenz von freiem Chlor vermindert dadurch den Abbau von Trichloramin. Solange freies Chlor im Badewasser vorhanden ist, ist der Trichloraminabbau nahe beim Selbstzerfall von Trichloramin im Reinstwasser.

Eine Senkung der freien Chlorkonzentration zur Reduktion der Trichloraminkonzentration ist in der Praxis nur soweit möglich, als dass die Desinfektion noch gewährleistet ist. Eine gängige Technik, die Konzentration des gebundenen Chlors im Badewasser zu senken, ist die UV-

---

Behandlung. In Schweizer Hallenbädern kommen hauptsächlich Mitteldruck- und weniger häufig Niederdruckstrahler zum Einsatz. In dieser Doktorarbeit wurde mit Versuchen im Labor bestätigt, dass eine UV-Bestrahlung Trichloramin unter den in der Badwasserbehandlung üblichen Bedingungen bis zu 30–50 % abbaut. Eine vergleichbare Elimination wurde bei zwei UV Reaktoren in einem Hallenbad gemessen. Trotz diesem deutlichen Abbau von Trichloramin (~50 %) im UV-Reaktor, wurde als Folge der UV-Behandlung die Konzentration von Trichloramin im Schwimmer- und im Planschbecken nur um ~10 %, beziehungsweise 20 % gesenkt. Die verhältnismässig geringe Abnahme der Trichloraminkonzentration in den Becken kann darauf zurück geführt werden, dass Trichloramin im Becken einer Dynamik unterliegt. Im Schwimmerbecken, in welchem das Badewasser eine Aufenthaltszeit von 4–5 Stunden hat, wird durch die Trichloramin-Bildung fast wieder dieselbe Gleichgewichtskonzentration erreicht wie ohne die UV-Behandlung. Die UV-Behandlung war effektiver im Planschbecken, in welchem das Wasser eine Aufenthaltszeit von nur ~1 Stunde hatte. Folglich ist die UV-Behandlung von Badewasser zur Minimierung der Trichloraminkonzentration nur in Becken mit einer kurzen Aufenthaltszeit wirksam und auch dort ist der Effekt limitiert durch die Trichloramin-Bildung im Becken.

Die Resultate im Kapitel 5 zeigen zudem auf, dass die Konzentration des gebundenen Chlors durch die UV Behandlung vermutlich gesenkt werden kann. Um diese Annahme zu bestätigen, müssten jedoch Langzeitstudien durchgeführt werden. Langzeitstudien sind auch nötig, um die Frage zu beantworten, ob die UV-Behandlung von Badewasser zu einer erhöhten Trihalomethankonzentration führt. Die während der Doktorarbeit durchgeführten Messungen konnten nur bestätigen, dass die Trihalomethankonzentration zwischen Ein- und Austritt des Badewassers in den UV Reaktor unverändert bleibt.

Den Einfluss der UV-Behandlung auf die Nitrosaminkonzentration, ein kanzerogenes Desinfektionsnebenprodukt, wurde in Kapitel 6 untersucht. Bisherige Studien zeigten, dass Nitrosamine (z.B. Nitrosodimethylamin (NDMA)) mit Nieder- und Mitteldruckstrahlern abgebaut werden können. Die UV-Behandlung von Badewasser kann hingegen die Bildung von NDMA erhöhen, da die Bestrahlung von Monochloramin und Dimethylamin zu schnell reagierenden NDMA-Vorläufersubstanzen (wie z.B. Stickstoffmonooxid) führen kann. Ob die UV-Behandlung von Badewasser die NDMA-Konzentration erhöht oder senkt hängt vom Verhältnis von NDMA zu den Vorläufersubstanzen und von der angewendeten UV-Dosis ab. In Kapitel 6 wird gezeigt, dass dieser Bildungsweg nicht nur für NDMA, sondern auch für andere Nitrosamine gilt. Der Effekt der UV-Behandlung auf die Nitrosaminekonzentration hängt also von den spezifischen Bedingungen im Badewasser und der Intensität der UV-Behandlung ab.

---

Zusammenfassend kann man sagen, dass im Rahmen dieser Doktorarbeit eine einfache und kostengünstige Trichloramin-Messmethode entwickelt wurde. Messungen mit dieser Methode haben gezeigt, dass die Trichloraminkonzentration im Badewasser normalerweise  $< 0.5 \mu\text{M}$  ist und stark von der freien Chlorkonzentration abhängt. Die Absenkung der freien Chlorkonzentration ist wahrscheinlich ein geeigneteres Mittel um die Trichloraminkonzentration im Badewasser zu senken als die Behandlung des Badewassers mit UV-Strahlung. Eine gesamtheitliche Beurteilung des Einflusses der UV-Behandlung auf die Qualität des Badewassers ist schwierig, da in dieser Doktorarbeit wie auch der bisherigen Literatur gezeigt wurde, dass sich die UV-Behandlung sowohl positiv wie auch negativ auf die Konzentration von einzelnen Desinfektionsnebenprodukten im Badewasser auswirken kann.



# **Chapter 1**

## **General Introduction**

## **1.1 History of swimming in pools**

The earliest archaeological reports of swimming are drawings in “the cave of swimmers” in Egypt, which date back to 2000–3000 B.C. (Encyclopaedia Britannica). During the same period, the first community baths were built in Pakistan, though the baths were rather used for religious ceremonials than for bathing (Gray, 1940). Later, swimming was also practiced in the Assyrian, Greek and Roman civilizations. It is no surprise that Romans build not only Roman baths but also heated swimming pools and that the Greeks organized occasionally swimming races. Thus, swimming was part of the education and the physical training in the Greek and Roman culture (Encyclopaedia Britannica). Swimming lost its popularity in Europe during the Middle Ages in which only knights trained this skill. It is hypothesised that this was caused by the church and the conservative society which disfavoured and partly prohibited naked bathing or by people’s fear of diseases being spread by swimming (Encyclopaedia Britannica; Fischer, 2005). Swimming as recreation and sports gained again popularity in the mid-19<sup>th</sup> century and especially after the Olympic Games included swimming races in 1896. The first indoor pools were constructed during the same period in England. Nowadays, swimming is one of the most popular sports worldwide and swimming pools are ubiquitous in industrialized countries (Blatchley and Cheng, 2010).

## 1.2 Water disinfection and pool water treatment

Swimming pools are commonly filled with fresh water of drinking water quality containing a few mg L<sup>-1</sup> of dissolved organic matter. Therefore, they initially represent an oligotrophic environment, which is not favourable for microbial growth. With bathers entering the pool, more and more nutrients are introduced into pool water by bather's urine, skin particles, sweat, saliva, hair, etc. This, together with the increased water temperature in heated pools, improves the conditions for most bacteria in comparison to drinking water. Furthermore, pool water is recycled to minimize the loss of water and energy (heated water), which results in a long residence time of the water in the pool system. With this combination, swimming pools represent a potential environment for growth of fecally-derived (which prefer growth medium with higher nutrient concentrations and higher temperatures) and non-fecally-derived viruses and bacteria introduced by bathers or from the pool surroundings (Figure 1.1). Consequently, there are many reports of severe health issues related to hygienic problems in swimming pools (WHO, 2006). The most common health issues are infections or irritations of the respiratory tract, the ears, the eyes, the skin and the alimentary tract (Singer, 1990). To prevent these problems, the standard norm for Swiss pool water (SIA 385/9) requires disinfection and treatment of pool water as well as a monitoring of microbiological parameters (Table 1.1) (SIA, 2013).

Besides the hygienic reasons, pool water is often disinfected to prevent the growth of algae, which are an aesthetic problem and can also reduce the functionality of the filters due to clogging.

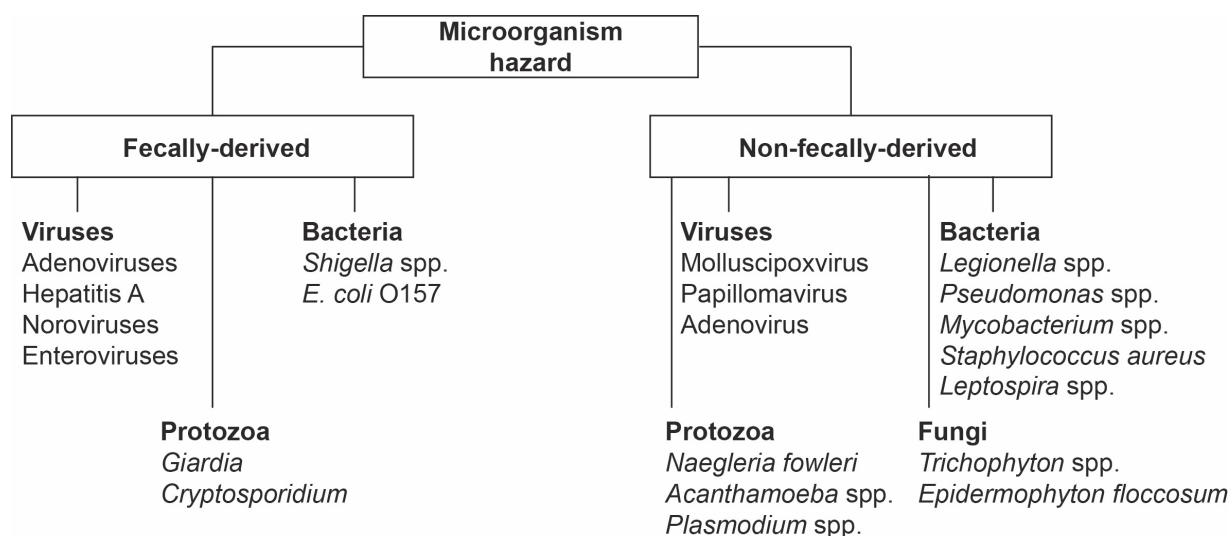


**Figure 1.1:** Hazardous microorganisms in swimming pools from fecal and non-fecal sources (from WHO (2006)).

**Table 1.1:** Regulations in Swiss pool water (adapted from SIA 385/9 (SIA, 2013)).

Parameter	Target value	Limit value <sup>a)</sup>	Unit
<b>Microbiological requirements</b>			
Heterotrophic plate count	-	1000	CFU <sup>b)</sup> mL <sup>-1</sup>
<i>Escherichia coli</i>	-	not detectable	CFU <sup>b)</sup> 100 mL <sup>-1</sup>
<i>Pseudomonas aeruginosa</i>	-	not detectable	CFU <sup>b)</sup> 100 mL <sup>-1</sup>
<i>Legionella spp.</i>	-	1	CFU <sup>b)</sup> 100 mL <sup>-1</sup>
<b>Chemical and physical requirements</b>			
Turbidity	< 0.2	0.5	NTU <sup>c)</sup>
pH	7.0 - 7.4	6.8 - 7.6	
TOC	< 2.0	3	mg C L <sup>-1</sup>
Free chlorine	swimming pool	0.2 - 0.4	mg L <sup>-1</sup> as Cl <sub>2</sub>
	hot tub	0.7 - 1.0	mg L <sup>-1</sup> as Cl <sub>2</sub>
Combined chlorine		0.2	mg L <sup>-1</sup> as Cl <sub>2</sub>
Trihalomethane (as chloroform)	-	0.02	mg L <sup>-1</sup>
Ozone	-	0.02	mg L <sup>-1</sup>
Chlorate	< 4	10	mg L <sup>-1</sup>
Bromate		0.2	mg L <sup>-1</sup>
Urea	indoor pool	< 1	mg L <sup>-1</sup>
	outdoor pool	< 2	mg L <sup>-1</sup>

<sup>a)</sup> measures must be taken

<sup>b)</sup> colony forming unit

<sup>c)</sup> nephelometric turbidity unit

### 1.2.1 Disinfection and microbiological parameters

Disinfection in Swiss pool water is ensured by the presence of residual free chlorine (Cl<sub>2</sub>, HOCl, OCl<sup>-</sup>). The norm imposes a limit value (lv) of 0.2–0.8 mg L<sup>-1</sup> as Cl<sub>2</sub> and a target value (tv) of 0.2–0.4 mg L<sup>-1</sup> as Cl<sub>2</sub> in pool water. These values are higher in whirlpools (0.7–1.0 and 0.7–1.5 mg L<sup>-1</sup> as Cl<sub>2</sub> for target and limit value, respectively). The distribution of free chlorine species is illustrated in Figure 1.2 and depends on the pH, the chloride concentration and temperature (eqs.1.1 and 1.2) according to the equilibrium constants given in Morris (1966).



Swiss pool water is controlled at a neutral pH (lv: 6.8–7.6, tv: 7.0–7.4) to ensure that most of the free chlorine is present as HOCl (pK<sub>HOCl, 25 °C</sub> = 7.54) (Morris, 1966; SIA, 2013). This is important since HOCl is significantly more active as a disinfectant than OCl<sup>-</sup>. The target values

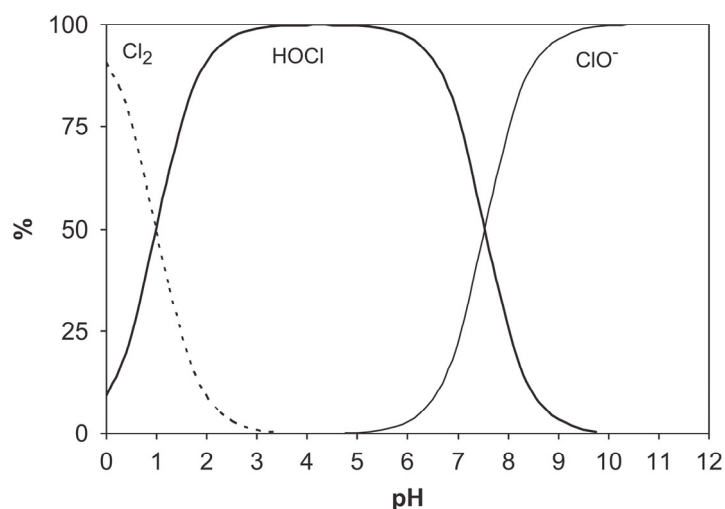


**Figure 1.2:** Distribution of free chlorine species as a function pH. The distribution is calculated for a chloride concentration of  $5 \times 10^{-3}$  M according to equation 1.1 and 1.2 (from Deborde and von Gunten (2008)).

of pH and free chlorine aim to guarantee a 4-log-inactivation of *pseudomonas aeruginosa* within 30 seconds.

Free chlorine is usually added as hypochlorite (in solution or produced from the electrolysis of sodium chloride or hydrochloric acid) or calcium hypochlorite. Its addition is regulated by the residual free chlorine concentration in pool water. In pool water, free chlorine (primary disinfectant) can react with nitrogenous compounds to organic and inorganic chloramines to secondary disinfectants (Deborde and von Gunten, 2008). While inorganic chloramines (mono-, di- and trichloramine also summarized as combined chlorine) still act as weak disinfectants, the chlorinated organic *N*-compounds demonstrate almost no germicidal efficiency (Donnermair and Blatchley, 2003).

Inorganic chloramines can either be formed from the chlorination of ammonia (eqs. 1.3–1.5, Jolley et al. (1983)) or from the hydrolysis and chlorination of primary or secondary amines (Blatchley and Cheng, 2010).



The chloramine species are in an equilibrium, which depends on the pH and on the chlorine:nitrogen ratio. Soulard et al. (1981) defined theoretically and experimentally the boundary of the predominant chlorine and chloramine species as a function of the pH and the

Cl:N ratio (Figure 1.3). Pool water has a circumneutral pH and a Cl:N ratio which is quite variable due to a permanent addition of free chlorine and bather input. Measurements in pool water showed that monochloramine is the predominant inorganic chloramine species under pool water conditions (Weaver et al., 2009). Since the Swiss norm for pool water limits the concentration of inorganic chloramines to  $0.2 \text{ mg L}^{-1}$  as  $\text{Cl}_2$ , the effect of the secondary disinfectants is minor in comparison to the primary disinfection with free chlorine since they are weaker oxidants. A 99%-inactivation of *E.coli* at 2–6 °C requires an exposure time of ~1 minute, ~100 minutes and ~400 minutes for HOCl, OCl<sup>-</sup> and monochloramine, respectively, at a concentration of 0.1 ppm (titrable chlorine) (White, 1986).

The disinfection of the water in the pool by residual free chlorine is amended by the water treatment in the recirculation (section 1.2.2). Many swimming pool operators enhance their mandatory filter system with an oxidation/disinfection step such as ozonation or UV treatment. These treatment steps are supposed to improve the disinfection and to reduce the concentration of disinfection by-products in pool water. A disinfection of the pool water only by ozonation or UV irradiation is not in agreement with the SIA 385/9. Pool water remains on average 4–5 hours in the swimming pool before it is treated again, wherefore a residual disinfectant in the pool is mandatory to prevent bacterial growth during that time. Nevertheless, a disinfection step in addition to chlorination is favourable because the microbial inactivation mechanisms of ozone and UV irradiation differ from chlorine. Hence, ozonation and/or UV treatment potentially deplete bacteria that are insensitive or resistant to free chlorine (LeChevallier et al., 1988).

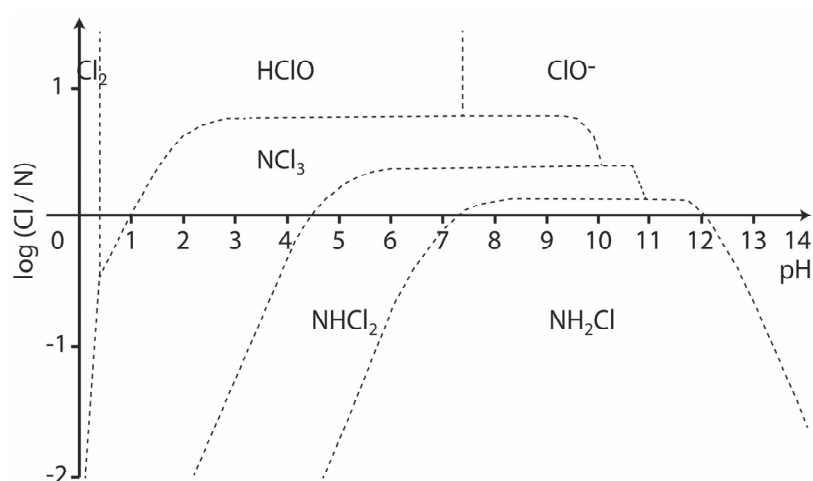


**Figure 1.3:** Illustration of the theoretically predominant chlorine and chloramine species as a function of pH and the Cl:N ratio (adapted from Soulard et al. (1981)).

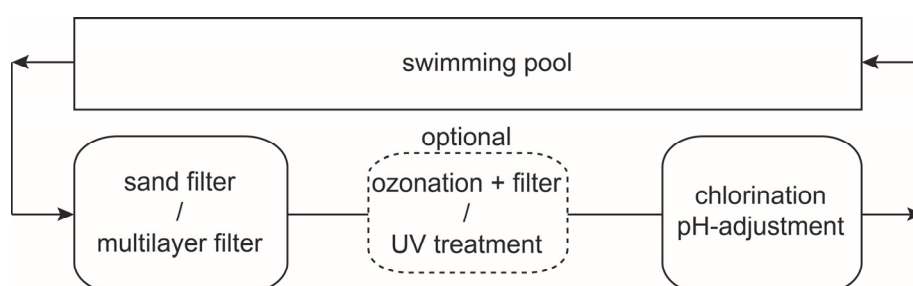
The SIA 385/9 contains limit values for four microbiological parameters (heterotrophic bacteria, *E. coli*, *Pseudomonas aeruginosa*, *Legionella spp.*) (Table 1.1). The heterotrophic plate count is a sum parameter for bacteria and fungi which are general indicators for the water quality. The bacterium *E. coli* itself is commonly not harmful to bathers but it indicates fecal contamination and the potential presence of other pathogens. The bacterium *Pseudomonas aeruginosa* is a pathogen that has shown multiple resistance against antibiotics. It can cause a large variability of disease e.g. pneumonia, infection of the urinary tract and otitis externa (Swimmer's ear). The pathogen *Legionella spp.* may cause severe adverse health effects such as pneumonia or pyelonephritis by inhalation of aerosols containing *Legionella spp.* Therefore, its presence in water for showering or in whirlpools is more problematic than in pool water. These four parameters must be monitored periodically to check whether the disinfection of the pool water is appropriate.

## 1.2.2 Pool water treatment

Scheme 1.1 shows a common pool water treatment according to the SIA 385/9, which foresees a filtration (flocculation and filter or precoated filter), an optional ozonation (ozonation plus sorption or multilayer filter) and a chlorination. Commonly, pH adjustment is done in the same step as the chlorination. There are no norms on UV treatment of pool water in the SIA 385/9, although it is widely applied in public pools in Switzerland.

### *Residence time and fresh water addition*

The pool operators must provide at least 2 m<sup>3</sup> of treated pool water per bather according to the Swiss norm (SIA, 2013). The norm does not imply hydraulic residence times (average time in the pool before being treated) but states recommendations to fulfil the regulations in Table 1.1. The recommended hydraulic residence time depends on the category of the pool. At a normal bather frequency, the residence times are about 3.5–5.5 hours, 1–2 hours and 0.05 hours for a swimming pool, a children pool and a hot tub, respectively (Table 1.2). The addition of the



**Scheme 1.1:** Required and optional treatment steps in pool water treatment.

**Table 1.2:** Recommended hydraulic residence times in swimming pools according to their category, water depths and flow rate (SIA, 2013).

	water depth (m)	flow rate (m <sup>3</sup> h <sup>-1</sup> )	residence time (h)
swimming pool	1.35 - 2.2	0.4 m h <sup>-1</sup> x A	3.4 - 5.5
diving pool	> 3.4	0.6 m h <sup>-1</sup> x A	> 5.7
children's pool	0.6 - 1.35	0.67 m h <sup>-1</sup> x A	0.9 - 2
wading pool	< 0.5	0.7 m h <sup>-1</sup> x A	0.7
hot tube (> 4 m <sup>3</sup> )	~ 1	20 h <sup>-1</sup> x V	0.05

A: surface area (m<sup>2</sup>), V: volume (m<sup>3</sup>)

treated water should occur in a way that a complete mixing of the pool water is guaranteed. Furthermore, a fresh water addition of at least 30 L per bather in pools and 75 L per bather in hot tubs is required. In consequence, the average exchange time of the pool water with fresh water in a competition pool (50 m × 25 m × 2.5 m) is 10–20 days in dependence on the bather frequency.

### ***Filtration, chlorination and pH adjustment***

The filtration step in Scheme 1.1 consists commonly of a sand or multilayer filter with flocculation (with aluminium or iron (III) salts) prior to sand filtration or to a precoated filter (with activated carbon). The filters eliminate particles from the pool water. They are backwashed weekly to restore their function and reduce the headloss. Ultrafiltration, which is an absolute barrier against bacteria and viruses, is rarely applied in the field of pool water treatment. For ultrafiltration, a flocculation and pre-filtration is recommended (SIA, 2013).

The most basic pool water treatment contains just a filter followed by chlorination and pH adjustment, which are regulated by measurements in the pool. The use of alkaline disinfectants (e.g. sodium hypochlorite) commonly requires a pH adjustment with an acid (HCl or H<sub>2</sub>SO<sub>4</sub>), while bases (e.g. Na<sub>2</sub>CO<sub>3</sub> or NaOH) are used for acidic disinfectants (e.g. Cl<sub>2</sub> (eq. 1.1)).

### ***Optional treatments: Ozonation and UV irradiation***

Ozonation and UV irradiation are efficient disinfection processes for bacteria, viruses and protozoa. They are implemented in pool water treatment as secondary disinfection steps to mitigate chlorine-resistant pathogens (Hijnen et al., 2006; Wang et al., 2013). A further important purpose for ozone is an oxidation of disinfection by-products and their precursors (section 1.3). Ozone, a strong oxidant, is usually produced on-site by corona discharge from oxygen. The ozone-containing oxygen gas is then bubbled into the water to target concentrations in the mg L<sup>-1</sup> range. UV treatment of pool water is done with low-pressure (LP) or, slightly more often, with medium-pressure (MP) mercury lamps. LP lamps have a



monochromatic emission at  $\lambda = 254$  nm while MP lamps emit over a range of 200–400 nm (Figure 1.4). The applied UV dose in the pool water treatment is around  $400\text{--}1000$   $\text{J m}^{-2}$ . This dose is referred for LP lamps to the emission at  $\lambda = 254$  nm and for MP lamps to the cumulative emission from  $\lambda = 200\text{--}300$  nm. The wavelengths below 240 nm are commonly eliminated an optical filter in drinking water treatment to prevent nitrite formation. This is not always the case for pool water treatment.

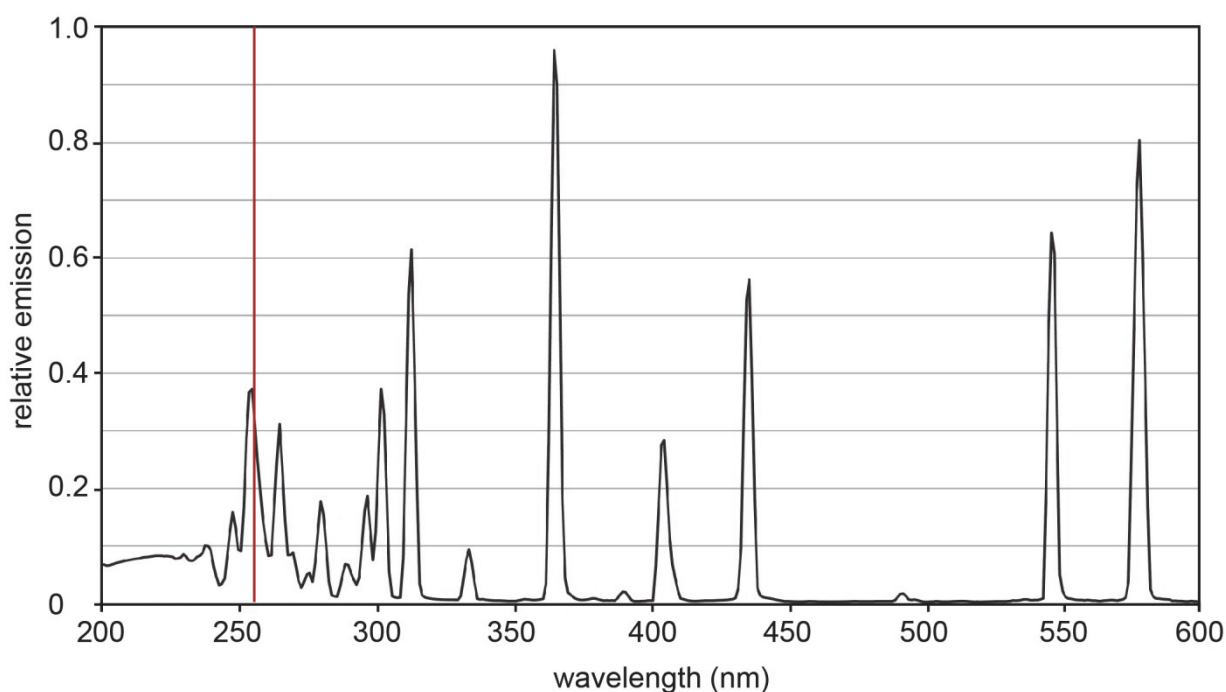


**Figure 1.4:** Emission spectra of low- (red line) and medium-pressure mercury lamps (black line) (adapted from Peschl Ultraviolet, online catalogue 2013, [www.peschl-ultraviolet.com](http://www.peschl-ultraviolet.com)).

## 1.3 Disinfection by-products

### 1.3.1. Formation, formation pathways and occurrence

#### *Precursors and formation*

Disinfection by-products (DBPs) are formed by the reaction of primary or secondary disinfectants (free chlorine, chloramines, ozone) with precursors or during disinfection processes (UV treatment). These precursors can either derive from the source/filling water, the bather input or from substances used for the pool water treatment (Figure 1.5). In Switzerland, filling water has drinking water quality containing commonly low mg L<sup>-1</sup> levels of dissolved organic carbon and almost no nitrogenous compounds. However, bather load such as urine, sweat, saliva, hair, skin particles, sunscreens and body lotions increases the concentration of nitrogen-containing compounds like urea, creatinine, uric acid and histidine. To date, three studies established artificial mixtures representing body fluid analogues (BFA) to imitate the bather load (Borgmann-Strahsen, 2003; Judd and Bullock, 2003; Goeres et al., 2004). A study about the DBP formation from the chlorination of filling waters and of the three BFAs revealed that trihalomethanes are mainly formed from precursors from the filling water while haloacetic acids from precursors from the BFAs (Kanan and Karanfil, 2011). The assumption that trihalomethanes mainly originate from the filling water is supported by Kim et al. (2002), who found a decreased trihalomethane formation if bather inputs (hair, saliva, lotion, etc.) were added to ground water. Additional input of natural organic matter in outdoor pools from the environment may also lead to higher trihalomethane concentrations than in indoor pools (Simard et al., 2013).

Differences in disinfection and in the filling water as well as the variations in bather load result in a huge variety of disinfection by-products in pool water (Table 1.3) (Zwiener et al., 2007; Richardson et al., 2010). The concentration and composition of the DBPs depend on the disinfectant and the precursor concentrations but also on pH and water temperature, which may

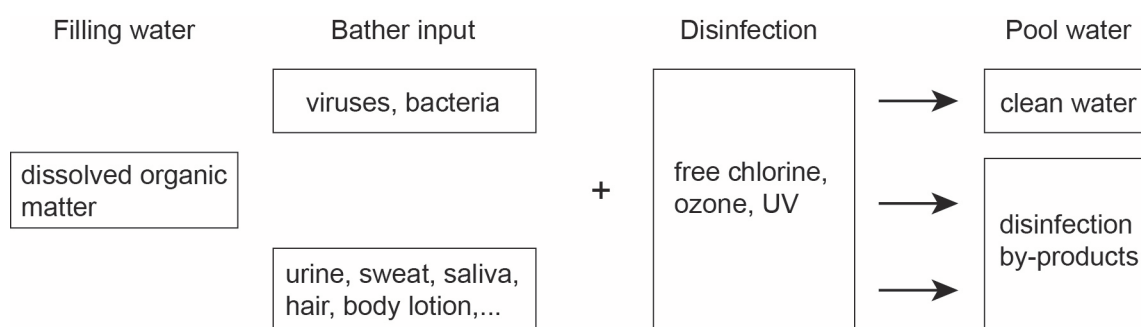


**Figure 1.5:** Disinfection and disinfection by-product formation in pool water.

**Table 1.3:** Selection of DBPs formed from chlorination, chloramination, ozonation and UV treatment in drinking water, pool water or purified water (Cassan et al., 2006; Krasner et al., 2006; Schreiber and Mitch, 2006; WHO, 2006; Weng et al., 2012; Xiao et al., 2012; Soltermann et al., 2013; Wang et al., 2013).

Disinfection	Disinfection by-products	
Chlorine / hypochlorite	trihalomethanes	chloral hydrate
	haloacetic acids	chloropicrin
	haloacetonitriles	cyanogen chloride
	haloketones	chlorate
	haloaldehydes	chloramines
	halobenzoquinones	halophenols
Chloramine	nitrosamines	cyanogen chloride
	trichloramine	haloacetaldehyde
Ozone	bromate	carboxylic acids
	aldehydes	bromoform
	ketones	nitrosamines
UV irradiation	enhanced DBP formation under specific conditions for	
	nitrosamines	cyanogen chloride
	haloacetonitriles	trihalomethanes (inconsistent data)

specifically influence the formation or the degradation/outgassing of certain DBPs (Hansen et al., 2012; Simard et al., 2013; Wang et al., 2013).

### **Formation pathways**

Figure 1.6 illustrates suggested formation pathways for trichloramine, *N*-nitrosodimethylamine and chloroform which were investigated in this doctoral thesis and belong to the most important DBPs in pool water (Boyce and Hornig, 1983; Schreiber and Mitch, 2006; Deborde and von Gunten, 2008; Blatchley and Cheng, 2010). Blatchley and Cheng (2010) suggest that the first chlorination step of urea occurs by the reaction with molecular chlorine ( $\text{Cl}_2$ ) and not with HOCl or  $\text{OCl}^-$  (Figure 1.6a). This first chlorination step is assumed to be the rate limiting step since the  $\text{Cl}_2$  fraction of the free chlorine is very small ( $\sim 10^{-6} = \frac{[\text{Cl}_2]}{[\text{HOCl}] + [\text{OCl}^-] + [\text{Cl}_2]}$ ) at common pool water conditions (pH 7,  $\text{Cl}^-$  conc.:  $\sim 150 \text{ mg L}^{-1}$ ). However, measured free chlorine, urea and trichloramine concentrations and the estimated trichloramine degradation in pool water suggest that this reaction is not the main trichloramine source or that the reaction rate is higher than assumed. Not only for trichloramine, but also for many DBPs it is difficult to evaluate the

main formation pathway in pool water due to the large variety of precursors and changing/unknown precursor concentrations.

Schreiber and Mitch (2006) revisited their previously published formation pathway for the *N*-nitrosodimethylamine (NDMA) formation from chloramines (Mitch and Sedlak, 2002). Originally, it was assumed that dimethylamine reacted with monochloramine to unsymmetrical dimethylhydrazine (UDMH) which then was oxidized by monochloramine to *N*-nitrosodimethylamine. Later, they suggested that the reaction of dichloramine with dimethylamine would lead to a faster NDMA formation. In this formation pathway, dichloramine reacts with dimethylamine to chlorinated UMDH (Figure 1.6b). According to Schreiber and Mitch (2006), the following oxidation of UMDH with dissolved oxygen is possible in the presence of metallic catalysts which facilitate the electron transfer. Whether this mechanism takes place and is the main source for NDMA in pool water is still open. Many

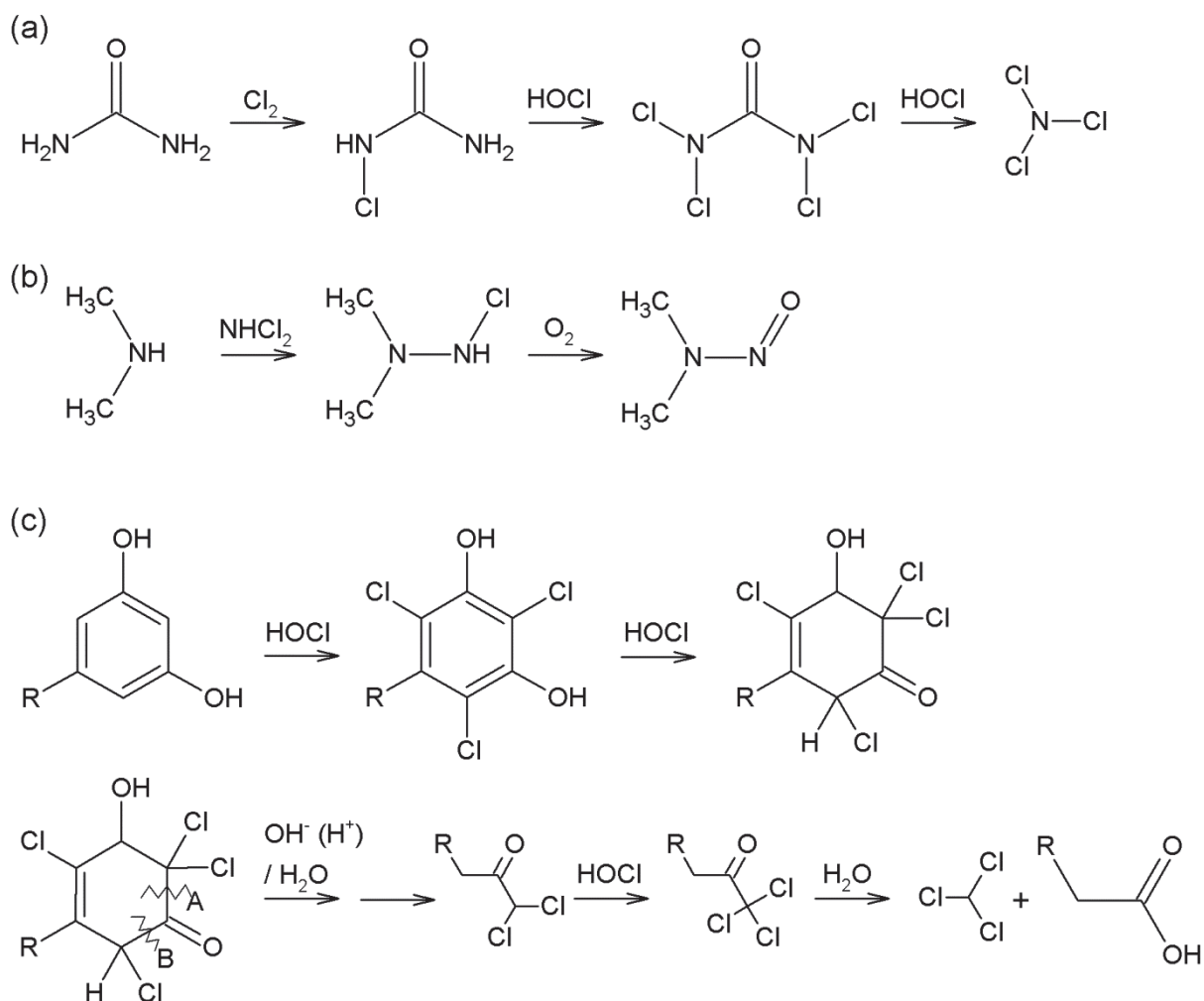


**Figure 1.6:** Suggested formation pathways for the formation of (a) trichloramine, (b) *N*-nitrosodimethylamine and (c) chloroform adapted from Blatchley and Cheng (2010), Schreiber and Mitch (2006) and Boyce and Hornig (1983), respectively.

other precursors and formation pathways are described in literature (Nawrocki and Andrzejewski, 2011; Shah and Mitch, 2011; Krasner et al., 2013).

The chloroform formation from the chlorination of various resorcinol-type compounds (as model compounds for humic acids) was investigated as a function of pH and chlorine concentration (Boyce and Hornig, 1983). According to the suggested formation pathway, the aromatic structure is first chlorinated (electrophilic substitution) before one carbon atom is further chlorinated with a second chlorine atom (Figure 1.6c). Hydrolysis and an oxidative bond cleavage at position A or B opens the ring structure and leads to a ketone structure which is further chlorinated by free chlorine. Chloroform is finally formed by the base-catalysed hydrolysis of this trichloromethyl keton. This illustrates that chloroform can be derived from ketones. However, this formation is rather slow and depends on the rate of the enolization.

### ***Occurrence***

As mentioned above, oxidative processes in pool water treatment can lead to a large variety of potentially hazardous DBPs in swimming pool water. Comparable to the situation in drinking water, there might be a large number of unknown DBPs in pool water (Weinberg et al., 2002; Krasner et al., 2006; Zwiener et al., 2007; Lakind et al., 2010). Especially polar DBPs with high molecular weight tend to remain unidentified because volatile and semivolatile DBPs are more easily extracted and measured with common techniques such as gas-chromatography mass spectrometry (Richardson and Postigo, 2012). In addition to the lack of data for unidentified DBPs, quantitative data is missing or scarce for many DBPs even for the highly toxic compounds such as nitrosamines and halobenzoquinones (Zwiener et al., 2007; Walse and Mitch, 2008; Richardson et al., 2010; Lee et al., 2013; Wang et al., 2013; Chowdhury et al., 2014). Depending on the DBP, concentrations in pool water can range from a few  $\text{ng L}^{-1}$  to several  $\text{mg L}^{-1}$ . Since the concentration of DBPs is influenced by many factors (pH, free chlorine concentration, source water, type of pool, treatment, etc.) and shows a diurnal and seasonal variation for some DBPs, a large number of measurements is required to gain an overview over the concentration range of a DBP in pool water or in indoor pool air. Trihalomethane concentrations in pool water and air as well as trichloramine concentrations in indoor pool air have been well investigated and summarized in previous studies (Bessonneau et al., 2011; Chowdhury et al., 2014). Table 1.4 shows a selection of studies in which DBPs in pool waters are summarized to give a overview on the range of measured DBPs. Trihalomethanes and trichloramine have concentrations in a similar range in pool water ( $\sim 10\text{--}100 \mu\text{g L}^{-1}$ ) and in indoor pool air ( $\sim 50\text{--}500 \mu\text{g m}^{-3}$ ). However, especially trihalomethane concentrations can vary significantly and reach higher concentrations depending on the pool

**Table 1.4:** Selection of DBP measurements in swimming pools based on information from literature.

DBP	Range / Mean / Median	Pool type	Remarks	Literature
Trihalomethanes	~ 15 - 150 $\mu\text{g L}^{-1}$	indoor pools	11 pools, measured bi-weekly for 6 months, free chlorine n.d. - 7.66 $\text{mg L}^{-1}$	Weaver et al. (2009)
Trihalomethanes	~ 4 - 313 $\mu\text{g L}^{-1}$	various pools	review, citing 3 studies	WHO (2006)
Trihalomethanes	39.8 $\pm$ 21.7 $\mu\text{g L}^{-1}$	indoor pools	5 pools	Fantuzzi et al. (2001)
Trihalomethanes	~6 - 155 $\mu\text{g L}^{-1}$	indoor pools	review, citing 5 studies	Chowdhury et al. (2014)
Trihalomethanes in air	~20 - 100 $\mu\text{g m}^{-3}$	indoor pools	1 pool continuously measured over 1 month	Kristensen et al. (2010)
Trihalomethanes in air	58.0 $\pm$ 22.1 $\mu\text{g m}^{-3}$	indoor pools	5 pools	Fantuzzi et al. (2013)
Trihalomethanes in air	~20 - 340 $\mu\text{g m}^{-3}$	indoor pools	review, citing 5 studies	Chowdhury et al. (2014)
Trichloramine	2 - 120 $\mu\text{g L}^{-1}$ (as $\text{Cl}_2$ )	indoor pools	11 pools, measured bi-weekly for 6 months, free chlorine n.d. - 7.66 $\text{mg L}^{-1}$	Weaver et al. (2009)
Trichloramine	~25 $\mu\text{g L}^{-1}$	indoor pools	1 pool continuously measured over 1 week	Gérardin et al. (2005)
Trichloramine in air	650 $\pm$ 200 $\mu\text{g m}^{-3}$	indoor pools	20 pools, free chlorine 1.3 $\pm$ 0.3 $\text{mg L}^{-1}$	Fantuzzi et al. (2013)
Trichloramine in air	110 $\pm$ 40 $\mu\text{g m}^{-3}$	indoor pools	30 pools, free chlorine 1.3 $\pm$ 0.3 $\text{mg L}^{-1}$	Parrat et al. (2013)
Trichloramine in air	100 - 700 $\mu\text{g m}^{-3}$	indoor pool	day-course in one indoor pool	Weng et al. (2011)
Halobenzoquinones	41 $\pm$ 18 $\text{ng L}^{-1}$	swimming pools	6 pools, 25° C, , free chlorine 0.60 - 1.82 $\text{mg L}^{-1}$ , DOC 4.9 - 8.1 $\text{mg C L}^{-1}$	Wang et al. (2013)
Halobenzoquinones	158 $\pm$ 100 $\text{ng L}^{-1}$	hot tubes	4 pools, 35° C, , free chlorine 1.34 - 1.72 $\text{mg L}^{-1}$ , DOC 8.1 - 10.7 $\text{mg C L}^{-1}$	Wang et al. (2013)
<i>N</i> -Nitrosodimethylamine	5.3 $\text{ng L}^{-1}$	outdoor pools	6 pools, median value, ~24° C	Walse et al. (2008)
<i>N</i> -Nitrosodimethylamine	32 $\text{ng L}^{-1}$	indoor pools	8 pools, median value, ~24° C	Walse et al. (2008)
<i>N</i> -Nitrosodimethylamine	n.d. - 46 $\text{ng L}^{-1}$	indoor pools	4 pools	Lee et al. (2013)
<i>N</i> -Nitrosodimethylamine	313 $\text{ng L}^{-1}$	hot tubes	9 pools, median value, ~41° C	Walse et al. (2008)
Cyanogen bromide / chloride	~ 1 - 10 $\text{ng L}^{-1}$	indoor pools	11 pools, measured bi-weekly for 6 months, free chlorine n.d. - 7.66 $\text{mg L}^{-1}$	Weaver et al. (2009)
Dichloroacetonitrile	~ 1 - 10 $\text{ng L}^{-1}$	indoor pools	11 pools, measured bi-weekly for 6 months, free chlorine n.d. - 7.66 $\text{mg L}^{-1}$	Weaver et al. (2009)

water conditions. Concentrations for other DBPs such as nitrosamines, halobenzoquinones, cyanogen chloride and dichloroacetonitrile are in the  $\text{ng L}^{-1}$  range.

### 1.3.2. Exposure and health effects

In the last years, concerns about swimming in chlorinated pools increased together with the number of identified DBPs in pool water (Figure 1.7). Whether a DBP represents a severe health risk for swimmers and pool workers depends on the toxicity of the DBP and on the exposure (concentration, exposure time and uptake pathway).

**Bladder Cancer and Exposure to Water Disinfection By-Products through  
Ingestion, Bathing, Showering, and Swimming in Pools**

**Health risks of early swimming pool attendance**

**Drowning in Disinfection Byproducts? Assessing  
Swimming Pool Water**

**The Good, the Bad, and the Volatile:  
Can We Have Both Healthy Pools  
and Healthy People?**

**Nitrosamine Carcinogens Also Swim  
in Chlorinated Pools**

Swimming pool chlorination: a health hazard?

**New Halogenated Disinfection Byproducts in Swimming Pool Water  
and Their Permeability across Skin**

**Figure 1.7:** A selection of publication titles about DBPs in swimming pools and their adverse health effects (Villanueva et al., 2007; Zwiener et al., 2007; Schoefer et al., 2008; Walse and Mitch, 2008; Lakind et al., 2010; Richardson et al., 2010; Xiao et al., 2012).

***Exposure pathways***

There are three exposure pathways of swimmers to DBPs: (i) oral uptake (all DBPs), (ii) dermal uptake (primarily lipophilic DBPs) and (iii) inhalation (volatile DBPs). The mean water ingestion during swimming was estimated to be about 10–50 mL h<sup>-1</sup>, with children ingesting up to 100 mL h<sup>-1</sup> in extreme cases (Dufour et al., 2006; Dorevitch et al., 2011). This shows that the weekly oral water uptake during swimming is much lower than for drinking water. Therefore, it is also assumed that this exposure pathway is of minor importance even though it is the only pathway for hydrophilic DBPs.

Dermal uptake and inhalation are relevant exposure pathways for various DBPs. The volatile trichloramine causes severe health effects (inflammation of the respiratory tract, asthma) after inhalation, while dermal uptake results in skin and eye irritations (Bernard et al., 2003; Parrat et al., 2012). For trihalomethanes (THMs), data about the main exposure pathway of swimmers are inconsistent. Aiking et al. (1994) and Aggazotti et al. (1990) measured THMs in swimmer's blood and suggested that the main uptake was via inhalation while Beech (1980) and Lindstrom et al. (1997) assumed dermal uptake to be the main exposure pathway. Erdinger et al. (2004) concluded that THMs in swimmer's blood resulted to 30% from the uptake via the skin and the rest stemmed from inhalation. Recently, Xiao et al. (2012) found halogenated phenols in swimming pool water and showed their permeation across the skin.

Basically, volatile DBPs which have a relatively high vapour pressure (>10 Pa, e.g. trichloramine and trihalomethane) are favourable for uptake via inhalation. The vapour pressure ( $p_i^*$  (Pa)) of a compound can be estimated from its Henry's law constant ( $K_{iH}$  (Pa M<sup>-1</sup>)) and its aqueous solubility ( $C_{iw}^{sat}$  (M)) according to equation 1.6 (Schwarzenbach et al., 2005). The air-

water partitioning of a substance is named as the “dimensionless” Henry constant ( $K_{iaw}$ ) and is defined by the Henry’s law constant ( $K_{iH}$ ), the universal gas constant ( $R$  ( $J K^{-1} mol^{-1}$ )) and the temperature ( $T$  ( $K^{-1}$ )) (eq. 1.7). The Henry constant ( $K_{iaw}$ ) is equal to the molar concentration of a substance in air ( $mol m^{-3}$ ) divided by the molar concentration in water ( $mol L^{-1}$ ). This air-water partitioning strongly depends on the polarity of a substance.

$$K_{iH} \cong \frac{p_i^*}{C_{iw}^{sat}} \quad (1.6)$$

$$K_{iaw} = \frac{K_{iH}}{R \times T} \quad (1.7)$$

The volatile trichloramine and chloroform have Henry constants  $K_{iaw}$  of about 435 and 124, respectively (Holzwarth et al., 1984; Nicholson et al., 1984). Aggazzotti et al. (1990) measured chloroform concentrations in the water and in the air of 3 indoor swimming pools during 18 sampling session (Table 1.5). In addition, they measured the chloroform concentration in the blood plasma of totally 127 visitors of the indoor pools. From these measurements, it can be calculated how close the ratios  $C_{air} / C_{water}$  and  $C_{air} / C_{blood}$  are to the Henry constant of chloroform. Since the ratio  $C_{air} / C_{water}$  is  $6.4 \pm 3.2$  and hence much smaller than the Henry constant of 124, it can be concluded that the air concentration is clearly below the equilibrium concentration. This might be due to the air ventilation of the indoor pools and the slow exchange of chloroform between the pool water with the indoor air. The same was also suggested for trichloramine (Schmalz et al., 2011a). A comparison of the Henry constant (124) to the ratio  $C_{air} / C_{blood}$  ( $215 \pm 75$ ) reveals that this distribution is close to the equilibrium concentration between air and water. This suggests that there is a fast gas exchange between the ambient air and the human blood. However, the results might be interfered by the dermal uptake of chloroform since the blood samples were taken after swimming in pool water and the importance of the dermal uptake is controversially discussed in literature (see above).

Generally, the dermal uptake can roughly be approximated with the equilibrium constant between lipids and water ( $K_{ilipw}$ ). Since there is an approximative correlation between the lipid-water and the octanol-water partitioning constant ( $K_{iow}$ ) (eq. 1.8), the  $K_{iow}$  is often used as an indicator to estimate the efficiency of the dermal uptake of contaminants to the fatty compartments of the human body.

$$K_{ilipw} = 3.2 \times K_{iow}^{0.91} \quad \text{for } \log K_{iow} \leq 6 \quad (1.8)$$



**Table 1.5:** Calculation of the chloroform concentration  $C_{\text{air}} / C_{\text{water}}$  and  $C_{\text{air}} / C_{\text{blood}}$  ratios for samples measured by Aggazzotti et al (1990).

Sampling session	$C_{\text{water}}$ (nmol L <sup>-1</sup> )	$C_{\text{air}}$ (nmol m <sup>-3</sup> )	$C_{\text{blood}}^{1)}$ (nmol L <sup>-1</sup> )	Ratio $C_{\text{air}} / C_{\text{water}}$ (nmol <sub>air</sub> m <sub>air</sub> <sup>-3</sup> / nmol <sub>water</sub> L <sub>water</sub> <sup>-1</sup> )	Ratio $C_{\text{air}} / C_{\text{blood}}$ (nmol <sub>air</sub> m <sub>air</sub> <sup>-3</sup> / nmol <sub>blood</sub> L <sub>blood</sub> <sup>-1</sup> )
1	394	5445	21.5	13.8	253.3
2	360	4674	21.6	13.0	216.4
3	377	1441	8	3.8	180.1
4	293	1918	6.8	6.5	282.1
5	326	1759	13.6	5.4	129.3
6	176	662	1.8	3.8	367.8
7	201	913	5.2	4.5	175.6
8	142	880	3	6.2	293.3
9	352	1558	5.9	4.4	264.1
10	385	2304	8.1	6.0	284.4
11	209	1030	4.3	4.9	239.5
12	198	1332	5.7	6.7	233.7
13	198	553	2	2.8	276.5
14	198	2237	12.7	11.3	176.1
15	360	1365	13.4	3.8	101.9
16	218	1441	9.7	6.6	148.6
17	343	1122	13.9	3.3	80.7
18	209	1572	9.4	7.5	167.2
Average	274.4	1789.2	9.3	6.5	193.3
stdev.	84.1	1254.3	5.7	3.1	73.2

<sup>1)</sup> average of chloroform concentration in the blood of all people measured in the sampling session (4-17 people)

This approximation is limited for large molecules with a reduced uptake due to their size (Schwarzenbach et al., 2005). Generally, apolar and weakly polar substances with a big size have high  $K_{iow}$  values. Thus, apolar substances are favourable for inhalation and dermal uptake. For this reason, the uptake of disinfection by-products with acid-base speciation is strongly affected by pH and the corresponding degree of protonation. For instance, halophenols have  $pK_a$  values around 8–10 and are therefore uncharged in circumneutral pool water, which makes them more accessible than in basic waters.

Conclusively, dermal uptake and inhalation are the main pathways for the DBP exposure of swimmers. However, exposure via inhalation depends on the DBP concentration in air, which is significantly lower for outdoor pools.

### ***Toxicity and adverse health effects***

Many of the DBPs in pool water have genotoxic and fewer also carcinogenic properties (Richardson et al., 2007; Walse and Mitch, 2008; Liviac et al., 2010; Zhang et al., 2010; Wang et al., 2013). Plewa et al. (2008) categorized the DBPs and summarized their cyto- and genotoxicity (Figure 1.8). These studies revealed that nitrogenous DBPs are more toxic than

carbonaceous ones and that the toxicity of the halogenated DBPs increases in the order  $\text{Cl} < \text{Br} < \text{I}$ . In a previous study, the toxicity of haloacetic acids on mouse embryos showed a similar trend with a toxicity of  $\text{F} < \text{Cl} < \text{Br}$  (Hunter et al., 1996). This effect is presumably related to a shift of the  $\text{pK}_a$  and the electrophilicity of the haloacetic acid depending on the substituent (Richard and Hunter, 1996). The transport and the bioavailability of haloacetic acids to cells in the embryo is increased for unionized acids. Therefore, a change in the speciation by a  $\text{pK}_a$  shift affects the toxicity. An increased electrophilicity of the haloacetic acids enhances the interactions with electron donors in the embryo cells.

To properly assess the toxicity of a DBP, it is also important to know the exposure pathway. For instance, THMs are less toxic via ingestion than via dermal absorption and inhalation due to a detoxification step in the liver (Villanueva et al., 2007).

Due to the presence of the genotoxic and carcinogenic DBPs, several publications postulate an increased or a potential risk of bladder cancer associated with swimming in chlorinated pools (Villanueva et al., 2007; Kogevinas et al., 2010; Lakind et al., 2010; Wang et al., 2013). A bioanalytical study with Australian pool water, which has commonly rather high DBP concentrations, revealed that there was no adverse health effect caused by the hydrophilic DBPs although there was a high concentration of haloacetic acids ( $\leq 2600 \mu\text{g L}^{-1}$ ) in the pool water (Yeh et al., 2014). Adverse health effects of swimming such as eye and skin irritation, inflammation of the respiratory tract and asthma are related to the volatile trichloramine (Bernard et al., 2003; Parrat et al., 2012). Although it was shown that trichloramine irritates lung cells, it is discussed controversially in literature whether trichloramine concentrations found in indoor pools cause asthma to swimmers and employees of the pool facility (Massin et al., 1998; Jacobs et al., 2007; Goodman and Hays, 2008; Bernard et al., 2009; Uyan et al., 2009; Weisel et al., 2009; Font-Ribera et al., 2011; Schmalz et al., 2011b). Especially the practice of infantile swimming and early pool attendance is questioned and judged as a health risk (Bernard et al., 2007; Schoefer et al., 2008; Voisin et al., 2010).

In conclusion, there are many substances in swimming pool that are known to be carcinogenic but there are only few epidemiological studies to confirm a correlation of regular swimming pool attendance with bladder cancer. Furthermore, toxicological data is missing for many potentially carcinogenic substances found in pool water (Bull et al., 2011). With regard to respiratory diseases, many studies suggest that pool attendance, especially at an early age, increases the risk of bronchiolitis or asthma and causes acute inflammations of the respiratory tract.

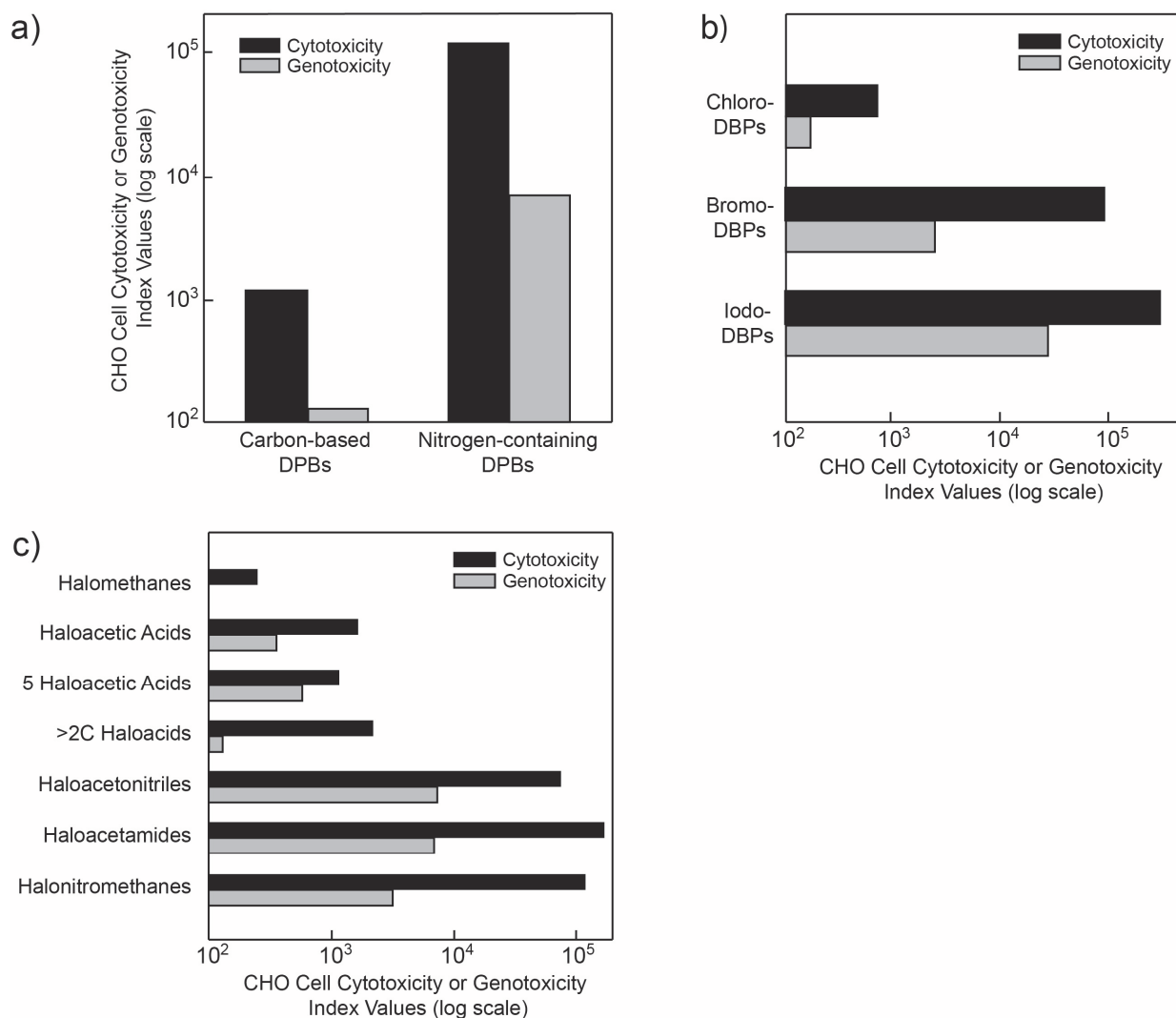


**Figure 1.8:** Cyto- and genotoxicity for (a) carbonaceous and nitrogenous DBPs, (b) halogenated DBPs (Cl-, Br-, I-) and (c) various classes of DBPs (from Plewa et al. (2008)). The CHO cell cytotoxicity and genotoxicity index values are derived from *in vitro* cellular toxicological assays with the Chinese hamster ovary (CHO) by measuring the reduction in cell density as a function of DBP concentration over 72 hours and the genomic DNA damage, respectively.

## **1.4 Disinfection by-product mitigation strategies**

Strategies to mitigate disinfection by-products are numerous, but the mitigation of a specific DBP often results in the formation of other DBPs, in an increased microbiological risk or in a loss of comfort for the swimmer. The most common mitigation strategies are discussed in the following sections.

### ***Natural swimming pool***

Instead of treating the pool water with a sand or multilayer filter, pool water is conducted to an artificial pond nearby where it seeps away. Similar to riverbank filtration, the water is pumped into the pool again from the aquifer below the pond. The removal of the viruses and bacteria occurs during the soil passage and no disinfection with a chemical oxidant is performed in the whole circulation system. Conclusively, there is no risk of forming disinfection by-products. The negative aspect of this treatment system is that a high water flow through the swimming pool is required to control the microbiological risk. As a consequence, a large surface is needed for the seepage, which makes the realisation of natural swimming pools costly. Once the dimensioning of the swimming pool and the pond is done, the water flow cannot be increased anymore. Therefore, it is difficult to react on an extreme microbiological contamination during an intense use of the pool or an accidental contamination.

### ***Fresh water addition***

The dilution of the DBPs by fresh water addition is inefficient for substances with a fast degradation since even with a strong increase of the fresh water addition, the dilution of the pool water still remains a slow process in comparison to the degradation. Therefore, the fresh water addition hardly affects the concentration of such substances. However, the concentrations of stable DBPs might be significantly reduced by an increased addition of fresh water but this costs water and energy (in heated pools).

### ***Temperature reduction***

Higher temperatures reduce the stability of free chlorine. This negative effect on the disinfection is compensated by an increased disinfection efficiency of free chlorine at higher temperatures. Hence, higher temperatures do not necessarily require higher free chlorine concentrations. In line with the reduced free chlorine stability at high temperatures, the DBP formation and degradation rates of DBPs change with temperature. Measurements of various DBPs revealed that DBP concentrations in pool waters increased with temperature leading to higher DBP levels in hot tubs > indoor pools > outdoor pools for the same precursor and oxidant concentration (Walse and Mitch, 2008; Simard et al., 2013; Wang et al., 2013).

### Variation of pH

As mentioned in section 1.3.2, the exposure to DBPs can change with pH since the degree of protonation may influence the charge of DBPs. The pH may also affect the DBP concentration by changing the speciation of free chlorine and the precursors as well as by accelerating acid-base-catalysed reactions. DBPs are commonly formed by electrophilic substitution or electron-transfer reactions of an electron-rich precursor with HOCl. As shown in Figure 1.2, the HOCl concentration decreases with increasing pH ( $pK_a(\text{HOCl}, 25^\circ\text{C}) = 7.54$ ). At the same time, the concentration of deprotonated precursors, which have higher electron density than the protonated ones, increase with increasing pH. Most precursors (e.g. ammonia, creatinine, histidine and phenolic compounds) have  $pK_a$  values of 9–11 and mainly their deprotonated form reacts with HOCl. Therefore, the reactions of precursors with free chlorine have commonly the highest apparent rate constant at a pH of  $\sim 8.75$  (Figure 1.9). To estimate the effect of pH on the DBP concentration, not only its effect on the rate of formation but also on the DBP stability must be considered.

Under pool water conditions, trihalomethane concentrations increase with increasing pH, while the opposite is the case for trichloramine, dichloroacetonitrile and the nitrosamine precursor dichloramine (Soulard et al., 1981; Hansen et al., 2012; Hansen et al., 2013a). Evaluating the optimal pH in terms of DBP mitigation, it should also be kept in mind that free chlorine loses its disinfection capacity if it is deprotonated (section 1.2.1).

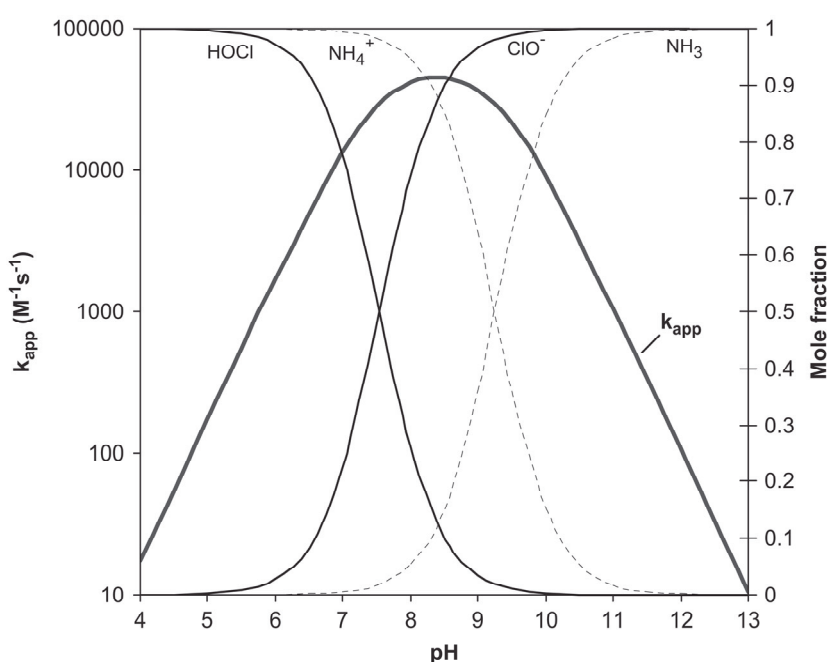


**Figure 1.9:** Example for the pH-dependence of the apparent second order rate constant ( $k_{\text{app}}$ ) due to the speciation of free chlorine and de-/protonation of the precursor ( $\text{NH}_4^+/\text{NH}_3$ ) (from Deborde and von Gunten (2008)).

### ***Precursor reduction by improved hygiene***

The impact of a bather on the precursor concentration in pool water can be analysed by the initial bather load, when the bather is entering the pool, and the continuous bather load during his activity in the pool (sweat, saliva, skin particles, ...). Showering for about 0.5–1 minute can significantly reduce the initial chemical and microbiological bather load (Keuten et al., 2012). The reduction of the chemical precursors by an improved hygiene of the pool visitors reduces nitrogen-containing precursors from the bather load. The mainly carbonaceous DBPs formed from the filling water cannot be mitigated by an enhanced hygiene.

### ***Selection and concentration of the oxidant***

The replacement of chlorine-based by bromine-based disinfectants results in an enhanced formation of brominated DBPs. This is not favourable since they are generally more toxic on a molar basis (Figure 1.6). By choosing between chlorine gas, hypochlorite or chlorine dioxide, the safety during the pool water treatment and for personnel must also be considered besides the DBP formation. Therefore, chlorine gas is not used anymore in swimming pools of the new generation. Generally, the dose of the disinfectant should be as low as possible to guarantee disinfection with minimal DBP formation.

### ***Ozonation***

The enhancement of pool water treatment with ozonation improves the disinfection and oxidizes potential DBP precursors and DBPs. Ozonation is commonly combined with biofiltration (e.g. sand filtration) to remove the biologically easily accessible reaction products of ozonation. This prevents the formation of new DBPs during post-chlorination. However, ozonation is known to form DBPs such as bromate and nitrosamines under certain conditions (von Gunten and Hoigne, 1994; Nawrocki and Andrzejewski, 2011; von Sonntag and von Gunten, 2012). Lee et al. (2010) found that the concentration of trihalomethanes, haloacetic acids, haloacetonitrile and chloral hydrate are significantly lower in pools with ozonation/chlorination in comparison to pools with only chlorination.

### ***UV irradiation***

Hansen et al. (2013b) assume that UV irradiation of pool water with a medium-pressure lamp mitigates significantly trichloronitromethane, chloral hydrate and bromine-containing haloacetonitriles and trihalomethanes. While UV irradiation is also known to photolyse other DBPs such as inorganic chloramines and nitrosamines in pure solutions, the effect of UV treatment in pool water has been studied scarcely (Li and Blatchley, 2009; De Laat et al., 2010; Nawrocki and Andrzejewski, 2011). The concentration of inorganic chloramines is assumed to

decrease with UV treatment, however, no such effect was observed for trichloramine (Gérardin et al., 2005; Cassan et al., 2006; Kristensen et al., 2009). A comparison of few pools showed that UV treatment of indoor pool water reduced its cytotoxicity and genotoxicity (Liviak et al., 2010; Plewa et al., 2011). However, several studies showed that UV treatment of humic substances at high UV doses can promote the formation of DBPs such as chloropicrin, chloroform, cyanogen chloride, dichloroacetonitril and haloacetic acid for the combination UV treatment/chlorination in comparison with chlorination alone (Liu et al., 2006; Shah et al., 2011; Weng et al., 2012; Weng and Blatchley, 2013; Cimetiere and De Laat, 2014).

## 1.5 Trichloramine in pool water and its mitigation by UV treatment

In the last 10–15 years, concerns about adverse health effects of trichloramine in indoor swimming pools increased (section 1.3.2). The hazardous effects of trichloramine and therefore also the limit value in Switzerland ( $0.2 \text{ mg m}^{-3}$ ) are related to its concentration in air (SIA, 2013). The trichloramine concentration in water is also important because pool water is the trichloramine source and reservoir, which allow for trichloramine mitigation. In spite of the need for an appropriate analytical method for trichloramine measurement in pool water, only a few methods are available. The few measurements of trichloramine in pool water show that its concentration is usually in the range of  $0.05\text{--}1 \text{ }\mu\text{M}$  (section 1.3.1). Trichloramine has been measured with a colorimetric method (based on *N,N*-dipropyl-*p*-phenylene-diamine (DPD)) (APHA, 2005). However, this method is often not sensitive enough for low trichloramine concentrations and suffers from interferences by other organic and inorganic chloramines (Shang and Blatchley, 1999). A more sophisticated, but costly method to measure trichloramine is membrane inlet mass spectrometry (MIMS). The lack of an appropriate analytic method hampers not only the regular measurement of trichloramine in pool water but also the investigation of mitigation strategies.

Nevertheless, some studies investigated options to decrease the trichloramine concentration in pool water such as by changing the pH of the pool water, introducing a stripping step or a UV irradiation in the treatment (Gérardin et al., 2005; Gérardin and Hery, 2005; Li and Blatchley, 2009; Hansen et al., 2012). UV treatment seems to be a promising option since trichloramine is sensitive to UV light and undergoes efficient photolysis (Li and Blatchley, 2009). However, measurements in pool facilities could not confirm the efficiency of this process (Gérardin et al., 2005).



## 1.6 Thesis outline

This doctoral thesis, funded by the Swiss Federal Office of Public Health (FOPH), aims to establish an accurate, low cost trichloramine measurement method and to investigate the occurrence of trichloramine in Swiss pool waters. Furthermore, UV treatment, the most used trichloramine mitigation strategy, was studied for its efficiency and for its risk of promoting the formation of other DBPs. The results and conclusions of this thesis are given in chapters 2–7.

**Chapter 1** gives a general overview of pool water treatment and its associated risks for disinfection by-product formation. Further, the consequential adverse health effects are discussed.

**Chapter 2** provides general kinetic data about trichloramine reactivity with model compounds and its dependence on pH and temperature. A comparison with the reactivity of free chlorine allows assumptions about the fate of trichloramine in pool water. Measurements of reaction products elucidate reaction mechanisms and allow an assessment of the potential of trichloramine to form DBPs such as chloroform.

**Chapter 3** presents software that was engineered in the frame of this thesis to generate and analyse data with membrane introduction mass spectrometry (MIMS). The software facilitates the automation of on-site sampling for long-term campaigns. It further helps to treat and analyse efficiently large data sets by performing automated peak identification and analysis.

**Chapter 4** introduces a low cost analytical method for trichloramine measurement, which is easily to apply and accurate for measurements in pool water. The method is validated by a comparison with MIMS. A survey of pool water samples showed the range of trichloramine concentrations in Swiss pool waters and the dependence of trichloramine concentration on various pool water parameters (free and combined chlorine concentrations, pH and urea concentration). On-site measurements were performed to further investigate these dependencies.

**Chapter 5** gives information on UV treatment of chloramines (especially trichloramine) with low- and medium-pressure lamps. The effect of UV irradiation on chloramines and particularly on trichloramine in pool water matrices was investigated. Measurements were conducted in a pool facility to assess the efficiency of trichloramine elimination with UV treatment and its effect on the trichloramine concentration in pool water.

**Chapter 6** focuses on the ambiguous effect of UV treatment on the *N*-nitrosodimethylamine concentration in pool water. On the one hand, UV is known to photodegrade nitrosamines

efficiently. On the other hand, it is shown in chapter 6 that UV irradiation of pool water can enhance the *N*-nitrosamine formation due to the increased formation of *N*-nitrosamine precursors. This highlights the complexity to assess the impact of UV treatment on pool water quality.

**Chapter 7** contains the final conclusions about the trichloramine problem in pool water with regard to its monitoring options, its concentrations in pool water, the factors affecting its concentration and potential mitigation strategies. Furthermore, it presents the options and limitations of pool water treatment with UV irradiation.

---

## References

- Aggazzotti, G., G. Fantuzzi, P. L. Tartoni and G. Predieri (1990). "Plasma Chloroform Concentrations in Swimmers Using Indoor Swimming Pools." *Archives of Environmental Health: An International Journal* 45(3): 175-179.
- Aiking, H., M. B. van Ackert, R. J. P. M. Schölten, J. F. Feenstra and H. A. Valkenburg (1994). "Swimming pool chlorination: a health hazard?" *Toxicology Letters* 72(1-3): 375-380.
- American Public Health Association (APHA) (2005). "Standard methods for the examination of water & wastewater."
- Beech, J. A. (1980). "Estimated worst case trihalomethane body burden of a child using a swimming pool." *Medical Hypotheses* 6(3): 303-307.
- Bernard, A., S. Carbonnelle, X. Dumont and M. Nickmilder (2007). "Infant swimming practice, pulmonary epithelium integrity, and the risk of allergic and respiratory diseases later in childhood." *Pediatrics* 119(6): 1095-1103.
- Bernard, A., S. Carbonnelle, O. Michel, S. Higuët, C. de Burbure, J. P. Buchet, C. Hermans, X. Dumont and I. Doyle (2003). "Lung hyperpermeability and asthma prevalence in schoolchildren: unexpected associations with the attendance at indoor chlorinated swimming pools." *Occupational and Environmental Medicine* 60(6): 385-394.
- Bernard, A., M. Nickmilder, C. Voisin and A. Sardella (2009). "Impact of chlorinated swimming pool attendance on the respiratory health of adolescents." *Pediatrics* 124(4): 1110-1118.
- Bessonneau, V., M. Derbez, M. Clément and O. Thomas (2011). "Determinants of chlorination by-products in indoor swimming pools." *International Journal of Hygiene and Environmental Health* 215(1): 76-85.
- Blatchley, E. R. and M. Cheng (2010). "Reaction Mechanism for Chlorination of Urea." *Environmental Science & Technology* 44(22): 8529-8534.
- Borgmann-Strahsen, R. (2003). "Comparative assessment of different biocides in swimming pool water." *International biodeterioration & biodegradation* 51(4): 291-297.
- Boyce, S. D. and J. F. Hornig (1983). "Reaction pathways of trihalomethane formation from the halogenation of dihydroxyaromatic model compounds for humic acid." *Environmental Science & Technology* 17(4): 202-211.
- Bull, R. J., D. A. Reckhow, X. Li, A. R. Humpage, C. Joll and S. E. Hrudey (2011). "Potential carcinogenic hazards of non-regulated disinfection by-products: Haloquinones, halo-cyclopentene and cyclohexene derivatives, N-halamines, halonitriles, and heterocyclic amines." *Toxicology* 286(1-3): 1-19.
- Cassan, D., B. Mercier, F. Castex and A. Rambaud (2006). "Effects of medium-pressure UV lamps radiation on water quality in a chlorinated indoor swimming pool." *Chemosphere* 62(9): 1507-1513.
- Chowdhury, S., K. Alhooshani and T. Karanfil (2014). "Disinfection byproducts in swimming pool: Occurrences, implications and future needs." *Water Research* 53(0): 68-109.
- Cimetiere, N. and J. De Laat (2014). "Effects of UV-dechloramination of swimming pool water on the formation of disinfection by-products: A lab-scale study." *Microchemical Journal* 112(0): 34-41.

De Laat, J., N. Boudiaf and F. Dossier-Berne (2010). "Effect of dissolved oxygen on the photodecomposition of monochloramine and dichloramine in aqueous solution by UV irradiation at 253.7 nm." *Water Research* 44(10): 3261-3269.

Deborde, M. and U. von Gunten (2008). "Reactions of chlorine with inorganic and organic compounds during water treatment--Kinetics and mechanisms: A critical review." *Water Research* 42(1-2): 13-51.

Donnermair, M. M. and E. R. Blatchley (2003). "Disinfection efficacy of organic chloramines." *Water Research* 37(7): 1557-1570.

Dorevitch, S., S. Panthi, Y. Huang, H. Li, A. M. Michalek, P. Pratap, M. Wroblewski, L. Liu, P. A. Scheff and A. Li (2011). "Water ingestion during water recreation." *Water Research* 45(5): 2020-2028.

Dufour, A., O. Evans, T. Behymer and R. Cantu (2006). "Water ingestion during swimming activities in a pool: a pilot study." *J Water Health* 4: 425-430.

Encyclopaedia Britannica. Academic Edition Retrieved 29.05.2014, from <http://www.britannica.com/EBchecked/topic/577062/swimming?anchor=ref8786>.

Erdinger, L., K. P. Kühn, F. Kirsch, R. Feldhues, T. Fröbel, B. Nohynek and T. Gabrio (2004). "Pathways of trihalomethane uptake in swimming pools." *International Journal of Hygiene and Environmental Health* 207(6): 571-575.

Fischer, J. (2005). *Schwimmen und Schwimmen lernen gestern und heute - Historische Entwicklungen und aktuelle Konzeptionen*, Pädagogische Hochschule Weingarten.

Font-Ribera, L., C. M. Villanueva, M. J. Nieuwenhuijsen, J. P. Zock, M. Kogevinas and J. Henderson (2011). "Swimming Pool Attendance, Asthma, Allergies, and Lung Function in the Avon Longitudinal Study of Parents and Children Cohort." *American Journal of Respiratory and Critical Care Medicine* 183(5): 582-588.

Gérardin, F., G. Hecht, G. Huber-Pelle and I. Subra (2005). "Traitement UV: Suivi de l'évolution des concentrations en chlorforme et en trichlorure d'azote dans les eaux de baignade d'un centre aquatique." *Hygiène et sécurité du travail - Cahiers de notes documentaires* 201: 19-30.

Gérardin, F. and M. Hery (2005). *Effects of nitrogen trichloride stripping on air quality in indoor swimming pools*. Budapest.

Goeres, D., T. Palys, B. Sandel and J. Geiger (2004). "Evaluation of disinfectant efficacy against biofilm and suspended bacteria in a laboratory swimming pool model." *Water research* 38(13): 3103-3109.

Goodman, M. and S. Hays (2008). "Asthma and Swimming: A Meta-Analysis." *Journal of Asthma* 45(8): 639-647.

Gray, H. F. (1940). "Sewerage in Ancient and Mediaeval Times." *Sewage Works Journal* 12(5): 939-946.

Hansen, K. M., H.-J. Albrechtsen and H. R. Andersen (2013a). "Optimal pH in chlorinated swimming pools--balancing formation of by-products." *Journal of water and health* 11(3): 465-472.

Hansen, K. M. S., S. Willach, M. G. Antoniou, H. Mosbaek, H. J. Albrechtsen and H. R. Andersen (2012). "Effect of pH on the formation of disinfection byproducts in swimming pool water - Is less THM better?" *Water Research* 46(19): 6399-6409.

Hansen, K. M. S., R. Zortea, A. Piketty, S. R. Vega and H. R. Andersen (2013b). "Photolytic removal of DBPs by Medium pressure UV in swimming pool water." *Science of the Total Environment* 443: 850-856.

- Hijnen, W. A. M., E. F. Beerendonk and G. J. Medema (2006). "Inactivation credit of UV radiation for viruses, bacteria and protozoan (oo)cysts in water: A review." *Water Research* 40(1): 3-22.
- Holzwarth, G., R. G. Balmer and L. Soni (1984). "The fate of chlorine and chloramines in cooling-towers - Henrys law constants for flashoff." *Water Research* 18(11): 1421-1427.
- Hunter, E. S., E. H. Rogers, J. E. Schmid and A. Richard (1996). "Comparative effects of haloacetic acids in whole embryo culture." *Teratology* 54(2): 57-64.
- Jacobs, J. H., S. Spaan, G. van Rooy, C. Meliefste, V. A. C. Zaat, J. M. Rooyackers and D. Heederik (2007). "Exposure to trichloramine and respiratory symptoms in indoor swimming pool workers." *European Respiratory Journal* 29(4): 690-698.
- Jolley, R. L., W. Brungs, J. Cotruvo, R. Cumming, J. Mattice and V. Jacobs (1983). "Water chlorination: environmental impact and health effects. Volume 4, Book 1. Chemistry and water treatment."
- Judd, S. J. and G. Bullock (2003). "The fate of chlorine and organic materials in swimming pools." *Chemosphere* 51(9): 869-879.
- Kanan, A. and T. Karanfil (2011). "Formation of disinfection by-products in indoor swimming pool water: The contribution from filling water natural organic matter and swimmer body fluids." *Water Research* 45(2): 926-932.
- Keuten, M. G. A., F. M. Schets, J. F. Schijven, J. Q. J. C. Verberk and J. C. van Dijk (2012). "Definition and quantification of initial anthropogenic pollutant release in swimming pools." *Water Research* 46(11): 3682-3692.
- Kim, H., J. Shim and S. Lee (2002). "Formation of disinfection by-products in chlorinated swimming pool water." *Chemosphere* 46(1): 123-130.
- Kogevinas, M., C. M. Villanueva, L. Font-Ribera, D. Liviac, M. Bustamante, F. Espinoza, M. J. Nieuwenhuijsen, A. Espinosa, P. Fernandez and D. M. DeMarini (2010). "Genotoxic effects in swimmers exposed to disinfection by-products in indoor swimming pools." *Environmental health perspectives* 118(11): 1531.
- Krasner, S. W., W. A. Mitch, D. L. McCurry, D. Hanigan and P. Westerhoff (2013). "Formation, precursors, control, and occurrence of nitrosamines in drinking water: A review." *Water research* 47(13): 4433-4450.
- Krasner, S. W., H. S. Weinberg, S. D. Richardson, S. J. Pastor, R. Chinn, M. J. Scilimenti, G. D. Onstad and A. D. Thruston (2006). "Occurrence of a New Generation of Disinfection Byproducts." *Environmental Science & Technology* 40(23): 7175-7185.
- Kristensen, G. H., M. M. Klausen, H. R. Andersen, L. Erdinger, F. Lauritsen, E. Arvin and H. J. Albrechtsen (2009). Full scale test of UV-based water treatment technologies at Gladsaxe Sport Centre—with and without advanced oxidation mechanisms. *Swimming Pool and Spa International Conference*.
- Lakind, J. S., S. D. Richardson and B. C. Blount (2010). "The Good, the Bad, and the Volatile: Can We Have Both Healthy Pools and Healthy People?" *Environmental Science & Technology* 44(9): 3205-3210.
- LeChevallier, M. W., C. D. Cawthon and R. G. Lee (1988). "Factors promoting survival of bacteria in chlorinated water supplies." *Applied and Environmental Microbiology* 54(3): 649-654.
- Lee, J., M.-J. Jun, M.-H. Lee, M.-H. Lee, S.-W. Eom and K.-D. Zoh (2010). "Production of various disinfection byproducts in indoor swimming pool waters treated with different disinfection methods." *International Journal of Hygiene and Environmental Health* 213(6): 465-474.

Lee, M., Y. Lee, F. Soltermann and U. von Gunten (2013). "Analysis of *N*-nitrosamines and other nitro (so) compounds in water by high-performance liquid chromatography with post-column UV photolysis/Griess reaction." *Water research* 47(14): 4893-4903.

Li, J. and E. R. Blatchley (2009). "UV Photodegradation of Inorganic Chloramines." *Environmental Science & Technology* 43(1): 60-65.

Lindstrom, A. B., J. D. Pleil and D. C. Berkoff (1997). "Alveolar breath sampling and analysis to assess trihalomethane exposures during competitive swimming training." *Environmental Health Perspectives* 105(6): 636-642.

Liu, W., L. M. Cheung, X. Yang and C. Shang (2006). "THM, HAA and CNCl formation from UV irradiation and chlor(am)ination of selected organic waters." *Water Research* 40(10): 2033-2043.

Liviac, D., E. D. Wagner, W. A. Mitch, M. J. Altonji and M. J. Plewa (2010). "Genotoxicity of Water Concentrates from Recreational Pools after Various Disinfection Methods." *Environmental Science & Technology* 44(9): 3527-3532.

Massin, N., A. B. Bohadana, P. Wild, M. Hery, J. Toamain and G. Hubert (1998). "Respiratory symptoms and bronchial responsiveness in lifeguards exposed to nitrogen trichloride in indoor swimming pools." *Occupational and Environmental Medicine* 55(4): 258-263.

Mitch, W. A. and D. L. Sedlak (2002). "Formation of *N*-nitrosodimethylamine (NDMA) from dimethylamine during chlorination." *Environmental Science & Technology* 36(4): 588-595.

Morris, J. C. (1966). "Acid ionization constant of HOCl from 5 to 35 degrees." *Journal of Physical Chemistry* 70(12): 3798-&.

Nawrocki, J. and P. Andrzejewski (2011). "Nitrosamines and water." *Journal of Hazardous Materials* 189(1-2): 1-18.

Nicholson, B., B. P. Maguire and D. B. Bursill (1984). "Henry's law constants for the trihalomethanes: effects of water composition and temperature." *Environmental Science & Technology* 18(7): 518-521.

Parrat, J., G. Donze, C. Iseli, D. Perret, C. Tomicic and O. Schenk (2012). "Assessment of Occupational and Public Exposure to Trichloramine in Swiss Indoor Swimming Pools: A Proposal for an Occupational Exposure Limit." *Annals of Occupational Hygiene* 56(3): 264-277.

Plewa, M. J., E. D. Wagner and W. A. Mitch (2011). "Comparative Mammalian Cell Cytotoxicity of Water Concentrates from Disinfected Recreational Pools." *Environmental Science & Technology* 45(9): 4159-4165.

Plewa, M. J., E. D. Wagner, M. G. Muellner, K.-M. Hsu and S. D. Richardson (2008). "Comparative mammalian cell toxicity of *N*-DBPs and *C*-DBPs." *Urbana* 51: 61801.

Richard, A. M. and E. S. Hunter (1996). "Quantitative structure-activity relationships for the developmental toxicity of haloacetic acids in mammalian whole embryo culture." *Teratology* 53(6): 352-360.

Richardson, S. D., D. M. DeMarini, M. Kogevinas, P. Fernandez, E. Marco, C. Lourencetti, C. Balleste, D. Heederik, K. Meliefste, A. B. McKague, R. Marcos, L. Font-Ribera, J. O. Grimalt and C. M. Villanueva (2010). "What's in the Pool? A Comprehensive Identification of Disinfection By-products and Assessment of Mutagenicity of Chlorinated and Brominated Swimming Pool Water." *Environmental Health Perspectives* 118(11): 1523-1530.

- Richardson, S. D., M. J. Plewa, E. D. Wagner, R. Schoeny and D. M. DeMarini (2007). "Occurrence, genotoxicity, and carcinogenicity of regulated and emerging disinfection by-products in drinking water: a review and roadmap for research." *Mutation Research/Reviews in Mutation Research* 636(1): 178-242.
- Richardson, S. D. and C. Postigo (2012). *Drinking water disinfection by-products. Emerging Organic Contaminants and Human Health*, Springer: 93-137.
- Schmalz, C., F. H. Frimmel and C. Zwiener (2011a). "Trichloramine in swimming pools - Formation and mass transfer." *Water Research* 45(8): 2681-2690.
- Schmalz, C., H. Wunderlich, R. Heinze, F. Frimmel, C. Zwiener and T. Grummt (2011b). "Application of an optimized system for the well-defined exposure of human lung cells to trichloramine and indoor pool air." *Journal of water and health* 9(3): 586-596.
- Schoefer, Y., A. Zutavern, I. Brockow, T. Schäfer, U. Krämer, B. Schaaf, O. Herbarth, A. von Berg, H. E. Wichmann and J. Heinrich (2008). "Health risks of early swimming pool attendance." *International Journal of Hygiene and Environmental Health* 211(3-4): 367-373.
- Schreiber, I. M. and W. A. Mitch (2006). "Nitrosamine Formation Pathway Revisited: The Importance of Chloramine Speciation and Dissolved Oxygen." *Environmental Science & Technology* 40(19): 6007-6014.
- Schwarzenbach, R. P., P. M. Gschwend and D. M. Imboden (2005). *Environmental organic chemistry*, John Wiley & Sons.
- Shah, A. D., A. D. Dotson, K. G. Linden and W. A. Mitch (2011). "Impact of UV Disinfection Combined with Chlorination/Chloramination on the Formation of Halonitromethanes and Haloacetonitriles in Drinking Water." *Environmental Science & Technology* 45(8): 3657-3664.
- Shah, A. D. and W. A. Mitch (2011). "Halonitroalkanes, halonitriles, haloamides, and N-nitrosamines: a critical review of nitrogenous disinfection byproduct formation pathways." *Environmental science & technology* 46(1): 119-131.
- Shang, C. and E. R. Blatchley (1999). "Differentiation and quantification of free chlorine and inorganic chloramines in aqueous solution by MIMS." *Environmental Science & Technology* 33(13): 2218-2223.
- Swiss society of engineers and architects (SIA) (2013). "Water and water treatment in public pools (German)."
- Simard, S., R. Tardif and M. J. Rodriguez (2013). "Variability of chlorination by-product occurrence in water of indoor and outdoor swimming pools." *Water Research* 47(5): 1763-1772.
- Singer, M. (1990). "The role of antimicrobial agents in swimming pools." *International Biodeterioration* 26(2-4): 159-168.
- Soltermann, F., M. Lee, S. Canonica and U. von Gunten (2013). "Enhanced N-nitrosamine formation in pool water by UV irradiation of chlorinated secondary amines in the presence of monochloramine." *Water Research* 47(1): 79-90.
- Soulard, M., F. Bloc and A. Hatterer (1981). "Diagrams of existence of chloramines and bromamines in aqueous solution." *Journal of the Chemical Society, Dalton Transactions*(12): 2300-2310.
- Uyan, Z. S., S. Carraro, G. Piacentini and E. Baraldi (2009). "Swimming pool, respiratory health, and childhood asthma: Should we change our beliefs?" *Pediatric Pulmonology* 44(1): 31-37.
- Villanueva, C. M., K. P. Cantor, J. O. Grimalt, N. Malats, D. Silverman, A. Tardon, R. Garcia-Closas, C. Serra, A. Carrato, G. Castaño-Vinyals, R. Marcos, N. Rothman, F. X. Real, M. Dosemeci and

M. Kogevinas (2007). "Bladder Cancer and Exposure to Water Disinfection By-Products through Ingestion, Bathing, Showering, and Swimming in Pools." *American Journal of Epidemiology* 165(2): 148-156.

Voisin, C., A. Sardella, F. Marcucci and A. Bernard (2010). "Infant swimming in chlorinated pools and the risks of bronchiolitis, asthma and allergy." *European Respiratory Journal* 36(1): 41-47.

von Gunten, U. and J. Hoigne (1994). "Bromate Formation during Ozonization of Bromide-Containing Waters: Interaction of Ozone and Hydroxyl Radical Reactions." *Environmental Science & Technology* 28(7): 1234-1242.

von Sonntag, C. and U. von Gunten (2012). *Chemistry of Ozone in Water and Wastewater Treatment*, IWA Publishing.

Walse, S. S. and W. A. Mitch (2008). "Nitrosamine carcinogens also swim in chlorinated pools." *Environmental Science & Technology* 42(4): 1032-1037.

Wang, W., Y. C. Qian, J. M. Boyd, M. H. Wu, S. E. Hrudey and X. F. Li (2013). "Halobenzoquinones in Swimming Pool Waters and Their Formation from Personal Care Products." *Environmental Science & Technology* 47(7): 3275-3282.

Weaver, W. A., J. Li, Y. L. Wen, J. Johnston, M. R. Blatchley and E. R. Blatchley (2009). "Volatile disinfection by-product analysis from chlorinated indoor swimming pools." *Water Research* 43(13): 3308-3318.

Weinberg, H. S., S. W. Krasner, S. D. Richardson and A. D. Thruston Jr (2002). The occurrence of disinfection by-products (DBPs) of health concern in drinking water: results of a nationwide DBP occurrence study, National Exposure Research Laboratory, Office of Research and Development, US Environmental Protection Agency.

Weisel, C. P., S. D. Richardson, B. Nemery, G. Aggazzotti, E. Baraldi, E. R. Blatchley III, B. C. Blount, K.-H. Carlsen, P. A. Eggleston and F. H. Frimmel (2009). "Childhood asthma and environmental exposures at swimming pools: state of the science and research recommendations." *Environmental health perspectives* 117(4): 500.

Weng, S. C. and E. R. Blatchley (2013). "Ultraviolet-Induced Effects on Chloramine and Cyanogen Chloride Formation from Chlorination of Amino Acids." *Environmental Science & Technology* 47(9): 4269-4276.

Weng, S. C., J. Li and E. R. Blatchley (2012). "Effects of UV254 irradiation on residual chlorine and DBPs in chlorination of model organic-N precursors in swimming pools." *Water Research* 46(8): 2674-2682.

White, G. C. (1986). *Handbook of chlorination*, Van Nostrand Reinhold Company.

World Health Organisation (WHO) (2006). "Guidelines for safe recreational water environments." Volume 2: Swimming pools and similar environments.

Xiao, F., X. R. Zhang, H. Y. Zhai, I. M. C. Lo, G. L. Tipoe, M. T. Yang, Y. Pan and G. H. Chen (2012). "New Halogenated Disinfection Byproducts in Swimming Pool Water and Their Permeability across Skin." *Environmental Science & Technology* 46(13): 7112-7119.

Yeh, R. Y. L., M. J. Farré, D. Stalter, J. Y. M. Tang, J. Molendijk and B. I. Escher (2014). "Bioanalytical and chemical evaluation of disinfection by-products in swimming pool water." *Water Research* 59(0): 172-184.



Zhang, S.-H., D.-Y. Miao, A.-L. Liu, L. Zhang, W. Wei, H. Xie and W.-Q. Lu (2010). "Assessment of the cytotoxicity and genotoxicity of haloacetic acids using microplate-based cytotoxicity test and CHO/HGPRT gene mutation assay." *Mutation Research/Genetic Toxicology and Environmental Mutagenesis* 703(2): 174-179.

Zwiener, C., S. D. Richardson, D. M. De Marini, T. Grummt, T. Glauner and F. H. Frimmel (2007). "Drowning in disinfection byproducts? Assessing swimming pool water." *Environmental Science & Technology* 41(2): 363-372.



# **Chapter 2**

## **Trichloramine reactions with nitrogenous and carbonaceous compounds: kinetics, products and chloroform formation**

Fabian Soltermann, Silvio Canonica and Urs von Gunten (2015)

*Water Research*, 71, 318-329

## Abstract

Trichloramine is a hazardous disinfection by-product that is of particular relevance in indoor swimming pools. To better understand its fate in pool waters, apparent second order rate constants ( $k_{app}$ ) at pH 7 for its reaction with several model compounds were determined.  $k_{app}$  values at pH 7 for nitrogenous compounds were found to increase in the following order: ammonia ~ amides ( $\sim 10^{-2}$ – $10^{-1}$  M<sup>-1</sup> s<sup>-1</sup>) < primary amines ( $\sim 10^{-1}$ – $10^0$  M<sup>-1</sup> s<sup>-1</sup>) < relevant body fluid compounds (L-histidine, creatinine) ( $\sim 10^0$ – $10^1$  M<sup>-1</sup> s<sup>-1</sup>) < secondary amines ( $\sim 10^1$ – $10^2$  M<sup>-1</sup> s<sup>-1</sup>) < trimethylamine ( $\sim 10^3$  M<sup>-1</sup> s<sup>-1</sup>).  $k_{app}$  values at pH 7 of trichloramine with hydroxylated aromatic compounds ( $\sim 10^2$ – $10^5$  M<sup>-1</sup> s<sup>-1</sup>) are higher than for the nitrogenous compounds and depend on the number and position of the hydroxyl groups (phenol < hydroquinone < catechol < resorcinol). The measurement of  $k_{app}$  as a function of pH revealed that mainly the deprotonated species react with trichloramine. The reaction of trichloramine with Suwannee River and Pony Lake fulvic acid standards showed a decrease of their reactivity upon chlorination, which can be related to the electron donating capacity and the SUVA<sub>254</sub>. Chlorinated nitrogenous compounds (e.g. uric acid) also have a reduced reactivity with trichloramine. Hence, the residual chlorine in pool water hinders a fast consumption of trichloramine. This explains why trichloramine degradation in pool water is lower than expected from the reactivity with the estimated bather input.

Trichloramine also has the potential to form secondary disinfection by-products such as chlorinated aromatic compounds or chloroform by electron transfer or Cl<sup>+</sup>-transfer reactions. The chloroform formation from the reaction of trichloramine with resorcinol occurs with a similar yield and rate as for chlorination of resorcinol. Since the trichloramine concentration in pool water is commonly about one order of magnitude lower than the free chlorine concentration, its contribution to the disinfection by-product formation is assumed to be minor in most cases but might be relevant for few precursors (e.g. phenols) that react faster with trichloramine than with free chlorine.

## 2.1 Introduction

Trichloramine is a volatile disinfection by-product (DBP), which is of concern in indoor swimming pools. In recent studies it has been suggested that the recommended guideline value of  $0.5 \text{ mg m}^{-3}$  of the World Health Organisation (WHO) for the trichloramine concentration in air might not be restrictive enough to protect swimmers and pool attendants from adverse health effects such as skin and eye irritations, inflammation of the respiratory tract or asthma (Bernard et al., 2003; WHO, 2006; Schmalz et al., 2011b; Parrat et al., 2012; Chu et al., 2013). Although health risks and regulations are related to trichloramine concentration in air, its concentration in water is of interest since pool water is the source and reservoir of trichloramine. Due to analytical challenges, only a few publications report trichloramine concentrations in pool water, which range commonly from  $0.1$  to  $0.5 \text{ }\mu\text{M}$  ( $0.02$ – $0.1 \text{ mg L}^{-1}$  as  $\text{Cl}_2$ ) (Gérardin and Subra, 2004; Weaver et al., 2009; Soltermann et al., 2014a). This is usually 2–10 % of the molar free chlorine concentration, which varies from about  $3$  to  $30 \text{ }\mu\text{M}$  ( $0.2$ – $2 \text{ mg L}^{-1}$  as  $\text{Cl}_2$ ) according to the regulatory guidelines and the actual pool operation. To prevent high trichloramine concentrations in pool water, numerous studies investigated the formation and abatement of trichloramine (Gérardin and Hery, 2005; Li and Blatchley, 2009; Blatchley and Cheng, 2010; Schmalz et al., 2011a; Soltermann et al., 2014b). Thereby, it was shown that trichloramine can be potentially formed from various precursors (e.g. urea, creatinine, histidine and uric acid), which are introduced by bathers (Schmalz et al., 2011a). However, recent studies on trichloramine concentrations in swimming pool water and in indoor swimming pool air revealed that the trichloramine concentration correlates much stronger with the free chlorine concentration than with the precursor concentration or the bather density (Chu et al., 2013; Soltermann et al., 2014a).

Free chlorine is not only an important factor for the trichloramine formation but also for the formation of other disinfection by-products (DBPs) in pool water (e.g. trihalomethanes (THM), halobenzoquinones, haloacetic acids) (Richardson et al., 2010; Wang et al., 2013). Additionally, free chlorine competes with trichloramine for reaction partners, wherefore its presence can increase trichloramine's stability (Soltermann et al., 2014b). While the free chlorine reactivity has been widely studied (Deborde and von Gunten, 2008), kinetic data for reactions of trichloramine is very scarce. Trichloramine reaction rate constants have been reported for the base-catalysed decomposition and reaction with chloramines and ammonia as well as for the reaction with anions ( $\text{Br}^-$ ,  $\text{CN}^-$ ,  $\text{SO}_3^-$ ,  $\text{I}^-$ ) (Table 2.1) (Kumar et al., 1987; Yiin and Margerum, 1990b; Yiin and Margerum, 1990a; Gazda et al., 1995; Schurter et al., 1995). The reactivity of

trichloramine with these anions correlates to the nucleophilic strength of the anions with a high sensitivity (Swain-Scott sensitivity factor ( $s$ ) = 6.6) (Gazda et al., 1995). Measurements of intermediates and reaction products suggest that a  $\text{Cl}^+$ -transfer from trichloramine to the anion is the first reaction step (Yiin and Margerum, 1990b; Gazda et al., 1995; Schurter et al., 1995).

To better understand the behaviour of trichloramine in pool water, it is crucial to investigate the reactivity of trichloramine with various compounds present in pool water. The reactivity of trichloramine is also of interest owing to the potential formation of disinfection by-products. Chlorination partially yields different disinfection by-products than chloramination (disinfection with monochloramine) while very little is known about the by-product formation from trichloramine (Sedlak and von Gunten, 2011).

In this study, the reactivity of trichloramine with various surrogate compounds was investigated to assess its stability in swimming pools and to compare its reactivity with free chlorine. The effect of temperature and pH on second order rate constants were studied for the reaction of trichloramine with selected model compounds. Furthermore, the products of the reaction of trichloramine with dimethylamine, hydroquinone and phenol were investigated to elucidate reaction pathways and assess the potential for DBP formation. Chloroform as an indicator for DBP formation was measured for the resorcinol-trichloramine reaction. Finally, the reactivity of trichloramine towards chlorinated fulvic acids was measured and its reaction with body fluid analogues was calculated to assess the fate of trichloramine in pool water.

## 2.2 Materials and Methods

### 2.2.1 Chemicals

The origin of all chemicals used in this study and the structures of the model compounds are given in the supporting information (SI, Text A.1 and Figure A.1). Suwanee River fulvic acid standard I (SRFA, 1S101F) and Pony Lake fulvic acid (PLFA, 1R109F) were obtained from the International Humic Substances Society (IHSS, St. Paul, MN). Stock solutions of mono-, di- and trichloramine were produced and quantified spectrophotometrically as described previously (Soltermann et al., 2014a). Mono- and trichloramine solutions were not stored for more than a few days while dichloramine solutions were used the same day. The hypochlorite stock solution was quantified daily photometrically ( $\epsilon_{292\text{nm}} = 350 \text{ M}^{-1} \text{ cm}^{-1}$ ) (Soulard et al., 1981). Ultrapurified water was produced by a “barnstead nanopure” system from Thermo Scientific.

### 2.2.2 Analytical methods

A Cary 100 Scan (Varian) and a Cary 100 UV-Vis (Agilent Technologies) spectrophotometer were used for absorbance measurements. Measurements of the pH were conducted with a 632 pH-meter (Metrohm), which was calibrated daily at pH 4 and 7 with standard solutions. Membrane inlet mass spectrometry (MIMS) was performed with a MIMS 2000 (Microlab, Aarhus, Denmark). The membrane temperature was controlled at 40 °C and the sample flow rate was set to  $\sim 8 \text{ mL min}^{-1}$ . The signal of the ion  $\text{N}^{35}\text{Cl}^{35}\text{Cl}^{++}$  ( $m/z = 84$ ) was used to measure trichloramine except for a few cases in which the reactant or a reaction product interfered with this ion. In such a case, the ions with lower abundance such as  $\text{N}^{35}\text{Cl}^{37}\text{Cl}^{++}$  ( $m/z = 86$ ) or  $\text{N}^{37}\text{Cl}^{37}\text{Cl}^{++}$  ( $m/z = 88$ ) were used. Trichloramine concentration was usually measured in the range of 0.1–1  $\mu\text{M}$  and in few cases of 0.02–0.2  $\mu\text{M}$ . It has been shown previously that trichloramine can be measured as low as 0.05  $\mu\text{M}$  with a standard deviation of about 5 % for signal 88  $m/z$  (Soltermann et al., 2014a). The signals 84  $m/z$  and 86  $m/z$  have a  $\sim 10$  and  $\sim 5$  times higher intensity, respectively, with a correspondingly lower quantification limit.

Phenol, mono- and dichlorophenols were measured by high performance liquid chromatography (HPLC, Ultimate 3000, Dionex) with a UV-visible diode array detector. Analyses were performed with an eluent consisting of methanol and phosphoric acid (10 mM) (ratio 40:60), a flow rate of  $0.5 \text{ mL min}^{-1}$ , a standard column (Cosmosil, 5C18-MS-II, 3.0 ID  $\times$  100 mm, Nacalai Tesque Ing.) and at a wavelength of 220 nm. The limit of quantification was 0.05  $\mu\text{M}$  for phenol and all chlorophenols with a standard deviation of about 10 %.

Total organic carbon (TOC) was measured with a Phoenix 8000 Analyzer (Tekmar-Dohrmann). Chloroform was measured by gas chromatography mass spectrometry (GC-MS) using a gas chromatograph Trace 2000 series (Thermo scientific) with a Rtx-VMS column (60 m length, 0.32 mm ID and 1.8  $\mu\text{m}$  film thickness) and a quadrupole MS (DSQ II, Thermo scientific).

### 2.2.3 Experimental procedure

#### *Kinetics of trichloramine reactions*

The trichloramine reactivity with model compounds was measured by adding trichloramine ( $\sim 1 \mu\text{M}$ ) to 1.1 L of a temperature-controlled ( $25 \pm 1 \text{ }^\circ\text{C}$ ) phosphate buffered (pH 7, 5 mM) solution. The fast reacting hydroxylated aromatic compounds were measured at pH 5 (phosphate buffer, 5 mM). The trichloramine solution was analysed with the MIMS for about 12 minutes until the trichloramine signal reached a steady-state and 1 L solution was left. Thereafter, the model compound was added in molar excess (10–75'000-fold, pseudo first order conditions), by adding 0.5–20 mL of a stock solution to the stirred trichloramine solution. The evolution of the trichloramine concentration was then continuously monitored by MIMS. The apparent second order rate constant ( $k_{\text{app}}$  ( $\text{M}^{-1} \text{ s}^{-1}$ )) at pH 7 was calculated from the observed rate constant ( $k_{\text{obs}}$  ( $\text{s}^{-1}$ )) at the corresponding concentration of the model compound ( $c_{\text{compound}}$  (M)) (eq. 2.1).

$$k_{\text{app}} = \frac{k_{\text{obs}}}{c_{\text{compound}}} \quad (2.1)$$

Usually,  $k_{\text{obs}}$  was measured five times at different model compound concentrations over a range of about one order of magnitude. The range in which the  $k_{\text{obs}}$  could be measured with MIMS was limited by two factors (SI, Figure B.1. and Text B.1): (i) The trichloramine signal slightly decreased in blank measurements due to its self-decay and outgassing ( $k_{\text{decay+outgassing}} \sim 4 \times 10^{-5} \text{ s}^{-1}$ ). (ii) The trichloramine signal did not drop to the baseline immediately after changing the inlet to ultrapurified water because of the outwashing of the trichloramine from the system ( $k_{\text{outwashing}} \sim 1.4 \times 10^{-2} \text{ s}^{-1}$ ). Therefore, only  $k_{\text{obs}}$  values in the range  $5 \times 10^{-3} \text{ s}^{-1} > k_{\text{obs}} > 4 \times 10^{-4} \text{ s}^{-1}$  were considered for the calculation of  $k_{\text{app}}$  (eq. 2.1) to ensure no influence of the self-decay or the outwashing.

Measurements of the trichloramine reactivity with chlorinated model humic substances (fulvic acids) were performed similarly to the experiments with model compounds. To assess the role of free chlorine, the SRFA and PLFA standards were treated with chlorine prior to the trichloramine experiment according to the procedure described by Wenk et al. (2013), in which



the oxidants and the fulvic acids were added to phosphate buffer (pH 7, 50 mM) and kept for 72 hours in the dark at room temperature.

### ***Product formation from trichloramine reactions***

Four experiments were conducted to investigate and compare the reaction products of the oxidation with free chlorine and with trichloramine: (i) Dimethylamine (5 mM) was added to free chlorine (0.24 mM) and to trichloramine (0.18 mM) buffered a pH 7 (phosphate buffer, 5 mM) and analysed directly after mixing by spectrophotometry to observe the formation of chlorinated dimethylamine. (ii) Hydroquinone in phosphate buffer (pH 7, 5 mM) was added to free chlorine or trichloramine solutions, once in excess of the oxidant (~15:1) and once in excess of hydroquinone (~1:12–1:30). The solutions were analysed spectrophotometrically to measure the concentration of benzoquinone, which is the product resulting from an electron transfer reaction. (iii) The formation of chlorinated phenols from the reaction of trichloramine with phenol was investigated. In this experiment, hydrogen peroxide (500  $\mu\text{M}$ ) was added to trichloramine (180  $\mu\text{M}$ ) at pH 5 (acetate buffer, 20 mM) to quench residual free chlorine in the trichloramine stock solution. Thereafter, phenol (10  $\mu\text{M}$ ) was added to the trichloramine solution. Samples were taken every 3 minutes with a dispenser and quenched with ascorbic acid (4 mM). The analysis of the samples for phenol, chlorophenols and dichlorophenols was performed by HPLC. (iv) The 24-hours chloroform formation potential was measured for different oxidant:resorcinol ratios (9:1, 27:1, 54:1, 81:1) at pH 7 (phosphate buffer 5 mM) for free chlorine and trichloramine. The samples were quenched with sodium sulfite (1 mM). In addition, the kinetics of the chloroform formation from the reaction of resorcinol (0.05  $\mu\text{M}$ ) with free chlorine (3.75  $\mu\text{M}$ ) or trichloramine (3.75  $\mu\text{M}$ ) were investigated over a time period of 4 hours (phosphate buffer 5 mM, pH 7).

## 2.3 Results and Discussion

### 2.3.1 Trichloramine reactivity

#### *Kinetics of the reaction of trichloramine with model compounds*

The kinetics of the reaction of trichloramine with various model compounds was determined in excess of the model compound (Figure 2.1). The structures of the model compounds are provided in the supporting information (SI, Figure A.1). The variation of the model compound concentration revealed that for some compounds the apparent second order rate constant ( $k_{\text{app}}$ ) depended on the model compound concentration even in large excess of the model compound (concentration ratio  $\geq 10$ ) (SI, Text C.2, which shows all measured  $k_{\text{app}}$  as a function of the model compound concentration). For these compounds,  $k_{\text{app}}$  tended to increase at lower molar ratios (model compound:trichloramine) and leveled off at higher molar ratios of the investigated range. This behavior was also observed by measurements with a second analytical method (colorimetric method) (SI, Text and Figure C.1). The increase of  $k_{\text{app}}$  at lower molar ratios might be explained by a competitive reaction of trichloramine and the model compound with primary or secondary reaction products. The  $k_{\text{app}}$  measured at high concentrations of the model compound corresponded to the  $k_{\text{app}}$  measured in excess of trichloramine (SI, Text and Figure C.1). Therefore, it is assumed that the  $k_{\text{app}}$  at higher molar ratios, where the  $k_{\text{app}}$  levels off, represents the rate constant of the reaction of trichloramine with the model compound.

The values of  $k_{\text{app, pH 7}}$  for the reaction of  $\text{NCl}_3$  with nitrogenous model compounds cover a wide range (Figure 2.1). The  $k_{\text{app}}$  with ammonia is very low and comparable to the reaction with electron-poor compounds such as amides (urea and acetamide). The electron density of  $\alpha$ -amino-acids is higher than for amides, wherefore they have an increased reactivity with trichloramine. Furthermore, secondary amines react faster than the primary amines.

For some compounds, the reactivity allows to draw conclusions about the reactive site of the compound. For instance, acetamide reacted much faster with trichloramine than the amides. Therefore, it is assumed that trichloramine does not react at the primary amine of acetamide but at the imine. Analogously, it can be concluded that L-histidine reacts preferentially at one of the imidazol-nitrogen and not at the  $\alpha$ -amino-acid site.

The  $k_{\text{app}}$  values measured in this study are in agreement with previous studies for trichloramine reactivity with dimethylamine ( $25 \text{ M}^{-1} \text{ s}^{-1}$ ), morpholine ( $160 \text{ M}^{-1} \text{ s}^{-1}$ ) (Soltermann et al., 2014b) and ammonia ( $\sim 2 \times 10^{-2} \text{ M}^{-1} \text{ s}^{-1}$ , estimated for pH 7 and phosphate buffer (5mM) according to Yiin and Margerum (1990a)). Second order rate constants were also measured for the reaction

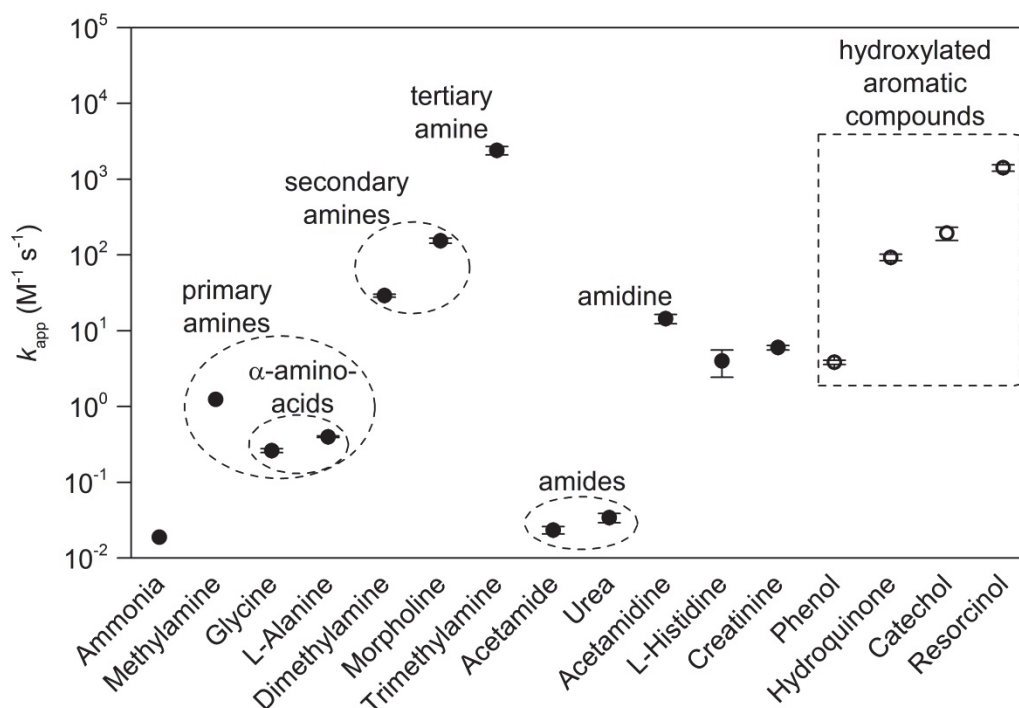


**Figure 2.1:** Measured  $k_{app}$  for the reaction of trichloramine with model compounds at pH 7 (closed symbols) and pH 5 (open symbols).  $k_{app}$  values were measured at varying concentrations of the model compounds. The error bars represent the standard deviations of all values used for the mean calculation. Ammonia and methylamine do not have error bars because they are derived from a linear regression with changing pH (SI, Text C.2).

of  $\text{NCl}_3$  with hydroxylated aromatic compounds. The corresponding  $k_{app}$  values were determined at pH 5 because the reaction was too fast to be measured with MIMS at pH 7. The  $k_{obs}$  at pH 5 were commonly  $\sim 100$  times lower than at pH 7 since trichloramine almost exclusively reacts with the deprotonated species (Figure 2.2a). The  $k_{app}$  values showed a strong dependence on the degree and position of the hydroxylation and increased in the order phenol < hydroquinone < catechol < resorcinol.

#### ***Factors affecting trichloramine reactivity: pH and temperature***

pH and temperature are two important parameters that influence chemical reactions in aqueous systems. To assess the effect of these parameters on trichloramine reactivity, the reaction of trichloramine was measured for several model compounds over the pH range 4–7 and the temperature range 15–30 °C. The results in Figure 2.2a show that the logarithm of  $k_{app}$  increases linearly (slope  $\sim 1$ ) with increasing pH. This suggests that trichloramine reacts predominantly with the deprotonated form of the investigated compounds because for most model compounds  $\text{pK}_a \geq 9$ . The temperature dependence of  $k_{app}$  can be approximated by the Arrhenius equation

$$k_{app} = A \times e^{\frac{-E_a}{RT}} \quad (2.2)$$

in which  $A$  is the frequency factor,  $E_a$  is the activation energy ( $\text{J mol}^{-1}$ ),  $R$  is the universal gas constant ( $\text{J K}^{-1} \text{mol}^{-1}$ ) and  $T$  is the temperature (K). Activation energies of 69, 86 and 92  $\text{kJ mol}^{-1}$  resulted for phenol, dimethylamine and acetamidine, respectively (Figure 2.2b). This is rather high in comparison to the activation energy of the reaction of chlorine with ammonia or monochloramine, which are  $\sim 15\text{--}20 \text{ kJ mol}^{-1}$  (Deborde and von Gunten, 2008).

In conclusion, trichloramine reactivity, which potentially lowers the trichloramine concentration, is about 2.5–4 times higher in a heated indoor pool ( $30 \text{ }^\circ\text{C}$ ) than in a colder outdoor pool ( $20 \text{ }^\circ\text{C}$ ). Additionally, the decreased stability and solubility of trichloramine in

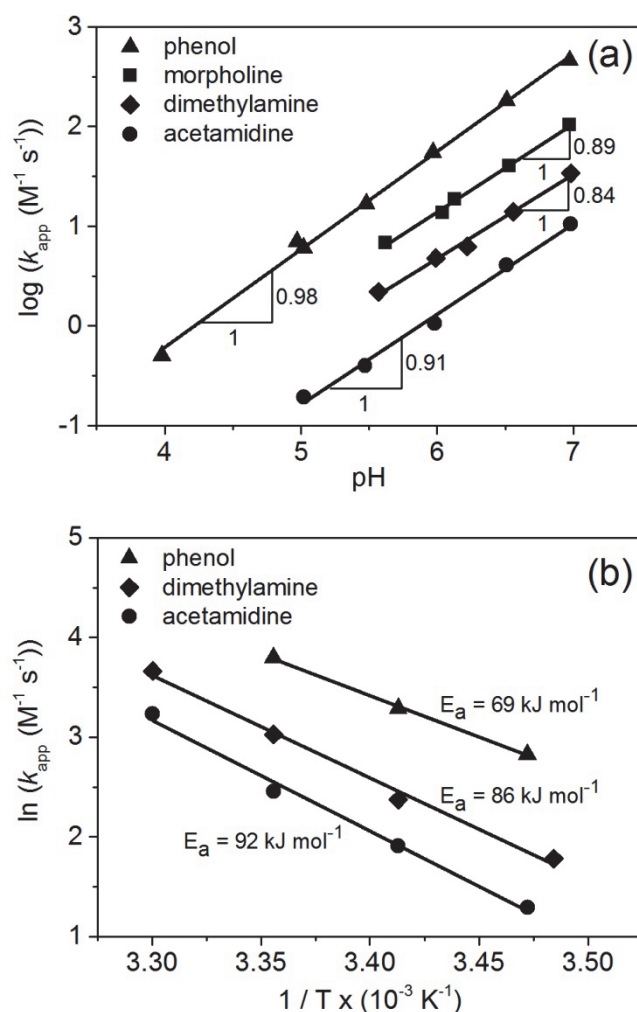


**Figure 2.2:** (a) Effect of pH on the  $k_{app}$  values for the reaction of trichloramine with various compounds at 25 ( $\pm 1$ )  $^\circ\text{C}$ . (b) Effect of temperature (15–30  $^\circ\text{C}$ ) on the  $k_{app}$  values of trichloramine reactions with various compounds at pH 7.0 ( $\pm 0.03$ ), represented by an Arrhenius-type plot. The equations for the linear regressions are for (a) phenol:  $y = 0.98x - 4.1$ , morpholine:  $y = 0.89x - 4.2$ , dimethylamine:  $y = 0.84x - 4.4$  and acetamidine:  $y = 0.91x - 5.4$  and for (b) phenol:  $y = 8.3x + 31.6$ , dimethylamine:  $y = 10.3x + 37.6$  and acetamidine:  $y = 11.1x + 39.8$ .

warm water may lead to a lower concentration. However, a higher temperature also accelerates trichloramine formation.

### ***Comparison of $k_{NCl_3}$ with $k_{HOCl}$***

A comparison of the measured  $k_{app}$  for trichloramine with values for free chlorine, calculated or estimated from literature values (Figure 2.3 and Table 2.1) reveals that trichloramine and free chlorine have similar reactivities with many model compounds at pH 7. Their  $k_{app}$  are in the same range and show an equal trend for phenol and chlorinated phenols as well as for anions such as sulfite, bromide, cyanide and iodide. A notable exception to this trend is given by ammonia and primary amines, which react much slower with trichloramine than with free chlorine. Additionally, the reactivity of trichloramine is smaller for primary than secondary amines (Figure 2.1) while for free chlorine the reactivity decreases in the order primary > secondary > tertiary amines (Abia et al., 1998). Another oxidant, namely chlorine dioxide, behaves similarly to trichloramine with a reactivity of primary < secondary < tertiary amines (Rosenblatt et al., 1967). The similarity becomes most evident if the reactivity of the oxidants with methylated amines is compared. Trichloramine and chlorine dioxide react the fastest with trimethylamine and the slowest with methylamine, while the opposite is the case for free chlorine (Hoigné and Bader, 1994; Deborde and von Gunten, 2008). The differences between the reactions of free chlorine and chlorine dioxide with amines can be explained by the different reaction mechanisms involved. Chlorine dioxide reacts mainly via an electron abstraction with the formation of an intermediate radical cation (Hull et al., 1967). This electron abstraction is assumed to be the rate limiting step, while the following H-abstraction occurs rapidly. Free chlorine mainly reacts with a chlorine addition to the amine, which is water-assisted in the case of primary and secondary amines (Abia et al., 1998). The increasing reactivity of trichloramine with a higher degree of methylation of the amines might be an indication that the rate limiting step of the reaction is an electron transfer (similar to chlorine dioxide), which leads to a nitrogen-centered radical cation. Because the results in section 2.3.2 reveal that the end product of the reaction of trichloramine with dimethylamine is chlorinated dimethylamine, it is hypothesized that the electron transfer is followed by a fast transfer of a chlorine atom (a potential product from the electron transfer step) to the nitrogen-centered radical – yielding in a net overall  $Cl^+$ -transfer.

The kinetics of the trichloramine reaction with hydroxylated aromatic compounds (phenol, hydroquinone, catechol and resorcinol) are rather comparable to the reaction of free chlorine and different from chlorine dioxide. The rate constants for trichloramine and free chlorine

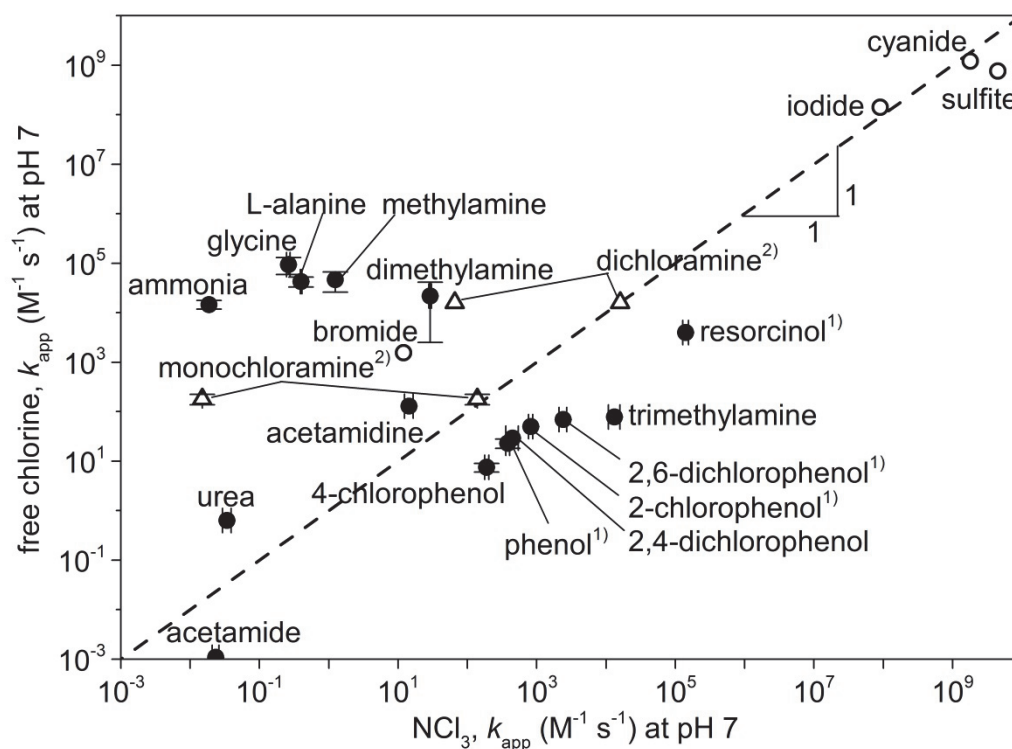


**Figure 2.3:** Comparison of  $k_{app}$  values for the reaction of trichloramine and chlorine with various model compounds at pH 7. Closed circles are  $k_{app}$  values for trichloramine which were measured in this study, open circles and triangles are measured and calculated values from literature, respectively. All plotted values are listed in Table 2.1 with additional information. <sup>1)</sup>  $k_{app}$  values for trichloramine were calculated from the measured  $k_{app}$  at pH 5. <sup>2)</sup>  $k_{app}$  values for the reaction of trichloramine with mono- and dichloramine are derived from two different models (see Table 2.1) and differ significantly from each other.

reactions with hydroxylated aromatic compounds increase in the order phenol < catechol < resorcinol while chlorine dioxide follows the order phenol ~ resorcinol < catechol (Hoigné and Bader, 1994; Deborde and von Gunten, 2008). The results in section 2.3.2 (below) reveal that trichloramine can react with hydroxylated aromatic compounds by an electron transfer (as with hydroquinone) or a  $Cl^+$ -transfer (as with phenol).

Other compounds of interest in pool water are mono- and dichloramine. The reactivity of trichloramine with mono- and dichloramine is difficult to assess due to analytical challenges and the difficulty to maintain a system at pH 7 with pure mono- or dichloramine solutions. Two studies present a model to calculate the chloramine speciation in chlorinated ammoniacal water (Yiin and Margerum, 1990a; Jafvert and Valentine, 1992). Both studies introduce base- and phosphate buffer-catalysed reactions in their model but they come up with very different rate constants for the reactions of trichloramine with mono- and dichloramine at pH 7. The

**Table 2.1:** Apparent second order rate constants ( $k_{app}$ ) for the reaction of various compounds with trichloramine and free chlorine at pH 7 and at  $25 \pm 1$  °C. Values in italic are derived from literature, values in bold were measured at pH 5.

Compound	pK <sub>a</sub>	Measured concentration range (mM)	$k_{app}$ for NCl <sub>3</sub> at pH 7 (or pH 5) (M <sup>-1</sup> s <sup>-1</sup> )	$k_{app}$ for free chlorine at pH 7 (M <sup>-1</sup> s <sup>-1</sup> )
Acetamide	15.1 <sup>o)</sup>	10–75	$2.3 \times 10^{-2}$	$1.1 \times 10^{-3}$ <sup>i)</sup>
Acetamidine	12.52 <sup>p)</sup>	0.025 – 0.25	$1.4 \times 10^1$	$1.3 \times 10^2$ <sup>k)</sup>
L-Alanine	9.87 <sup>o)</sup>	1 – 4	$4.0 \times 10^{-1}$	$4.3 \times 10^4$ <sup>j)</sup>
Ammonia	9.25 <sup>o)</sup>	25 – 125	$1.9 \times 10^{-2}$ <sup>a)</sup>	$1.5 \times 10^4$ <sup>j)</sup>
Catechol	9.34 <sup>o)</sup>	0.005 – 0.02	<b><math>1.9 \times 10^2</math></b> <sup>b)</sup>	
2-chlorophenol	8.56 <sup>o)</sup>		<b><math>8.2 \times 10^0</math></b> <sup>c,d)</sup>	$5.0 \times 10^1$ <sup>j)</sup>
4-chlorophenol	9.41 <sup>o)</sup>	0.1 – 0.25	$1.9 \times 10^2$ <sup>e)</sup>	$7.5 \times 10^0$ <sup>j)</sup>
Creatinine	9.2 <sup>o)</sup>	0.05 – 0.4	$6.0 \times 10^0$	
2,4-dichlorophenol	7.85 <sup>n)</sup>	0.01	$4.6 \times 10^2$ <sup>f)</sup>	$2.9 \times 10^1$ <sup>j)</sup>
2,6-dichlorophenol	6.97 <sup>n)</sup>	0.01 – 0.015	<b><math>1.3 \times 10^2</math></b>	$7.8 \times 10^1$ <sup>j)</sup>
Dimethylamine	10.73 <sup>o)</sup>	0.01 – 0.05	$2.9 \times 10^1$	$2.2 \times 10^4$ <sup>j)</sup>
Glycine	9.78 <sup>o)</sup>	1 – 10	$2.6 \times 10^{-1}$	$9.4 \times 10^4$ <sup>j)</sup>
L-Histidine	9.33 <sup>o)</sup>	0.05 – 2.5	$4.0 \times 10^0$	
Hydroquinone	9.85 <sup>o)</sup>	0.005 – 0.02	<b><math>9.3 \times 10^1</math></b>	
Methylamine	10.66 <sup>o)</sup>	0.25 – 1	$1.2 \times 10^0$ <sup>a)</sup>	$4.7 \times 10^4$ <sup>j)</sup>
Morpholine	8.50 <sup>o)</sup>	0.015 – 0.03	$1.5 \times 10^2$	
Phenol	9.99 <sup>o)</sup>	0.2 – 0.8	<b><math>3.8 \times 10^0</math></b>	$2.3 \times 10^1$ <sup>j)</sup>
Resorcinol	9.32 <sup>o)</sup>	0.001 – 0.005	<b><math>1.4 \times 10^3</math></b> <sup>b)</sup>	$4 \times 10^3$ <sup>j)</sup>
Trimethylamine	9.80 <sup>o)</sup>	0.01 – 0.15	$2.4 \times 10^3$ <sup>b)</sup>	$6.9 \times 10^1$ <sup>j)</sup>
Urea	13.82 <sup>o)</sup>	10 – 100	$3.4 \times 10^{-2}$	$6.3 \times 10^{-1}$ <sup>k)</sup>
Literature values				
Bromide			$1.2 \times 10^1$ <sup>g)</sup>	$1.2 \times 10^3$ <sup>h)</sup>
Cyanide	9.2 <sup>n)</sup>		$1.8 \times 10^9$ <sup>g)</sup>	$9.3 \times 10^8$ <sup>h)</sup>
Dichloramine			$6.5 \times 10^1$ <sup>m)</sup>	
Dichloramine			$5.6 \times 10^3$ <sup>l)</sup>	$1.6 \times 10^4$ <sup>l)</sup>
Monochloramine				$2.0 \times 10^2$ <sup>l)</sup>
Monochloramine			$1.4 \times 10^2$ <sup>l)</sup>	$2.2 \times 10^2$ <sup>l)</sup>
Monochloramine			$1.5 \times 10^{-2}$ <sup>m)</sup>	$1.2 \times 10^2$ <sup>m)</sup>
Iodide			$9.0 \times 10^7$ <sup>g)</sup>	$1.1 \times 10^8$ <sup>h)</sup>
Sulfite	7.2 <sup>n)</sup>		$4.5 \times 10^9$ <sup>g)</sup>	$5.9 \times 10^8$ <sup>h)</sup>

<sup>a)</sup> Calculated by a linear regression from the pH-dependence. <sup>b)</sup> NCl<sub>3</sub> concentration  $\leq 0.5$   $\mu$ M to ensure excess of the model compound. <sup>c)</sup> Measured in excess of NCl<sub>3</sub>, acetate buffer (10 mM), analysed with HPLC. <sup>d)</sup> Measured at room temperature (22–23 °C). <sup>e)</sup> Measured at low concentration to avoid interferences. <sup>f)</sup> Measured at pH 6.9. <sup>g)</sup> Cited in or from Schurter et al. (1995). <sup>h)</sup> Calculated for pH 7 from rate constants for HOCl and OCl<sup>-</sup> cited in Schurter et al. (1995). <sup>i)</sup> Calculated from  $k_{HOCl}$  cited in Deborde and von Gunten (2008). <sup>j)</sup> Average of calculated values cited in Deborde and von Gunten (2008). <sup>k)</sup> At pH 7.3 or 7.2–7.4 cited in Deborde and von Gunten (2008). <sup>l)</sup> Calculated according to the model by Jafvert and Valentine (1992). <sup>m)</sup> Calculated according to the model by Yiin and Margerum (1990). <sup>n)</sup> Deborde and von Gunten (2008). <sup>o)</sup> CRC Handbook of Chemistry and Physics (2014). <sup>p)</sup> Albert et al. (1948).

calculated  $k_{\text{app,pH7}}$  in Yiin and Margerum (1990a) for the reaction of trichloramine with mono- and dichloramine is about 10'000 and 100 times smaller, respectively, than in Jafvert and Valentine (1992). A typical combined chlorine concentration in Swiss pool water is close to the guideline value of 0.2 mg L<sup>-1</sup> as Cl<sub>2</sub>, which corresponds to an estimated mono- and dichloramine concentration of ~2 μM and ~0.5 μM, respectively, assuming a similar speciation as measured by Weaver et al. (2009). In the model with the higher  $k_{\text{app,pH7}}$  by Jafvert and Valentine (1992), this chloramine concentration would result in a trichloramine decay of  $2.8 \times 10^{-4} \text{ s}^{-1}$  and  $2.8 \times 10^{-3} \text{ s}^{-1}$  at pH 7 for the reaction with mono- and dichloramine, respectively. This estimated trichloramine decay is clearly faster than what was measured in pool water ( $2\text{--}8 \times 10^{-5} \text{ s}^{-1}$ , in 4 pool water samples with combined chlorine concentrations of 0.15–0.25 mg L<sup>-1</sup> as Cl<sub>2</sub>) (Soltermann et al., 2014a). The calculated trichloramine decays for the reaction with mono- and dichloramine from the model of Yiin and Margerum (1990a) are much lower with values of  $3 \times 10^{-8} \text{ s}^{-1}$  and  $3.3 \times 10^{-5} \text{ s}^{-1}$ , respectively. These values also appear to be plausible for a swimming pool system.

### 2.3.2 Reaction products of chlorination and trichloramination

#### *Reaction of free chlorine and trichloramine with dimethylamine*

The reactions of dimethylamine (5 mM) in excess with trichloramine (0.18 mM) and free chlorine (0.24 mM), respectively, were investigated spectrophotometrically to compare the reaction products (Figure 2.4). The spectra were measured immediately after mixing (~30 s) and after a reaction time of 2 minutes. Because the spectra remained unchanged and were different from the sum of the spectra of the reactants, it can be concluded that the reaction was complete after a reaction time of 30 seconds. Both the trichloramine and free chlorine peaks at 337 nm and 292 nm, respectively, disappeared after the reaction. The absorbance of the reaction products suggest that trichloramination and chlorination of dimethylamine form the same reaction product because they have very similar absorbance spectra in the range of 270–320 nm, while the higher absorbance between 225–250 nm for the trichloramination might be due to other reaction products or by-products present in the trichloramine solution from the trichloramine production (see below). Abbia et al. (1998) showed that chlorination of dimethylamine results in the formation of chlorinated dimethylamine (CDMA), with an absorbance peak at 262 nm. Therefore, the formation of the peak at ~260 nm suggests that the reaction of trichloramine with dimethylamine results in a net Cl<sup>+</sup>-transfer (SI, Figure E.1). The molar CDMA yield of the trichloramination is ~1.3 times higher than of chlorination. The 30% higher CDMA yield for trichloramination might be explained by the reaction of dimethylamine



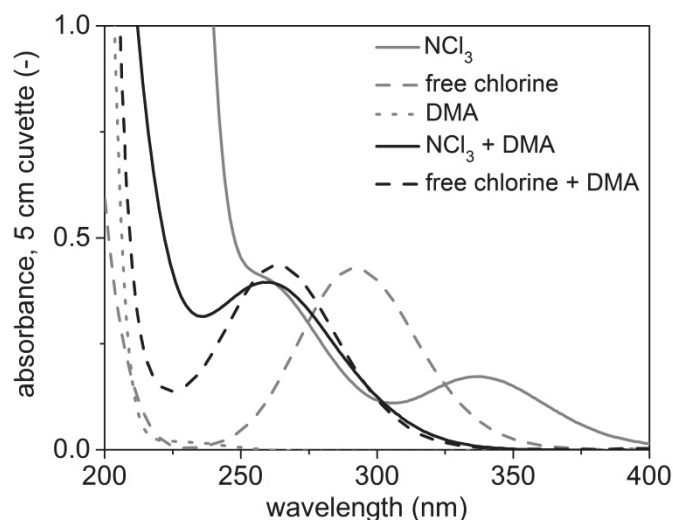


**Figure 2.4:** Absorption spectra of unbuffered trichloramine ( $\text{NCl}_3$  (0.18 mM)), free chlorine ( $\text{HOCl} / \text{OCl}^-$  (0.24 mM)), dimethylamine (DMA (5 mM)) and the products of the reactions of DMA with trichloramine and free chlorine, respectively, in phosphate buffer ( $\text{pH } 7.00 \pm 0.05$ , 5 mM) after a reaction time of 30 seconds.

with other chlorine-containing reaction products from the trichloramination or by the presence of free chlorine in the trichloramine stock solution (about 5% of the trichloramine concentration according to Kumar et al. (1987)).

#### ***Reaction of trichloramine with hydroquinone***

It has been shown that other oxidants such as chlorine dioxide and free chlorine react by an electron transfer with hydroquinone to form the *p*-benzoquinone (Wajon et al., 1982; Criquet et al., in preparation). To evaluate whether trichloramine also reacts via electron transfer, the formation of benzoquinone from the reaction of hydroquinone (10  $\mu\text{M}$ ) with trichloramine in excess (100  $\mu\text{M}$ ) was monitored spectrophotometrically at pH 7 (Figure 2.5a and SI, Figure E.1). The same experiment was performed with free chlorine (150  $\mu\text{M}$ ) (Figure 2.5b). The results in Figure 2.5 illustrate that both oxidants react with hydroquinone to form benzoquinone, which has an absorption peak at 248 nm. This reaction was completed within seconds for trichloramine whereas for free chlorine an increase of the benzoquinone concentration was observed for ~12 min before it decreased again slowly (Figure 2.5c). Adding trichloramine (100  $\mu\text{M}$ ) and free chlorine (150  $\mu\text{M}$ ) to benzoquinone revealed that the benzoquinone concentration remained rather stable with trichloramine but clearly decreased with free chlorine (~20% in 10 min) (SI, Figure E.3). This reaction of benzoquinone with free chlorine is less obvious in Figure 2.5c (decrease of ~10% from minutes 10–20) because there was a simultaneous benzoquinone formation from the reaction of hydroquinone with free

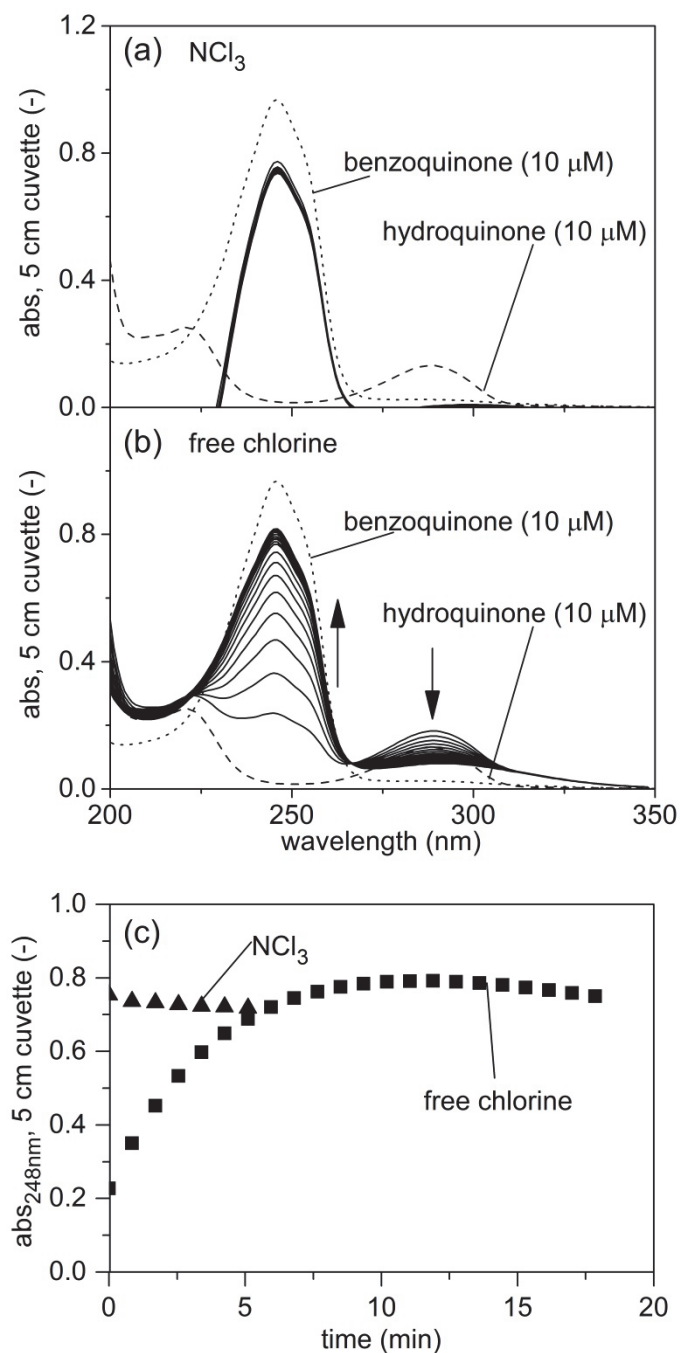
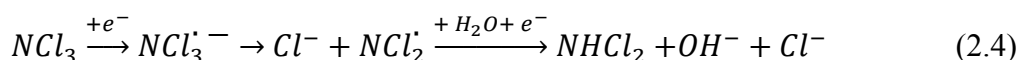


**Figure 2.5:** Absorption spectra of hydroquinone (10  $\mu\text{M}$ ) and benzoquinone (10  $\mu\text{M}$ ) (dashed or dotted lines) and (a) the absorption spectra of hydroquinone (10  $\mu\text{M}$ ) in presence of trichloramine (100  $\mu\text{M}$ ) at pH 6.9 measured every 0.8 minutes for 5 minutes (lines) (trichloramine (100  $\mu\text{M}$ ) absorbance subtracted, trichloramine absorbance  $< 235$  nm out of measurement range), (b) the absorption spectra of hydroquinone (10  $\mu\text{M}$ ) in presence of free chlorine (150  $\mu\text{M}$ ) at pH 7 measured every 0.8 minutes for ~20 minutes (lines). (c) Absorbance at 248 nm as a function of time for the reaction of hydroquinone (10  $\mu\text{M}$ ) with trichloramine (triangles, 100  $\mu\text{M}$ , from (a)) and with free chlorine (squares, 150  $\mu\text{M}$ , from (b)).

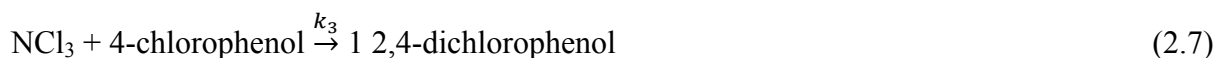
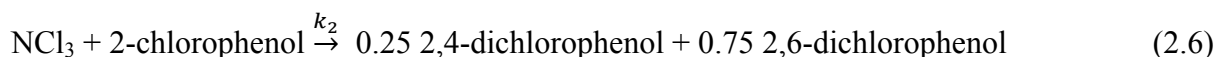
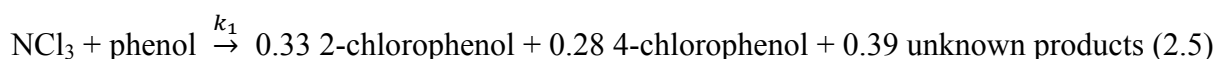
chlorine. The reaction of trichloramine (3.0–7.4  $\mu\text{M}$ ) with hydroquinone in excess (100  $\mu\text{M}$ ) confirmed that the yield of the benzoquinone formation is constant at  $\sim 80\%$  (SI, Figure E.2). The second order rate constant of the reaction between trichloramine and hydroquinone was determined as  $k_{\text{app,pH5}} = 93 \text{ M}^{-1} \text{ s}^{-1}$ . Assuming a two electron transfer reaction between trichloramine and hydroquinone, dichloramine is a potential reaction product (eq. 2.3–2.4).



Furthermore, the evolution of the absorbance suggests that after the fast benzoquinone formation with trichloramine a slow benzoquinone formation by the reaction of hydroquinone with trichloramine reaction products such as dichloramine takes place (SI, Figure E.2c). This is also supported by the fact that monochloramine and dichloramine react with hydroquinone to benzoquinone but much slower than trichloramine ( $k_{\text{trichloramine}} \gg k_{\text{dichloramine}} > k_{\text{monochloramine}}$ ) (SI, Figure E.4).

### ***Trichloramine reaction with phenol***

The reaction of trichloramine (180  $\mu\text{M}$ ) with phenol (10  $\mu\text{M}$ ) at pH 5 and room temperature ( $22 \pm 1$   $^\circ\text{C}$ ) was studied in detail to investigate the formation of the reaction products 2- and 4-chlorophenol as well as 2,4- and 2,6-dichlorophenol (Figure 2.6). The reactivity of trichloramine with each of these compounds was measured separately to perform model calculations with the Kintecus software based on eqs. 2.5 – 2.9 (Ianni, 2008).



The rate constant for the reaction of trichloramine with phenol ( $k_1 = 2.8 \text{ M}^{-1} \text{ s}^{-1}$ ) in the model was derived from the experimental data in Figure 2.6. This measured rate constant at room temperature was close to the one measured at 25  $^\circ\text{C}$  ( $3.8 \text{ M}^{-1} \text{ s}^{-1}$ , Table 2.1). The other rate constants in the model ( $k_2 = 8.2 \text{ M}^{-1} \text{ s}^{-1}$ ,  $k_3 = 1.9 \text{ M}^{-1} \text{ s}^{-1}$ ,  $k_4 = 4.5 \text{ M}^{-1} \text{ s}^{-1}$  and  $k_5 = 133 \text{ M}^{-1} \text{ s}^{-1}$ ) were derived from the values in Table 2.1 by dividing  $k_{\text{app,pH7,25}^\circ\text{C}}$  by 100 to estimate  $k_{\text{app,pH5,22}^\circ\text{C}}$ .

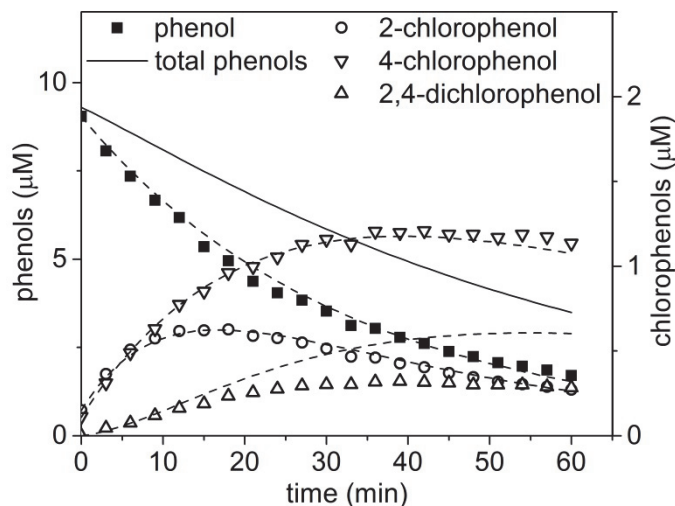


**Figure 2.6:** Evolution of phenol and chlorophenol concentrations during the reaction of phenol (10  $\mu\text{M}$ ) with trichloramine (180  $\mu\text{M}$ ) at pH 5 and room temperature ( $22 \pm 1$   $^{\circ}\text{C}$ ) (symbols = experimental data). The dashed lines are model results and the solid line represents the sum of phenol and all chlorinated phenols in the model.

The stoichiometric factors in equations 2.5 and 2.6 were derived from fitting the model to the measured concentrations (see below) and from literature on chlorination of phenols, respectively (Acero et al., 2005).

The measured rate constants reveal that chlorine addition to phenol affects its reactivity with trichloramine. Firstly, the rate constants in equations 2.5–2.9 show that a chlorine substitution at the ortho-position increases the apparent second order rate constant ( $k_2 > k_1$ ,  $k_5 > k_2$ ) and at the para-position lowers the apparent second order rate constant ( $k_1 > k_3$ ,  $k_2 > k_4$ ). Secondly, the chlorine addition changes the  $\text{pK}_a$  values (Table 2.1). Because trichloramine reacts predominantly with the deprotonated phenols (section 2.3.1), the  $\text{pK}_a$  change induced by chlorine substitution affects the apparent rate constant of trichloramine with chlorinated phenols. In previous studies the second order rate constants for the reaction of HOCl with chlorinated phenols followed much clearer the  $\text{pK}_a$  shift induced by chlorine substitution (Acero et al., 2005) than the apparent rate constants for the corresponding reactions with trichloramine.

Previous studies have shown that phenol chlorination and chloramination with mono- or dichloramine lead preferentially to 2-chloro and not to 4-chlorophenol (ratio 4:1) (Hesley et al., 2004; Acero et al., 2005). This preference is less pronounced for trichloramine which shows a ratio of  $\sim 1$  according to the fit in the model. The measured second order rate constants for the reaction of trichloramine with phenol ( $k_1$ ) and with 2- and 4-chlorophenol ( $k_2$  and  $k_3$ ) suggest

that the reaction of trichloramine with phenols leads also to unknown products (~40 %). Since trichloramine is able to undergo electron transfer reactions (section 2.3.2), phenol coupling products potentially belong to this group of unknown products. The incomplete mass balance (solid line, Figure 2.6) suggests that also at a later stage unknown products (e.g. trichlorophenols) are formed in the system. While the concentration of the secondary product 2,4-dichlorophenol rose to a peak concentration of 0.3  $\mu\text{M}$ , the concentration of 2,6-dichlorophenol remained below the detection limit ( $<0.05 \mu\text{M}$ ), which is caused by the fast further reaction of 2,6-dichlorophenol with trichloramine. However, the model overestimates the 2,4-dichlorophenol concentration (dashed line, Figure 2.6), which suggests that either (i) the stoichiometric factors leading to 2,4-dichlorophenol are lower than in the model and other products (e.g. by electron transfer) are formed, (ii) the rate constant of the reaction of trichloramine with 2,4-dichlorophenol ( $k_4$ ) is higher than estimated from the measured constant at pH 7 or (iii) 2,4-dichlorophenol reacts with other reaction products than trichloramine. The hypothesis that other products than 2,4-dichlorophenol are formed is supported by the fact that other peaks were detected in the HPLC analysis of the phenolic compounds. Conclusively, phenol forms similar reaction products by the reaction with trichloramine and free chlorine but with slightly different yields.

### **2.3.3 Chloroform formation from the reaction of resorcinol with trichloramine or free chlorine**

In pools with continuous fresh water addition it is assumed that THMs, which belong to the most abundant DBPs in pool water, are mainly formed by the reaction of free chlorine with NOM from the filling water and not with precursors introduced by bathers (Kanan and Karanfil, 2011). Resorcinol-like structures were found to be responsible for the fast THM formation from the reaction of free chlorine with NOM (Gallard and von Gunten, 2002). The reaction of resorcinol with monochloramine also leads to the formation of chloroform (Heasley et al., 1999). However, chloramination of NOM with monochloramine results in less THM formation than chlorination for the same oxidant exposure (Lu et al., 2009). For this reason, some drinking water treatment plants mainly in the USA switched their treatment process from chlorination to chloramination (Sedlak and von Gunten, 2011). Trichloramine was assumed not to form chloroform by the reaction with resorcinol since no disruption of the phenolic ring structure was expected (Heasley et al., 1999). Nevertheless, the chloroform formation potential and its kinetics for the reaction of resorcinol with trichloramine was investigated in this study

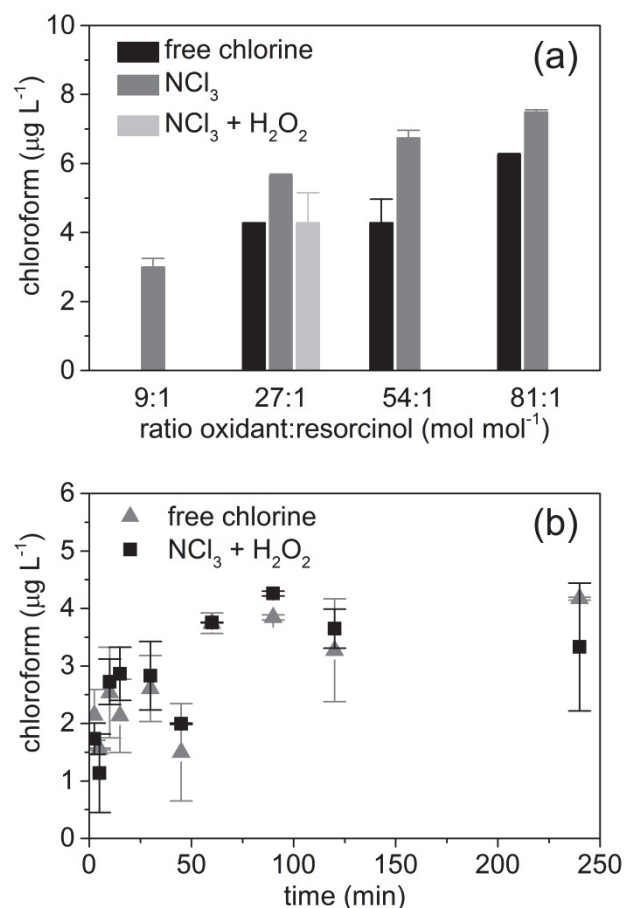


**Figure 2.7:** Chloroform formation by the reaction of resorcinol ( $0.05 \mu\text{M}$ ) at pH 7 (a) with free chlorine or trichloramine for various molar ratios of oxidant:resorcinol ( $[\text{CHCl}_3]$  after 24 hours) and (b) with free chlorine ( $3.75 \mu\text{M}$ ) or trichloramine ( $3.75 \mu\text{M}$ ) as a function of time. Hydrogen peroxide ( $100 \mu\text{M}$ ) was added to the trichloramine stock solution ( $15 \mu\text{M}$ ) in one sample in (a) and all the trichloramine samples in (b). The experiments in (b) were performed in duplicates. The boundaries of the error bars indicate measured values for the duplicates and the symbols represent the average of the duplicates.

because at pH 7 trichloramine has an even higher reactivity with resorcinol than free chlorine (Table 2.1).

The chloroform formation after a reaction time of 24 hours was measured for the reaction of resorcinol ( $0.05 \mu\text{M}$ ) with trichloramine and free chlorine at pH 7 (phosphate buffer ( $5 \text{mM}$ )) for varying molar oxidant:resorcinol ratios. In the case of trichloramine, a part of the chloroform formation might also result from reactions involving products from the trichloramine-resorcinol reaction or residual free chlorine in the trichloramine stock solution. To estimate the contribution of these effects, hydrogen peroxide ( $100 \mu\text{M}$ ) was added to the trichloramine stock solution ( $15 \mu\text{M}$ ) to quench the residual free chlorine. It has been shown

that hydrogen peroxide does not react with trichloramine (McKay et al., 2013) but reduces HOCl quickly to Cl<sup>-</sup> (Held et al., 1978). The results in Figure 2.7a show that the chloroform concentration increased with an increasing oxidant:resorcinol ratio. For the same molar oxidant:resorcinol ratio, the chloroform formation from chlorination was similar to the formation from the reaction with trichloramine in presence of hydrogen peroxide and slightly lower than with trichloramine in the absence of hydrogen peroxide (Figures 2.7a and 2.7b). This shows that the trichloramine-resorcinol reaction has a similar chloroform yield as the corresponding reaction with free chlorine.

The kinetics of the chloroform formation were almost identical for the reactions of resorcinol (0.05 μM) with free chlorine (3.75 μM) and with trichloramine (3.75 μM) in presence of hydrogen peroxide (Figure 2.7b). The experiment was conducted in duplicates for each time step and resulted in a high variability for a few samples (> 40 %) although analytical uncertainty was only about 10 %. Nevertheless, Figure 2.7b illustrates that trichloramine has similar chloroform formation potential and formation kinetics as free chlorine. Because trichloramine is commonly present in swimming pools at a lower molar concentration than free chlorine (2–10 %), free chlorine is most likely the main oxidant responsible for chloroform formation and the contribution of trichloramine is expected to be minor.

### **2.3.4 Trichloramine reactivity with fulvic acids and its dependence on pre-chlorination**

The results from the previous sections suggest that trichloramine reacts quickly with hydroxylated aromatic compounds. Pool water contains natural organic matter (NOM), which consists partly of hydroxylated aromatic compounds. However, due to their reaction with free chlorine they are often in a chlorinated form in pool water. To explore the reactivity of trichloramine with NOM, the rate constant for the reaction of trichloramine with two (non-)chlorinated fulvic acids (SRFA and PLFA) was measured. It was shown previously that the electron donating capacity (EDC) and the specific UV absorbance at  $\lambda = 254$  nm per mg L<sup>-1</sup> DOC (SUVA<sub>254</sub>) decrease during chlorination (Wenk et al., 2013). The SUVA<sub>254</sub> decreases linearly with chlorination, slightly faster for SRFA than for PLFA (Figure 2.8b). The EDCs measured by Wenk et al. (2013) show a stronger decrease than the SUVA<sub>254</sub> and a non-linear evolution for PLFA (Figure 2.8b). The EDC for (non-)chlorinated SRFA is about 3 times higher than the EDC of PLFA, reflecting the higher content of phenolic moieties in SRFA which results in a generally higher reactivity of oxidants with SRFA (Wenk et al., 2013). This is in line with the measured  $k_{app}$  for trichloramine with non-chlorinated SRFA and PLFA (Figure 2.8a).

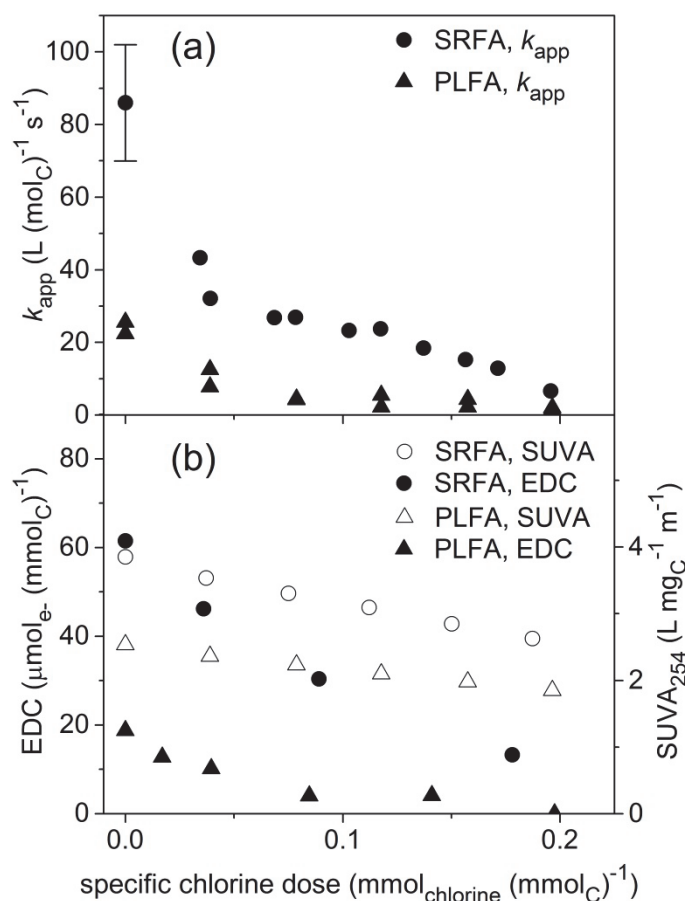


**Figure 2.8:** (a) Apparent second order rate constants for the reaction of trichloramine ( $C_0 \sim 1 \mu\text{M}$ ) with (non-)chlorinated SRFA ( $1\text{--}3 \mu\text{M}_{\text{C}}$ ) and PLFA ( $3 \mu\text{M}_{\text{C}}$ ) at pH 7 and  $25 \text{ }^\circ\text{C}$  (closed symbols). (b) Evolution of the specific UV absorbance ( $\text{SUVA}_{254}$ , open symbols) and the electron donating capacity (EDC, values from Wenk et al. (2013), closed symbols) as a function of chlorination for SRFA and PLFA.

Furthermore, the evolution of the  $k_{\text{app}}$  as a function of the degree of chlorination is very similar to the evolution of the EDC and fits also to the evolution of the  $\text{SUVA}_{254}$ . This suggests that the EDC, and partially also the  $\text{SUVA}_{254}$ , are reasonable qualitative indicators for the reactivity of organic matter with trichloramine and that dissolved organic matter loses its reactivity to trichloramine with increasing exposure to free chlorine.

### 2.3.5 Trichloramine reactivity in swimming pool water

Trichloramine in swimming pool water can either react with compounds from the filling water (mainly dissolved organic matter) or from the bather input (mainly nitrogenous compounds). In previous studies, various body fluid analogues (BFAs) were used to imitate the input of bathers to swimming pools (Borgmann-Strahsen, 2003; Judd and Bullock, 2003; Goeres et al., 2004; Kanan and Karanfil, 2011). To assess the contribution of the individual compounds of the BFAs



to the trichloramine degradation in pool water, the reactivity of trichloramine with components of BFAs was calculated (SI, Table D.1). For a better comparability, the concentrations of the BFA components were normalised to  $1 \text{ mg L}^{-1}$  of urea, which is the guideline value for urea in pool water in Switzerland (SIA, 2013). Two BFAs contain a small molar ratio of uric acid (1 % of urea on a molar basis) which has a high reactivity with trichloramine ( $> 10^4 \text{ M}^{-1} \text{ s}^{-1}$ ) (SI, Text and Figure D.2). Accounting for the reactivity of the various compounds in the normalised BFA with trichloramine, uric acid dominates trichloramine consumption ( $> 99 \%$ ) (SI, Table D.1). The calculated consumption rate of trichloramine by uric acid in the normalised BFAs ( $k_{\text{obs, pH7}} = 1\text{--}2 \text{ s}^{-1}$ ,  $t_{1/2} = 0.35\text{--}0.7 \text{ s}$ ) is much higher than for creatinine ( $k_{\text{obs, pH7}} = 2.9\text{--}6.4 \times 10^{-3} \text{ s}^{-1}$ ,  $t_{1/2} = 110\text{--}240 \text{ s}$ ) (SI, Table D.1), which is the second most important trichloramine consumer. The trichloramine decay rate in pool water was previously measured to be  $2\text{--}8 \times 10^{-5} \text{ s}^{-1}$  ( $t_{1/2} = 2.4\text{--}9.6 \text{ h}$ ), which is within or slightly above the range of trichloramine self-decay ( $k_{\text{decay}} = 0.75\text{--}4 \times 10^{-5} \text{ s}^{-1}$ ) (SI, Figure B.1) (Saguinsin and Morris, 1975; Kumar et al., 1987; Soltermann et al., 2014a). The difference between the calculated reactivity of trichloramine with the normalised BFA and the measured trichloramine decay in pool water might be explained by the fact that trichloramine is in competition with free chlorine. Commonly, trichloramine represents only  $\leq 10 \%$  of the molar free chlorine concentration (Weaver et al., 2009; Soltermann et al., 2014a). As shown in the previous sections, free chlorine has a higher  $k_{\text{app, pH7}}$  than trichloramine for many model compounds. The chlorination of potential reaction partners for trichloramine lowers their reactivity with trichloramine significantly as it was shown for uric acid, secondary amines, fulvic acids and UV-irradiated pool water (SI, section D and Soltermann et al. (2014b)). This is possibly the reason why trichloramine is more stable in pool water than calculated from its reactions with non-chlorinated BFAs.

## 2.4 Conclusions

The disinfection by-product trichloramine can cause adverse health effects to swimmers and attendants of indoor swimming pools. Although these effects are linked to the trichloramine concentrations in air, it is crucial to understand the trichloramine formation and degradation in pool water. Measurements of the trichloramine reactivity at pH 7 showed that trichloramine reacts slowly with ammonia, amides and primary amines and faster with secondary amines. Other compounds such as uric acid or hydroxylated aromatic compounds react more than two orders of magnitude faster with trichloramine than primary and secondary amines. For many of the selected compounds, the second order rate constants for the reaction with free chlorine are equal or higher than for trichloramine.

The calculated first order rate constants for the reaction of trichloramine with body fluid analogues (BFAs), at concentrations they are realistically introduced in swimming pool water, are much higher than the measured trichloramine decay in pool water. This might be explained by the reaction of free chlorine (usually present at a ~10 times higher molar concentration in pool water than trichloramine) with the BFA. The resulting chlorinated compounds react much slower with trichloramine than the parent compounds, wherefore the presence of free chlorine increases the stability of trichloramine in pool water.

Trichloramine has the ability to undergo electron transfer and electrophilic substitution reactions. Disinfection by-products such as chlorinated aromatic compounds or chloroform from the reaction of trichloramine with model compounds (resorcinol and phenol) were detected in this study. Chloroform was formed with similar yields and kinetics from the reaction of trichloramine with resorcinol as from the reaction of free chlorine with resorcinol. Since the trichloramine concentration is commonly small compared to the free chlorine concentration, its contribution to chlorinated disinfection by-product formation in pool water is assumed to be minor. However, it might be significant for disinfection by-products formed from a few compounds for which their higher reactivity with trichloramine compared to free chlorine can compensate for the lower trichloramine concentration (e.g. phenolic compounds and trimethylamine).

Conclusively, the presence of free chlorine plays an important role for the stability of trichloramine since it has a higher reactivity than trichloramine with many constituents of the pool matrix and the chlorination of these compounds lowers their reactivity with trichloramine. This was shown exemplarily by the reaction of trichloramine with chlorinated SRFA and

PLFA, which revealed that the trichloramine reactivity decreased with the degree of chlorination.

## **Acknowledgements**

This work was supported by the Swiss Federal Office of Public Health (FOPH). The authors thank Elisabeth Salhi and Philippe Périsset (Eawag) for laboratory support and Gérard Donzé (FOPH) for fruitful discussions.

---

## References

- Abia, L., X. L. Armesto, M. Canle, M. V. Garcia and J. A. Santaballa (1998). "Oxidation of aliphatic amines by aqueous chlorine." *Tetrahedron* 54(3-4): 521-530.
- Acero, J. L., P. Piriou and U. Von Gunten (2005). "Kinetics and mechanisms of formation of bromophenols during drinking water chlorination: Assessment of taste and odor development." *Water Research* 39(13): 2979-2993.
- Albert, A., R. Goldacre and J. Phillips (1948). "455. The strength of heterocyclic bases." *J. Chem. Soc.:* 2240-2249.
- Bernard, A., S. Carbonnelle, O. Michel, S. Higuët, C. de Burbure, J. P. Buchet, C. Hermans, X. Dumont and I. Doyle (2003). "Lung hyperpermeability and asthma prevalence in schoolchildren: unexpected associations with the attendance at indoor chlorinated swimming pools." *Occupational and Environmental Medicine* 60(6): 385-394.
- Blatchley, E. R. and M. Cheng (2010). "Reaction Mechanism for Chlorination of Urea." *Environmental Science & Technology* 44(22): 8529-8534.
- Borgmann-Strahsen, R. (2003). "Comparative assessment of different biocides in swimming pool water." *International biodeterioration & biodegradation* 51(4): 291-297.
- CRC Handbook of Chemistry and Physics. (2014). CRC Press. Editor-in-chief Haynes, W.M.
- Chu, T.-S., S.-F. Cheng, G.-S. Wang and S.-W. Tsai (2013). "Occupational exposures of airborne trichloramine at indoor swimming pools in Taipei." *Science of The Total Environment* 461: 317-322.
- Criquet, J., E. M. Rodriguez Francoa, S. Allard, S. Wellauer, E. Salhi, C. Joll and U. von Gunten (in prepration). "Reaction of bromine and chlorine with phenolic compounds and natural organic matter extracts – oxidation and electrophilic aromatic substitution."
- Deborde, M. and U. von Gunten (2008). "Reactions of chlorine with inorganic and organic compounds during water treatment--Kinetics and mechanisms: A critical review." *Water Research* 42(1-2): 13-51.
- Gallard, H. and U. von Gunten (2002). "Chlorination of natural organic matter: kinetics of chlorination and of THM formation." *Water Research* 36(1): 65-74.
- Gazda, M., K. Kumar and D. W. Margerum (1995). "Nonmetal redox kinetics - oxidation of bromide ion by nitrogen trichloride." *Inorganic Chemistry* 34(13): 3536-3542.
- Gérardin, F. and M. Hery (2005). Effects of nitrogen trichloride stripping on air quality in indoor swimming pools. 1st International Conference on Health and Water Quality Aspects of the Man Made Recreational Water Environment. Budapest.
- Gérardin, F. and I. Subra (2004). "Development of a sampling and analysis method for trichloramine in water (French)." INRS: Hygiène et sécurité du travail - Cahiers de notes documentaires 194: 39-49.
- Goeres, D., T. Palys, B. Sandel and J. Geiger (2004). "Evaluation of disinfectant efficacy against biofilm and suspended bacteria in a laboratory swimming pool model." *Water research* 38(13): 3103-3109.
- Heasley, V. L., M. B. Alexander, R. H. Deboard, J. C. Hanley, T. C. McKee, B. D. Wadley and D. F. Shellhamer (1999). "Reactions of resorcinol and its chlorinated derivatives with monochloramine: Identification of intermediates and products." *Environmental Toxicology and Chemistry* 18(11): 2406-2409.

Heasley, V. L., A. M. Fisher, E. E. Herman, F. E. Jacobsen, E. W. Miller, A. M. Ramirez, N. R. Royer, J. M. Whisenand, D. L. Zoetewey and D. F. Shellhamer (2004). "Investigations of the Reactions of Monochloramine and Dichloramine with Selected Phenols: Examination of Humic Acid Models and Water Contaminants†." *Environmental Science & Technology* 38(19): 5022-5029.

Held, A. M., D. J. Halko and J. K. Hurst (1978). "Mechanisms of chlorine oxidation of hydrogen peroxide." *Journal of the American Chemical Society* 100(18): 5732-5740.

Hoigné, J. and H. Bader (1994). "Kinetics of reactions of chlorine dioxide (OCIO) in water—I. Rate constants for inorganic and organic compounds." *Water Research* 28(1): 45-55.

Hull, L. A., G. T. Davis, D. H. Rosenblatt, H. K. R. Williams and R. C. Weglein (1967). "Oxidations of amines. III. Duality of mechanism in the reaction of amines with chlorine dioxide." *Journal of the American Chemical Society* 89(5): 1163-1170.

Ianni, J. C. (2008). "Windows Version 2.80."

Jafvert, C. T. and R. L. Valentine (1992). "Reaction Scheme for the chlorination of ammoniacal water." *Environmental Science & Technology* 26(3): 577-586.

Judd, S. J. and G. Bullock (2003). "The fate of chlorine and organic materials in swimming pools." *Chemosphere* 51(9): 869-879.

Kanan, A. and T. Karanfil (2011). "Formation of disinfection by-products in indoor swimming pool water: The contribution from filling water natural organic matter and swimmer body fluids." *Water Research* 45(2): 926-932.

Kumar, K., R. W. Shinness and D. W. Margerum (1987). "Kinetics and mechanisms of the base decomposition of nitrogen trichloride in aqueous-solution." *Inorganic Chemistry* 26(21): 3430-3434.

Li, J. and E. R. Blatchley (2009). "UV Photodegradation of Inorganic Chloramines." *Environmental Science & Technology* 43(1): 60-65.

Lu, J., T. Zhang, J. Ma and Z. Chen (2009). "Evaluation of disinfection by-products formation during chlorination and chloramination of dissolved natural organic matter fractions isolated from a filtered river water." *Journal of Hazardous Materials* 162(1): 140-145.

McKay, G., B. Sjelin, M. Chagnon, K. P. Ishida and S. P. Mezyk (2013). "Kinetic study of the reactions between chloramine disinfectants and hydrogen peroxide: Temperature dependence and reaction mechanism." *Chemosphere* 92(11): 1417-1422.

Parrat, J., G. Donze, C. Iseli, D. Perret, C. Tomicic and O. Schenk (2012). "Assessment of Occupational and Public Exposure to Trichloramine in Swiss Indoor Swimming Pools: A Proposal for an Occupational Exposure Limit." *Annals of Occupational Hygiene* 56(3): 264-277.

Richardson, S. D., D. M. DeMarini, M. Kogevinas, P. Fernandez, E. Marco, C. Lourencetti, C. Balleste, D. Heederik, K. Meliefste, A. B. McKague, R. Marcos, L. Font-Ribera, J. O. Grimalt and C. M. Villanueva (2010). "What's in the Pool? A Comprehensive Identification of Disinfection By-products and Assessment of Mutagenicity of Chlorinated and Brominated Swimming Pool Water." *Environmental Health Perspectives* 118(11): 1523-1530.

Rosenblatt, D. H., L. A. Hull, D. C. De Luca, G. T. Davis, R. C. Weglein and H. K. R. Williams (1967). "Oxidations of amines. II. Substituent effects in chlorine dioxide oxidations." *Journal of the American Chemical Society* 89(5): 1158-1163.

Saguinsin, J. L. S. and J. C. Morris (1975). *The chemistry of aqueous nitrogen trichloride. Disinfection Water and Wastewater.* J. D. Johnson. Michigan, Ann Arbor Science: 277-299.

- Schmalz, C., F. H. Frimmel and C. Zwiener (2011a). "Trichloramine in swimming pools - Formation and mass transfer." *Water Research* 45(8): 2681-2690.
- Schmalz, C., H. Wunderlich, R. Heinze, F. Frimmel, C. Zwiener and T. Grummt (2011b). "Application of an optimized system for the well-defined exposure of human lung cells to trichloramine and indoor pool air." *Journal of water and health* 9(3): 586-596.
- Schurter, L. M., P. P. Bachelor and D. W. Margerum (1995). "Nonmetal redox kinetics - monochloramine, dichloramine, and trichloramine reactions with cyanide ion." *Environmental Science & Technology* 29(4): 1127-1134.
- Sedlak, D. L. and U. von Gunten (2011). "The Chlorine Dilemma." *Science* 331: 42-43.
- Swiss society of engineers and architects (SIA) (2013). "Water and water treatment in public pools (German)."
- Soltermann, F., T. Widler, S. Canonica and U. von Gunten (2014a). "Comparison of a novel extraction-based colorimetric (ABTS) method with membrane introduction mass spectrometry (MIMS): Trichloramine dynamics in pool water." *Water Research* 58: 258-268.
- Soltermann, F., T. Widler, S. Canonica and U. von Gunten (2014b). "Photolysis of inorganic chloramines and efficiency of trichloramine abatement by UV treatment of swimming pool water." *Water research* 56: 280-291.
- Soulard, M., F. Bloc and A. Hatterer (1981). "Diagrams of existence of chloramines and bromamines in aqueous solution." *Journal of the Chemical Society, Dalton Transactions*(12): 2300-2310.
- Wajon, J. E., D. H. Rosenblatt and E. P. Burrows (1982). "Oxidation of phenol and hydroquinone by chlorine dioxide." *Environmental Science & Technology* 16(7): 396-402.
- Wang, W., Y. C. Qian, J. M. Boyd, M. H. Wu, S. E. Hrudey and X. F. Li (2013). "Halobenzoquinones in Swimming Pool Waters and Their Formation from Personal Care Products." *Environmental Science & Technology* 47(7): 3275-3282.
- Weaver, W. A., J. Li, Y. L. Wen, J. Johnston, M. R. Blatchley and E. R. Blatchley (2009). "Volatile disinfection by-product analysis from chlorinated indoor swimming pools." *Water Research* 43(13): 3308-3318.
- Wenk, J., M. Aeschbacher, E. Salhi, S. Canonica, U. von Gunten and M. Sander (2013). "Chemical Oxidation of Dissolved Organic Matter by Chlorine Dioxide, Chlorine, And Ozone: Effects on Its Optical and Antioxidant Properties." *Environmental Science & Technology* 47(19): 11147-11156.
- World Health Organisation (WHO) (2006). "Guidelines for safe recreational water environments." Volume 2: Swimming pools and similar environments.
- Yiin, B. S. and D. W. Margerum (1990a). "Nonmetal redox kinetics - reactions of trichloramine with ammonia and with dichloramine." *Inorganic Chemistry* 29(11): 2135-2141.
- Yiin, B. S. and D. W. Margerum (1990b). "Nonmetal redox kinetics: reactions of sulfite with dichloramines and trichloramine." *Inorganic Chemistry* 29(10): 1942-1948.





# **Supporting Information for Chapter 2**

## **Trichloramine reactions with nitrogenous and carbonaceous compounds: kinetics, products and chloroform formation**

Fabian Soltermann, Silvio Canonica and Urs von Gunten (2015)

*Water Research*, 71, 318-329

## **A Additional information on chemical substances**

### **Text A.1.**

Acetamide, acetamidine hydrochloride, acetic acid, creatinine, dimethylamine, glycine, L-alanine, L-histidine, methylamine, morpholine, resorcinol, sodium hypochlorite (6-14 %), trimethylamine, urea, uric acid, 2-chlorophenol and 2,2'-azino-bis(3-ethylbenzothiazoline-6-sulphonic acid) (ABTS) were purchased from Sigma-Aldrich. Ammonium chloride, hydrogen peroxide (35 %), hydroquinone, ortho-phosphoric acid, phenol, sodium sulfite anhydrous, 1,4-benzoquinone, 2,6-dichlorophenol and 4-chlorophenol were obtained from Fluka. Disodium hydrogen phosphate dihydrate, L-ascorbic acid, pyrocatechol (catechol), perchloric acid, sodium dihydrogen phosphate monohydrate, sodium acetate trihydrate and sodium hydroxide pellets were purchased from Merck. Other chemicals were 2,4-dichlorophenol from Riedel-de Haën, methanol from Fisher Scientific and trihalomethan calibration mix from Supelco. All chemicals were analytical grade and used without further purification.

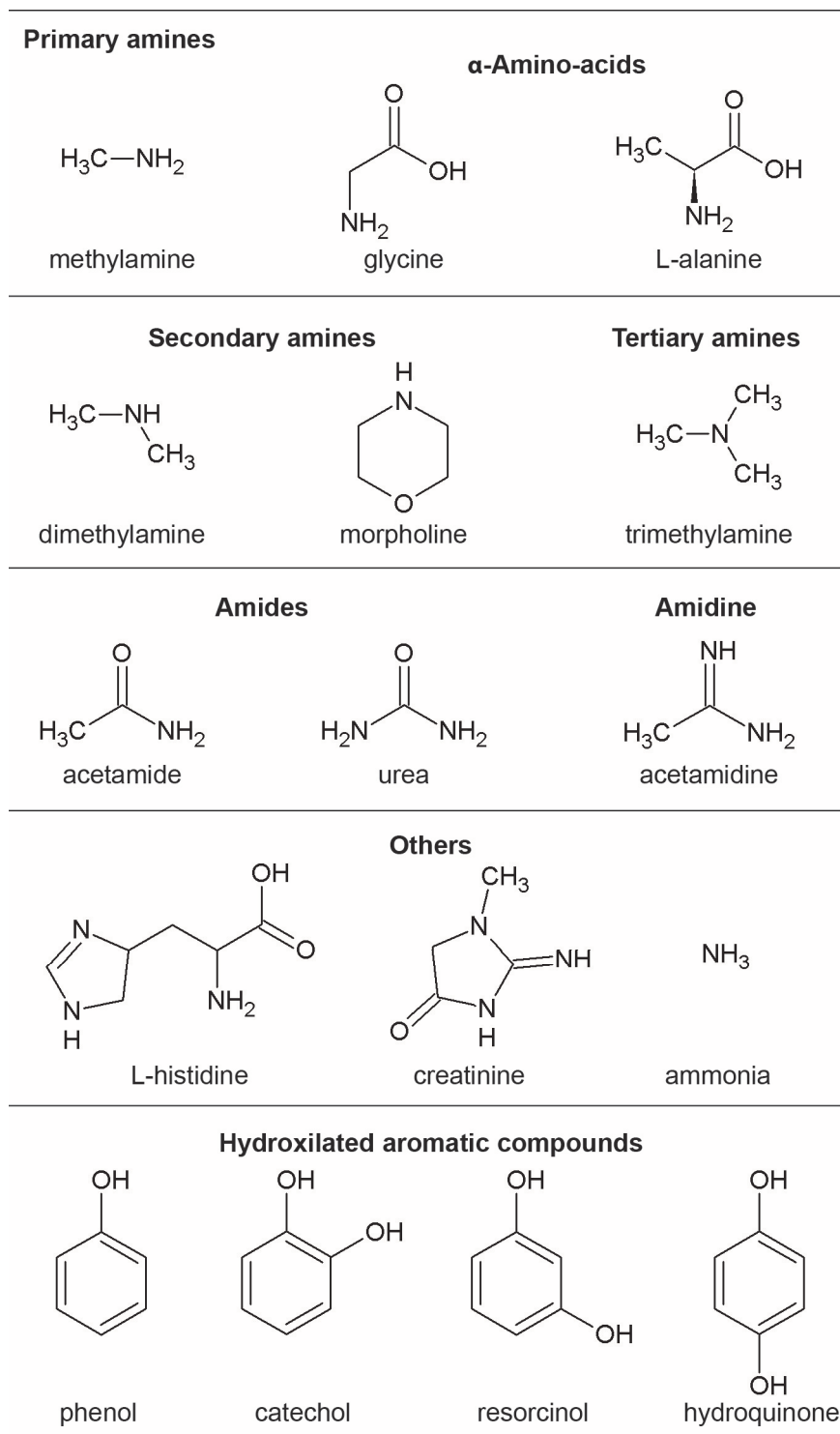


**Figure A.1.** Chemical structures of the model compounds for which the reactivity with trichloramine was measured.

## **B** Details on the experimental procedure

### **Text B.1.**

Figure B.1 shows the evolution of the signal 84 m/z (main fragment of trichloramine) for two series of trichloramine measurements, one representing the trichloramine wash out and one the self-decay. In both series, ultrapurified water was flowing initially in front of the membrane (signal at time < 500 s, which corresponds to the baseline). Thereafter, the inlet valve was switched to trichloramine ( $\sim 1 \mu\text{M}$ ,  $25 \text{ }^\circ\text{C}$ , aspirated from the bottom of a 1L bottle), whereby the signal 84 m/z increased until it reached a steady-state (within  $\sim 12$  minutes).

In the first series, the valve remained on the trichloramine position for the rest of the measurement (Figure B.1) to investigate the decrease of the trichloramine signal due to self-decay and outgassing. For this series, the trichloramine signal was stable for 40 minutes before it started to decrease ( $k_{\text{decay}} = 4 \times 10^{-5} \text{ s}^{-1}$ ). The decrease of the trichloramine concentration to determine the rate constants was commonly not measured for more than 40 minutes. To ensure that there is no impact of the trichloramine self-decay on the observed rate constants ( $k_{\text{obs}}$ ), only  $k_{\text{obs}}$  values higher than  $4 \times 10^{-4} \text{ s}^{-1}$  were considered for the calculation of the apparent second order rate constant ( $k_{\text{app}}$ ).

For the second series, the inlet valve was switched back to water after the steady-state signal was reached. The signal 84 m/z dropped rapidly ( $k_{\text{washout}} = 1.4 \times 10^{-2} \text{ s}^{-1}$ ). However, the signal did not drop immediately to the baseline because residual trichloramine in the tubing, in the dead volume attached to the membrane and in the membrane had to be washed out first. Therefore,  $k_{\text{obs}}$  values higher than  $5 \times 10^{-3} \text{ s}^{-1}$  were rejected for the calculation of the  $k_{\text{app}}$ . Trichloramine reactions with high concentrations of fast reacting compounds (e.g. resorcinol) resulted in an even faster decrease of the trichloramine signal than during the washout since trichloramine was not only washed out by convection but also degraded in the system. Nevertheless, for the calculation of the  $k_{\text{app}}$  only values of  $5 \times 10^{-3} \text{ s}^{-1} > k_{\text{obs}} > 4 \times 10^{-4} \text{ s}^{-1}$  were considered to avoid an impact of the out washing on  $k_{\text{obs}}$ .

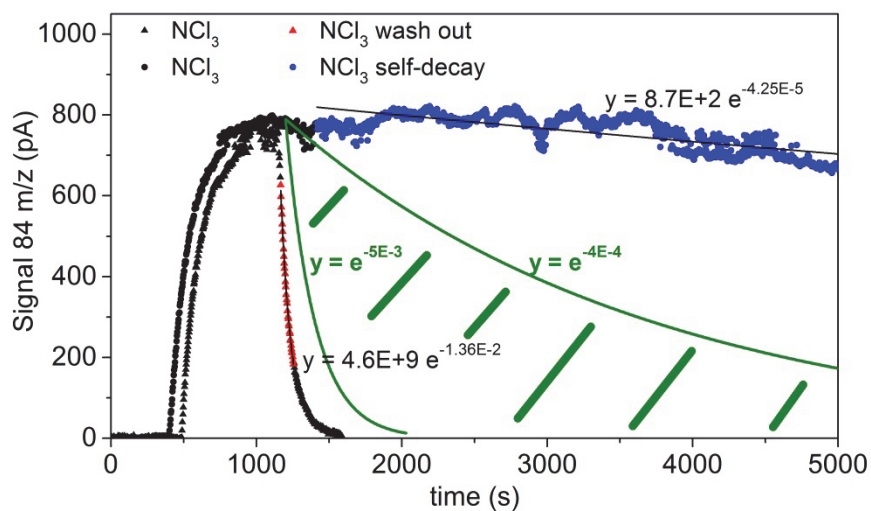


**Figure B.1.** Evolution of the trichloramine signal 84 m/z after switching the valve to the trichloramine solution (1  $\mu\text{M}$ ) followed by a wash out (red triangles) or by a continuous measurement of the self-decay (blue circles). The green lines show the boundary conditions used to determine trichloramine kinetics.

## C Trichloramine reactivity with model substances

### Text C.1.

Measured apparent second order rate constants ( $k_{app}$ ) of a few model substances (such as L-histidine or phenol) showed a dependence on the concentration of the model compound (Figure C.1). To evaluate whether this is an artefact of the MIMS measurements and to determine an unbiased second order rate constant,  $k_{app}$  of the reaction of trichloramine with phenol was measured in three different ways at room temperature ( $22 \pm 1$  °C) and pH 5 (acetate buffer, 10 mM) (Figure C.1):

(i)  $k_{app}$  was determined as described previously for the model compounds (phenol in excess, trichloramine (0.2–2  $\mu\text{M}$ ) and analysis with MIMS) but with acetate buffer (pH 5, 10 mM) since the buffer capacity of phosphate buffer at pH 5 was not high enough. Signal 86 (m/z) was used for the trichloramine analysis because signal 84 (m/z) and 88 (m/z) showed interferences if the reaction was performed in acetate buffer.

(ii)  $k_{app}$  was measured with phenol in excess and at room temperature by measuring the trichloramine decrease with 2,2'-azino-bis(3-ethylbenzothiazoline-6-sulphonic acid) (ABTS). Trichloramine (1  $\mu\text{M}$ ) was added to a phosphate buffered solution (pH 5, 5 mM). Because the trichloramine stock solution may contain free chlorine which interferes with ABTS (Gazda et al., 1995; Pinkernell et al., 2000), hydrogen peroxide (10  $\mu\text{M}$ ) was added 5 minutes prior to the reaction since hydrogen peroxide reacts very slowly with trichloramine (too slow to be differentiated from trichloramine self-decay, McKay et al. (2013)) but quickly with free chlorine ( $\text{HO}_2^- + \text{HOCl}$  ( $k_{25\text{ }^\circ\text{C}} = 4.4 \times 10^7 \text{ M}^{-1} \text{ s}^{-1}$ ), Held et al. (1978)). Thereafter, phenol (25–500  $\mu\text{M}$ ) was added to the trichloramine solution. The trichloramine decrease was monitored by measuring the absorbance ( $\lambda = 405 \text{ nm}$ ) of the  $\text{ABTS}^{\bullet -}$  which is formed by the reaction of trichloramine with ABTS (50  $\mu\text{M}$ ). The absorbance was immediately ( $< 30$  seconds) measured after mixing with ABTS because the absorbance is not stable at this pH (Soltermann et al., 2014).

(iii)  $k_{app}$  for the reaction of trichloramine with phenol (2–10  $\mu\text{M}$ ) in excess of trichloramine (20–180  $\mu\text{M}$ ) was measured at room temperature. Trichloramine was added to an acetate buffered solution (pH 5, 10 mM) in presence of hydrogen peroxide (550  $\mu\text{M}$ ). After 5 minutes, phenol was added and the kinetics of the reaction were determined by quenching the reaction with ascorbic acid at various time points followed by phenol analysis with HPLC.

The results in Figure C.1 show that there is a dependence of the  $k_{app}$  on the phenol concentration at low phenol concentrations for both analytical methods (MIMS and ABTS).

The  $k_{\text{app}}$  showed a trend towards  $2\text{--}3 \text{ M}^{-1} \text{ s}^{-1}$  for higher concentrations, which corresponds to the measured  $k_{\text{app}}$  with phenol in excess. Conclusively, it can be assumed that the increase of the  $k_{\text{app}}$  with decreasing phenol concentration is not an artifact of the MIMS analysis. An explanation for this effect might be that primary or secondary reaction products undergo competitive reactions to the reaction of trichloramine with phenol. Therefore,  $k_{\text{app}}$  can only be measured in presence of sufficiently high phenol concentrations, which prevent the reaction of trichloramine with primary or secondary reaction products. Dichloramine is not important in this context, because the measured  $k_{\text{app}}$  for its reaction with phenol ( $k_{\text{app, pH 4.9}} = 4.6 \times 10^{-3} \text{ M}^{-1} \text{ s}^{-1}$ , this study) was too low.

The  $k_{\text{app}}$ , derived from the experiment in excess of trichloramine, is similar to the  $k_{\text{app}}$  at high phenol concentrations (Figure C.1). Therefore, it is assumed that  $k_{\text{app}}$  for the reaction of trichloramine with phenol corresponds to the value obtained at high phenol concentrations.

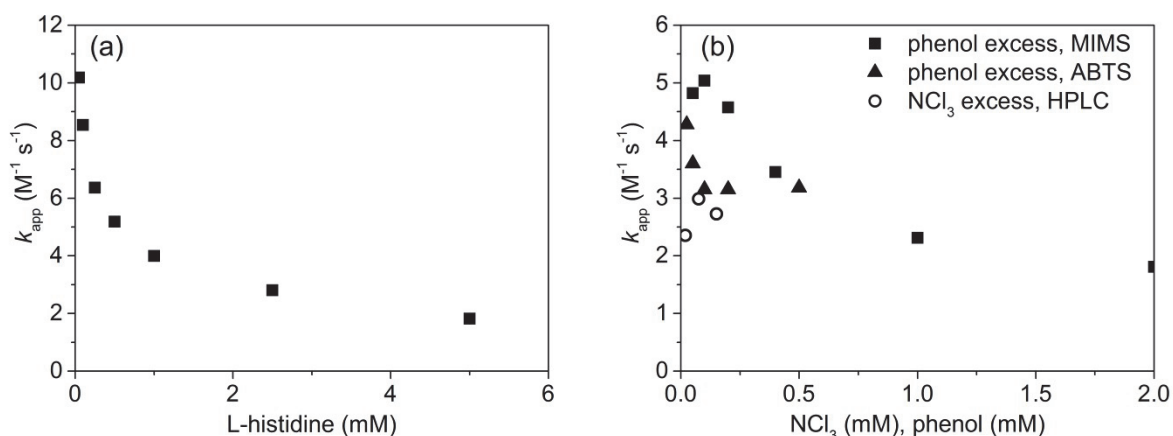


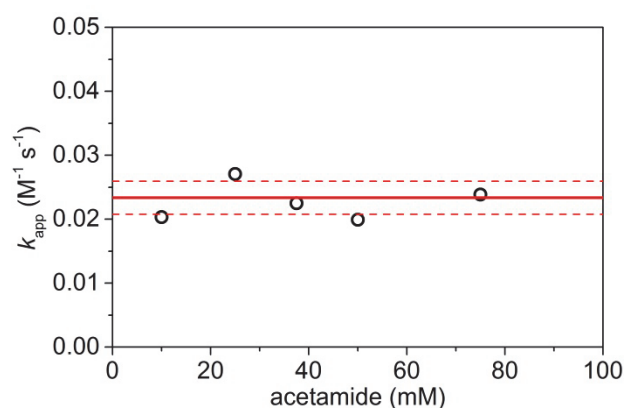
**Figure C.1.** (a) Reaction of trichloramine with L-histidine: Dependence of  $k_{\text{app}}$  on the concentration of L-histidine. (b) Measurement of  $k_{\text{app}}$  for the reaction of trichloramine with phenol in excess of phenol (squares and triangles, measured with MIMS and ABTS) and in excess of trichloramine (circles, measured with HPLC). The  $k_{\text{app}}$  determined in excess of phenol showed a dependence on the phenol concentration. For experimental conditions see Text C.1)

**Text C.2.**

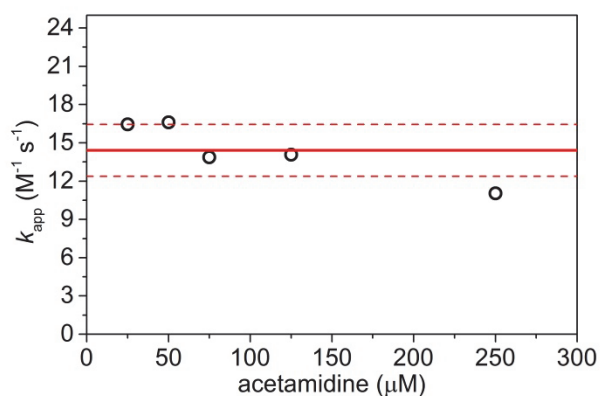
The reactivity of various model compounds with trichloramine was measured with MIMS. Thereby, trichloramine ( $\sim 1 \mu\text{M}$ ) was added to a phosphate buffered solution (5 mM) at pH 7 and pH 5 for slow reacting compounds and fast reacting phenols, respectively. After the trichloramine signal reached a steady-state ( $\sim 12$  min), the model compound was added to the trichloramine solution. The decrease of the trichloramine concentration was continuously monitored by MIMS. These measurements were conducted at different concentrations, always in excess of the model compound. In few experiments, the initial trichloramine concentration was lower than  $\sim 1 \mu\text{M}$  to ensure an excess of the model compound. The  $k_{\text{app}}$  values given in Table 1 of the main text are the averages of the measured  $k_{\text{app}}$  at different concentrations. For some model compounds, the  $k_{\text{app}}$  values showed a dependence on the concentration of the model compound (SI, Text C.1) with increasing  $k_{\text{app}}$  values at low model compound concentrations. If this was the case, the  $k_{\text{app}}$  was calculated from the values at high model compound concentrations (for explanation, see SI Text C.1). For few model compounds, the buffer capacity of the phosphate buffer was not high enough to keep the pH constant after the addition of the model compound (ammonia and methylamine). In these cases, the  $k_{\text{app}}$  for pH 7.0 was derived from a linear regression of  $k_{\text{app}}$  versus pH (from experiments using different concentrations of the model compound).

The figures below show the measured  $k_{\text{app}}$  as a function of compound concentration. Furthermore, information about the experimental conditions are given for each compound. The red lines (circles for ammonia and methylamine) in the plots correspond to the determined  $k_{\text{app}}$  given in Table 2.1 of the main text. This value is assumed to be the best fit considering various factors such as concentration effect (SI, Text C.1), pH changes and interferences. The standard deviations are plotted in dashed red lines and correspond to the standard deviations given in Figures 2.1 and 2.3 in the main text, which show the  $k_{\text{app}}$  for the reaction of trichloramine with model compounds and compare them to the  $k_{\text{app}}$  for the reaction of free chlorine with the model compounds, respectively.

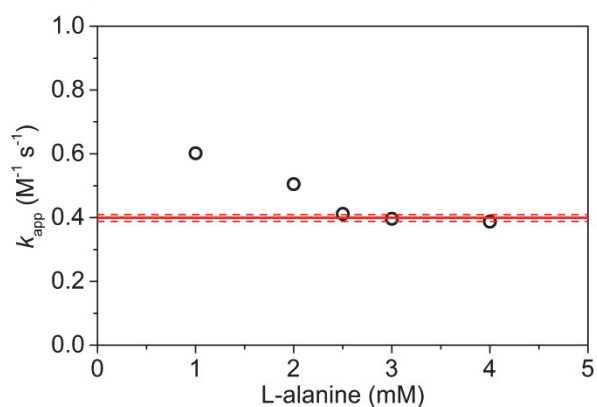


**Acetamide****Remarks:**

- $[NCl_3]_0$ :  $\sim 1 \mu M$ , pH 7, molar ratio  $NCl_3$ :acetamide: 1:10'000–1:75'000.
- Unstable pH, dropped to 6.9 for high acetamide concentrations.
- Acetamide (10 mM):  $k_{obs} < 4 \times 10^{-4} s^{-1}$ , therefore not considered for the mean calculation.

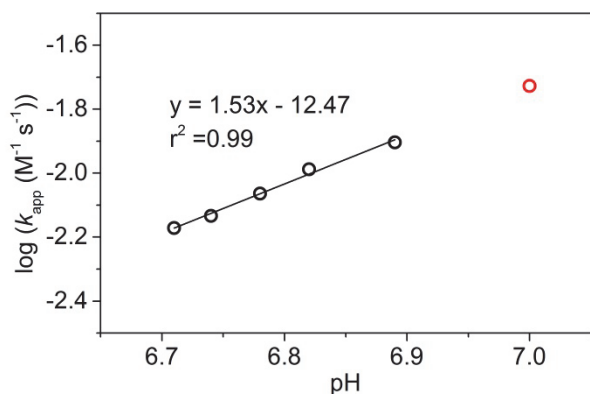
**Acetamidine****Remarks:**

- $[NCl_3]_0$ :  $\sim 1 \mu M$ , pH 7, molar ratio  $NCl_3$ :acetamidine: 1:25–1:250.

**L-Alanine****Remarks:**

- $[NCl_3]_0$ :  $\sim 1 \mu M$ , pH 7, molar ratio  $NCl_3$ :L-alanine: 1:1000–1:4000.
- The two lowest concentrations were omitted for the mean calculation of  $k_{app}$ .

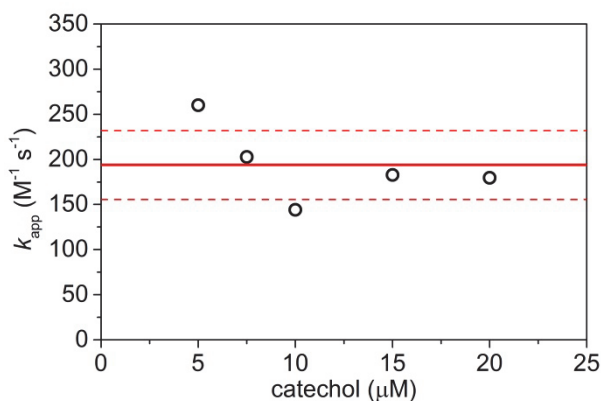
## Ammonia



## Remarks:

- $[NCl_3]_0$ :  $\sim 1 \mu M$ , pH 7, molar ratio  $NCl_3$ :ammonia: 1:25'000–1:125'000.
- pH varied from 6.7–6.9 for  $C_0$  of ammonia 25–125 mM, although the pH of the ammonia solution was lowered with perchloric acid prior to the experiment.
- Ionic strength might have an effect on the reaction.
- Calculation of  $k_{app,pH7}$  with linear regression. (red circle).

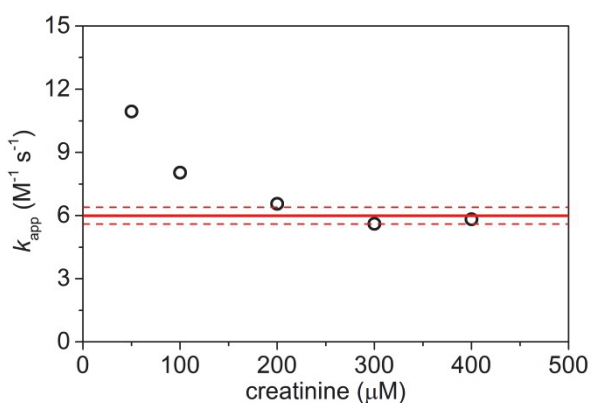
## Catechol



## Remarks:

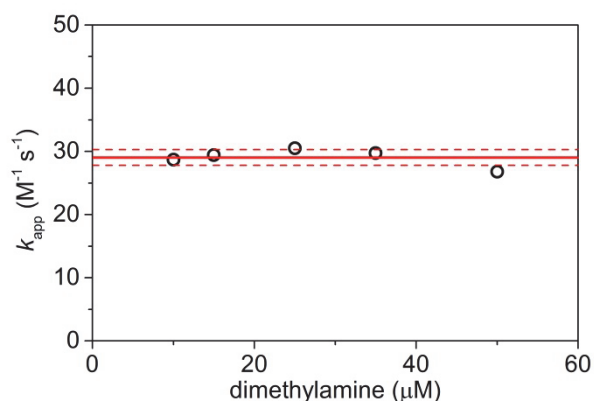
- $[NCl_3]_0$ :  $\sim 0.5 \mu M$ , pH 5, molar ratio  $NCl_3$ :catechol: 1:10–1:40.
- pH unstable (4.9–5.0).

## Creatinine

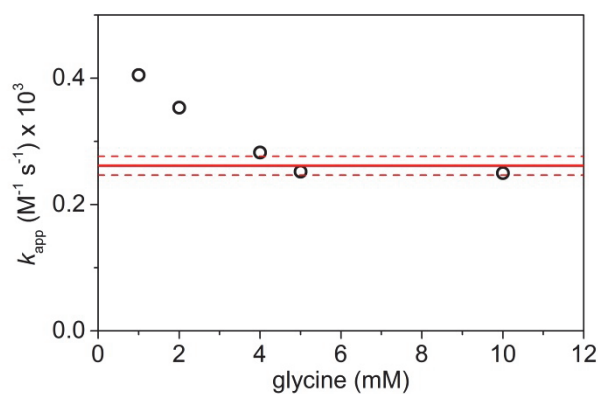


## Remarks:

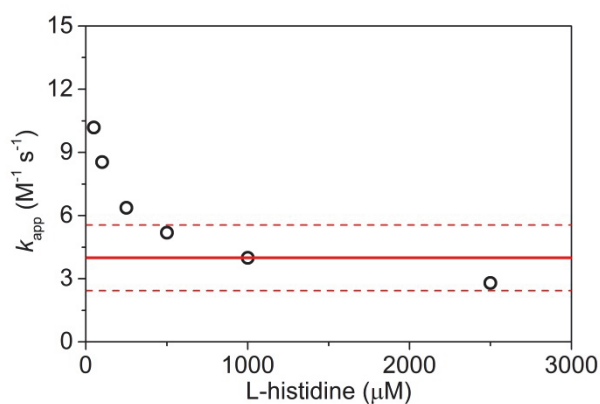
- $[NCl_3]_0$ :  $\sim 1 \mu M$ , pH 7, molar ratio  $NCl_3$ :creatinine: 1:50–1:400.
- The two lowest concentrations were omitted for the mean calculation of  $k_{app}$ .

**Dimethylamine****Remarks:**

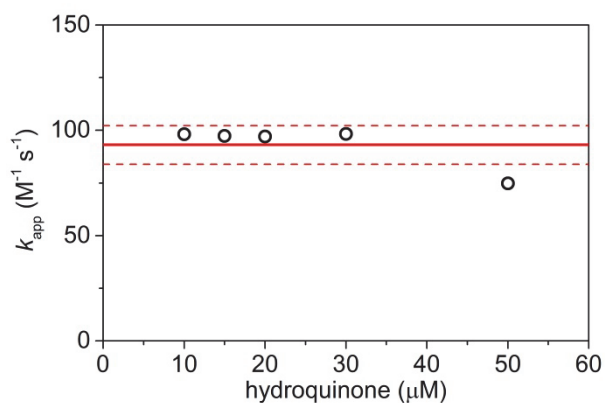
- $[\text{NCl}_3]_0$ :  $\sim 1 \mu\text{M}$ , pH 7, molar ratio  $\text{NCl}_3$ :dimethylamine: 1:10–1:50.

**Glycine****Remarks:**

- $[\text{NCl}_3]_0$ :  $\sim 1 \mu\text{M}$ , pH 7, molar ratio  $\text{NCl}_3$ :glycine: 1:1000–1:10'000.
- The two lowest concentrations were omitted for the mean calculation of  $k_{\text{app}}$ .

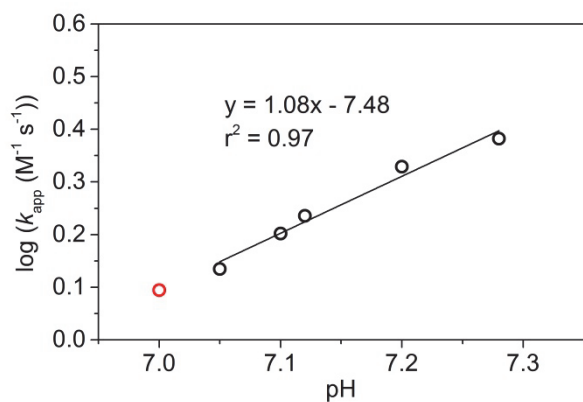
**L-Histidine****Remarks:**

- $[\text{NCl}_3]_0$ :  $\sim 1 \mu\text{M}$ , pH 7, molar ratio  $\text{NCl}_3$ :L-histidine: 1:50–1:2500.
- The three lowest concentrations were omitted for the mean calculation of  $k_{\text{app}}$ .
- The range used for the mean calculation showed a slight dependence on the L-histidine concentration.

**Hydroquinone**

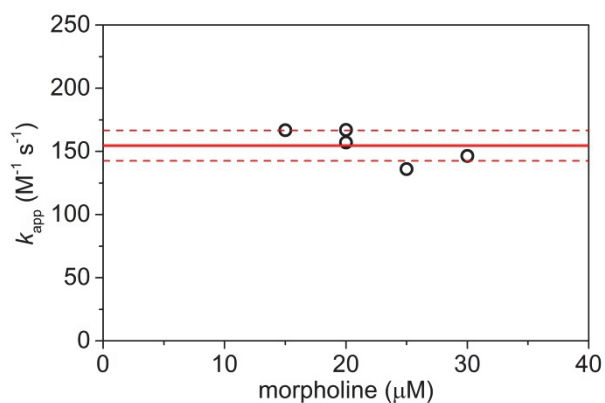
Remarks:

- $[\text{NCl}_3]_0$ :  $\sim 1 \mu\text{M}$ , pH 5, molar ratio  $\text{NCl}_3$ :hydroquinone: 1:10–1:50.

**Methylamine**

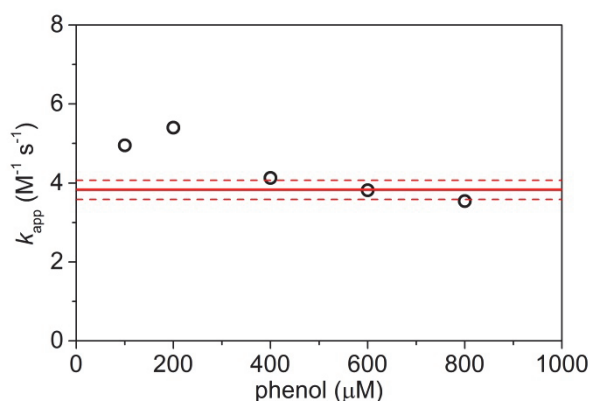
Remarks:

- $[\text{NCl}_3]_0$ :  $\sim 1 \mu\text{M}$ , [methylamine]: 0.25–1 mM, molar ratio  $\text{NCl}_3$ :methylamine: 1:250–1:1000.
- pH unstable (7.05–7.3).
- Calculation of  $k_{\text{app,pH 7}}$  with linear regression (red circle).

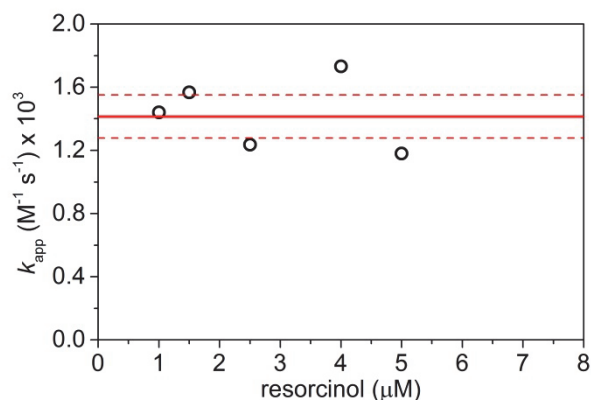
**Morpholine**

Remarks:

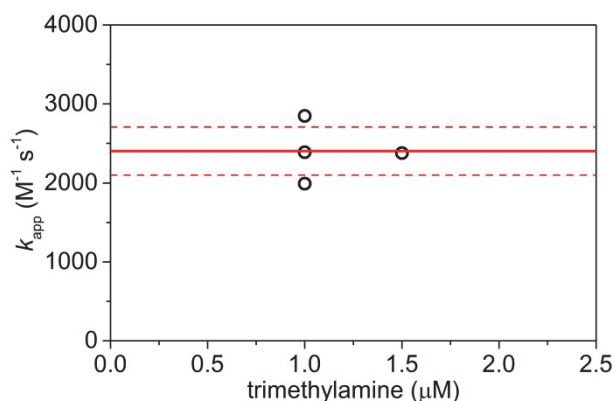
- $[\text{NCl}_3]_0$ :  $\sim 1 \mu\text{M}$ , pH 7, molar ratio  $\text{NCl}_3$ :morpholine: 1:15–1:30.

**Phenol****Remarks:**

- $[\text{NCl}_3]_0$ :  $\sim 1 \mu\text{M}$ , pH 5, molar ratio  $\text{NCl}_3$ :phenol: 1:100–1:800.
- pH values for concentrations  $\geq 400 \mu\text{M}$  were slightly below 5 (4.93–4.95).
- The range used for the mean calculation showed a slight dependence on the phenol concentration.

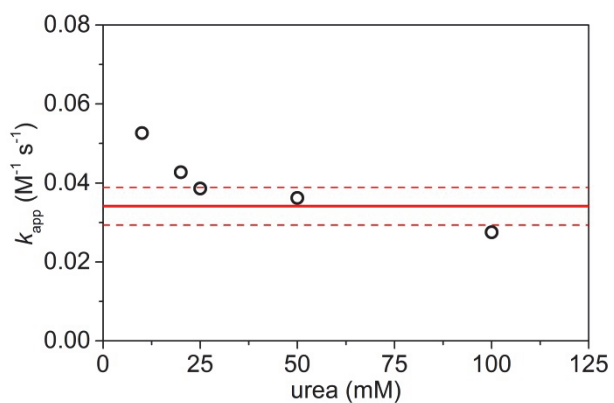
**Resorcinol****Remarks:**

- $[\text{NCl}_3]_0$ :  $\sim 0.1$ – $0.5 \mu\text{M}$ , molar ratio  $\text{NCl}_3$ :resorcinol: 1:10–1:25.
- pH unstable: 5.0–5.1.
- The measurements of resorcinol at 4 and 5  $\mu\text{M}$  had a  $k_{\text{obs}} > 5 \times 10^{-3} \text{s}^{-1}$  and were therefore not considered for the mean calculation.

**Trimethylamine****Remarks:**

- $[\text{NCl}_3]_0$ :  $\sim 0.1 \mu\text{M}$ , pH 7, molar ratio  $\text{NCl}_3$ :trimethylamine: 1:10–1:15.

## Urea



## Remarks:

- $[NCl_3]_0$ :  $\sim 1 \mu M$ , pH 7, molar ratio  $NCl_3$ :urea: 1:10'000–1:100'000
- The three lowest concentrations were omitted for the mean calculation of  $k_{app}$ .
- The range used for the mean calculation showed a slight dependence on the urea concentration.

## D Reactivity of trichloramine with chlorinated uric acid and calculated reactivity with bather fluid analogues (BFAs)

### Text D.1.

A uric acid (structure in Figure D.1) stock solution (5 mM) was chlorinated with free chlorine at various molar ratios (Figure D.2). The solution was stored for > 10 minutes to guarantee complete reaction. Thereafter, the reactivity of trichloramine (1  $\mu\text{M}$ ) with chlorinated uric acid (2.5–75  $\mu\text{M}$ ) was investigated at pH 7. Due to its fast reaction, the solutions with a ratio  $\leq 2:1$  (free chlorine:uric acid) were too fast to be accurately measured with MIMS without influence of the trichloramine washout. Therefore, the expected  $k_{\text{app}}$  for these ratios are higher than the measured ones.

The results in Figure D.2 show that non-chlorinated or low chlorinated (molar free chlorine:uric acid ratios of 1:1 and 2:1) uric acid has a high  $k_{\text{app}}$ , which is comparable to the range of  $k_{\text{app}}$  for hydroxylated aromatic compounds. This might be due to the conjugated double-ring structure of the molecule. If uric acid is more chlorinated (molar free chlorine:uric acid ratios of 3:1 and 4:1), it has a reactivity with trichloramine in the range of other secondary amines ( $10^1$ – $10^3 \text{ M}^{-1} \text{ s}^{-1}$ ). It is assumed that at this degree of chlorination the electrons cannot move freely in the ring system. At the same time, not all of the nitrogen in the molecule are chlorinated wherefore the uric acid reacts similar to secondary amines. At a higher extend of chlorination (free chlorine:uric acid ratios of 5:1 and 6:1), the uric acid is almost unreactive towards trichloramine similar to primary amines or amides (see Figure 1, main text).

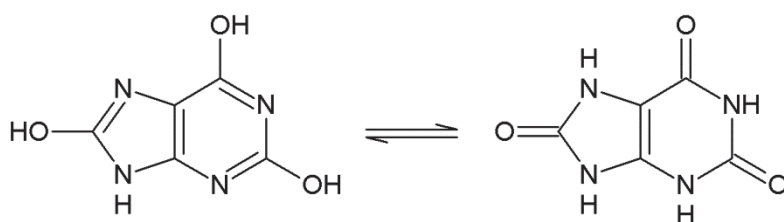


**Figure D.1.** Structures of the two uric acid tautomers.

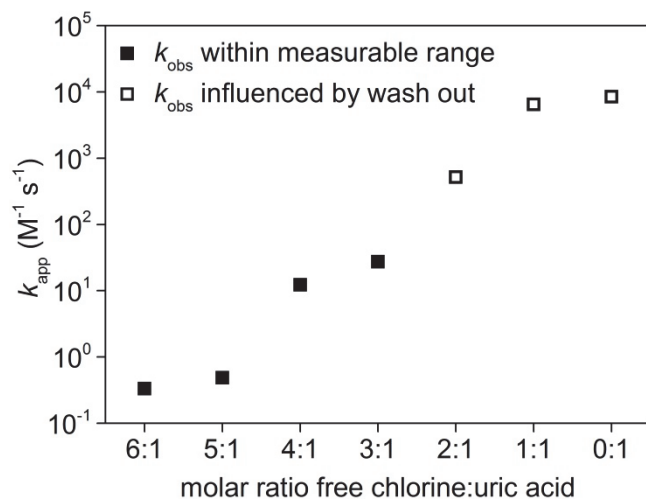


**Figure D.2.** Measured  $k_{app}$  for the reaction of chlorinated uric acid (2.5–75  $\mu M$ ) with trichloramine (1  $\mu M$ ) at pH 7 for various free chlorine:uric acid ratios. The kinetics of the ratios 0:1, 1:1 and 2:1 were too fast to be measured without influence of the trichloramine out washing. The uric acid concentration was only in a small excess (2.5 times) to trichloramine for the measurements at the ratios 0:1 and 1:1.



**Table D.1**

Concentrations and calculated contributions of bather fluid components to the trichloramine degradation for three different body fluid analogues BFA (G) (Goeres et al., 2004), BFA (B) (Borgmann-Strahsen, 2003) and BFA (J) (Judd and Bullock, 2003). The  $k_{app, pH7}$  for uric acid (red) is an estimated value for the non-chlorinated uric acid.

BFA (G)	concentration (mg L <sup>-1</sup> )	normalised to 1 mg L <sup>-1</sup> urea	molar mass (g mol <sup>-1</sup> )	norm. conc. (mmol L <sup>-1</sup> )	$k_{app, pH7}$ (M <sup>-1</sup> s <sup>-1</sup> )	$k_{obs, pH7}$ (s <sup>-1</sup> )	contribution to NCl <sub>3</sub> - degradation (%)
urea	62.6	1.00	60.1	16.65	3.4E-02	5.7E-04	0.04%
creatinine	4.3	0.07	113.1	0.61	6.0E+00	3.6E-03	0.25%
uric acid	1.5	0.02	168.1	0.14	1.0E+04	1.4E+00	99.70%
lactic acid	3.3	0.05	90.1	0.59			
albumin	9.7	0.15					
glucuronic acid	1.2	0.02	194.1	0.10			
ammonium chloride	7	0.11	53.5	2.09	1.9E-02	3.9E-05	0.00%
sodium chloride	22.1	0.35	58.4	6.04			
sodium sulfate	35.3	0.56	142.0	3.97			
sodium bicarbonate	6.7	0.11	84.0	1.27			
potassium phosphate	11.4	0.18					
potassium sulfate	10.1	0.16	174.3	0.93			
					sum	1.4E+00	

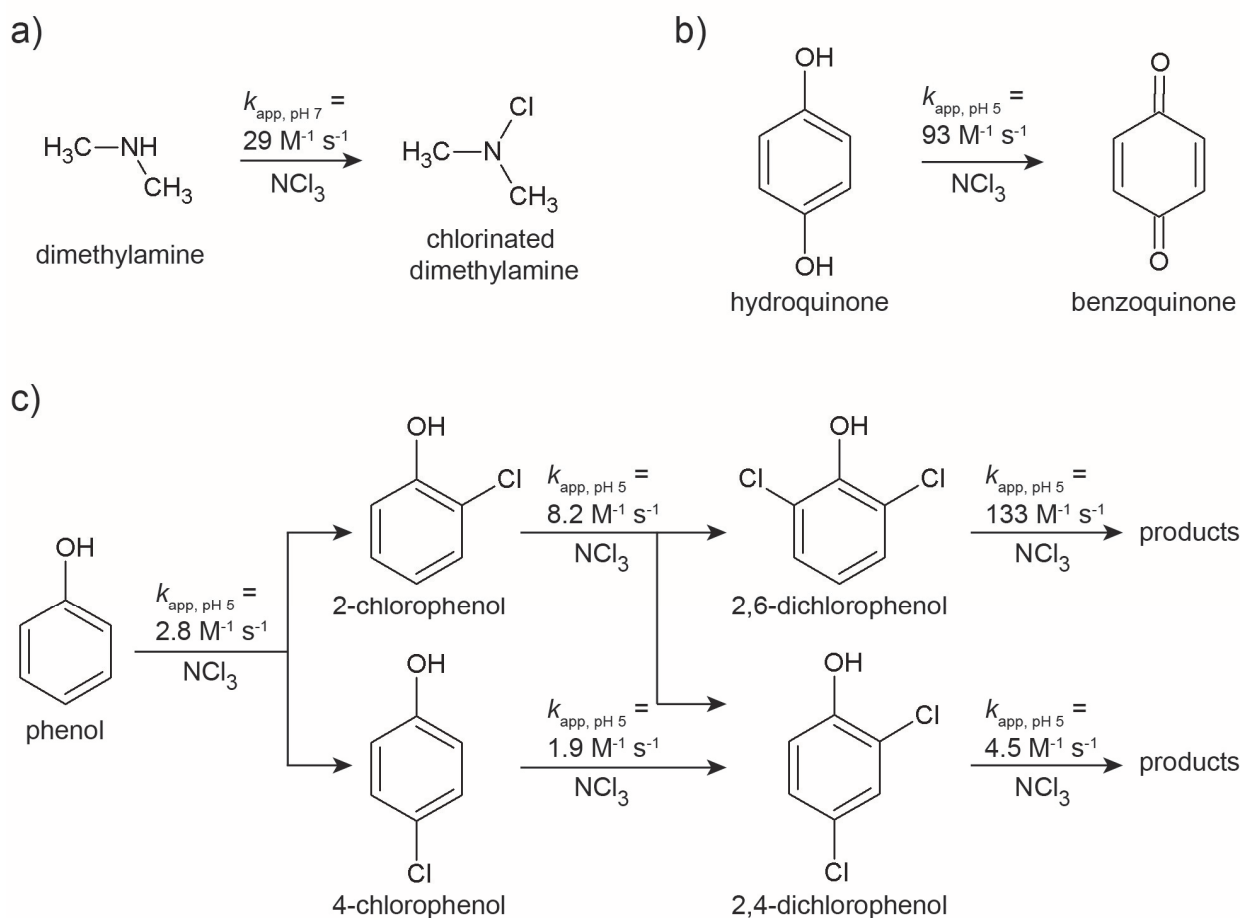
  

BFA (B)	concentration (mg L <sup>-1</sup> )	normalised to 1 mg L <sup>-1</sup> urea	molar mass (g mol <sup>-1</sup> )	norm. conc. (mmol L <sup>-1</sup> )	$k_{app, pH7}$ (M <sup>-1</sup> s <sup>-1</sup> )	$k_{obs, pH7}$ (s <sup>-1</sup> )	contribution to NCl <sub>3</sub> - degradation (%)
urea	23000	1.00	60.1	16.65	3.4E-02	5.7E-04	15.19%
creatinine	1250	0.05	113.1	0.48	6.0E+00	2.9E-03	77.00%
glutamic acid	300	0.01	147.1	0.09			
aspartic acid	830	0.04	133.1	0.27			
glycine	450	0.02	75.1	0.26	2.6E-01	6.8E-05	1.83%
histidine	200	0.01	155.2	0.06	4.0E+00	2.2E-04	5.98%
lysine	75	0.00	146.2	0.02			
					sum	3.7E-03	

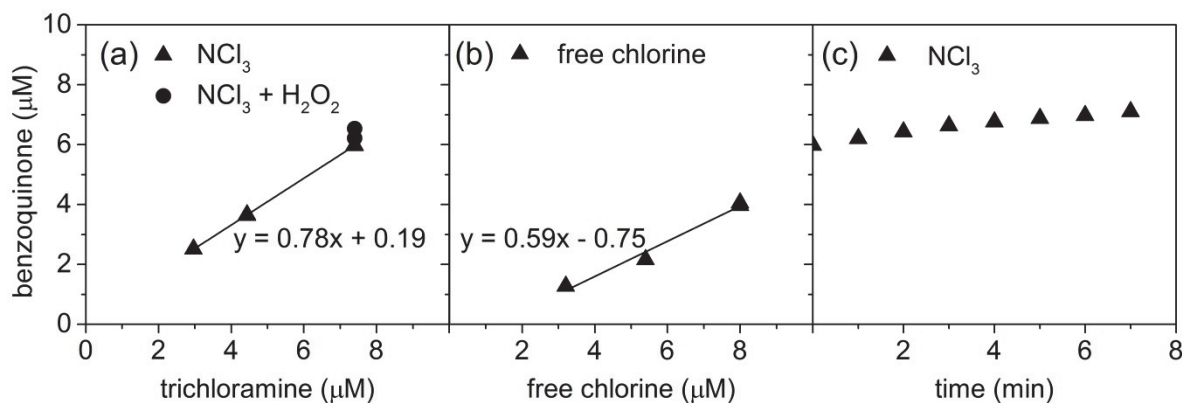
  

BFA (J)	concentration (mg L <sup>-1</sup> )	normalised to 1 mg L <sup>-1</sup> urea	molar mass (g mol <sup>-1</sup> )	norm. conc. (mmol L <sup>-1</sup> )	$k_{app, pH7}$ (M <sup>-1</sup> s <sup>-1</sup> )	$k_{obs, pH7}$ (s <sup>-1</sup> )	contribution to NCl <sub>3</sub> - degradation (%)
urea	14800	1.00	60.1	16.65	3.4E-02	5.7E-04	0.03%
creatinine	1800	0.12	113.1	1.08	6.0E+00	6.4E-03	0.33%
uric acid	490	0.03	168.1	0.20	1.0E+04	2.0E+00	99.54%
citric acid	640	0.04	192.1	0.23			
histidine	1210	0.08	155.2	0.53	4.0E+00	2.1E-03	0.11%
hippuric acid	1710	0.12	179.2	0.64			
ammonium chloride	2000	0.14	53.5	2.53	1.9E-02	4.7E-05	0.00%
sodium phosphate	4300	0.29					
					sum	2.0E+00	

## E Reactivity of chloramines with dimethylamine, phenol, chlorophenols, hydroquinone and benzoquinone



**Figure E.1.** Major reaction pathways for the reaction of trichloramine with (a) dimethylamine, (b) hydroquinone and (c) phenol. The  $k_{\text{app}}$  in (a) and (b) are the measured values at pH 7 and 5, respectively. The  $k_{\text{app}}$  in (c) correspond to the values used in the model for the reaction of trichloramine with phenol at pH 5 and room temperature (22–23 °C).



**Figure E.2.** Measured benzoquinone formation from the reaction of hydroquinone (100  $\mu\text{M}$ ) with (a) trichloramine and (b) free chlorine. The slope of the measured benzoquinone formation depends on the trichloramine concentration and reveals that the benzoquinone yield was about 80% for the reaction of trichloramine with hydroquinone. The same conclusion cannot be drawn for the free chlorine reaction since benzoquinone was not stable in presence of free chlorine (Figure E.3). (c) The reaction of trichloramine (7.4  $\mu\text{M}$ ) with hydroquinone (100  $\mu\text{M}$ ) leads to a fast, immediate benzoquinone formation and a slower benzoquinone formation thereafter, which might be induced by primary or secondary reaction products.

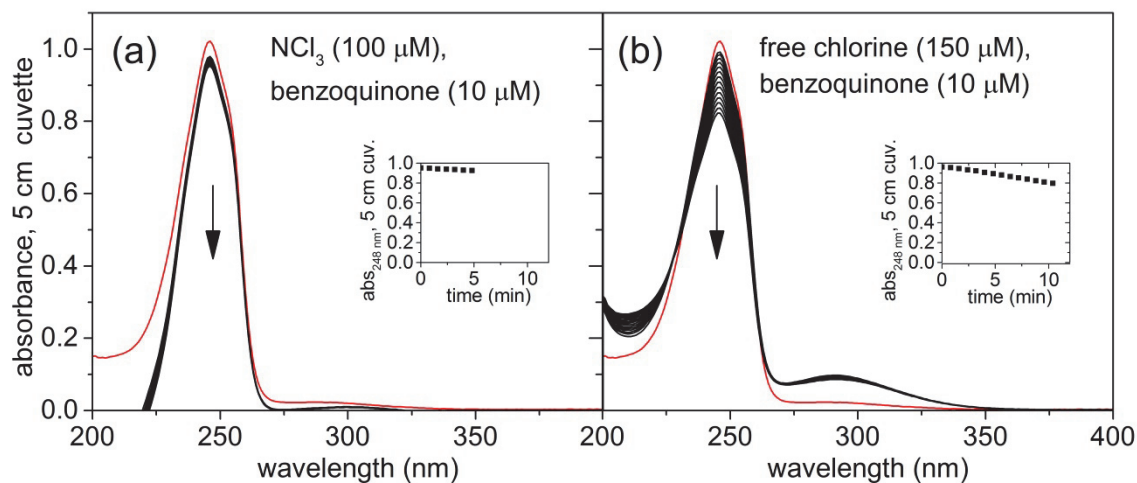


**Figure E.3.** Evolution of the absorbance of benzoquinone (10  $\mu\text{M}$ ) in presence of (a) trichloramine (100  $\mu\text{M}$ ) and (b) free chlorine (150  $\mu\text{M}$ ) at pH 7 (phosphate buffer, 5 mM). The spectrum of benzoquinone (10  $\mu\text{M}$ ) is shown by the red line. The spectrum of the reaction product in (a) is corrected for the trichloramine absorbance (100  $\mu\text{M}$ ). Due to the high absorbance of trichloramine at wavelengths  $< 230$  nm, the spectrum was out of measurable range of the instrument for  $\lambda < 230$  nm and should therefore not be considered.

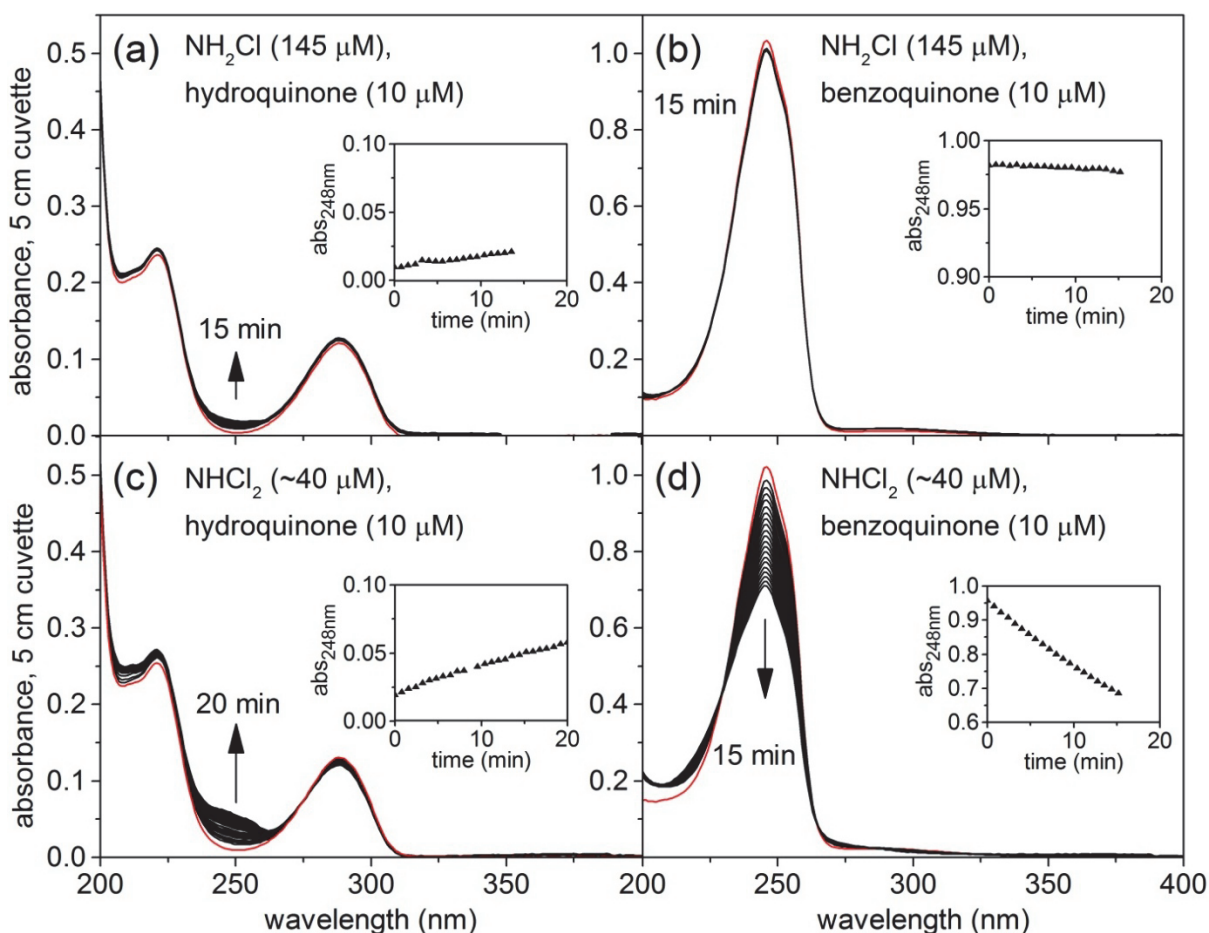


**Figure E.4.** Evolution of the absorbance after the reaction of (a, b) monochloramine (145  $\mu\text{M}$ ) and (c, d) dichloramine ( $\sim 40$   $\mu\text{M}$ ) with hydroquinone (10  $\mu\text{M}$ ) and benzoquinone (10  $\mu\text{M}$ ) at pH 7 (phosphate buffer, 5 mM). The red lines represent the absorbance of hydroquinone (10  $\mu\text{M}$ ) and benzoquinone (10  $\mu\text{M}$ ), respectively. All spectra were corrected for the absorbance of (a, b) the monochloramine (145  $\mu\text{M}$ ) and (c, d) the dichloramine ( $\sim 40$   $\mu\text{M}$ ) absorbance. The insets show the evolution with time, note that the y-axes have different scales. The dichloramine solution was produced by lowering the pH of a monochloramine solution but keeping the pH constantly above 4.5 to avoid trichloramine formation. The dichloramine solution still contained a small portion of monochloramine, which could interfere in the measurements.

## References

Borgmann-Strahsen, R. (2003). "Comparative assessment of different biocides in swimming pool water." *International biodeterioration & biodegradation* 51(4): 291-297.

Gazda, M., K. Kumar and D. W. Margerum (1995). "Nonmetal redox kinetics - oxidation of bromide ion by nitrogen trichloride." *Inorganic Chemistry* 34(13): 3536-3542.

Goeres, D., T. Palys, B. Sandel and J. Geiger (2004). "Evaluation of disinfectant efficacy against biofilm and suspended bacteria in a laboratory swimming pool model." *Water research* 38(13): 3103-3109.

Held, A. M., D. J. Halko and J. K. Hurst (1978). "Mechanisms of chlorine oxidation of hydrogen peroxide." *Journal of the American Chemical Society* 100(18): 5732-5740.

Judd, S. J. and G. Bullock (2003). "The fate of chlorine and organic materials in swimming pools." *Chemosphere* 51(9): 869-879.

McKay, G., B. Sjelín, M. Chagnon, K. P. Ishida and S. P. Mezyk (2013). "Kinetic study of the reactions between chloramine disinfectants and hydrogen peroxide: Temperature dependence and reaction mechanism." *Chemosphere* 92(11): 1417-1422.

Pinkernell, U., B. Nowack, H. Gallard and U. von Gunten (2000). "Methods for the photometric determination of reactive bromine and chlorine species with ABTS." *Water Research* 34(18): 4343-4350.

Soltermann, F., T. Widler, S. Canonica and U. von Gunten (2014). "Comparison of a novel extraction-based colorimetric (ABTS) method with membrane introduction mass spectrometry (MIMS): Trichloramine dynamics in pool water." *Water Research* 58: 258-268.



# **Chapter 3**

**Software for the valve control of a membrane introduction  
mass spectrometer (MIMS 2000) and for MIMS data  
analysis: MIMS-VICI Driver and MIMS-VICI Analysis**

Fabian Soltermann, Philippe Périsset and Urs von Gunten (2014)

## **Abstract**

Membrane inlet mass spectrometry (MIMS) is a widely used technique to measure volatile and semi-volatile substances in environmental samples. It allows for online and on-site measurements of multiple analytes. To measure and analyse multiple samples over a long time-period, it is essential to control automatically the inlet valve of the MIMS and to record the temporal sequence of the valve position. The data of the mass spectrometer (MS) must be analysed in connection to the valve position. A software (MIMS-VICI Driver) was developed to operate the inlet valve of a MIMS device (MIMS 2000) manually or with a defined method. Furthermore, the software monitors continuously the valve position. A second software (MIMS-VICI Analysis) was developed to facilitate the analysis of the MS data for the three standard measurement techniques (flow-injection, steady-state and continuous-flow measurements). Thereby, the original data set is reduced drastically to an essential data set without work-intensive and arbitrary data processing such as manual peak finding and analysis. Both programs were successfully tested in the laboratory and in a field campaign with long-term measurements.



### 3.1 Introduction

Membrane introduction mass spectrometry (MIMS) is an analytical technique with broad applications in the field of environmental chemistry and biology due to its ability to measure volatile and semi-volatile compounds in gaseous, liquid and solid samples (Ketola et al., 2010; Mächler et al., 2012). The technique is based on the coupling of a mass spectrometer (MS) with a membrane inlet, which separates the sample from the vacuum chamber of the MS. Commonly, a peristaltic pump aspirates the sample and pumps it via the inlet valve to the membrane. The analyte pervaporates through the membrane, a process which consists of the adsorption of the analyte on the membrane, the permeation through the membrane and the desorption into the vacuum (Johnson et al., 2000). The diffusion of the analyte through the membrane is often the rate limiting step. The maximal analyte response depends on the steady-state permeation of the analyte through the membrane which can be calculated with Fick's Law

$$I_m(x, t) = -AD \left( \frac{\partial C_m(x,t)}{\partial x} \right) \quad (3.1)$$

where  $I_m(x, t)$  is the analyte flow ( $\text{mol sec}^{-1}$ ),  $A$  the membrane surface ( $\text{cm}^2$ ),  $D$  the diffusivity ( $\text{cm}^2 \text{sec}^{-1}$ ), which is a property of the analyte and the membrane, and  $C_m(x, t)$  is the concentration of the analyte  $m$  at time  $t$  and depth  $x$  in the membrane (Johnson et al., 2000). Hence, the gradient of the concentration of the analyte in the membrane  $\frac{\partial C_m(x,t)}{\partial x}$  is decisive for the analyte flow through the membrane. This gradient can also be expressed using Henry's Law ( $C_m = SP_m$ ) which results in an equation for the total fluence of the analyte  $m$  ( $I_{\text{total},m}$  ( $\text{mol s}^{-1}$ )) as follows

$$I_{\text{total},m} = ADS(P_m/L) \quad (3.2)$$

where  $S$  is the solubility of the analyte ( $\text{mol atm}^{-1} \text{cm}^{-3}$ ),  $P_m$  the partial pressure (atm) of the analyte  $m$  (Johnson et al., 2000) and  $L$  the membrane thickness (cm). The most frequently used membrane in MIMS analysis is a silicon membrane, which renders MIMS an appropriate technique for the measurement of volatile, nonpolar substances. Equation 3.2 also illustrates that the fluence of the analyte into the vacuum chamber of the MS is positively correlated to the membrane surface and negatively to the membrane thickness. Several interfaces are known for the membrane introduction, whereof the most frequently used are shown in Figure 3.1.

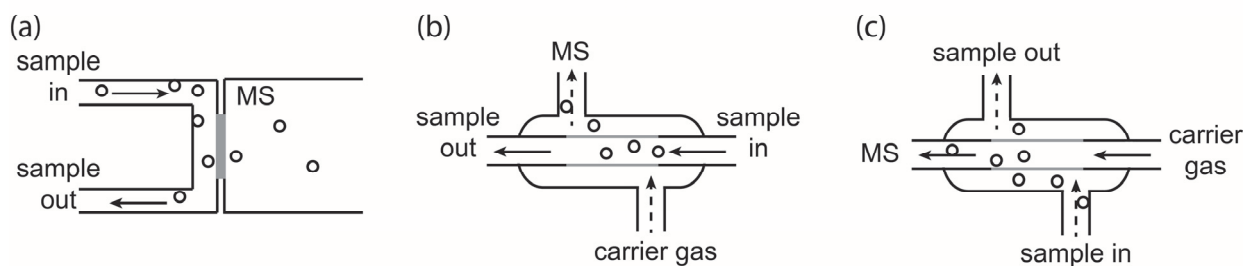


**Figure 3.1:** Examples of interfaces for membrane (gray) introduction with (a) a flat sheet membrane, (b) a sample flow through the membrane tube and (c) a sample flow around the membrane tube.

A thin membrane with a high surface increases the flux of the analyte and consequently its signal in the MS. Increasing temperature can also maximize analyte flux since diffusivity, solubility and partial pressure are dimensions which strongly depend on temperature. However, all aforementioned parameters must be optimized because an increased analyte flux is always accompanied by an increased flux of the sample matrix through the membrane. Under optimized conditions a high analyte flux is reached, while the membrane still discriminates the sample matrix. This results in a high signal-to-noise ratio. A last factor is the sample flow velocity. High sample flow in front of the membrane ensures that there is no analyte concentration drop on the membrane surface due to the permeation into the membrane. Low sample flow improves the contact with the membrane surface. In this study, MIMS was operated with a sample flow of  $5\text{--}15\text{ mL min}^{-1}$ .

The MIMS differs from more conventional MS systems such as liquid chromatography-MS (LC-MS) or gas chromatography-MS (GC-MS) mainly by the fact that there is no chromatographic separation. Furthermore, no sample pre-treatment, such as for instance salt addition to the sample, is necessary and using a flat sheet membrane allows for measurements without a carrier gas. This results in a number of advantages and disadvantages comparing MIMS with conventional MS systems (Table 3.1). MIMS facilitates online and on-site measurements with a temporal resolution, which is only restricted by the membrane transport rate. The price for the fact that online measurements are feasible is that there is no separation of the compounds. Therefore, analytes can only be measured if they have specific ions  $m/z$  which are free of interferences. If this is the case, multiple analytes can be measured simultaneously by monitoring the corresponding ions. MIMS measurements are commonly conducted by one of the three following analysis methods: (i) flow-injection, (ii) steady-state or (iii) continuous-flow measurements (Figure 3.2). (i) In steady-state measurements, the sample is measured when a steady-state signal is reached (Figure 3.2a). The time to reach a steady-state depends on

**Table 3.1:** Comparison of membrane inlet systems with systems containing a chromatographic separation prior to the MS.

	<b>Strengths</b>	<b>Weaknesses</b>
Membrane introduction	<ul style="list-style-type: none"> <li>- no sample pre-treatment</li> <li>- on-line, continuous</li> <li>- on-site possible</li> <li>- small matrix effects</li> </ul>	<ul style="list-style-type: none"> <li>- requires a compound specific ion</li> <li>- resolution time limited by permeation through membrane</li> <li>- requires considerable sample volume</li> </ul>
Liquid / gas-chromatography	<ul style="list-style-type: none"> <li>- analyte seperation</li> <li>- measurement of the ion with the highest abundance</li> </ul>	<ul style="list-style-type: none"> <li>- limited by compound stability in the chromatography</li> <li>- discrete measurements</li> </ul>

the analyte as well as on its concentration and on parameters such as membrane temperature and sample flow. (ii) Flow-injection is a method in which the sample is flowing in front of the membrane for a short, defined time period, which is commonly in the range of 30–180 s (Figure 3.2b). Thereafter, the sample is washed out by water. The MS signal increases in the first phase and decreases again during the washing out. The analyte is quantified by analysing the peak height. This method is used to measure analytes which need a long time to reach a steady-state signal or which are present in high concentrations. Additionally, this method is an option for measurements with restricted sample volume. (iii) Continuous-flow measurement means that one sample is continuously measured for a longer time period (Figure 3.2c). Changes in the signal correspond directly to changes of the analyte concentration in the sample if the temporal variation of the concentration is not faster than the transport of the analyte through the membrane. This allows to monitor the evolution on an analyte in the sample with a high temporal resolution.

Because of its ability to measure multiple analytes online and without sample pre-treatment, MIMS analyses are used in a wide field of applications such as bioreactor studies on microbiological and enzymatic activity (i.e. medical research, pharmaceutical production and environmental sciences), measurements of volatile and semi-volatile contaminants in the environment and monitoring of industrial processes or disinfection by-products in pool water (Johnson et al., 2000; Kristensen et al., 2010; Soltermann et al., 2014b).

Because many of these applications require measurement times in the order of hours and days and the MS measures one ion every 100–1000 ms, an efficient data processing is essential. The MIMS used in this study was a commercially available device named MIMS 2000, which is suited for on-site measurements. Unfortunately, only a software to operate the MS (Quadera) and a very basic software to control the inlet valve were delivered. As a consequence, three

important requirements for efficient measurements were not met by the MIMS 2000 and the associated software: (i) the operation of the inlet valve was not user-friendly, (ii) the MS data could not be linked with the corresponding position of the inlet valve, which is mandatory to interpret the MS data when measuring multiple samples and (iii) no automatic data analysis

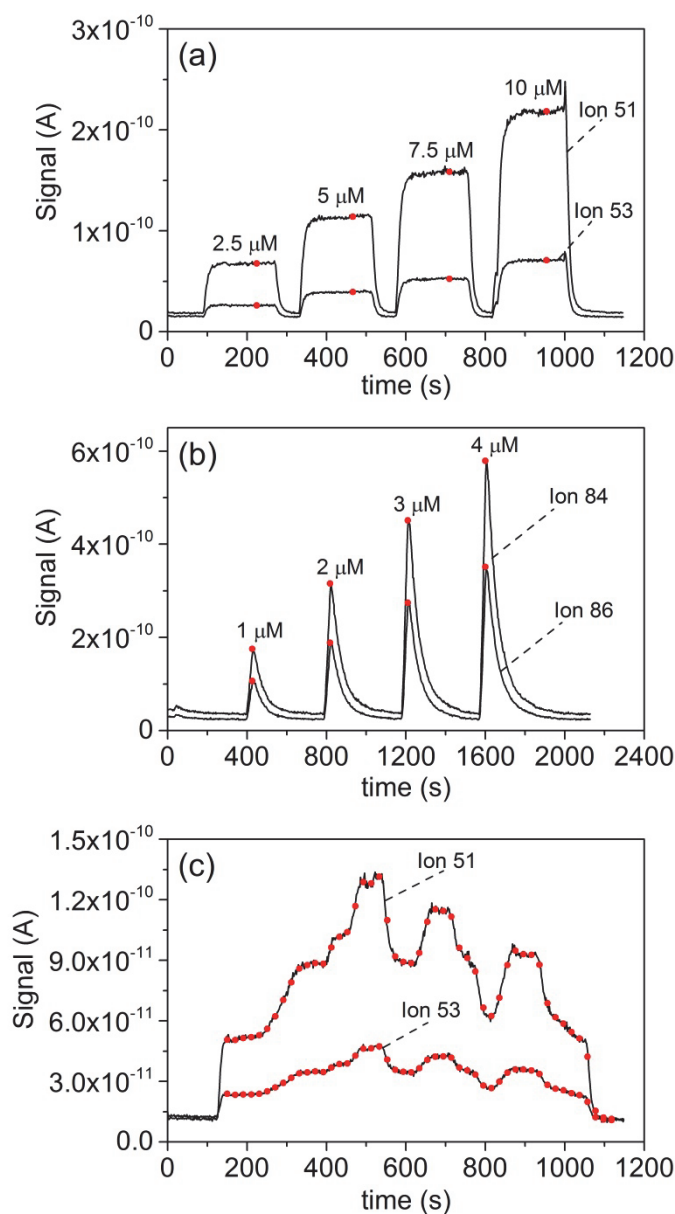


**Figure 3.2:** MS-signal during (a) the calibration of monochloramine (0–10  $\mu\text{M}$ ) with a steady-state measurement, (b) the calibration of trichloramine (0–4  $\mu\text{M}$ ) with a flow-injection measurement and (c) a continuous-flow measurement of a changing monochloramine solution. One ion is measured each 0.5 s. The red dots are the computed results with the software MIMS-VICI Analysis. For the continuous-flow measurement (c) an interval of 20 s was chosen.

such as peak finding or analysis of steady-state signals was provided. Therefore, two software were engineered to facilitate a routine control of the inlet valve and to perform efficient data analysis without work-intense and arbitrary manual peak recognition or mean determination.

## **3.2 Materials and Methods**

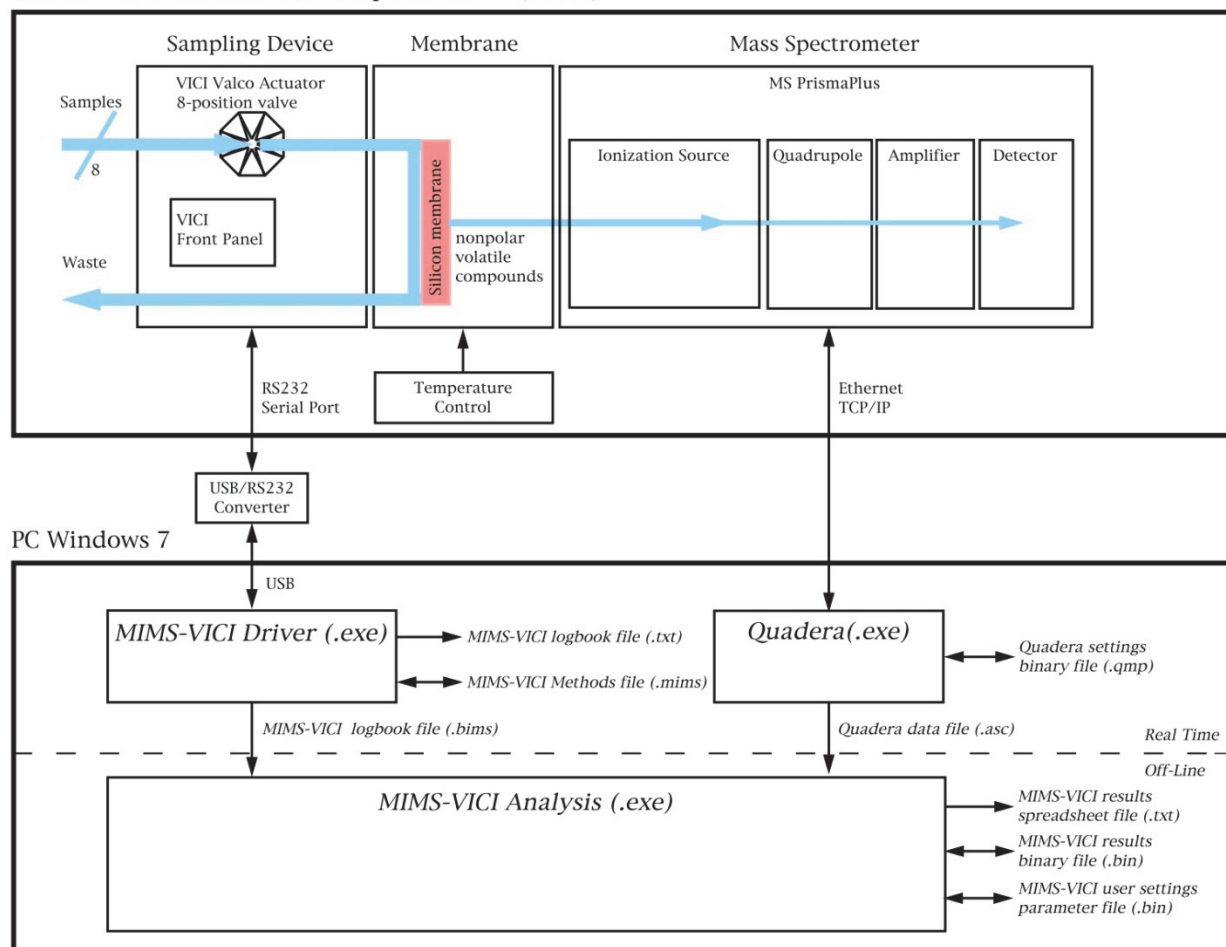
### **3.2.1 Programming environment**

MIMS-VICI Driver and MIMS-VICI Analysis were developed in a programming environment called Laboratory Virtual Instrument Engineering Workbench (LabView, National Instruments). LabView has a visual programming language which supports the development of software for data processing, instrument control and automation of processes. LabView allows for a user-friendly software handling since it facilitates the creation of user interfaces.

### **3.2.2 Overview of MIMS 2000 and its associated software**

MIMS 2000 is composed by a sampling device (8-position inlet valve), a membrane inlet (temperature-controlled by a thermostat) and the MS-part (consisting of an electron ionization source, a quadrupole, an amplifier and a detector) (Scheme 3.1). This hardware is controlled by two programs: (i) The MIMS-VICI Driver software operates the inlet valve and (ii) the Quadera software controls the MS. Both software have an own user interface and work independently. Data on temporal positions of the inlet valve were generated and saved with the MIMS-VICI Driver while data on analyte signals are collected and saved with the Quadera software. The MIMS-VICI Analysis software enables to link both data. After loading the two data sets, MIMS-VICI Analysis also facilitates the data processing by automation of peak finding or steady-state analysis. Computed results can be saved as a spreadsheet file and used for further treatment (e.g., with excel).

## Membrane Introduction Mass Spectrometer (MIMS)



**Scheme 3.1:** Overview of MIMS 2000 and its associated software (from Soltermann et al. (2014a)). The programs *MIMS-VICI Driver* and *MIMS-VICI Analysis* were developed in this study while *Quadera* is a commercially available software.

## 3.3 Results and Discussion

### 3.3.1 MIMS-VICI Driver

The software MIMS-VICI Driver consists of two interfaces to operate the inlet valve ('Manually' and 'Method', SI Figure A.1 and A.2) and one interface which allows to export a logbook of the valve positions. The inlet valve can be controlled by three means: (i) directly on the front panel of the device, (ii) manually or (iii) automatically with the software MIMS-VICI Driver. On the interface 'Manually', the positions of the inlet valve can be named and the inlet valve can be manually set to a position. Additionally, the front panel can be locked to prevent unwanted interactions. On the interface 'Method', a method can be defined which sets the inlet valve automatically to the desired position for a defined time period.

Figure 3.3 shows the interface 'Logbook' on which data about all the changes of the inlet valve position are recorded (absolute time, time on this position, position, position name, type of change (front panel, manually, method)). This data can be exported (as .txt and .bims) to be used by other software such as Excel or MIMS-VICI Analysis.

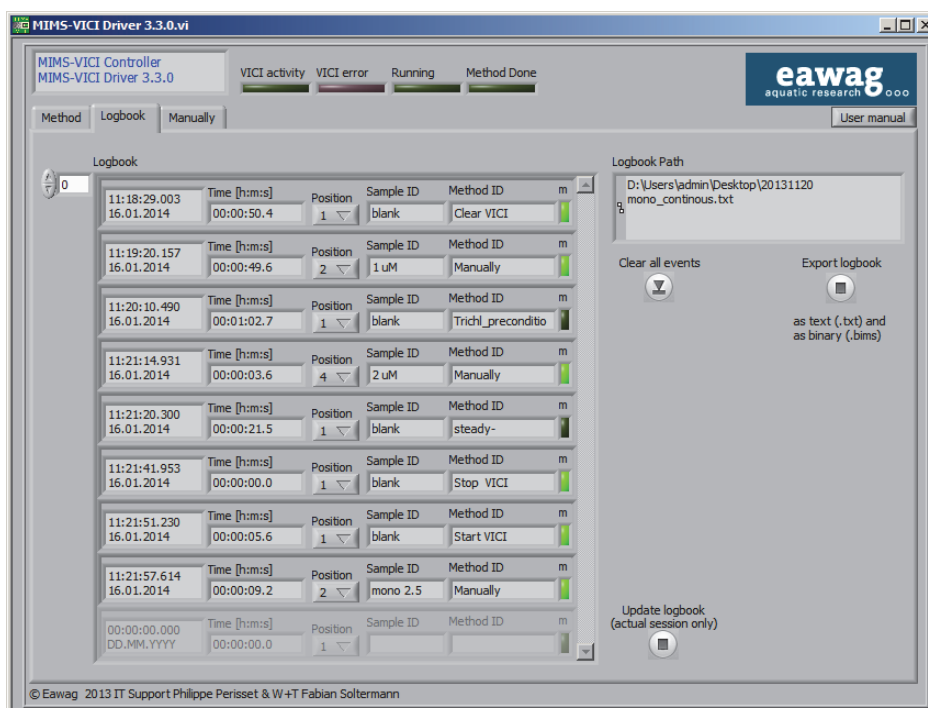


**Figure 3.3:** The interface 'Logbook' shows a record of data about all valve positions during the running time of the software MIMS-VICI-Driver.



### 3.3.2 MIMS-VICI Analysis

The software MIMS-VICI Analysis helps to combine and treat data of the mass spectrometer (Quadera) and the inlet valve (MIMS-VICI Driver). On the first two interfaces, data from Quadera and MIMS-VICI Driver can be loaded, illustrated and labelled (SI, Figure B.1 and B.2). These two data sets are linked and illustrated in one single graph on the next interface (Figure 3.4).

This facilitates decisively the interpretation of the MS data of long-term measurements with several samples. With the software provided by the manufacturers, no information on the valve position is automatically gathered although no analysis of the MS-signal is possible without knowing the corresponding valve position.

Raw data of long-term measurements with MIMS consist of large data matrixes since commonly several ions are measured in various samples. According to the settings of the MS, one ion is measured every 100–1000 ms. This tremendous amount of data can be significantly reduced by performing a steady-state, flow-injection or continuous-flow analysis, which are

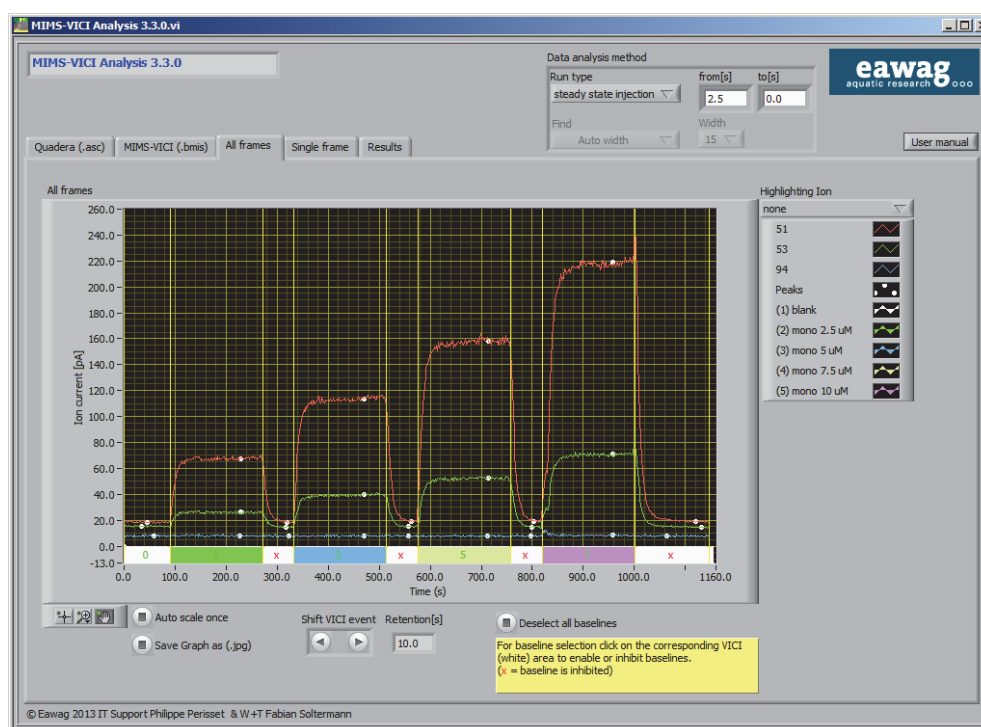


**Figure 3.4:** This interface shows a graph including the MS signal (red, green and blue lines) as a function of time and the corresponding valve position (colored bars at the bottom of the graph). Changes of the valve position are indicated with yellow lines. Samples which are considered as baseline measurements are shown in white. Calculated mean values for each ion and sample are marked with a white dot.

supported by the software (SI, Text B.1). Furthermore, the data processing is less arbitrary than by a manual analysis. In the case that one sample shows some irregularities during the measurement, the software offers in the second last interface the option to manually analyse the data for individual samples (SI, Figure B.3). The results of the analysis are summarized in the last interface, which also allows for saving the performed data treatment and for exporting the result table (SI, Figure B.4).

### 3.3.3 Application

The two software were successfully applied during several experiments in the laboratory and a field campaign (Soltermann et al., 2014a; Soltermann et al., 2014b). Especially during a sampling campaign, the software MIMS-VICI Driver simplified the data collection by the automatic valve control and provided data on the valve position at any time. The campaign lasted for about one month, which resulted in a four dimensional (time, valve position, ion, ion signal) data matrix with about one million data points. Figure 3.5 shows the data of one sampling day and how this four dimensional data is illustrated with the software MIMS-VICI Analysis. The top graph in Figure 3.5 shows the whole data set with the measured ion currents for selected ions (colored lines) and the corresponding valve positions (colored bars at the bottom of the graph) as a function of time. The results of the performed steady-state analysis are included in the same graph (dots). To illustrate this better, the middle graph of Figure 3.5 provides a zoom into a section of the whole data set (27595.9–34416.8 s). In this graph, the mean values calculated from the steady-state analysis (white dots) are better visible. These computed results can be exported to an Excel table, which facilitates an efficient treatment of the reduced data set. The bottom graph of Figure 3.5 gives an example of how the reduced data can be illustrated. It shows the evolution of the signal for the ion 83 m/z for the samples of the 5 different valve positions.

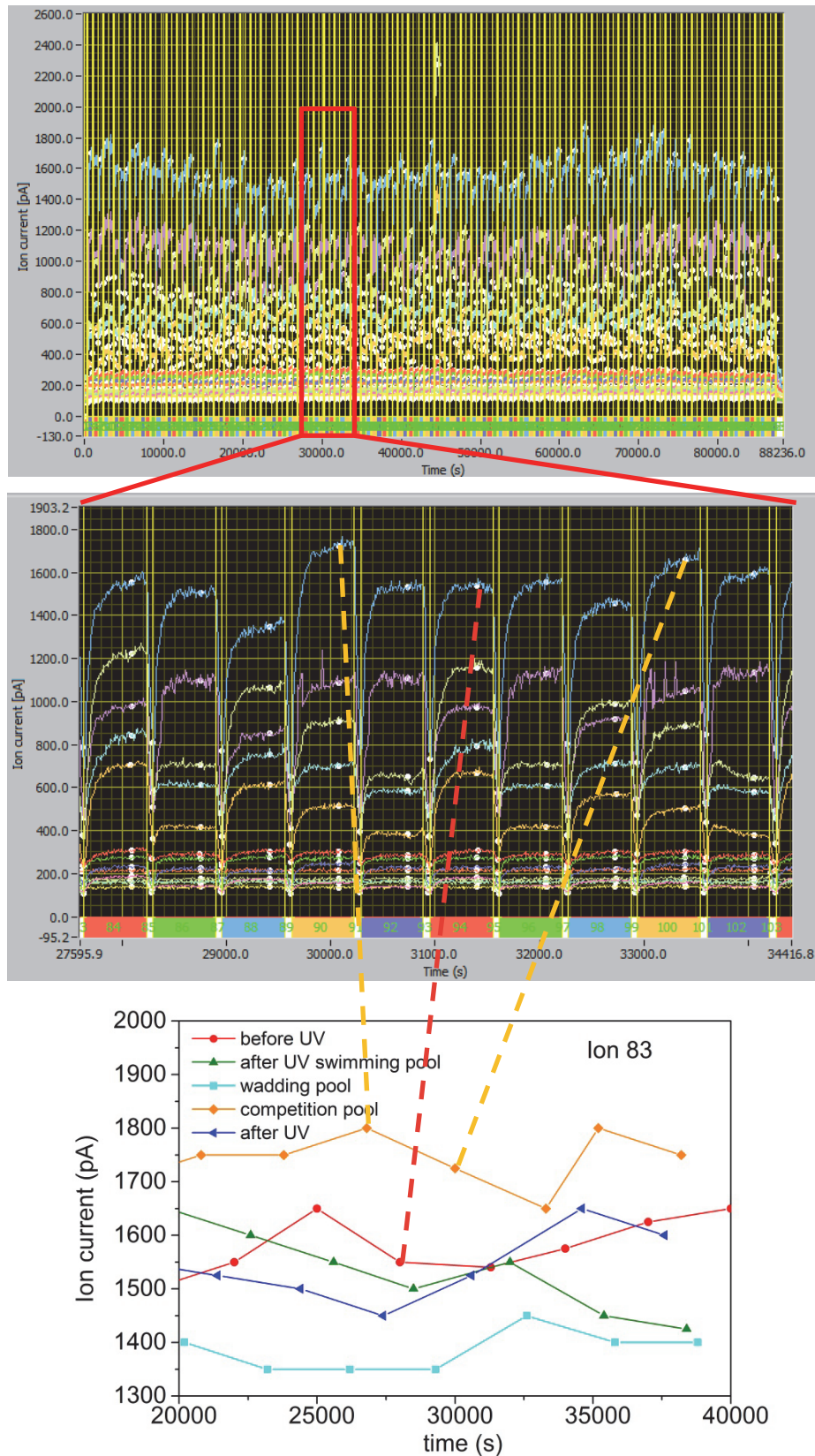


**Figure 3.5:** The top graph shows a one-day data set of the sampling campaign in a swimming pool facility. 5 samples were continuously measured for 12 minutes each and 14 ions were analysed for each sample (0.5 s measurement period). The middle graph shows a zoom into the

data set (27595.9–34416.8 s). The coloured lines show the evolution of the ion current for the measured ion. The colours at the bottom of the graph indicate the valve position. The dots show the automatically calculated mean values for the steady-state conditions. The mean values are exported to an Excel table. The bottom graph gives an example of the data analysis showing the evolution of the signal for the ion 83 m/z (representative for trihalomethanes) for the 5 different samples.

### 3.4 Conclusions

Membrane introduction mass spectrometry (MIMS) is a widely used method to analyse apolar, volatile compounds in environmental and laboratory samples. It is a suitable method for continuous and on-line monitoring of systems such as bioreactors or abiotic chemical reactors. However, so far measurements with MIMS 2000 suffered strong restrictions because data on the position of the inlet valve were not registered.

The software MIMS-Driver allows for an easy control of the inlet valve and monitors continuously the position of the inlet valve. This data facilitates the software MIMS-VICI Analysis to perform three types of data analysis: steady-state, flow injection and continuous-flow analyses. All three types of data analyses reduce significantly the data volume, which enables to analyse data of long-term measurements of multiple samples. Measurements in the laboratory and during a field campaign showed the necessity of the two software.

The case of the MIMS 2000 clearly shows that analytical devices are not always limited by their hardware. Often a large amount of data is quickly generated but its analysis requires a lot of tedious work. An automation of this work with a software provides the advantage of more efficiency and less arbitrariness.

## **Acknowledgements**

This study was supported by the Swiss Federal Office of Public Health (FOPH).

---

## References

Johnson, R. C., R. G. Cooks, T. M. Allen, M. E. Cisper and P. H. Hemberger (2000). "Membrane Introduction Mass Spectrometry: Trends and Application." *Mass Spectrometry Reviews* 19: 1-19.

Ketola, R. A., T. Kotiaho and F. R. Lauritsen (2010). Sample preparation in membrane introduction mass spectrometry. *Handbook of Sample Preparation* Chichester, England, John Wiley & Sons.

Kristensen, G. H., M. M. Klausen, V. A. Hansen and F. R. Lauritsen (2010). "On-line monitoring of the dynamics of trihalomethane concentrations in a warm public swimming pool using an unsupervised membrane inlet mass spectrometry system with off-site real-time surveillance." *Rapid Communications in Mass Spectrometry* 24(1): 30-34.

Mächler, L., M. S. Brennwald and R. Kipfer (2012). "Membrane Inlet Mass Spectrometer for the Quasi-Continuous On-Site Analysis of Dissolved Gases in Groundwater." *Environmental Science & Technology* 46(15): 8288-8296.

Soltermann, F., T. Widler, S. Canonica and U. von Gunten (2014a). "Comparison of a novel extraction-based colorimetric (ABTS) method with membrane introduction mass spectrometry (MIMS): Trichloramine dynamics in pool water." *Water Research* 58: 258-268.

Soltermann, F., T. Widler, S. Canonica and U. von Gunten (2014b). "Photolysis of inorganic chloramines and efficiency of trichloramine abatement by UV treatment of swimming pool water." *Water research* 56: 280-291.





# **Supporting Information for Chapter 3**

**Software for the valve control of a membrane introduction  
mass spectrometer (MIMS 2000) and for MIMS data  
analysis: MIMS-VICI Driver and MIMS-VICI Analysis**

Fabian Soltermann, Philippe Périsset and Urs von Gunten (2014)

## A Software “MIMS-VICI Driver”

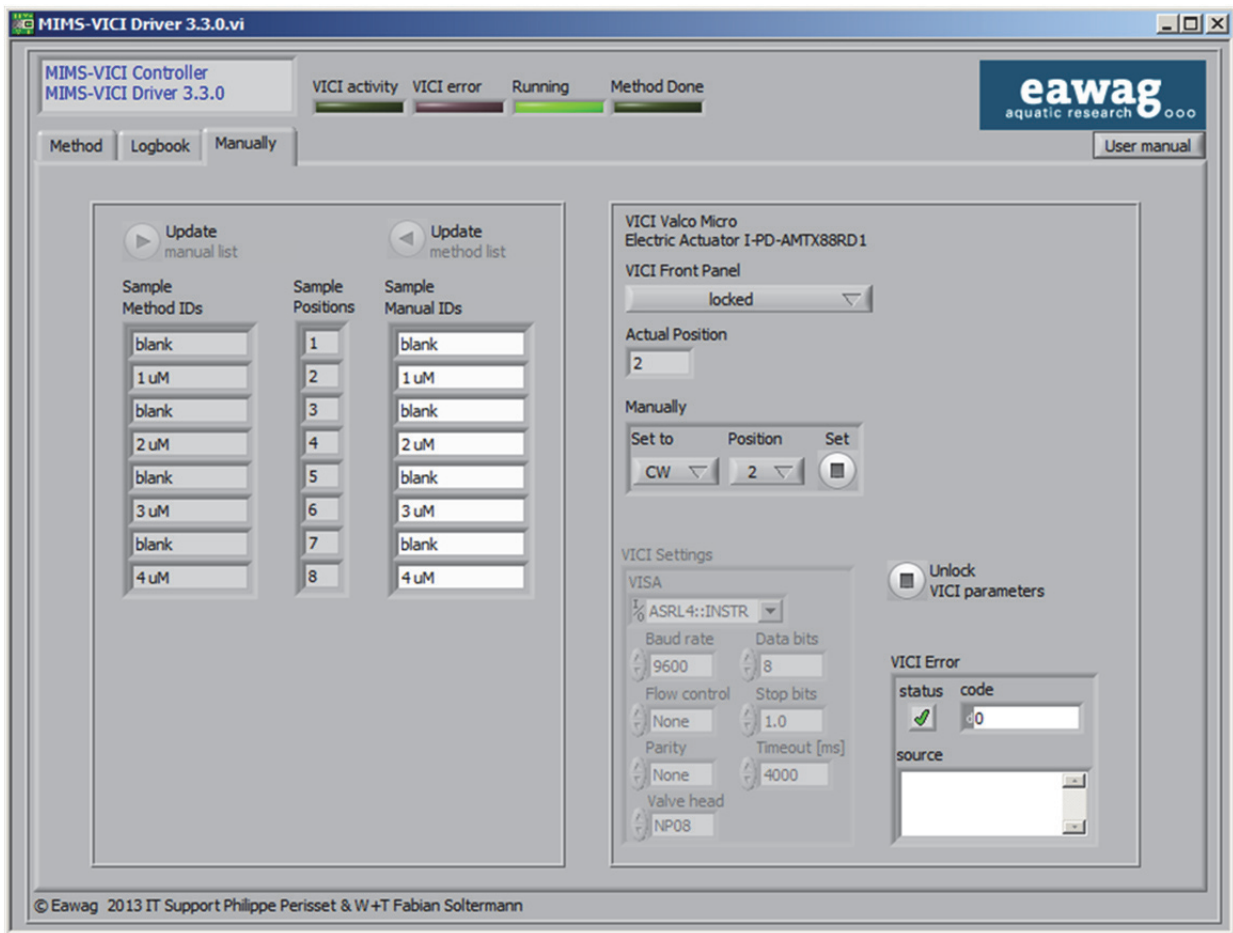


**Figure A.1.** The interface “Manually” of the MIMS-VICI Driver offers the option to define information on the inlet valve, to set the inlet valve position and to name the valve positions. Furthermore, the front panel on the hardware of the MIMS can be locked or unlocked.

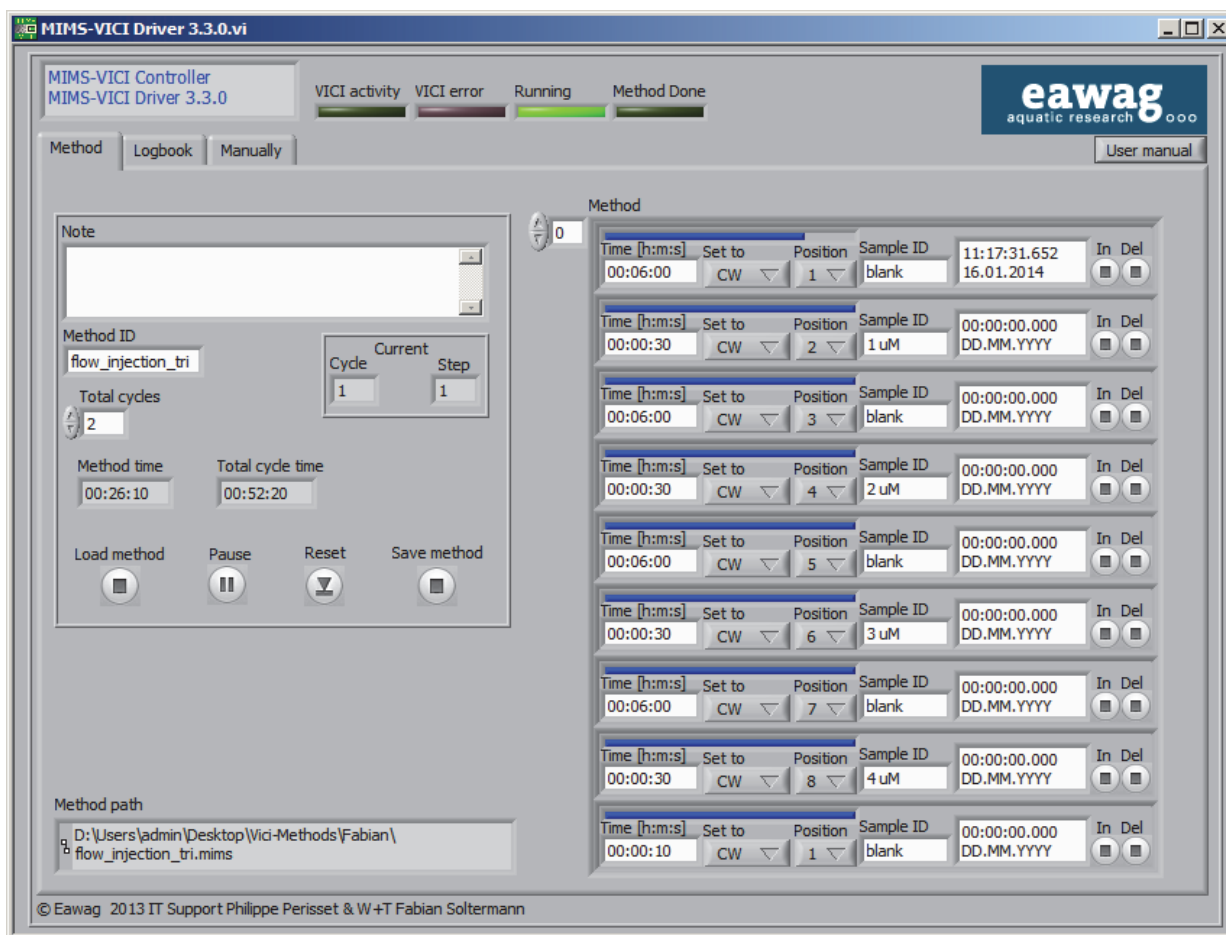


**Figure A.2.** The interface “Method” of the MIMS-VICI Driver offers the option to automatically control the inlet valve by defining a sequence of measurement steps (measurement time, turning direction, valve position and sample name) and the number of repetitions of the sequence.

## B Software “MIMS-VICI Analysis”

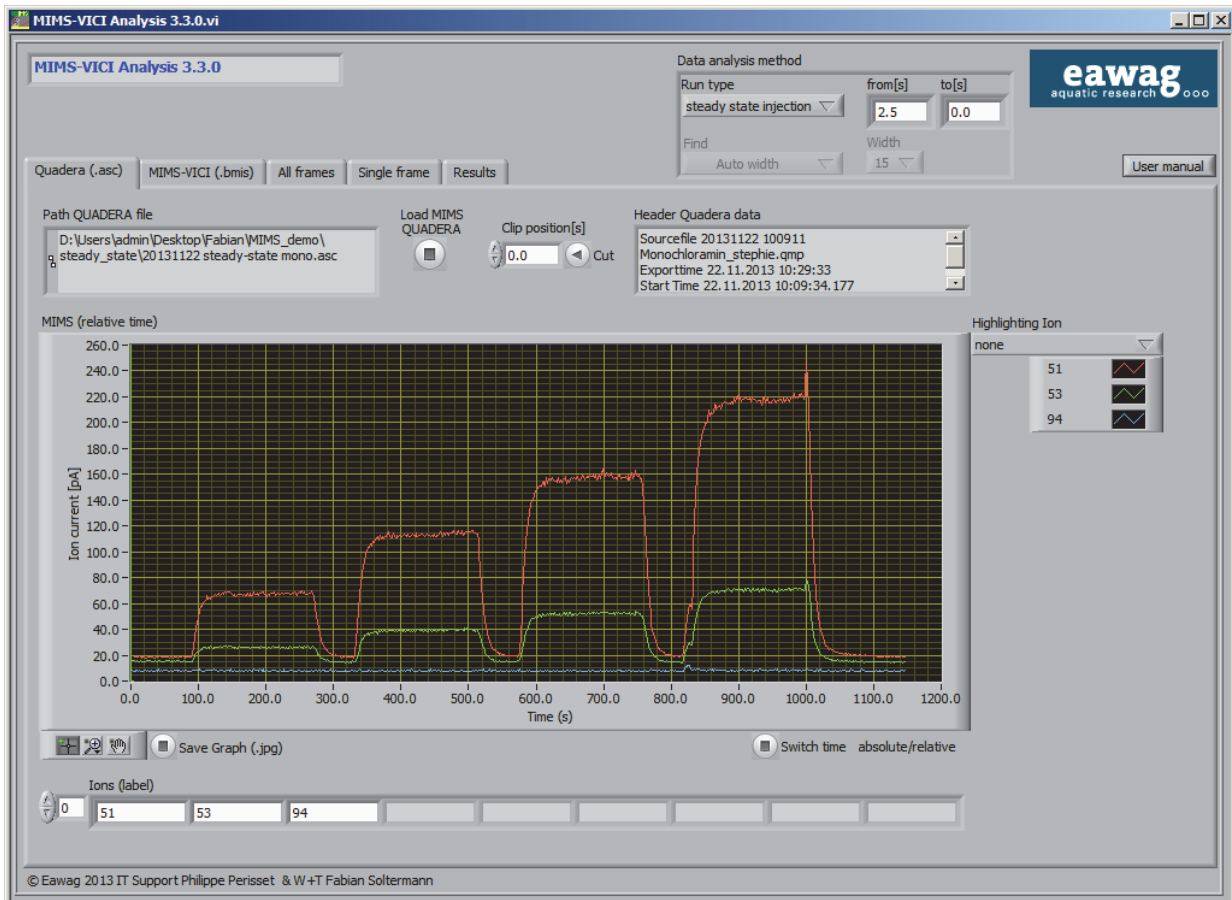


**Figure B.1.** Data of the MS signals can be loaded and plotted on this page.

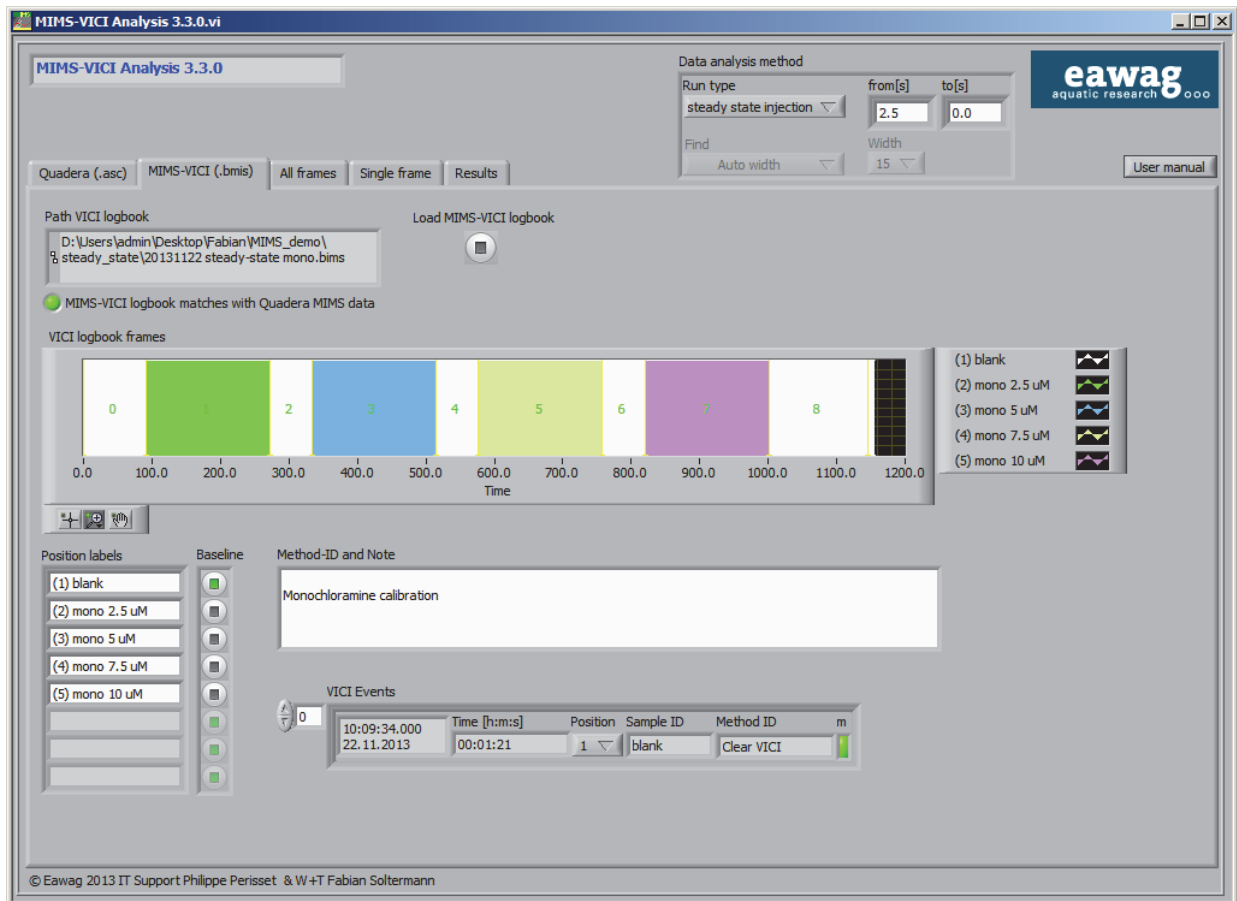


**Figure B.2.** The logbook on the inlet valve position can be loaded and the names of the valve positions adjusted. Furthermore, the valve position(s) of the blank sample(s) can be defined as baseline(s).

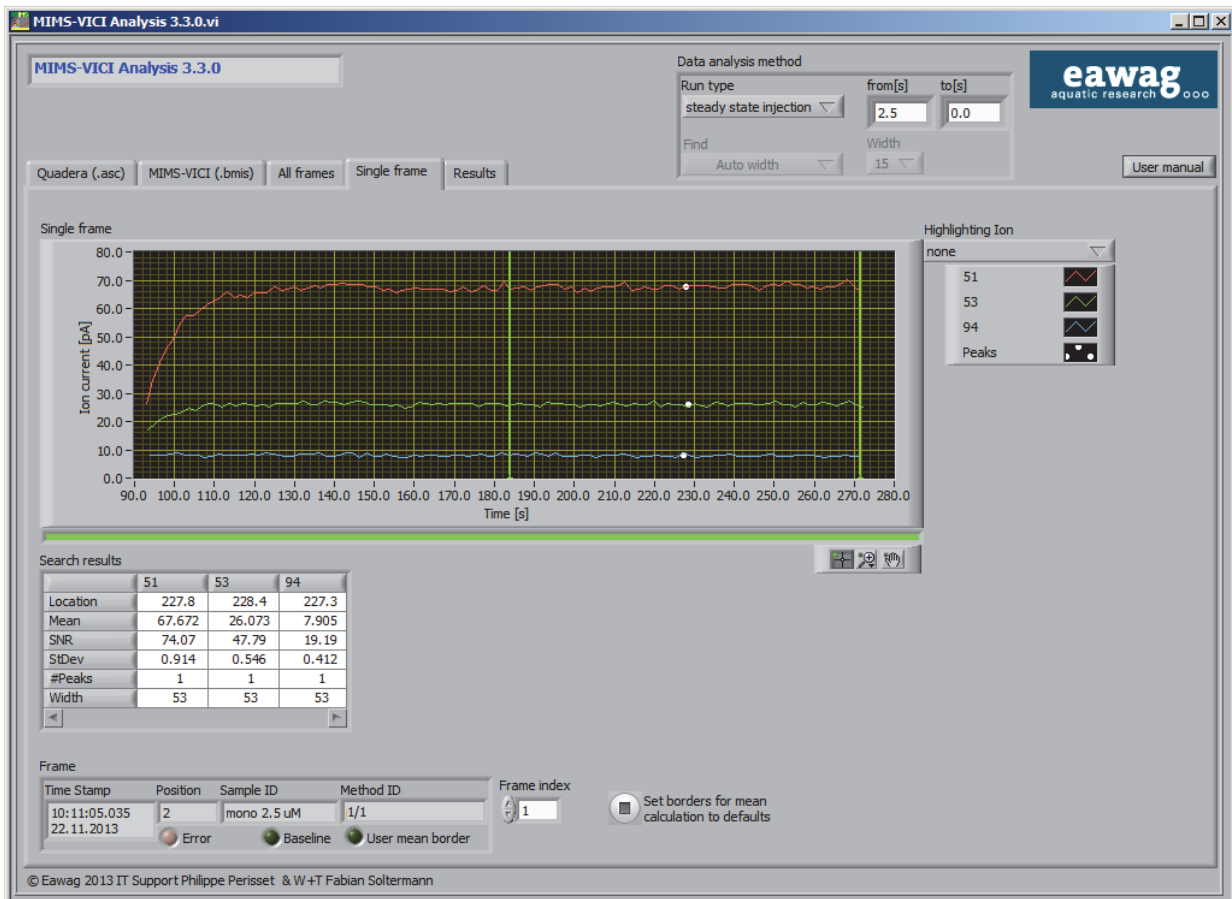


**Figure B.3.** The software offers the option to individually treat analysis of the steady-state signal by adjusting the limits for the mean calculation (green lines).

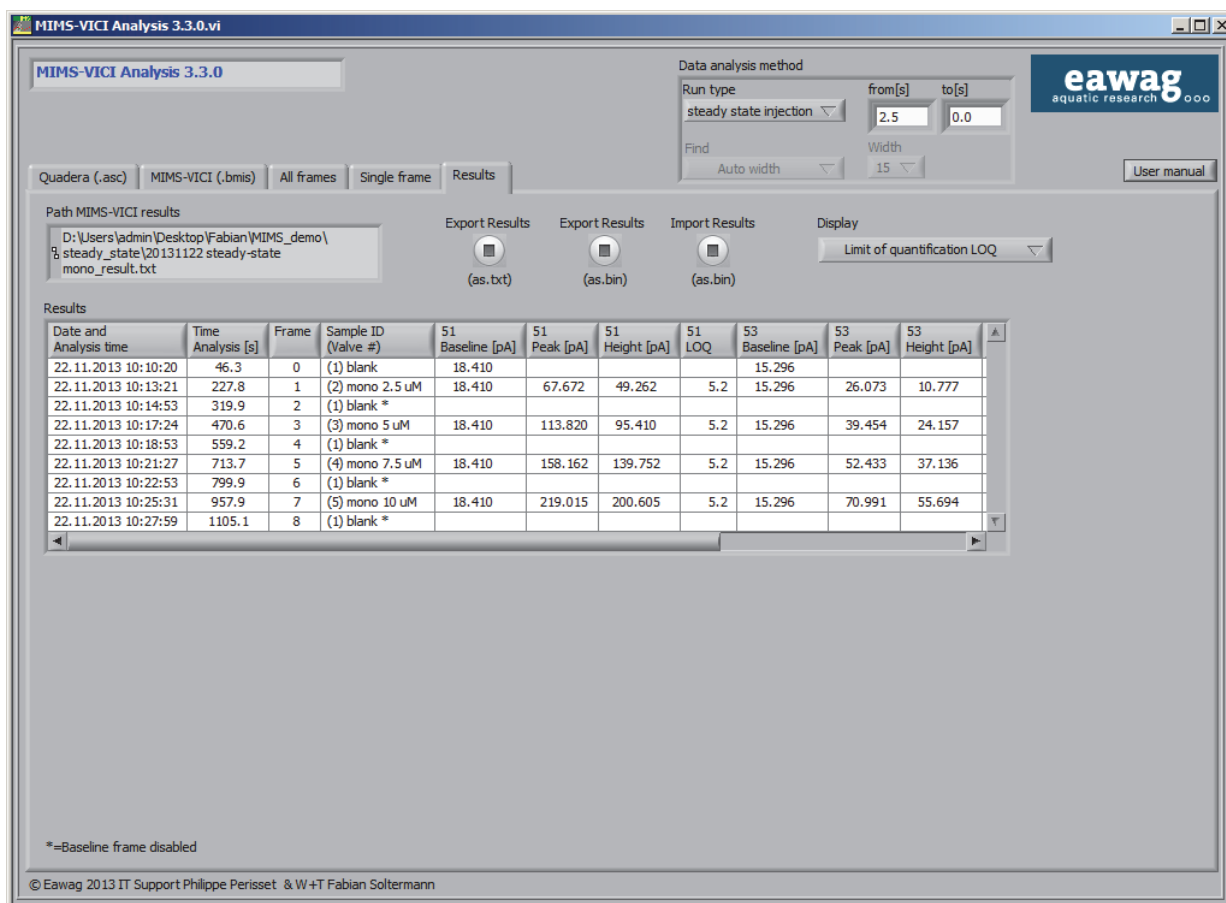


**Figure B.4.** A table containing all results can be saved as a .txt-file for further processing. The software also allows to save the data together with the current settings in order to reproduce treated data.

**Text B.1. Procedure for the computation of flow-injection, steady-state and continuous-flow analysis, inclusive baseline values.**

The software “MIMS-VICI Analysis” supports three types of data analyses: flow-injection, steady-state and continuous-flow analyses. All three methods have in common that the signal height/intensity is calculated by subtracting a baseline value from the signal peak. The user of the software defines which samples are treated as baseline values. In these samples, the baseline is calculated by adding  $2\sigma$  ( $\sigma$  = standard deviation of the sample) to the minima of the sample signal, which is found with a quadratic fit algorithm. The signal values for the three analyses types are computed as follows:

**Flow-injection analysis:** A quadratic fit algorithm is used to find the maxima of the sample peak. The user can set a parameter to define the number of points that are used in the fit algorithm.

**Steady-state analysis:** The sample peak is the mean value of the sample signals during the second half of the sampling period. The software offers the option to manually set the borders for the mean calculation if necessary.

**Continuous-flow analysis:** The user defines for which time-interval the samples are analysed. A signal value is extracted after every time-interval.



# Chapter 4

## **Comparison of a novel extraction-based colorimetric (ABTS) method with membrane introduction mass spectrometry (MIMS): trichloramine dynamics in pool water**

Fabian Soltermann, Tobias Widler,

Silvio Canonica and Urs von Gunten (2014)

*Water Research*, 58, 258-268

## Abstract

Trichloramine is a hazardous disinfection by-product, which is present in chlorinated swimming pools. Although it is primarily taken up by inhalation, the concentration in pool water is important to monitor pool water quality and to assess trichloramine mitigation strategies. To date, scarce data is available on trichloramine concentration in pool water due to the lack of a suitable and easily applicable analytical method. This study presents a novel low cost, colorimetric method which is easy to operate and suitable for on-site measurements of trichloramine concentrations  $\geq 0.05 \mu\text{M}$  ( $\geq 0.01 \text{ mg L}^{-1}$  as  $\text{Cl}_2$ ). The analytical method (termed “extraction-based ABTS method”) consists of, (i) trichloramine stripping from pool water samples, (ii) passing it through a solid phase filter, composed of silica gel impregnated with sulfamic acid to eliminate interferences and (iii) trichloramine reaction with the indicator 2,2'-azino-bis(3-ethylbenzothiazoline-6-sulfonic acid) diammonium salt (ABTS) to produce the colored  $\text{ABTS}^{\cdot -}$  radical, which is measured at  $\lambda = 405 \text{ nm}$  to determine the trichloramine concentration in the pool water sample. A comparison of the extraction-based ABTS method with membrane introduction mass spectrometry (MIMS) for 28 pool samples revealed a good correlation of the two methods.

The trichloramine concentration in pool samples is correlated to  $\text{HOCl}$ , which is the most important factor for its formation. Other parameters such as combined chlorine and pH play a minor role while no correlation between trichloramine and the urea or the TOC concentration was observed. On-site measurements with MIMS in a wading pool over 6 days with a time resolution of 1 h confirmed that trichloramine concentrations strongly responded to changes in free chlorine concentrations. A diurnal measurement of trichloramine with a time resolution of 20 min revealed that trichloramine concentrations reacted quickly and sensitively to the bather load and that urea is probably not the main precursor for its formation.

## 4.1 Introduction

Swimming is popular worldwide for recreation and sport. To provide safe pool water for customers, pool facilities face an optimization problem: to lower the formation of undesired disinfection by-products (DPBs) they have to reduce the disinfectant dose, with the consequential risk of hygienic problems. The variety of potential DBPs in pool waters is large (e.g. haloamines, nitrosamines, trihalomethanes, haloacetic acids) (Walse and Mitch, 2008; Richardson et al., 2010). Among these DBPs, the volatile trichloramine is of particular concern in indoor swimming pools since this malodorous compound is assumed to cause skin and eye irritations as well as irritations of the respiratory tract and possibly asthma (Massin et al., 1998; Bernard et al., 2003; Schmalz et al., 2011b).

Because the adverse health effects of trichloramine are mainly related to its presence in air, different methods for trichloramine measurement in the air of indoor pools were developed. Henry et al. (1995) introduced a method in which air is first aspirated through a filter (silica gel impregnated with sulfamic acid) to eliminate potential interferences from free chlorine and other chloramines before trichloramine is reduced to chloride by diarsenic trioxide. The trichloramine concentration is quantified by measuring the chloride concentration by ion chromatography (IC) after 180 minutes of continuous sampling. This method was adopted as a standard by the National Research and Safety Institute, France (INRS) and then used in various studies (Massin et al., 1998; Parrat et al., 2012). More recently, alternative methods such as colorimetric impinger methods (based on *N,N*-dipropyl-*p*-phenylene-diamine (DPD), which avoids the use of toxic diarsenic trioxide and IC analysis) were presented and applied for trichloramine measurement in indoor pool air (Schmalz et al., 2011b; Weng et al., 2011; Predieri and Giacobazzi, 2012; Fantuzzi et al., 2013).

Several studies reported trichloramine concentrations in indoor pool air of up to  $2 \text{ mg m}^{-3}$  but with most values below  $0.5 \text{ mg m}^{-3}$ , which is the recommended maximum level by the INRS and the World Health Organisation (WHO) (Héry et al., 1995; WHO, 2006; INRS, 2007; Weng et al., 2011; Parrat et al., 2012). It has been shown that trichloramine concentrations in indoor pool air depend on air ventilation and on the mass transfer from water to air induced by bather activity (Schmalz et al., 2011a; Weng et al., 2011).

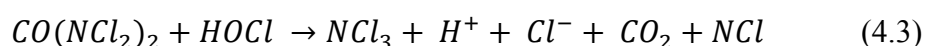
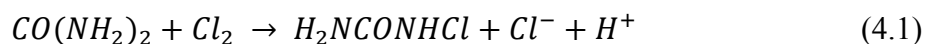
Since trichloramine is formed in the pool water, it is essential to measure it in the aqueous phase to evaluate pool water quality and to develop mitigation strategies. Trichloramine in pure solution and at a high concentration is commonly quantified by direct spectrophotometry ( $\epsilon = 190 \text{ M}^{-1} \text{ cm}^{-1}$  at  $\lambda = 336 \text{ nm}$ ) (Gazda et al., 1995), but multiple methods are available to measure

low concentrations of chloramines in real waters (Kinani et al., 2012). However, only a few of these methods are free of interferences and sensitive enough to measure trichloramine concentrations in pool water. Most of the methods suited for trichloramine analysis take advantage of the marked volatility of trichloramine, since its Henry's constant (mole fraction in the air / mole fraction in the water) of 435 is much higher than for the interfering species (e.g.  $\text{NH}_2\text{Cl}$ : 0.45,  $\text{NHCl}_2$ : 1.52,  $\text{HOCl}$ : 0.043) (Holzwarth et al., 1984). Gérardin et al. (2005) measured trichloramine in pool water by stripping trichloramine from pool water followed by trichloramine measurement in air with the diarsenic trioxide method. The sampling time was 1–2 hours in order to accumulate sufficient chloride for analysis by IC. In other studies, mass spectrometry (MS) was used in two different combinations, namely gas chromatography-MS (GC-MS) and membrane introduction MS (MIMS), to quantify trichloramine in drinking water and pool water (Shang and Blatchley, 1999; Weaver et al., 2009; Kosaka et al., 2010). GC-MS measurements have the advantage to minimize interferences due to the separation by the column. MIMS is favourable because it separates volatile, nonpolar compounds from others through a membrane, which facilitates on-site and online measurements without sample pre-treatment. However, only substances with unique fragments ( $m/z$  signals) can be analysed, otherwise interferences must be subtracted from the signal (Johnson et al., 2000). For trichloramine, only the fragment 88  $m/z$  is assumed to be free of interferences in pool water, but this fragment occurs with low abundance (Weaver et al., 2009). A drawback of MS-based methods is that they rely on expensive equipment and can only be operated by skilled personnel. *N,N*-diethyl-*p*-phenyldiamine (DPD)-based standard methods for chloramine analysis are inexpensive alternatives which can also be conducted by pool attendants (APHA, 2005). However, trichloramine concentrations are usually near or below the measurable range of DPD-based methods. Furthermore, it has been shown that the DPD methods suffer from interferences by the other inorganic chloramines ( $\text{NH}_2\text{Cl}$ ,  $\text{NHCl}_2$ ) and it is difficult to individually quantify the three inorganic chloramines by these methods (Shang and Blatchley, 1999; Shang et al., 2000).

Due to these analytical challenges, trichloramine concentrations in pool waters have only been measured in few studies, which yielded levels of up to  $150 \mu\text{g L}^{-1}$  as  $\text{Cl}_2$  ( $\sim 0.7 \mu\text{M}$ ), with most values in the  $20\text{--}100 \mu\text{g L}^{-1}$  range ( $0.1\text{--}0.5 \mu\text{M}$ ) (Gérardin et al., 2005; Li and Blatchley, 2008; Weaver et al., 2009).

Although various potential precursors are present in pool water, several studies suggest that trichloramine is mainly formed through the reaction of urea with molecular chlorine and hypochlorous acid (eqs. 4.1–4.3) (Blatchley and Cheng, 2010; De Laat et al., 2011; Schmalz et

al., 2011a). Thereby, it is assumed that the amide nitrogen of urea is first chlorinated by molecular chlorine ( $\text{Cl}_2$ , present in small concentrations during chlorination) and then further chlorinated by hypochlorous acid before trichloramine is released (Blatchley and Cheng, 2010).  $\text{NCl}$  in eq. 4.3 is a hypothetical intermediate, which further reacts to more stable nitrogenous species such as nitrous oxide ( $\text{N}_2\text{O}$ ).



Because urea concentrations in pool water are typically in the lower  $\text{mg L}^{-1}$  range (10–50  $\mu\text{M}$ ), it is in excess on a molar basis relative to free chlorine ( $\text{HOCl}/\text{OCl}^-$ ,  $\text{Cl}_2$ ), which is regulated at 0.2–0.8  $\text{mg L}^{-1}$  as  $\text{Cl}_2$  (3–11  $\mu\text{M}$ ) in Switzerland (De Laat et al., 2011; Schmalz et al., 2011a; SIA, 2013). However, conditions in small pools such as wading pools can change quickly due to temporal changes of bather load and chlorine addition. Schmalz et al. (2011a) assumed that under pool water conditions, only about 1 % of the urea is converted to trichloramine. They showed that the yield of trichloramine formation depends on the chlorine:urea ratio and the pH. An increasing trichloramine formation with decreasing pH for a constant free chlorine concentration was reported in other studies (Blatchley and Cheng, 2010; Hansen et al., 2012). Blatchley and Cheng (2010) also showed that trichloramine formation from the reaction of free chlorine with urea is a slow process. Furthermore, trichloramine concentrations might be related to combined chlorine concentrations since monochloramine can be chlorinated to trichloramine and trichloramine dechlorinated to monochloramine (Jafvert and Valentine, 1992). To date it is not entirely clarified which parameter (free chlorine, pH, precursor or combined chlorine) is mainly influencing the trichloramine concentration. It is only assumed that outgassing marginally affects the trichloramine mass balance in a swimming pool unless it is a shallow pool with high bather activity (wading pool) or with an unconventional water inlet (e.g. artificial waterfall, fountain) (Schmalz et al., 2011a; Weng et al., 2011).

To overcome the aforementioned problems of the currently available trichloramine measurement methods, this study aimed to develop a fast, robust and low-cost method for on-site trichloramine analysis, suitable for pool personnel. This method has a unique design and is based on the oxidation of 2,2-azino-bis(3-ethylbenzothiazoline-6-sulfonic acid) diammonium salt (ABTS), an indicator which was previously used for free chlorine and monochloramine measurements (Pinkernell et al., 2000). The method was validated by comparison with MIMS analysis using ultrapurified water and pool water samples. Furthermore, additional parameters

such as pH, free and combined chlorine and urea were measured to investigate their relationship to trichloramine concentration in pool water. In addition, on-line measurements were conducted in a pool facility to gain more information about trichloramine dynamics in swimming pools.

## 4.2 Materials and Methods

### 4.2.1 Reagents

#### *Chemicals*

All chemicals were analytical grade and used without further purification. Sodium hypochlorite (6–14 % active chlorine), ammonium chloride, ortho-phosphoric acid, silica gel 60, sulfamic acid and 2,2'-azino-bis(3-ethyl-benzothiazole-6-sulfonic acid) diammonium salt (ABTS) were purchased from Sigma-Aldrich. Sodium dihydrogenphosphate, sodium hydroxide pellets, hydrochloric acid, perchloric acid, titriplex III, urea and urease were obtained from Merck. Glass wool (silane treated) was purchased from Supelco. A “Barnstead nanopure” water purification system from Thermo Scientific was used to produce ultrapurified water.

#### *Chloramine, ABTS and buffer solutions*

Monochloramine ( $\text{NH}_2\text{Cl}$ ) stock solutions were produced as described previously (Soltermann et al., 2013). Dichloramine ( $\text{NHCl}_2$ ) stock solutions were produced freshly prior to each experiment by lowering the pH of a monochloramine solution. Perchloric acid was added dropwise to a stirred monochloramine solution until the pH remained almost stable, slightly above pH 4. Dichloramine was aged for more than one hour until the reaction was complete. During that time, dichloramine formation was monitored spectrophotometrically with a method described by Schreiber and Mitch (2005) in which absorptions at  $\lambda = 245$  and  $295$  nm ( $\text{NH}_2\text{Cl}$ :  $\epsilon_{245\text{nm}} = 445 \text{ M}^{-1}\text{cm}^{-1}$ ,  $\epsilon_{295\text{nm}} = 14 \text{ M}^{-1}\text{cm}^{-1}$ ;  $\text{NHCl}_2$ :  $\epsilon_{245\text{nm}} = 208 \text{ M}^{-1}\text{cm}^{-1}$ ,  $\epsilon_{295\text{nm}} = 267 \text{ M}^{-1}\text{cm}^{-1}$ ) were used for quantification. Trichloramine solutions were prepared by mixing ammonium chloride (5 mM) and hypochlorous acid (15 mM) with a dual syringe pump with a T-mixing system at pH 3.5. Perchloric acid was used to adjust the pH of the stock solutions. Trichloramine solutions were aged for at least 20 hours to ensure completion of the reactions. Trichloramine yield was constantly 42–46 % and analysis of the absorption spectra suggested that the solution did not contain  $\text{NHCl}_2$ . Trichloramine solutions were produced weekly and they were monitored spectrophotometrically ( $\epsilon_{336\text{nm}} = 190 \text{ M}^{-1}\text{cm}^{-1}$  and  $\epsilon_{360\text{nm}} = 126 \text{ M}^{-1}\text{cm}^{-1}$ ) before each experiment (Schurter et al., 1995). ABTS stock solutions (5 mM) were produced freshly daily. If not stated otherwise, phosphate buffer (0.1 M, pH 2.6) was used for the extraction-based ABTS method.

***Filter production (impregnated silica gel)***

Silica gel (particle size: 35–75  $\mu\text{m}$ ) was washed with ultrapurified water. 200 mL of a sulfamic acid solution (25 mg  $\text{L}^{-1}$ ) was added to 125 g of silica gel (dry weight). This mixture was dried with a rotary evaporator at 58°C and ~75–110 mPa until it became solid. Afterwards, the silica gel was dried overnight in an oven at 60 °C until the tap density (weight of silica gel in a mass flask after knocking several times on the mass flask) was ~0.77  $\text{g cm}^{-3}$  (tap density prior to impregnation was around 0.50  $\text{g cm}^{-3}$ ). To control the tap density after the drying process is important as silica gel retains trichloramine at low concentrations more efficiently under dryer conditions.

**4.2.2 Apparatus*****ABTS module***

The equipment for trichloramine measurement with the extraction-based ABTS method, except for the spectrophotometer, was placed in a box (40 cm  $\times$  32 cm  $\times$  30 cm) to make it suitable for transportation and on-site measurements. This device consists of four main parts (Figure 4.1): (i) an air pump and a pressure-reducing valve to provide a constant and adjustable air flow, (ii) an extraction impinger to strip trichloramine from the sample, (iii) a filter to reduce interferences by free chlorine and other chloramines, and (iv) a collection impinger containing an ABTS solution to quench and quantify trichloramine.

The air pump (Type N86KN.18,  $p_{\text{max}}$  2.4 bar, KNF, Balterswil, Switzerland) provided a constant air pressure and with the help of the reducing valve (Type FDV 30 KPZ, 0.5–2.5 bar, Balterswil, Switzerland), the air flow through the impingers was regulated. The resulting air flow was controlled with an air flow meter (Fisher Control). The pressure in the extraction impinger was above one bar due to the resistance of the frits in the impingers. A gate valve was installed before the first impinger to start and stop the air flow and to prevent a backflow of the liquid after stopping the pump. The impingers were 25 cm long and had an inner diameter of 16 and 14 mm for the extraction and the collection impinger, respectively. The frits (diameter: 8 mm, P 40 = 16–40  $\mu\text{m}$ ) were inclined to prevent the formation of big bubbles. The extraction and the collection impingers were connected with a U-shaped glass tube (inner diameter: 8 mm) which contained the filter material (impregnated silica gel). The filter material was filled into the glass tube and blocked on both sides with a ball of silane treated glass wool. The glass wool commonly absorbed trichloramine in the first measurements but could be recycled afterwards without influencing the trichloramine measurements. PVC tubing was used before the extraction impinger and after the collection impinger.



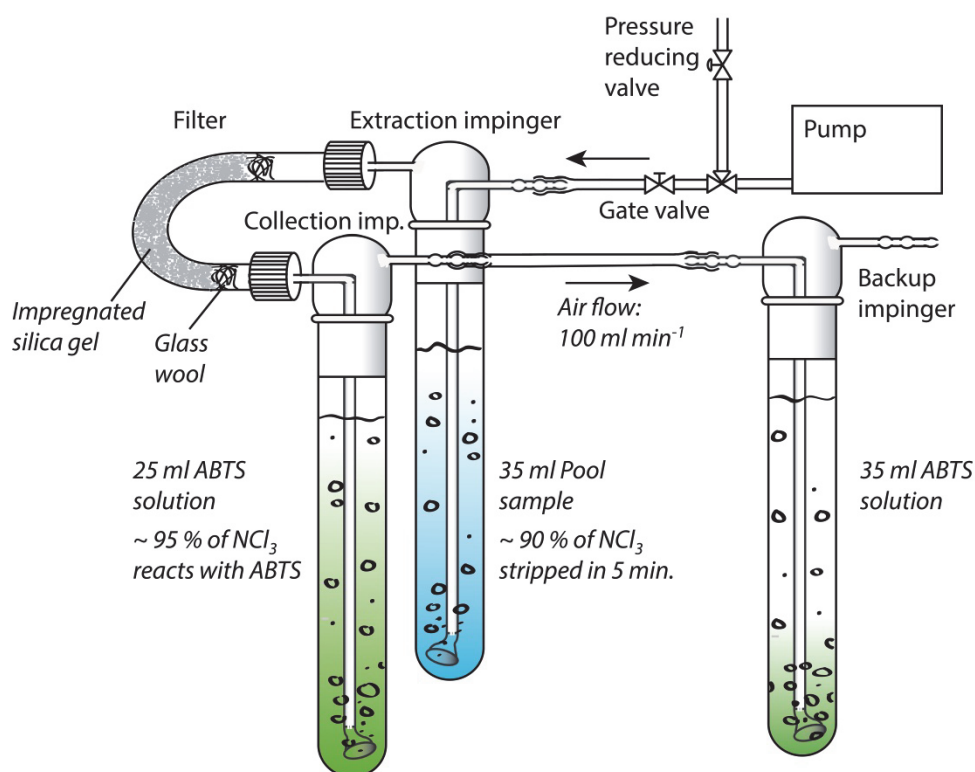


**Figure 4.1:** Scheme of the device for trichloramine measurements with the extraction-based ABTS method. Trichloramine is stripped from the pool water sample (extraction impinger) and enters the collection impinger where it reacts with ABTS. Trichloramine is quantified by measuring the absorbance change of the ABTS solution at  $\lambda = 405 \text{ nm}$ . Potential interferences are eliminated by the filter.

### *Analytical devices*

Membrane introduction mass spectrometry (MIMS) measurements were performed with a MIMS 2000 (Microlab, Aarhus, Denmark). Spectrophotometric measurements in the laboratory were conducted with a Cary 100 Scan (Varian) or a UVIKON 940 (Kontron Instruments) spectrophotometer, while for the determination of urea (see section 4.2.3.) a Beckman DU 640 spectrophotometer was utilized. A 632 pH-meter (Metrohm) was used for pH measurements and was calibrated with standard solutions at pH 4, 7 and 9, daily. Free and combined chlorine were measured using a DPD method-based test kit (Chematest 20 S) for grab samples, and with an on-line measurement device (Analyzer AMI Codes II-CC) from SWAN Analytical Instruments AG, Hinwil, Switzerland for the on-site study. Total organic carbon (TOC) was analysed with a Phoenix 8000 Analyzer (Tekmar-Dohrmann).

### 4.2.3 Analytical methods

#### *Trichloramine*

Trichloramine measurement with the extraction-based ABTS method is described in detail in sections 4.3.1 and 4.3.2. For trichloramine analysis with MIMS, the membrane inlet temperature was set to 40 °C and the sample flow rate to 8 mL min<sup>-1</sup>. Trichloramine quantifications in pool water were performed analysing the signal of fragment 88 m/z assuming that this fragment is the only trichloramine fragment free of interferences from other substances in pool water (Weaver et al., 2009). This assumption could be validated by trichloramine analysis with the second, independent trichloramine measurement method (extraction-based ABTS method). The steady-state signals in MIMS analysis were reached after a few minutes and measured for about 8–12 minutes. The analyses of the steady-state signals and the control of the inlet valve were done by a self-engineered software (SI, section A).

#### *Free chlorine, chloramine and urea analysis*

Free and combined chlorine in the laboratory and on-site were measured with commercially available test sets based on the colorimetric DPD method (APHA, 2005). Urea analyses were performed by enzymatic cleavage of urea to ammonia by urease followed by the photometric measurement of ammonia by the reaction with sodium dichloroisocyanurate (FOPH, 2007).

### 4.2.4 Pool water samples

Pool water samples were collected to compare the extraction-based ABTS method with MIMS and to investigate the correlation of trichloramine concentrations with various parameters (free chlorine, pH, urea and TOC). Single samples were collected from 30 different pools. Each pool had an individual water treatment (partly enhanced with UV treatment or ozonation) except for three pools which shared the water treatment (SI, Table C.1). The samples were taken by filling a 2 L glass bottle 30–40 cm below the water surface. The bottles were brought to the laboratory in an insulating box within 1–3 hours. Free and combined chlorine as well as pH were measured on-site and also in the laboratory simultaneously to trichloramine. In most cases, trichloramine was measured by MIMS and the extraction-based ABTS method sequentially from the same bottle while in a few cases trichloramine was measured simultaneously from two different bottles. Samples for urea and TOC measurements were quenched with sodium thiosulfate (40 µM) and titriplex III (100 µM) after the arrival in the laboratory, stored at 4 °C and analysed within 4 days.

#### **4.2.5 Pool facility for on-site measurements**

On-site trichloramine measurements were conducted at a pool facility with three pools: a wading pool (56 m<sup>3</sup>), a swimming pool (1'580 m<sup>3</sup>) and a diving pool (370 m<sup>3</sup>). The pools had a common water treatment which included fresh water addition. Chlorination of the pools was individual and residence time differed for each pool (~1, ~3 and 4–5 hours for the wading, diving and swimming pool, respectively). Further information on the pool facility is given in the supporting information (SI, section E)

## 4.3 Results and Discussion

### 4.3.1 Extraction-based ABTS method

#### *General approach*

The extraction-based ABTS method was designed to be a fast, simple and low-cost method for trichloramine measurement in pool water. The method works as follows: trichloramine is stripped from the pool water sample (extraction impinger) and passes through a filter, which eliminates potential interferences from free and combined chlorine (Figure 4.1). Then, trichloramine enters the collection impinger where it oxidizes  $\text{ABTS}^{2-}$  to the greenish  $\text{ABTS}^{\bullet-}$  radical. Trichloramine is quantified by measuring spectrophotometrically the absorbance of  $\text{ABTS}^{\bullet-}$  at  $\lambda = 405 \text{ nm}$ , immediately after stripping. Calibrations with trichloramine solutions were performed daily before the measurements and found to be constant (SI, Table B.2) which potentially allows for measurements without daily calibrations.

#### *Extraction procedure*

Water samples (35 mL) were cautiously added from a bottle containing pool water with a dispenser to the extraction impinger. A phosphate buffered solution (0.1 M, pH 2.6) and 250  $\mu\text{L}$  of the ABTS stock solution were added to a 25 mL volumetric flask and poured into the collection impinger. After mounting the filter, the water sample was stripped for 5 minutes with a gas flow of  $100 \text{ mL min}^{-1}$ .

#### *Extraction impinger (trichloramine stripping)*

To lower the detection limit, a high ratio of pool sample (extraction impinger) to ABTS solution volume (collection impinger) is desirable. However, by increasing the sample volume, either the stripping time or the air flow must be increased to result in a similar stripping efficiency. The optimization of the stripping time and the air flow revealed that a reasonable stripping efficiency of  $86 \pm 4 \%$  was reached with an air flow of  $100 \text{ mL min}^{-1}$  during 5 minutes (SI, Figure B.1 and Table B.1). Under these conditions,  $\sim 95 \%$  of the trichloramine entering the collection impinger reacted with  $\text{ABTS}^{2-}$  to  $\text{ABTS}^{\bullet-}$  (SI, Figure B.4).

To avoid the little interference from pool air, measurements should not be performed next to the swimming pool. Trichloramine concentration in swimming pool air is regulated to  $0.2 \text{ mg m}^{-3}$  in Switzerland (SIA, 2013). Such a level is expected to increase the aqueous trichloramine concentration measured with the extraction-based ABTS method by  $< 0.011 \mu\text{M}$  ( $2.3 \mu\text{g L}^{-1}$  as  $\text{Cl}_2$ ).

***Filter (elimination of interferences from pool water)***

Oxidants such as free chlorine, monochloramine and dichloramine oxidize  $\text{ABTS}^{2-}$  to the greenish  $\text{ABTS}^{\bullet-}$  radical (Pinkernell et al., 2000). Although these chlorine species have a much lower Henry's constant than trichloramine, they can be substantially stripped from pool water (Holzwarth et al., 1984). Similar to filter systems described previously, a filter consisting of impregnated silica gel (3 g) was introduced to eliminate these interferences (Héry et al., 1995; INRS, 2007). The filter efficiently eliminates interferences of  $\text{HOCl} / \text{OCl}^-$  ( $< 10 \mu\text{M}$  ( $0.7 \text{ mg L}^{-1}$  as  $\text{Cl}_2$ )),  $\text{NH}_2\text{Cl}$  ( $< 50 \mu\text{M}$  ( $3.5 \text{ mg L}^{-1}$  as  $\text{Cl}_2$ )), and  $\text{NHCl}_2$  ( $< 5 \mu\text{M}$  ( $0.7 \text{ mg L}^{-1}$  as  $\text{Cl}_2$ )) (SI, Figure B.2). In Swiss pool water, concentrations of these substances are below the aforementioned limits if standards are met (SIA, 2013). The filter also affects the trichloramine concentration with a loss of about 45 % which is accounted for by the calibration. Trichloramine elimination was even higher if the impregnated silica gel was dried completely after the impregnation. The trichloramine loss in the filter did not affect the good reproducibility of the method (Figure 4.3 and SI, Figure B.2) if the silica gel was produced according to the description in section 4.2.1.

***Collection impinger (trichloramine quantification)***

For the quantitative absorption of trichloramine, the indicator in the collection impinger has to fulfil the following criteria: (i) a very fast reaction with trichloramine, (ii) the reaction product exerts a high molar absorbance, (iii) the reaction of the quenching agent with trichloramine has a constant stoichiometric factor and (iv) the product of the reaction between trichloramine and the quencher has sufficient stability, at least several minutes.

ABTS has been chosen as an indicator in the collection impinger because trichloramine oxidizes  $\text{ABTS}^{2-}$  very quickly to its radical form ( $\text{ABTS}^{\bullet-}$ ) which has a high molar absorption coefficient ( $\epsilon_{405 \text{ nm}} = 31'600 \text{ M}^{-1}\text{cm}^{-1}$ ) (Pinkernell et al., 1997). Requirements (iii) and (iv) are only met under optimized and well-defined conditions as outlined below.

Trichloramine addition ( $0.55 \mu\text{M}$ ) to an ABTS solution ( $50\text{--}200 \mu\text{M}$ ) with phosphate buffer (pH 2.6, 0.1 M) revealed that the absorbance depended on the ABTS concentration (Figure 4.2a) even if ABTS was in high excess ( $\sim 100\text{--}400$ -fold). Since increasing ABTS concentration increased the absorbance of the blank even more than that of the sample, lowering the ABTS concentrations improves the sensitivity. Figure 4.2b shows the absorption of a buffered ABTS solution (pH 1.6–5), measured immediately after the addition of trichloramine. The buffer stock solution had a pH of 2.5 which was adjusted with  $\text{H}_2\text{SO}_4$  or  $\text{NaOH}$  prior to the reaction. The absorbance of the ABTS solution after the reaction with trichloramine decreased with

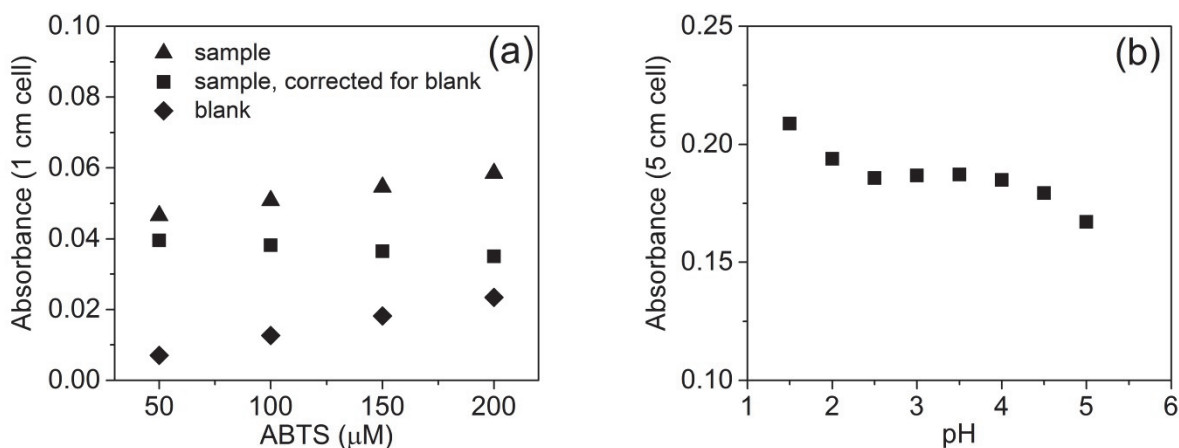


**Figure 4.2:** (a) Absorbance (1 cm path length) measured immediately after mixing trichloramine ( $0.55 \mu\text{M}$ ) with ABTS ( $50\text{--}200 \mu\text{M}$ ) and phosphate buffer ( $0.1 \text{ M}$ , pH 2.6). (b) Absorbance (5 cm path length) measured immediately after mixing trichloramine ( $0.53 \mu\text{M}$ ) with ABTS ( $125 \mu\text{M}$ ) and phosphate buffer ( $0.1 \text{ M}$ , pH 2.5) and adjusting the pH in the range of 1.6–5 with  $\text{H}_2\text{SO}_4$  or  $\text{NaOH}$ .

increasing pH. Hence, pH, ionic strength, sulfate and buffer concentrations may potentially influence the absorbance of the ABTS solution. Furthermore, only buffer solutions with pH of 2.6–3 resulted in a stable absorbance while the absorbance increased with time for ABTS solutions with  $\text{pH} < 2.5$  and decreased for solutions with  $\text{pH} > 3$  (SI, Figure B.3). Stoichiometric factors of the reaction of trichloramine with ABTS shown in Figure 4.2a and 4.2b were calculated to be  $\sim 2\text{--}3$ . If a complete reduction of chlorine in trichloramine ( $\text{Cl}^{\text{I}}$  to  $\text{Cl}^{\text{I}}$ ) induced an oxidation of  $\text{ABTS}^{2-}$  to  $\text{ABTS}^{*-}$ , the maximal stoichiometric factor would be 6. It has been found previously that trichloramine does not react quantitatively with reducing agents (e.g. iodide) (Kumar et al., 1986).

Nevertheless, a constant stoichiometric factor for the reaction of trichloramine with ABTS is only reached if the ABTS concentration, pH and the buffer concentration are kept constant. Therefore, the conditions in the collection impinger were set to ABTS concentration =  $50 \mu\text{M}$  and phosphate buffer =  $0.1 \text{ M}$  at pH 2.6.

To check whether trichloramine reacts to completion in the collection impinger, a second impinger (backup impinger) containing an identical ABTS solution was added at the outlet of the collection impinger. Based on the trichloramine concentrations in the collection and the backup impinger, about 95 % of the trichloramine was captured in the collection impinger for an air flow of  $100 \text{ mL min}^{-1}$  (SI, Figure B.4). This high yield was achieved because of the small bubble size in the collection impinger. Besides the small pore size of the frit and the low air

flow, two other factors are important for the bubble size: (i) the addition of the backup impinger increased the pressure in the collection impinger and (ii) the high concentration of the phosphate buffer (0.1 M) increased the surface tension and the viscosity of the solution. Based on this optimized procedure the volume of the ABTS solution could be minimized to 25 mL, which leads to an enrichment factor of 1.4 for trichloramine (volume of extraction is 35 mL).

### 4.3.2 Comparison of the extraction-based ABTS method with MIMS: standard solutions and standard addition

A first assessment of the extraction-based ABTS method and the MIMS was done by checking the signal response and the accuracy of trichloramine measurements. Trichloramine solutions (0.05–0.5  $\mu\text{M}$ ) in ultrapurified water were measured in triplicate with MIMS and the extraction-based ABTS method (Figure 4.3). For trichloramine analysis with MIMS, fragment 86 m/z was analyzed because this fragment has a higher signal intensity than fragment 88 m/z (SI, Figure B.7) and is free of interferences in pure solutions (but not in pool water). Both methods performed with good linearity and with little standard deviation. In the extraction-based ABTS method, linearity was only observed for trichloramine concentrations  $\geq 0.05 \mu\text{M}$  ( $0.01 \text{ mg L}^{-1}$  as  $\text{Cl}_2$ ). This sensitivity is sufficient to measure Swiss pool water since only 3 of 30 pool water samples had a trichloramine concentration  $< 0.05 \mu\text{M}$  (SI, Table C.1.). The sensitivity of the MIMS varied slightly and depended on the operational setting, but it was comparable to that of the extraction-based ABTS method.

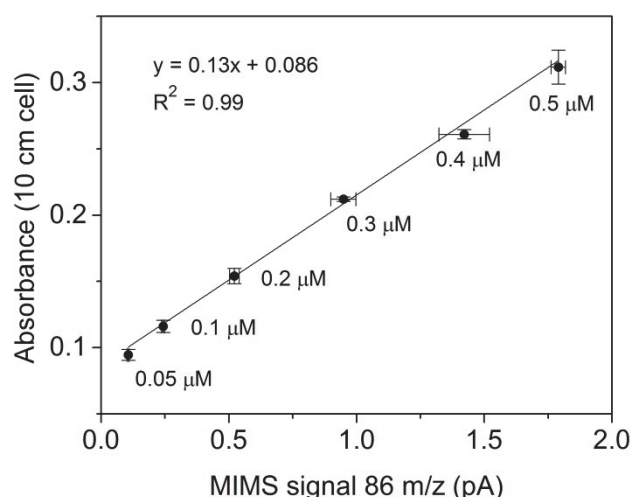


**Figure 4.3:** Trichloramine standards (0.05–0.5  $\mu\text{M}$  ( $0.01$ – $0.11 \text{ mg L}^{-1}$  as  $\text{Cl}_2$ )) measured with the extraction-based ABTS method (10 cm path length) and MIMS in ultrapurified water. Each sample was measured in triplicate with the extraction-based ABTS method and with MIMS (error bars show standard deviation).

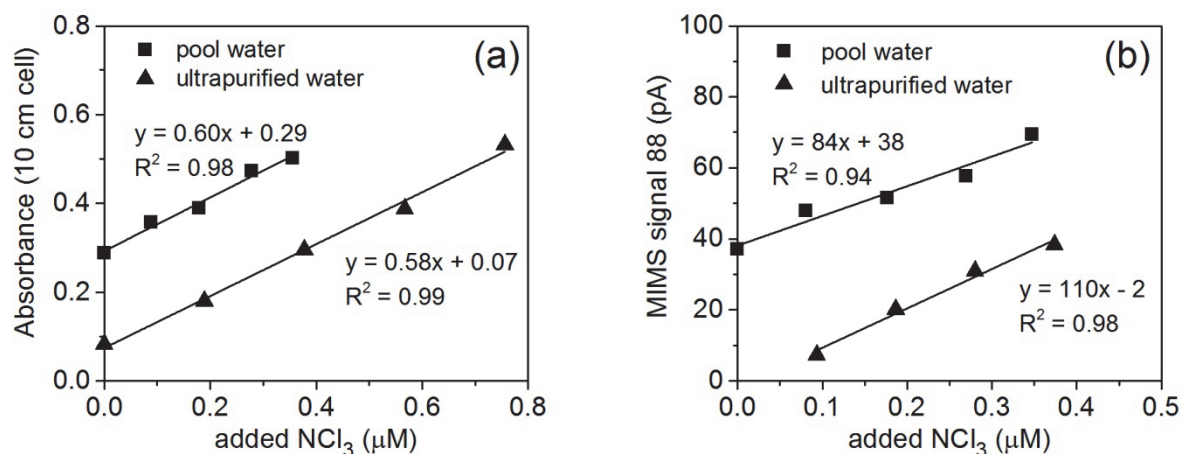


**Figure 4.4:** Trichloramine calibration curves in ultrapurified and pool water with (a) the extraction-based ABTS method (absorbance of  $\text{ABTS}^{\bullet-}$ , 10 cm cell) and (b) MIMS. Pool water was taken from a pool, which was regulated to pH 7.2 and to a free chlorine concentration of  $0.45 \text{ mg L}^{-1}$  as  $\text{Cl}_2$ .

To assess whether pool water matrices affect trichloramine measurements with the ABTS method or with MIMS, calibrations in ultrapurified water were compared to standard additions in pool water (Figure 4.4). Pool water samples with standard addition were first measured with MIMS and less than 15 minutes later with the extraction-based ABTS method. A comparison of the performed calibrations revealed that slopes (i.e. absorbance increase with concentration) in the extraction-based ABTS method were similar in ultrapurified water and in pool water (Figure 4.4a). In contrast, the slope in the calibration with MIMS was clearly lower in pool water than in ultrapurified water (Figure 4.4b). This suggests that MIMS measurements are affected by the matrix. This effect is likely not related to changes in salinity or temperature (SI, B.5) but it shows that trichloramine in pool water can only be quantified if calibrations are performed by standard addition to pool water.

### 4.3.3 Comparison of the extraction-based ABTS method with MIMS: pool water samples

Three trichloramine measurement series with 9–10 different pool water samples each were conducted to further assess the effect of the pool water matrix and to compare the performance to the two methods (Figure 4.5). For two series (a) and (b), MIMS calibrations were performed with trichloramine solution in ultrapurified water. The MIMS calibration in series (c) was derived from standard addition to pool water. The results in Figure 4.5 show that there was a good linearity between the two methods for all series. However, trichloramine concentrations measured with the extraction-based ABTS method were consistently about a factor of 1.4



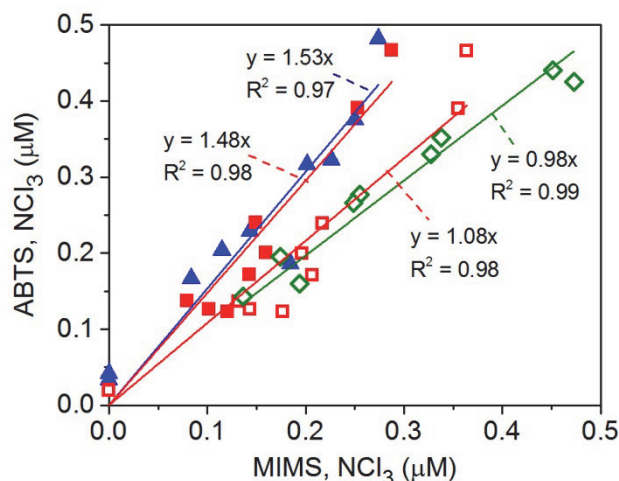


**Figure 4.5:** Comparison of trichloramine concentrations in pool water measured by the extraction-based ABTS method and by MIMS (28 pool waters). For series (a) (closed triangles) and (b) (closed squares) (for explanation, see text): MIMS calibration was performed with trichloramine in ultrapurified water. MIMS measurements of series (b) were corrected with a factor to consider the matrix effect of the pool water (open squares). Calibration for series (c) (open diamonds) was conducted with a trichloramine standard addition to pool water.

higher than with the MIMS for series (a) and (b). In series (b), pool samples were also spiked with a known trichloramine concentration and measured again with MIMS. The measured increase of the MIMS signal after trichloramine addition was systematically a factor of  $\sim 1.4$  lower than expected from calibration in ultrapurified water (SI, Table B.3). Dividing each trichloramine concentration measured with MIMS in series (b) by this factor, trichloramine concentrations fit well to trichloramine concentrations measured with the extraction-based ABTS method. In series (c), trichloramine calibration was performed in pool water with standard addition (signal 83  $m/z$  is independent from trichloramine addition and was therefore used as an internal standard to overcome the MIMS instability (SI, B.7)) and a good agreement between the extraction-based ABTS method and MIMS was observed for this case.

Although it seems necessary to do a trichloramine calibration in pool water, one should be aware of some restrictions: (i) Because a calibration of the MIMS with steady-state signals requires at least 40 minutes, only pool waters with stable trichloramine signals can be used. Trichloramine concentrations in pool water are rather stable, except for pool waters with low free chlorine concentrations (SI, B.6). (ii) Signal 83  $m/z$ , which represents mainly trihalomethanes (chloroform and dichlorobromomethane), can be used as internal standard for calibrations with MIMS. The signal is assumed to be equal in all calibration solutions since

trihalomethanes are fairly stable in pool water. However, one should be cautious because signal 83  $m/z$  needs slightly longer to reach a steady-state.

#### 4.3.4 Factors influencing trichloramine concentrations

It has been shown previously that there are various potential *N*-precursors for trichloramine formation in pool water, and urea is considered to be a dominant source (Blatchley and Cheng, 2010; De Laat et al., 2011; Schmalz et al., 2011a). However, other studies showed that trichloramine can also be formed from the chlorination of ammonia, monochloramine or dichloramine (Soulard et al., 1981). These compounds may interconvert, depending on the Cl:N ratio and pH. A low pH and high free chlorine concentration do not only shift the degree of chlorination toward trichloramine, but also enhance trichloramine formation from urea (see eqs. 4.1–4.3)).

Figures 4.6a–d show trichloramine concentrations of different pool waters in relation to free chlorine, HOCl, combined chlorine ( $\text{NH}_2\text{Cl}$ ,  $\text{NHCl}_2$ ,  $\text{NCl}_3$ ), pH and urea concentrations. A first glance at the data reveals that the trichloramine concentration correlates most strongly with the HOCl concentration. Two samples are regarded as outliers: (i) A sample from a small whirlpool ( $3 \text{ m}^3$ ), in which the trichloramine concentration was much lower than expected from the HOCl concentration. This was likely due to the increased outgassing during use of the whirlpool. (ii) The second sample originates from a pool facility whose pH control was not running properly, with a pH of 5.5 which is much lower than the regulatory range (6.8–7.6) (SIA, 2013). Therefore, the trichloramine concentration in this pool was elevated and the MIMS analysis suggested that dichloramine represented a higher share of the combined chlorine in comparison to the other samples.

Multiple linear regression models (t-test) of the data with the statistics program R (Team R Development Core, 2013) revealed the following (SI, section C): (i) Trichloramine shows a clearly significant correlation with the HOCl concentration measured in the laboratory. This correlation is stronger than the correlation with free chlorine, which suggests that trichloramine is rather formed by the reaction with HOCl than with  $\text{OCl}^-$  (Figure 4.6 and SI, Table C.2, model 1 + 2) as expected for typical chlorination reactions (Deborde and von Gunten, 2008). (ii) Trichloramine reacted rather quickly to changes in the HOCl concentrations. This conclusion is derived from the observation that the HOCl concentrations measured on-site were constantly higher than those measured in the laboratory (SI, Figure C.1) and that the correlation between trichloramine and HOCl measured on-site improved by inserting a term into the statistical model which describes the HOCl loss during the sample transport to the laboratory

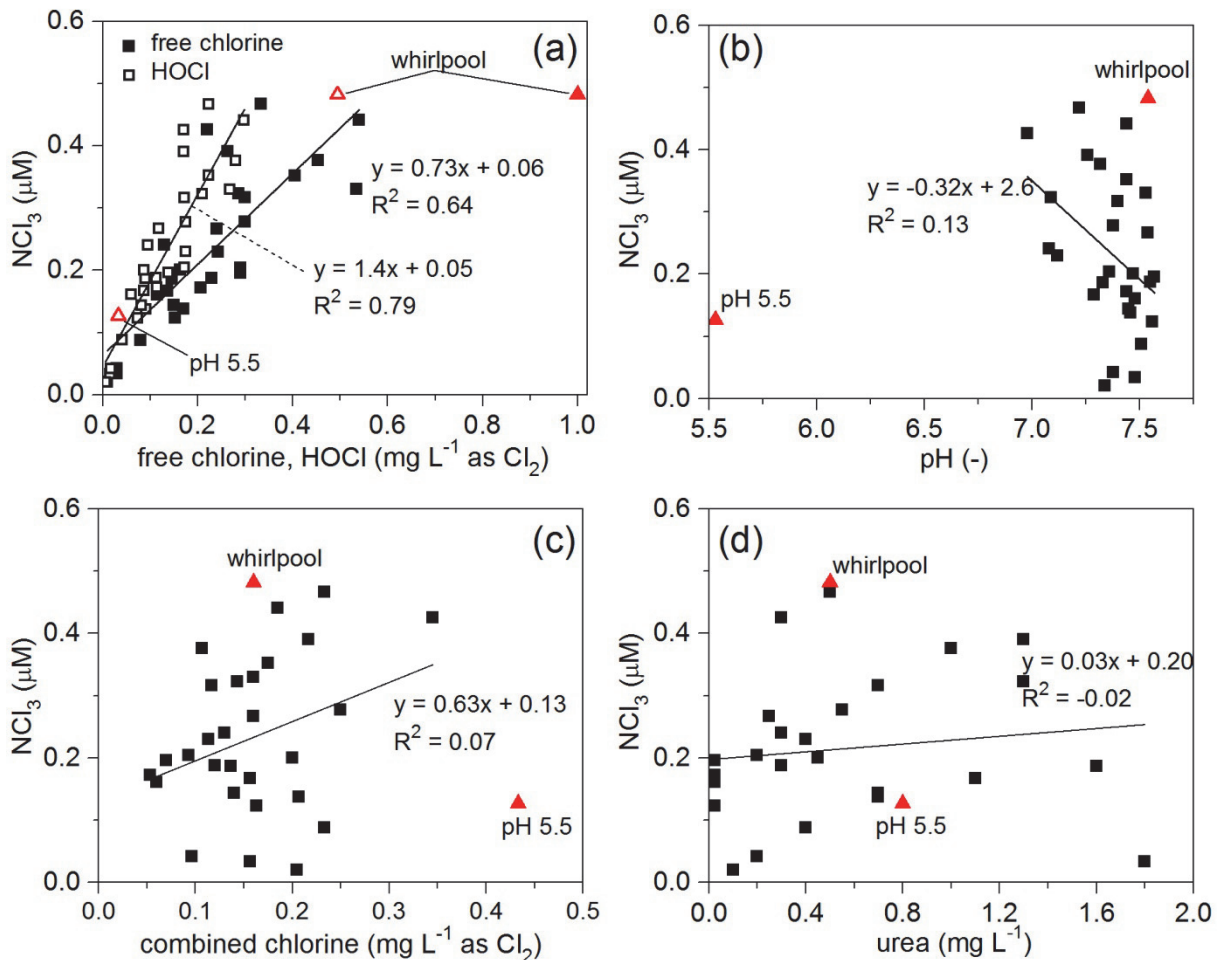


**Figure 4.6:** Correlation of trichloramine concentrations with a) free chlorine (closed symbols) and HOCl (open symbols), b) pH, c) combined chlorine and d) urea in 30 pool samples. Two outliers (triangles, samples of whirlpool and at pH 5.5) were not considered in the linear regressions.

(SI, Text C.1 and Table C.2, model 3 + 4). Because this term did not improve the model with the HOCl measured in the laboratory, trichloramine concentrations were rather related to the actual HOCl concentration in the laboratory and not to the HOCl concentration in the swimming pool (SI, Table C.2, model 2 + 5). Therefore, trichloramine concentrations decreased similarly to free chlorine concentrations, and concentrations measured in the laboratory might be slightly lower than the effective trichloramine concentrations on-site. (iii) Small pH variations as observed in the pool water samples (pH 7–7.5) did not significantly influence trichloramine levels (Figure 4.6b and SI, Table C.2, model 6). (iv) Measured combined chlorine also includes trichloramine. To investigate the influence of combined chlorine on the trichloramine concentration, combined chlorine concentrations were corrected by subtracting the measured trichloramine concentration (Figure 4.6c). This corrected combined chlorine

concentration was slightly significantly correlated to trichloramine in a statistical model including interactions but not in other models (SI, Table C.2, model 7). (v) Urea and TOC concentrations did not significantly correlate with the trichloramine concentration in any of the models (Figure 4.6d and SI, Table C.2, model 8). This finding is supported by the fact that four pool samples, whereof three were from pool facilities with ozone treatment, had urea concentrations below the detection limit ( $0.05 \text{ mg L}^{-1}$ ) and did not have especially low trichloramine concentrations. However, combined chlorine levels were remarkably lower in these three cases. Urea concentration in the other pool samples was  $\leq 1.3 \text{ mg L}^{-1}$  with an average concentration of  $0.67 \text{ mg L}^{-1}$ . A total of 12 pool water samples were additionally analysed with size exclusion chromatography coupled to organic carbon and organic nitrogen detection (SEC-OCD-OND) (SI, section D). This analysis revealed that urea accounted on average for 66% (ranging from 37 to 85%) of the organic nitrogen in the swimming pool samples (SI, Table D.1). Hence, urea represents the major fraction of organic nitrogen but is likely not the dominant trichloramine precursor.

#### **4.3.5 Field study on parameters affecting trichloramine concentration**

To test the findings from section 4.3.4, a MIMS and an online analyzer for free and combined chlorine (Analyzer AMI Codes II-CC, SWAN Analytical Instruments AG) were installed in a pool facility with a wading, diving and a swimming pool (SI, section E). Figure 4.7 shows the evolution of trichloramine, free chlorine, combined chlorine and urea concentrations in the wading pool during a period of eight days. The free chlorine concentration was intentionally lowered (from  $0.35$  to  $0.2 \text{ mg L}^{-1}$ ) for three days (days 4–6), while the pH was controlled at 7.2. The urea concentration was observed to be often elevated in the afternoons but usually dropped to a constant level overnight ( $0.55$ – $0.65 \text{ mg L}^{-1}$ ). The increased free chlorine concentration on day 2 may have been caused by a problem with the chlorine regulation while the short increase before the period with low free chlorine concentration was an operational error. Trichloramine showed a very good correlation with the free chlorine concentration, especially during the night when the pool water was not influenced by changing inputs from the bathers. Even short term changes in the free chlorine concentration were followed by changes in the trichloramine concentration. This correlation does not coincide with a study by Weng and Blatchley (2011) who found that free chlorine concentrations decreased during heavy use of a swimming pool leading to increased trichloramine concentrations.

Combined chlorine concentrations also increased in the afternoons but less pronouncedly. Trichloramine and combined chlorine concentrations were often correlated leading to distinct

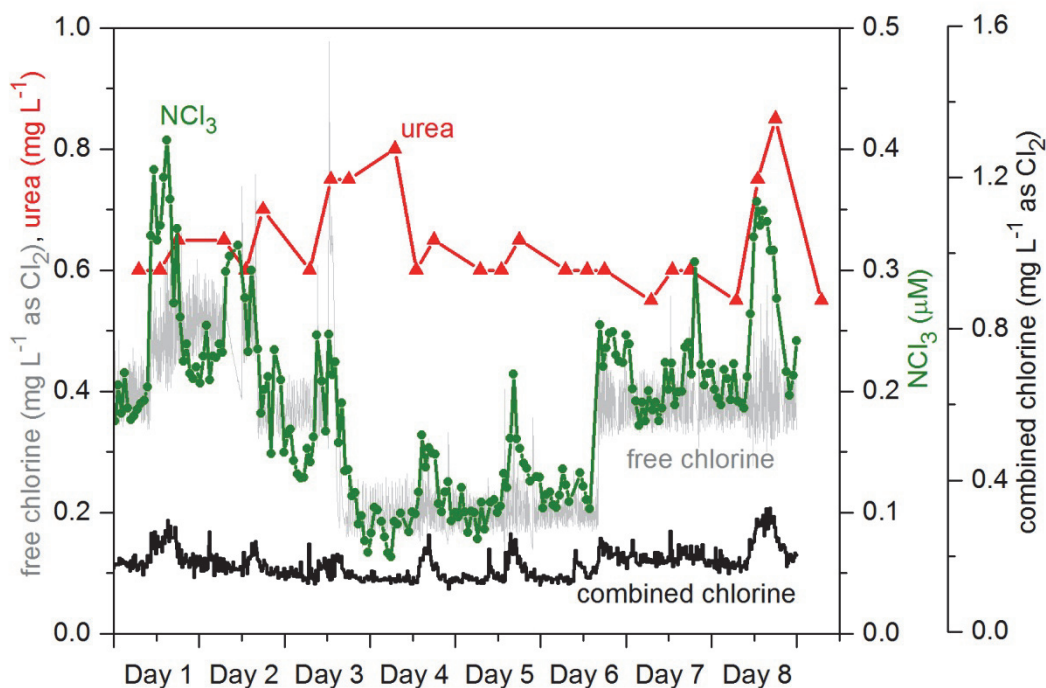


**Figure 4.7:** Evolution of trichloramine (circles), free chlorine (grey line), combined chlorine (black line) and urea (triangles) in a wading pool over eight days. The free chlorine level was lowered from day 4 to 6 from 0.35 to 0.2 mg L<sup>-1</sup> as Cl<sub>2</sub>.

peaks in the afternoons. Evolution of trichloramine in the swimming pool was much less dynamic than in the wading pool since the water volume was 30 times higher, which ensured a better dilution because of the lower bather density. The trichloramine concentration in the swimming pool was the highest from 15:00–20:00 when bather load was highest (SI, Figure E.3). Interestingly, trihalomethanes (signal 83 m/z) had an opposite daily pattern with the lowest concentration during the period with the highest bather attendance (SI, Figure E.3). This suggests that trihalomethanes were not or not immediately formed from precursors introduced by bathers and that their concentrations were influenced by the outgassing caused from bather activity. A more detailed diurnal pattern of the trichloramine concentration is illustrated in Figure 4.8. The trichloramine and urea concentrations reacted quickly and sensitively to bathers. Previous studies revealed that free chlorine reacts rather slowly with urea (Blatchley and Cheng, 2010; Schmalz et al., 2011a). Therefore, the immediate increase of the trichloramine concentration in the pool water is likely due to other precursors than urea. The increase might be more pronounced in a wading pool of which the water treatment is not connected to a large swimming pool as in this study.

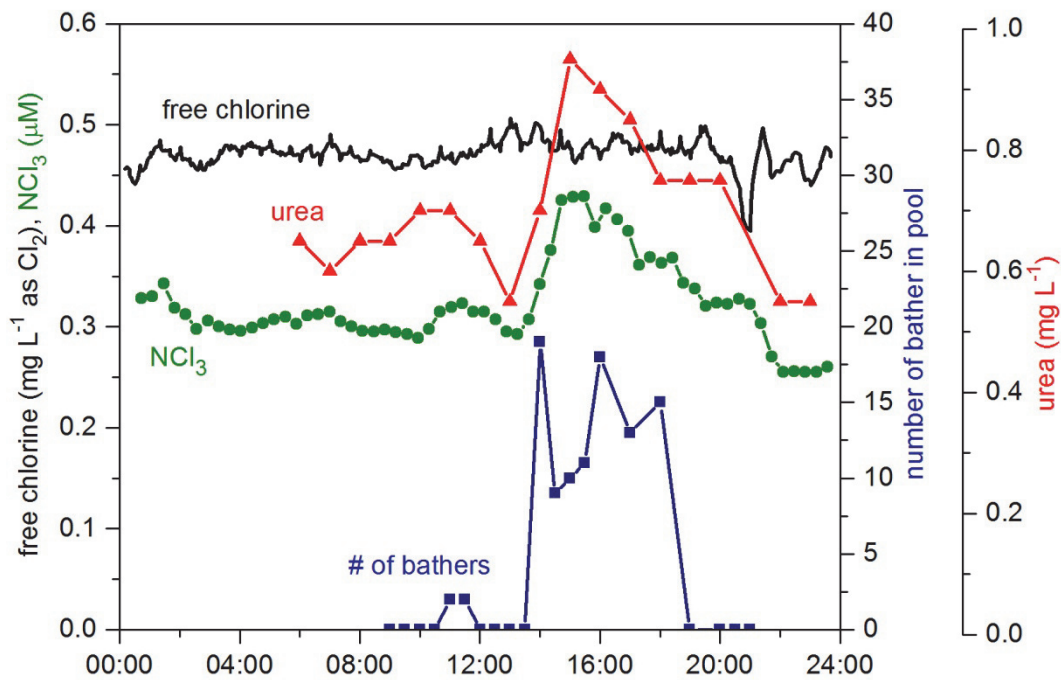


**Figure 4.8:** A typical diurnal pattern of free chlorine, trichloramine and urea concentrations in relation to the number of bathers in the wading pool. The trichloramine concentration was smoothed by plotting the moving average (3 measurements).

### 4.3 Conclusions

Trichloramine is one of various disinfection by-products with adverse health effects that is present in chlorinated swimming pools. Until now, there are only few studies on trichloramine concentrations in air and even less information on trichloramine in pool water. This is due to the lack of a suitable method which is sensitive enough for trichloramine measurements free of interferences in pool waters.

In this study, an accurate, fast, easily applicable and low cost method for trichloramine analysis in water was developed, which is suitable for on-site measurements in pool facilities. The method is based on stripping of trichloramine, passing it through a solid phase filter to reduce interferences from other chlorine species ( $\text{HOCl}$ ,  $\text{NH}_2\text{Cl}$ ,  $\text{NHCl}_2$ ) and its reaction with  $\text{ABTS}^{2-}$  producing the coloured product  $\text{ABTS}^{\bullet-}$ . Trichloramine was accurately measured in Swiss pool waters with a quantification limit of  $0.05 \mu\text{M}$  ( $0.01 \text{ mg L}^{-1}$  as  $\text{Cl}_2$ ). Comparison with MIMS measurements revealed that the developed method was free of interferences and represents therefore a valid option for routine measurements of trichloramine in pool water. Measurement of 30 different pool samples showed that the trichloramine concentration was strongly linked to the  $\text{HOCl}$  concentration and responded quickly when this changed. Therefore, transport of pool samples to the laboratory can affect trichloramine concentrations. Other parameters such as combined chlorine or pH were much less, and urea and TOC not correlated to the trichloramine concentration. On-site measurements in a wading pool confirmed the close relationship between the trichloramine and the free chlorine concentration at a constant pH. Similar to urea, trichloramine responded quickly to the bather load. However, because the formation of trichloramine during chlorination of urea is a slow process, it can be assumed that trichloramine in the wading pool is formed from the reaction of chlorine with other nitrogen-containing precursors. Lowering the free chlorine concentration is an effective means for trichloramine mitigation, however may lead to a limited disinfection.

## **Acknowledgements**

This work was supported by the Swiss Federal Office of Public Health (FOPH). The authors thank Rene Schittli (Kantonales Labor Zürich) for collaboration in pool water sampling and analysis, Elisabeth Salhi, Jacqueline Traber and Philippe Périsset (Eawag) for technical support and Gérard Donzé (FOPH) for the fruitful discussions.



## References

- American Public Health Association (APHA) (2005). "Standard methods for the examination of water & wastewater."
- Bernard, A., S. Carbonnelle, O. Michel, S. Higuët, C. de Burbure, J. P. Buchet, C. Hermans, X. Dumont and I. Doyle (2003). "Lung hyperpermeability and asthma prevalence in schoolchildren: unexpected associations with the attendance at indoor chlorinated swimming pools." *Occupational and Environmental Medicine* 60(6): 385-394.
- Blatchley, E. R. and M. Cheng (2010). "Reaction Mechanism for Chlorination of Urea." *Environmental Science & Technology* 44(22): 8529-8534.
- De Laat, J., W. Feng, D. A. Freyfer and F. Dossier-Berne (2011). "Concentration levels of urea in swimming pool water and reactivity of chlorine with urea." *Water Research* 45(3): 1139-1146.
- Deborde, M. and U. von Gunten (2008). "Reactions of chlorine with inorganic and organic compounds during water treatment--Kinetics and mechanisms: A critical review." *Water Research* 42(1-2): 13-51.
- Fantuzzi, G., E. Righi, G. Predieri, P. Giacobazzi, B. Petra and G. Aggazzotti (2013). "Airborne trichloramine (NCl<sub>3</sub>) levels and self-reported health symptoms in indoor swimming pool workers: dose-response relationships." *Journal of Exposure Science and Environmental Epidemiology* 23(1): 88-93.
- Federal Office of Public Health (FOPH), Switzerland (2007). "Determination of ammonia in drinking water, photometrically (German)."
- Gazda, M., K. Kumar and D. W. Margerum (1995). "Nonmetal redox kinetics - oxidation of bromide ion by nitrogen trichloride." *Inorganic Chemistry* 34(13): 3536-3542.
- Gérardin, F., G. Hecht, G. Huber-Pelle and I. Subra (2005). "Traitement UV: Suivi de l'évolution des concentrations en chloroforme et en trichlorure d'azote dans les eaux de baignade d'un centre aquatique." *Hygiène et sécurité du travail - Cahiers de notes documentaires* 201: 19-30.
- Hansen, K. M. S., S. Willach, M. G. Antoniou, H. Mosbaek, H. J. Albrechtsen and H. R. Andersen (2012). "Effect of pH on the formation of disinfection byproducts in swimming pool water - Is less THM better?" *Water Research* 46(19): 6399-6409.
- Héry, M., G. Hecht, J. M. Gerber, J. C. Gendre, G. Hubert and J. Rebuffaud (1995). "Exposure to chloramines in the atmosphere of indoor swimming pools." *Annals of Occupational Hygiene* 39(4): 427-439.
- Holzwarth, G., R. G. Balmer and L. Soni (1984). "The fate of chlorine and chloramines in cooling-towers - Henry's law constants for flashoff." *Water Research* 18(11): 1421-1427.
- National Institute for Research and Security (INRS) (2007). "Trichloramine and other chlorinated products (French)."
- Jafvert, C. T. and R. L. Valentine (1992). "Reaction Scheme for the chlorination of ammoniacal water." *Environmental Science & Technology* 26(3): 577-586.
- Johnson, R. C., R. G. Cooks, T. M. Allen, M. E. Cisper and P. H. Hemberger (2000). "Membrane Introduction Mass Spectrometry: Trends and Application." *Mass Spectrometry Reviews* 19: 1-19.
- Kinani, S., B. Richard, Y. Souissi and S. Bouchonnet (2012). "Analysis of inorganic chloramines in water." *TrAC Trends in Analytical Chemistry* 33(0): 55-67.

Kosaka, K., K. Seki, N. Kimura, Y. Kobayashi and M. Asami (2010). "Determination of trichloramine in drinking water using headspace gas chromatography/mass spectrometry." *Water Science & Technology: Water Supply* 10: 23-29.

Kumar, K., R. A. Day and D. W. Margerum (1986). "Atom-transfer redox kinetics: general-acid-assisted oxidation of iodide by chloramines and hypochlorite." *Inorganic Chemistry* 25(24): 4344-4350.

Li, J. and E. R. Blatchley (2008). Formation of Volatile Disinfection Byproducts from Chlorination of Organic-N Precursors in Recreational Water. *Disinfection by-Products in Drinking Water: Occurrence, Formation, Health Effects, and Control*. T. Karanfil, S. W. Krasner and Y. Xie. Washington, Amer Chemical Soc. **995**: 172-181.

Massin, N., A. B. Bohadana, P. Wild, M. Hery, J. Toamain and G. Hubert (1998). "Respiratory symptoms and bronchial responsiveness in lifeguards exposed to nitrogen trichloride in indoor swimming pools." *Occupational and Environmental Medicine* 55(4): 258-263.

Parrat, J., G. Donze, C. Iseli, D. Perret, C. Tomicic and O. Schenk (2012). "Assessment of Occupational and Public Exposure to Trichloramine in Swiss Indoor Swimming Pools: A Proposal for an Occupational Exposure Limit." *Annals of Occupational Hygiene* 56(3): 264-277.

Pinkernell, U., H. J. Luke and U. Karst (1997). "Selective photometric determination of peroxy-carboxylic acids in the presence of hydrogen peroxide." *Analyst* 122(6): 567-571.

Pinkernell, U., B. Nowack, H. Gallard and U. von Gunten (2000). "Methods for the photometric determination of reactive bromine and chlorine species with ABTS." *Water Research* 34(18): 4343-4350.

Predieri, G. and P. Giacobazzi (2012). "Determination of nitrogen trichloride (NCl<sub>3</sub>) levels in the air of indoor chlorinated swimming pools: An impinger method proposal." *International Journal of Environmental Analytical Chemistry* 92(6): 645-654.

Richardson, S. D., D. M. DeMarini, M. Kogevinas, P. Fernandez, E. Marco, C. Lourencetti, C. Balleste, D. Heederik, K. Meliefste, A. B. McKague, R. Marcos, L. Font-Ribera, J. O. Grimalt and C. M. Villanueva (2010). "What's in the Pool? A Comprehensive Identification of Disinfection By-products and Assessment of Mutagenicity of Chlorinated and Brominated Swimming Pool Water." *Environmental Health Perspectives* 118(11): 1523-1530.

Schmalz, C., F. H. Frimmel and C. Zwiener (2011a). "Trichloramine in swimming pools - Formation and mass transfer." *Water Research* 45(8): 2681-2690.

Schmalz, C., H. Wunderlich, R. Heinze, F. Frimmel, C. Zwiener and T. Grummt (2011b). "Application of an optimized system for the well-defined exposure of human lung cells to trichloramine and indoor pool air." *Journal of water and health* 9(3): 586-596.

Schreiber, I. M. and W. A. Mitch (2005). "Influence of the order of reagent addition on NDMA formation during chloramination." *Environmental Science & Technology* 39(10): 3811-3818.

Schurter, L. M., P. P. Bachelor and D. W. Margerum (1995). "Nonmetal redox kinetics - monochloramine, dichloramine, and trichloramine reactions with cyanide ion." *Environmental Science & Technology* 29(4): 1127-1134.

Shang, C. and E. R. Blatchley (1999). "Differentiation and quantification of free chlorine and inorganic chloramines in aqueous solution by MIMS." *Environmental Science & Technology* 33(13): 2218-2223.

Shang, C., W. L. Gong and E. R. Blatchley (2000). "Breakpoint chemistry and volatile byproduct formation resulting from chlorination of model organic-N compounds." *Environmental Science & Technology* 34(9): 1721-1728.

- Swiss society of engineers and architects (SIA) (2013). "Water and water treatment in public pools (German)."
- Soltermann, F., M. Lee, S. Canonica and U. von Gunten (2013). "Enhanced N-nitrosamine formation in pool water by UV irradiation of chlorinated secondary amines in the presence of monochloramine." *Water Research* 47(1): 79-90.
- Soulard, M., F. Bloc and A. Hatterer (1981). "Diagrams of existence of chloramines and bromamines in aqueous solution." *Journal of the Chemical Society, Dalton Transactions*(12): 2300-2310.
- Team R Development Core (2013). "R: A language and environment for statistical computing." R Foundation for Statistical Computing. Vienna, Austria, 2013. ISBN 3-900051-07-0. <http://www.R-project.org>.
- Walse, S. S. and W. A. Mitch (2008). "Nitrosamine carcinogens also swim in chlorinated pools." *Environmental Science & Technology* 42(4): 1032-1037.
- Weaver, W. A., J. Li, Y. L. Wen, J. Johnston, M. R. Blatchley and E. R. Blatchley (2009). "Volatile disinfection by-product analysis from chlorinated indoor swimming pools." *Water Research* 43(13): 3308-3318.
- Weng, S.-C., W. A. Weaver, M. Z. Afifi, T. N. Blatchley, J. S. Cramer, J. Chen and E. R. Blatchley (2011). "Dynamics of Gas-phase Trichloramine (NCl<sub>3</sub>) in Chlorinated, Indoor Swimming Pool Facilities." *Indoor Air* 21(5): 391-399.
- Weng, S. C. and E. R. Blatchley (2011). "Disinfection by-product dynamics in a chlorinated, indoor swimming pool under conditions of heavy use: National swimming competition." *Water Research* 45(16): 5241-5248.
- World Health Organisation (WHO) (2006). "Guidelines for safe recreational water environments." Volume 2: Swimming pools and similar environments.



# **Supporting Information for Chapter 4**

## **Comparison of a novel extraction-based colorimetric (ABTS) method with membrane introduction mass spectrometry (MIMS): trichloramine dynamics in pool water**

Fabian Soltermann, Tobias Widler,

Silvio Canonica and Urs von Gunten (2014)

*Water Research*, 58, 258-268

## **A Valve inlet control and signal analysis of MIMS 2000**

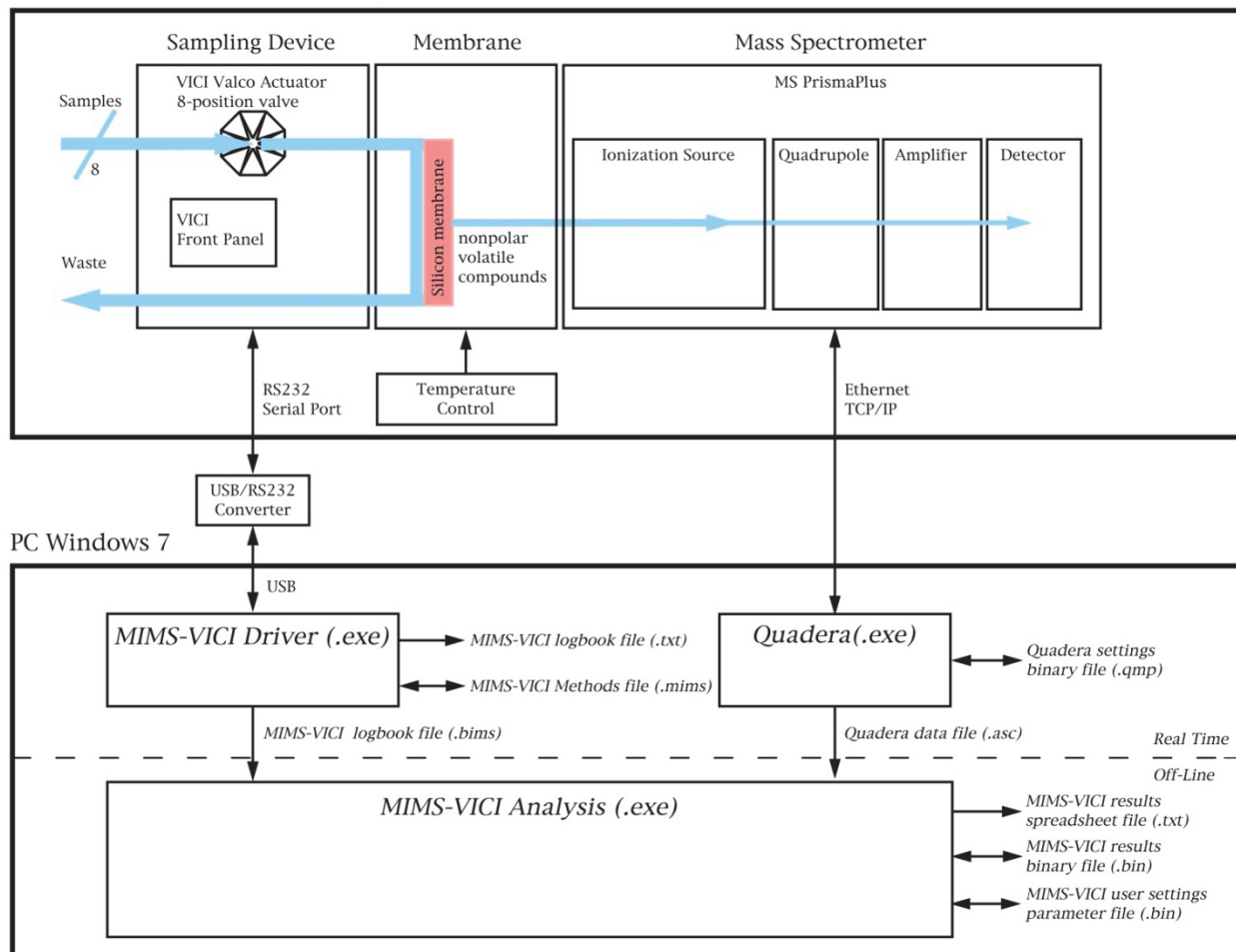
### **Text A.1.**

The MIMS 2000 apparatus (Microlab Aarhus, Denmark) is commonly delivered with a multi-port valve to facilitate automatic measurement of multiple samples. The inlet valve can be controlled by a basic software which has the disadvantage that it does not log the valve positions. Such a log-book is crucial since the control and data acquisition software of the mass spectrometer (QUADERA) is completely independent from the valve control software. An interpretation of the MS signals requires that signals can be linked to changes of the valve position. Therefore, a new software (MIMS-VICI driver) to conveniently control the inlet valve and to log the valve position was developed (Scheme A.1).

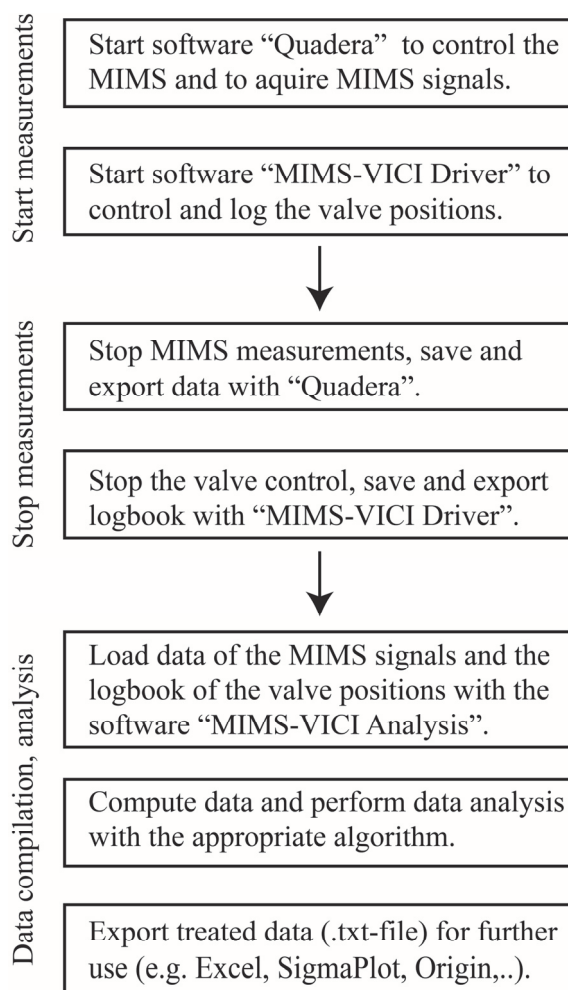
A second new software (MIMS-VICI Analysis) was engineered to link the MS signals exported from QUADERA with the logged data of the valve position. This software illustrates the combined data graphically. Additionally, the software facilitates data processing and analysis which is essential since data volume increases rapidly with duration of the measurement (commonly one measurement is performed every 500 ms). The software reduces the data volume tremendously by analysing steady-state measurements (extraction of mean values), flow-injections (extraction of peak values) and continuous measurements (extraction of signals after defined time-steps). The reduced data can be exported in tables as .txt-files containing measurement time, sample ID and compiled values for the different ions (Scheme A.2).

Results used in this study were all based on steady-state measurements. The implemented algorithm in the software averages the values over the second half of the measurement period. The resulting average is plotted in a graph with the signal. If the steady-state signal is not reached after half of the measurement or the MIMS measurement is influenced by air bubbles or other problems, the user has the option to manually set the ranges for the steady-state analysis.

## Membrane Introduction Mass Spectrometer (MIMS)



Scheme A.1. Overview of the software used for MIMS measurements.



**Scheme A.2.** Chronological overview of the procedure for MIMS measurements.



## B Further information on the extraction-based ABTS method and on trichloramine analysis with MIMS

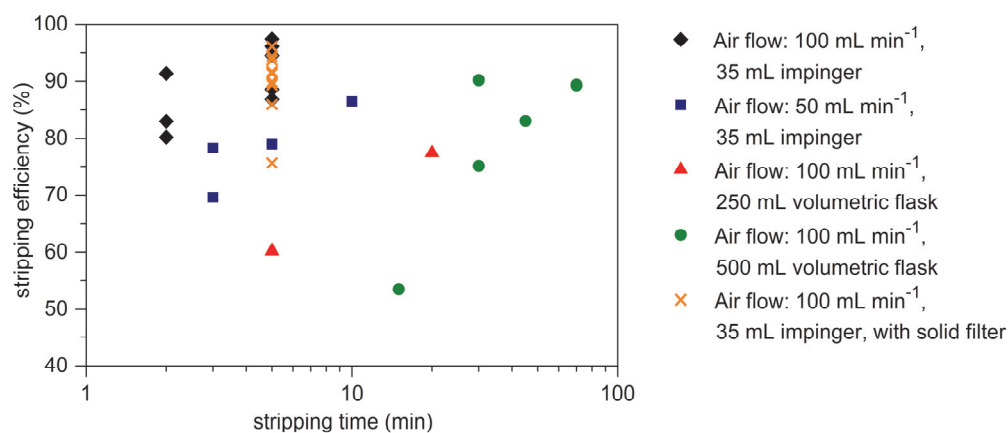


**Figure B.1.** Stripping efficiency (percentage of trichloramine stripped) with different air flows, stripping time and volume of the extraction impinger. Stripping efficiencies near 90% were reached with an air flow of  $100 \text{ mL min}^{-1}$  and a 35 mL impinger.

**Table B.1** Trichloramine concentration in ultrapurified water measured before and after stripping (5 min, air flow  $100 \text{ mL min}^{-1}$ ) by the direct reaction with buffered ABTS solution ( $5 \mu\text{M}$  ABTS,  $0.05 \text{ M}$  phosphate buffer with pH 2.6).

Run	Absorbance (1 cm cell)		Stripping efficiency (%)
	before stripping	after stripping	
1	0.068	0.013	81
2	0.067	0.008	88
3	0.069	0.009	87
4	0.071	0.009	87
5	0.069	0.010	86
6	0.069	0.007	89
7	0.408	0.043	90
8	0.393	0.043	89
9	0.408	0.075	82
10	0.421	0.073	83
11	0.427	0.043	90
12	0.376	0.055	85
13	0.380	0.073	81
14	0.387	0.079	79
		average	86
		std.-dev.	4

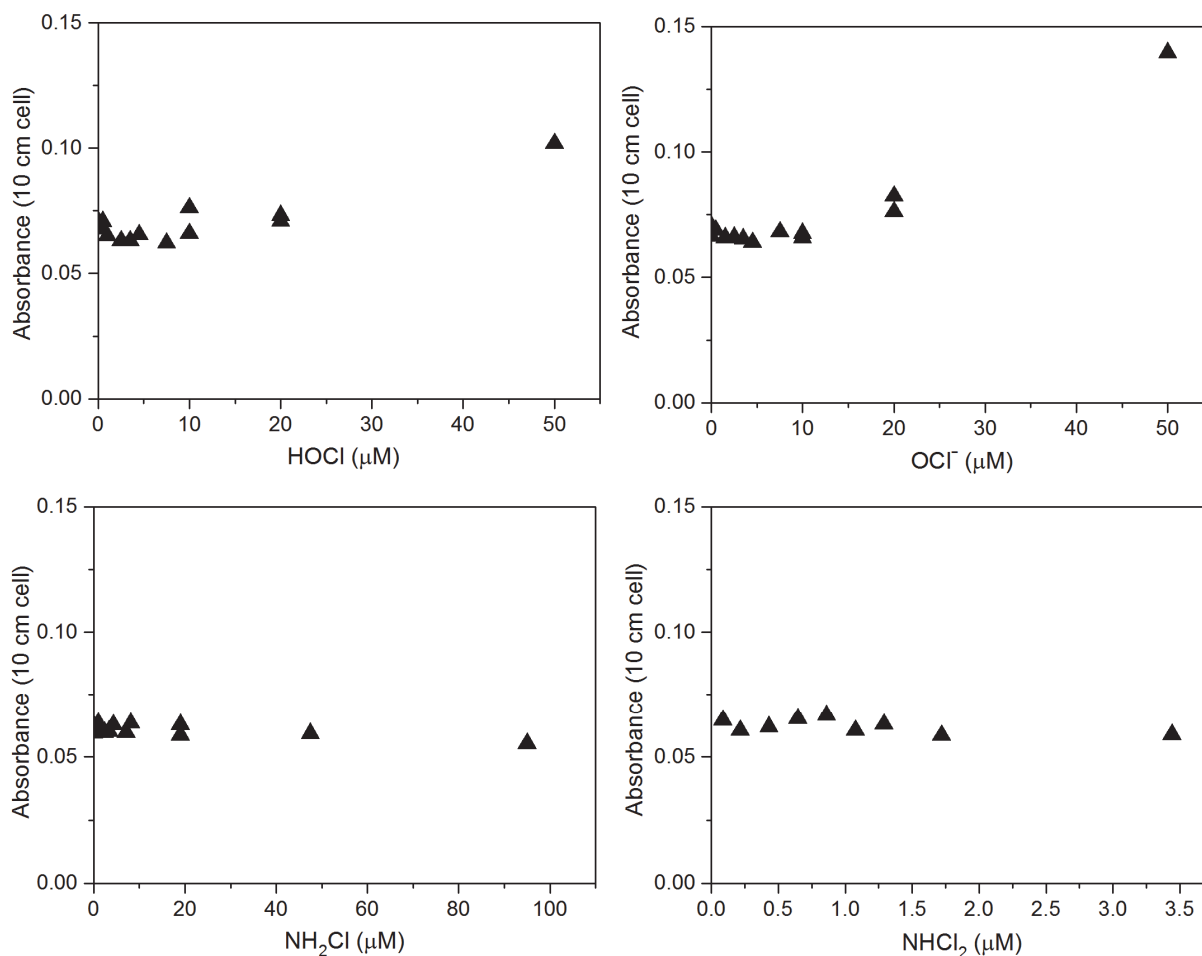


**Figure B.2.** Elimination of interferences with the filter (impregnated silica gel). Measurements with the extraction-based ABTS method were conducted with solutions of potentially interfering substances (HOCl (pH 3.3), OCl<sup>-</sup> (pH 8.9), NH<sub>2</sub>Cl and NHCl<sub>2</sub>) in the extraction impinger. Absorption remained for all concentrations on the level of the blank absorption (no interference) if the concentration was within the limits imposed by Swiss pool water regulations (free chlorine: 0.2–0.8 mg L<sup>-1</sup> as Cl<sub>2</sub> equals ~3–10  $\mu\text{M}$  HOCl or OCl<sup>-</sup>; combined chlorine: < 0.2 mg L<sup>-1</sup> as Cl<sub>2</sub> equals ~3  $\mu\text{M}$  NH<sub>2</sub>Cl or 1.5  $\mu\text{M}$  NHCl<sub>2</sub>) (SIA, 2013).

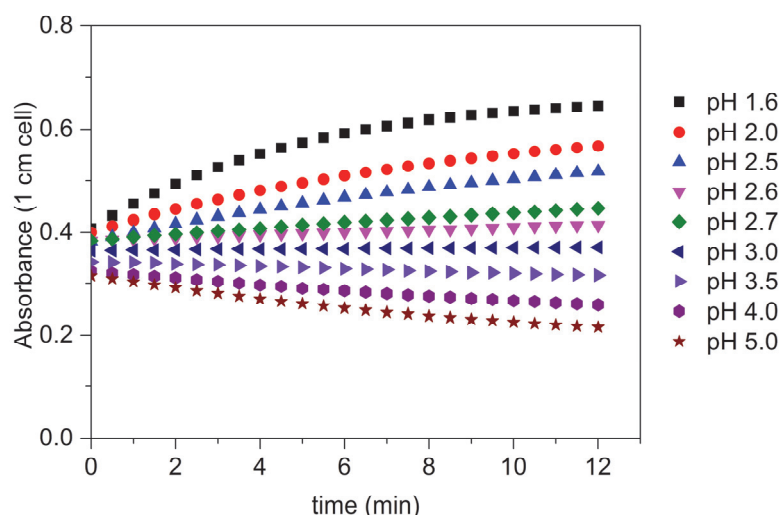


**Figure B.3.** Evolution of the absorbance of an ABTS solution (125  $\mu\text{M}$ ) with time after the reaction with trichloramine (0.75  $\mu\text{M}$ ). Solutions were buffered with phosphate buffer (0.15 M) at various pH values. The original pH of the buffer solution (2.5) was adjusted with 1 and 5 M  $\text{H}_2\text{SO}_4$  and 1 and 5 M NaOH. The results indicate that the ABTS solutions buffered at pH 2.6–3 gave the most stable readings.

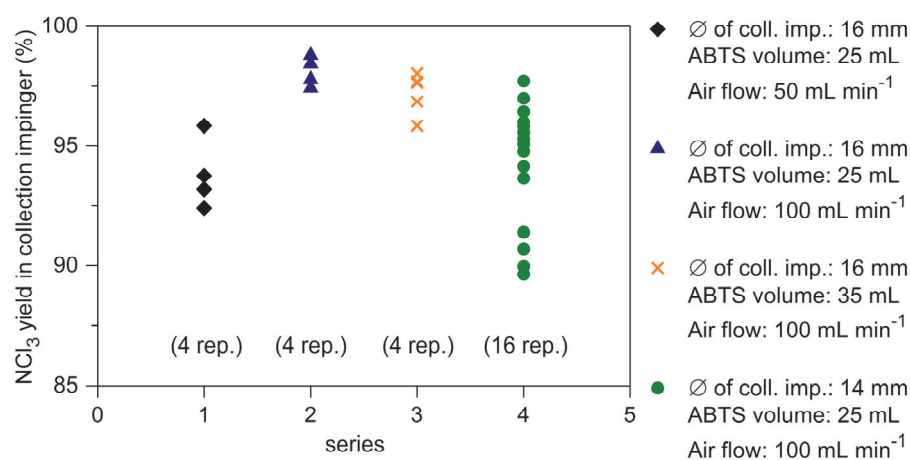


**Figure B.4.** Yield of the trichloramine reaction in the collection impinger ( $\text{NCl}_3$  reacting in collection impinger / ( $\text{NCl}_3$  reaction in collection impinger +  $\text{NCl}_3$  reaction in backup impinger)). Different parameters, such as the volume of the collection impinger (inner diameter of the impinger 14 or 16 mm), the volume of the ABTS solution (25 or 35 mL) and the air flow (50 or 100  $\text{mL min}^{-1}$ ), were varied. The trichloramine concentrations in the extraction impinger was  $\sim 1 \mu\text{M}$ .

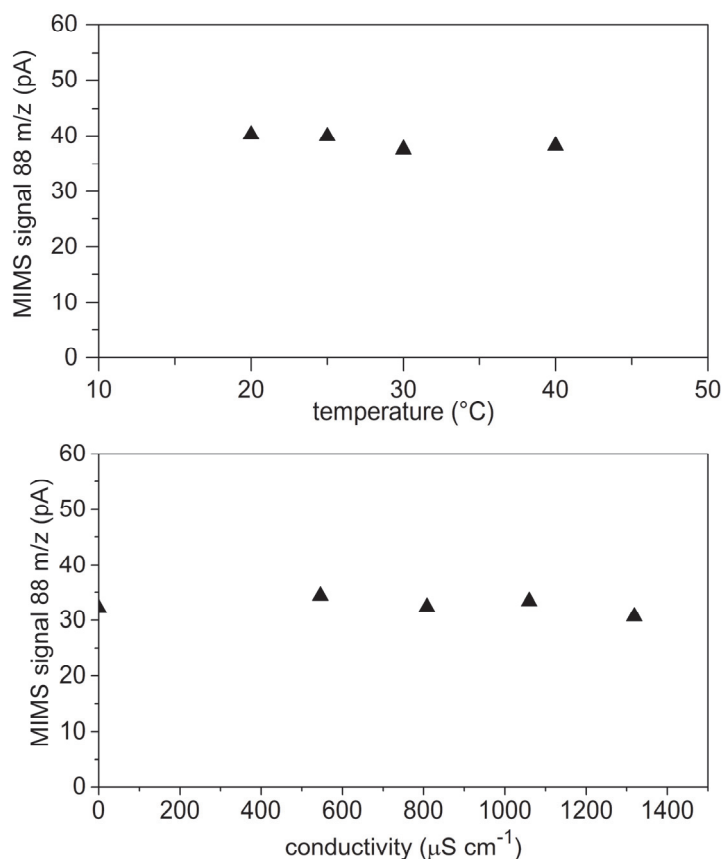


**Figure B.5.** Influence of sample (a) temperature and (b) conductivity on the trichloramine signal ( $0.5 \mu\text{M}$ ) measured with MIMS. The same amount of trichloramine was added simultaneously to all samples which were measured successively. The conductivity was adjusted by the addition of KCl ( $525 \text{ mg L}^{-1}$  KCl corresponded a conductivity of  $\sim 1000 \mu\text{S cm}^{-1}$ ).

**Table B.2.** Slopes of the trichloramine calibration lines with the extraction-based ABTS method. Data obtained from 5 calibrations on 3 different days with different solutions.

calibration	slope
1	0.53
2	0.55
3	0.53
4	0.50
5	0.48
average	0.52
standard dev.	0.02
%-standard dev.	5%

**Table B.3.** Ratio between expected (from calibration in purified water) and measured MIMS signal for added  $\text{NCl}_3$  ( $\sim 0.4 \mu\text{M}$ ) in 9 different pool waters.

Sample	ratio expected / measured signal
1	1.53
2	1.45
3	1.40
4	1.41
5	1.65
6	1.27
7	1.22
8	1.45
9	1.46
average	1.43

### Text B.1.

Trichloramine stability was measured by two different ways (Figure B.6.):

(i) 10 different pool waters ( $\blacktriangle$ , including a whirlpool sample (open symbol)) were spiked with trichloramine ( $\sim 1.5 \mu\text{M}$ ) and trichloramine concentrations were regularly checked in the untreated samples. Exponential decay rates ( $\text{s}^{-1}$ ) were deduced from these blank measurements ( $R^2$  values were commonly  $> 0.9$ ). Decay rates clearly increased with decreasing initial free chlorine concentration.

(ii) In 4 pool water samples ( $\blacksquare$ ), trichloramine concentrations were continuously measured with MIMS. For these measurements, pool water was constantly withdrawn from the bottom of a 2 L bottle. The resulting decay rates were slightly lower than from the 10 samples measured in (i). This might be a consequence of the potential trichloramine outgassing during the experiments performed in (i), in which trichloramine solution was continuously taken from the 2 L bottle with a dispenser resulting in an increased mixing of the trichloramine solution and an increased headspace.

To investigate the effect of the free chlorine concentration on trichloramine stability, the trichloramine concentration was measured continuously in one sample ( $\blacksquare$ , containing  $0.25 \text{ mg L}^{-1}$  as  $\text{Cl}_2$ ) after the addition of free chlorine ( $0.45 \text{ mg L}^{-1}$  as  $\text{Cl}_2$ ). Blank measurement (pool sample plus free chlorine, no trichloramine spiked) revealed that there was trichloramine formation induced by the free chlorine addition. Trichloramine stability in the pool water increased with the addition of free chlorine. If the induced trichloramine formation (determined

from the blank experiment) was subtracted ( $\square$ ), trichloramine stability was similar to the one in the sample without free chlorine addition. Hence, the increased trichloramine stability was mainly due to the chlorine-induced trichloramine formation.

Conclusively, it seemed that trichloramine decay was enhanced for low free chlorine concentrations but reached a value of  $2\text{--}5 \times 10^{-5} \text{ s}^{-1}$  for higher free chlorine concentrations. This is in agreement with two different studies reporting trichloramine decay rates of  $7.5 \times 10^{-6} \text{ s}^{-1}$  and  $3.4 \times 10^{-5} \text{ s}^{-1}$  in phosphate buffered and purified water, respectively (Saguinsin and Morris, 1975; Kumar et al., 1987).

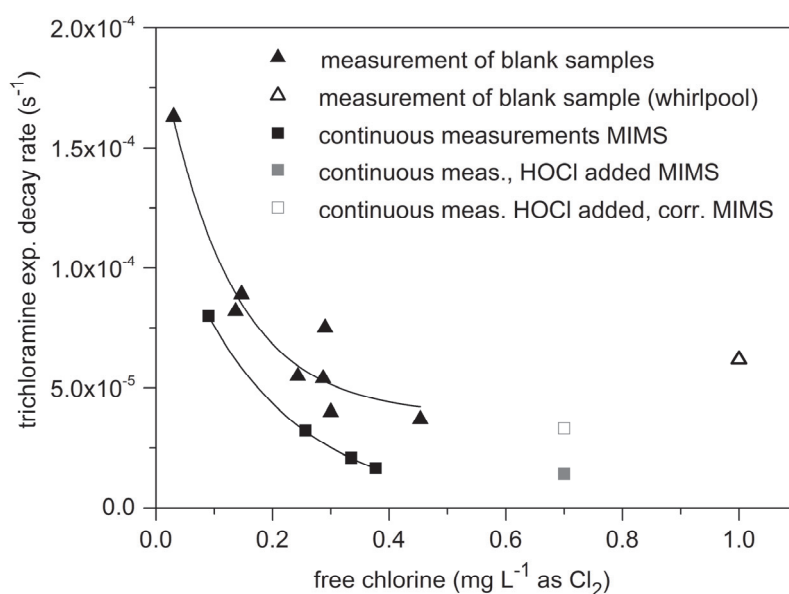


**Figure B.6.** Experimental decay rates for spiked trichloramine in pool water as a function of the free chlorine concentration for the two measurement methods: 1. Trichloramine decay was measured regularly (5 times within 2 hours) in the blank samples of experiments and 2. trichloramine decay was measured continuously with MIMS from a 2 L bottle.

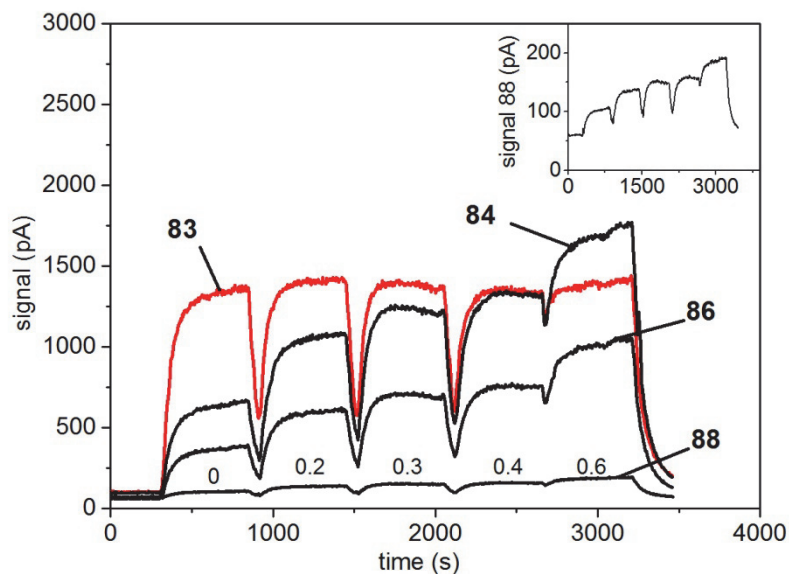


**Figure B.7.** Trichloramine calibration with standard addition of trichloramine (0, 0.2, 0.3, 0.4 and 0.6  $\mu\text{M}$ ) to pool water. The absolute MIMS signals depend strongly on the setting of the amplifier while the ratios remain constant. Signal 88 m/z is much weaker than signals 86 m/z and 84 m/z. However, trichloramine in pool water was always analysed with signal 88 m/z since it is the only one which is assumed to be free of interferences. Signal 83 m/z (assumed to represent chloroform and dichlorobromoform) was stable since THM concentrations remained unchanged by the trichloramine addition. Therefore, it can be used as an internal standard to correct for short term variations in MIMS sensitivity.

## **C Statistical analysis of data from pool sample measurements**

**Text C.1.** Statistical analysis of the pool water samples was performed with the software “R” (Team R Development Core, 2013). Data from Table C.1. were analysed with the following procedure:

- All samples containing NA (not available) for one parameter were omitted.
- Whirlpool sample “O 12” was omitted (outlier, probably because the whirlpool was used right before sampling –  $\text{NCl}_3$  might have been stripped).
- Sample “OB 2” was omitted (outlier, which had a very low pH (5.5) because of a malfunctioning pH control of the pool water).
- Urea concentrations below the detection limit ( $< 0.05 \text{ mg L}^{-1}$ ) were set to  $0.025 \text{ mg L}^{-1}$ .
- A parameter describing the relative loss of free chlorine during the transportation to the laboratory was introduced ( $\text{c.loss} = \text{free chlorine in the laboratory} / \text{free chlorine on-site}$ ).
- A parameter describing the combined chlorine concentration without trichloramine was introduced (combined chlorine ( $\text{mg L}^{-1}$  as  $\text{Cl}_2$ ) – trichloramine ( $\text{mg L}^{-1}$  as  $\text{Cl}_2$ ))
- Analysis was performed with a stepwise reduction of the parameters starting from a model containing all parameters. Parameters were taken either from on-site measurements or from measurements in the laboratory but no model was calculated by mixing parameters measured on-site and measured in the laboratory (e.g. free chlorine laboratory and free chlorine on-site).
- Analysis was performed with/without transformation according to standard statistical practice (concentrations = log-transformation, ratios = root-square-transformation, pH = no transformation) and with/without interactions (not more than two-way interactions).



**Table C.1.** Data set used for statistical analysis with R (T.ABTS = trichloramine measured with ABTS method ( $\mu\text{M}$ ), fc = free chlorine ( $\text{mg L}^{-1}$  as  $\text{Cl}_2$ ), cc = combined chlorine ( $\text{mg L}^{-1}$  as  $\text{Cl}_2$ ), cc.corr = combined chlorine - trichloramine conc. ( $\text{mg L}^{-1}$  as  $\text{Cl}_2$ ), HOCl = calculated from fc and pH ( $\text{mg L}^{-1}$  as  $\text{Cl}_2$ ), c.loss = calculated free chlorine loss (fc / fc.os), fc.os = free chlorine on-site ( $\text{mg L}^{-1}$  as  $\text{Cl}_2$ ), cc.os = combined chlorine on-site ( $\text{mg L}^{-1}$  as  $\text{Cl}_2$ ), pH.os = pH on-site, HOCl.os = calculated from fc.os and pH.os ( $\text{mg L}^{-1}$  as  $\text{Cl}_2$ ), toc = total organic carbon ( $\text{mg C L}^{-1}$ ) and NA = not available). The last three pools in the list had a shared water treatment.

sample	T.ABTS	fc	cc	cc.corr	pH	HOCl	urea	c.loss	treatment	pool.type	fc.os	cc.os	pH.os	HOCl.os	toc
PF 2	0.09	0.08	0.23	0.22	7.51	0.04	0.4	0.4	Filter	beginner	0.19	0.24	7.35	0.11	1.5
PF12	0.19	0.23	0.12	0.11	7.55	0.11	0.3	0.7	ozone - activated carbon	non-swimmer	0.33	0.11	7.3	0.21	1
HK4	0.03	0.03	0.16	0.16	7.48	0.02	1.8	0.4	Filter	swimmer	0.08	0.17	7.25	0.05	2.2
HK 12	0.32	0.29	0.14	0.12	7.09	0.21	1.3	0.7	UV	whirlpool	0.43	0.15	6.9	0.35	3.4
K 1	0.38	0.45	0.11	0.08	7.32	0.28	1	0.8	UV	swimmer	0.55	0.08	7.1	0.4	1.5
K 2	0.19	0.15	0.14	0.13	7.33	0.09	1.6	0.4	UV	non-swimmer	0.36	0.15	7.2	0.25	2
D 8	0.23	0.24	0.11	0.09	7.12	0.18	0.4	1	Filter	swimmer	0.23	0.06	6.9	0.19	1.2
Wa 6	0.04	0.03	0.1	0.10	7.38	0.02	0.2	0.6	UV	beginner	0.05	0.14	7.2	0.03	1.2
B 9	0.2	0.29	0.09	0.08	7.36	0.17	0.2	0.9	aggregation filter	swimmer	0.33	0.09	NA	NA	0.6
B 10	0.32	0.3	0.12	0.10	7.4	0.17	0.7	0.9	aggregation filter	non-swimmer	0.35	0.17	NA	NA	1.1
O 11	0.17	0.14	0.16	0.15	7.29	0.09	1.1	1.4	Filter	non-swimmer	0.1	0.24	7.19	0.07	1.1
O 12	0.48	1	0.16	0.13	7.54	0.49	0.5	1	Filter	whirlpool	0.96	0.15	8.02	0.23	0.8
T 4	0.02	0.01	0.21	0.21	7.34	0.01	0.1	0	ozone - activated carbon	non-swimmer	0.25	0.16	7.15	0.18	0.5
T 6	0.17	0.21	0.05	0.04	7.44	0.11	0.025	0.5	ozone - activated carbon	therapeutic pool	0.42	0.07	7.25	0.28	0.4
T 10	0.39	0.26	0.22	0.19	7.26	0.17	1.3	0.6	UV	non-swimmer	0.45	0.15	7.1	0.33	1.8
OB 2	0.13	0.03	0.43	0.42	5.53	0.03	0.8	0.2	Filter	beginner	0.15	0.4	5.6	0.15	1.9
OB 4	0.14	0.17	0.21	0.20	7.46	0.09	0.7	0.6	Filter	beginner	0.3	0.2	7.25	0.2	1.2
OB 6	0.47	0.33	0.23	0.20	7.22	0.22	0.5	0.7	multilayer filter	beginner	0.5	0.15	6.9	0.41	1.5
E 4	0.2	0.16	0.2	0.19	7.47	0.09	0.45	0.6	Filter	multiple use	0.25	0.15	7.3	0.16	1.2
E 6	0.24	0.13	0.13	0.11	7.08	0.1	0.3	0.7	Filter	beginner	0.2	0.12	6.9	0.16	0.6
E 8	0.12	0.15	0.16	0.15	7.56	0.07	0.025	0.5	multilayer filter	swimmer	0.3	0.12	7.4	0.17	1.7
RE 2	0.43	0.22	0.35	0.32	6.98	0.17	0.3	0.5	aggregation filter	beginner	0.48	0.28	6.8	0.4	1.3
RE 4	0.16	0.12	0.06	0.05	7.48	0.06	0.025	0.3	ozone - activated carbon	swimmer	0.36	0.05	7.25	0.24	0.3
RE 6	0.2	0.29	0.07	0.06	7.57	0.14	0.025	0.7	ozone - activated carbon	warm water	0.4	0.06	7.35	0.24	0.4
RE 8	0.28	0.3	0.25	0.23	7.38	0.18	0.55	0.7	aggregation filter	multiple use	0.42	0.21	7.2	0.29	1.2
RE 10	0.14	0.15	0.14	0.13	7.45	0.08	0.7	0.6	UV	swimmer	0.25	0.13	7.3	0.16	3.5
RE 12	0.27	0.24	0.16	0.14	7.54	0.12	0.25	0.5	multilayer filter	non-swimmer	0.46	0.17	7.35	0.28	0.9
W s	0.44	0.54	0.19	0.16	7.44	0.3	NA	NA	UV	swimmer	NA	NA	NA	NA	NA
W ch	0.33	0.54	0.16	0.14	7.53	0.27	NA	NA	UV	non-swimmer	NA	NA	NA	NA	NA
W d	0.35	0.41	0.18	0.16	7.44	0.22	NA	NA	UV	jump	NA	NA	NA	NA	NA

**Table C.2.** Selection of results for model 1-9 indicating the included model parameters, the  $R^2$  of the model and the significance of the parameters (significance codes: 0 < '\*\*\*' < 0.001 < '\*\*' < 0.01 < '\*' < 0.05 < '.' < 0.1 < '' < 1).

<b>Comparison free chlorine vs. HOCl</b>			
model 1	$R^2$	Pr(> t )	
log (T.ABTS) ~ log (fc)	<b>0.89</b>	1.9E-11	***
log (fc)			
model 2	$R^2$	Pr(> t )	
log (T.ABTS) ~ log (HOCl)	<b>0.93</b>	6.2E-14	***
log (HOCl)			
<b>Effect of free chlorine loss</b>			
model 3	$R^2$	Pr(> t )	
log (T.ABTS) ~ log (HOCl.os)	<b>0.55</b>	5.4E-05	***
log (HOCl.os)			
model 4	$R^2$	Pr(> t )	
log (T.ABTS) ~ log (HOCl.os) + sqrt (c.loss)	<b>0.92</b>	9.8E-11	***
log (HOCl.os)		3.5E-09	***
sqrt (c.loss)			
model 5	$R^2$	Pr(> t )	
log (T.ABTS) ~ log (HOCl) + sqrt (c.loss)	<b>0.94</b>	1.1E-11	***
log (HOCl)		2.7E-01	
sqrt (c.loss)			
<b>Influence of pH</b>			
model 6	$R^2$	Pr(> t )	
log (T.ABTS) ~ log (HOCl) + pH	<b>0.94</b>	8.1E-13	***
log (HOCl)		3.3E-01	
pH			
<b>Influence of combined chlorine</b>			
model 7	$R^2$	Pr(> t )	
log (T.ABTS) ~ log (HOCl) * log (cc)	<b>0.95</b>	8.0E-06	***
log (HOCl)		1.7E-02	*
log (cc)		3.4E-02	*
log (HOCl) : log (cc)			
<b>Influence of urea and toc</b>			
model 8	$R^2$	Pr(> t )	
log (T.ABTS) ~ log (HOCl) + log (urea) + log (toc)	<b>0.95</b>	9.2E-13	***
log (HOCl)		6.2E-01	
log (urea)		4.1E-01	
log (toc)			

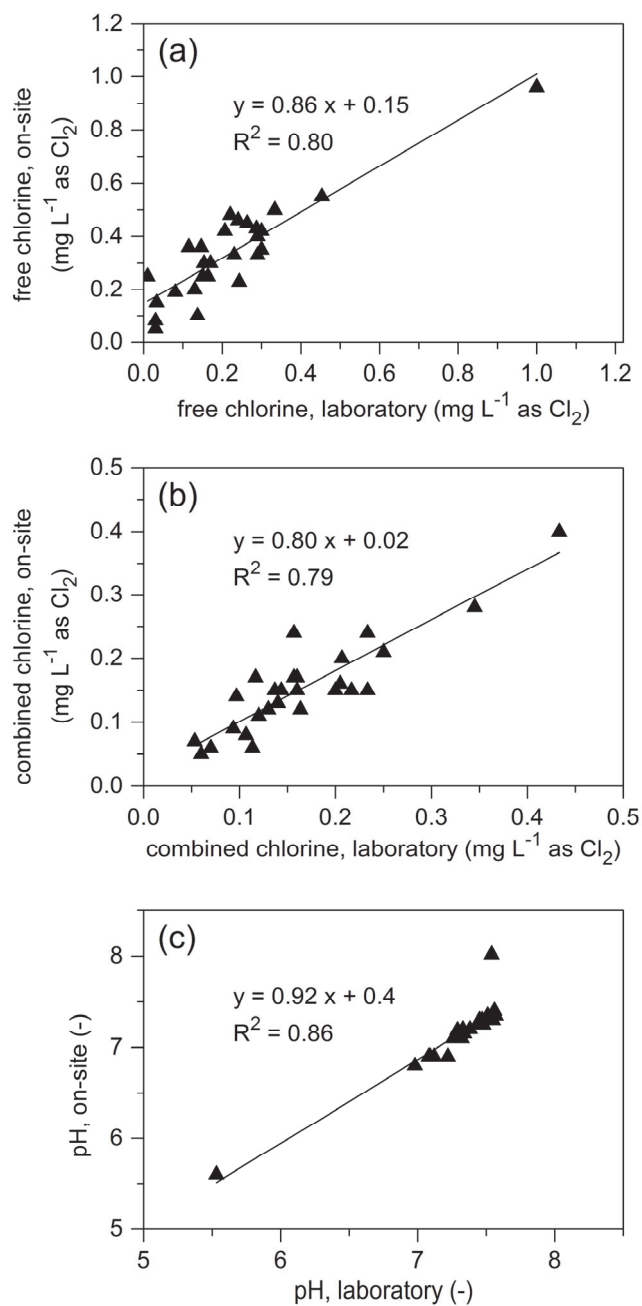


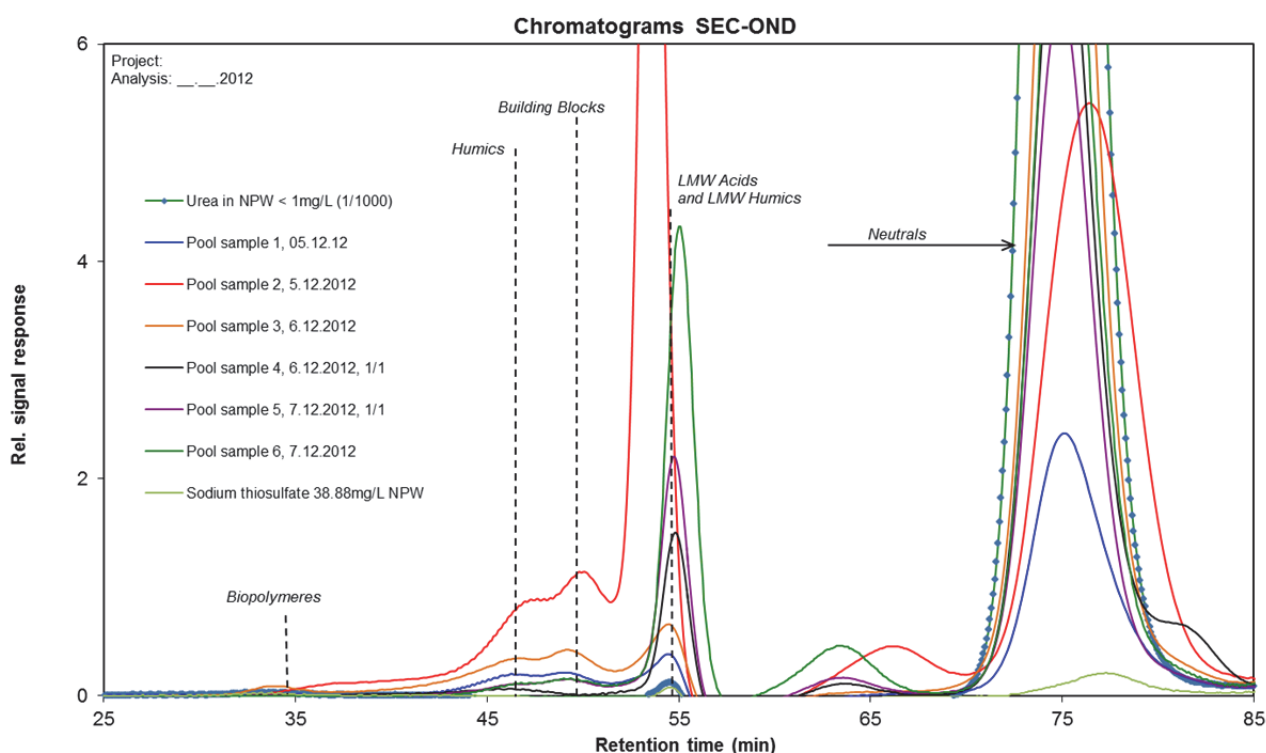
**Figure C.1** Comparison of on-site and laboratory measurements of (a) free chlorine, (b) combined chlorine and (c) pH.

## D Further information on pool samples

### Text D.1.

#### Analytical procedure of SEC-OND measurements

The samples were quenched with thiosulfate before electro dialysis was performed in order to reduce the nitrate concentration (reduction of conductivity: 75 %). High nitrate concentrations as found in pool water can lead to a big peak at the end of the SEC-OND chromatogram (low molecular weight compounds) which overlaps with the organic nitrogen compounds (Chon et al., 2013). After electro dialysis, samples were measured with an analytical system according to Huber et al. (2011a; 2011b) to characterize dissolved organic matter (DOM) and urea. The SEC column used (Toyopearl TSK HW-50S, 250 x 20 mm) had a fractionation range of 100–20'000 D. The system was running with a phosphate- buffer as eluent (24 mM, pH 6.6) at a flow rate of 1 mL min<sup>-1</sup>. Organic carbon was fully oxidized to CO<sub>2</sub>, whereas the organic nitrogen components were oxidized to nitrate in parallel (Huber et al., 2011a; Huber et al., 2011b). Results were quantified and interpreted with a customized software (Fiffikus, Huber Germany 2006). With an injection volume of 1 mL, the limit of detection (LOD) for organic carbon was 10 µg C L<sup>-1</sup>, while for organic nitrogen the LOD was 5 µg N L<sup>-1</sup>.



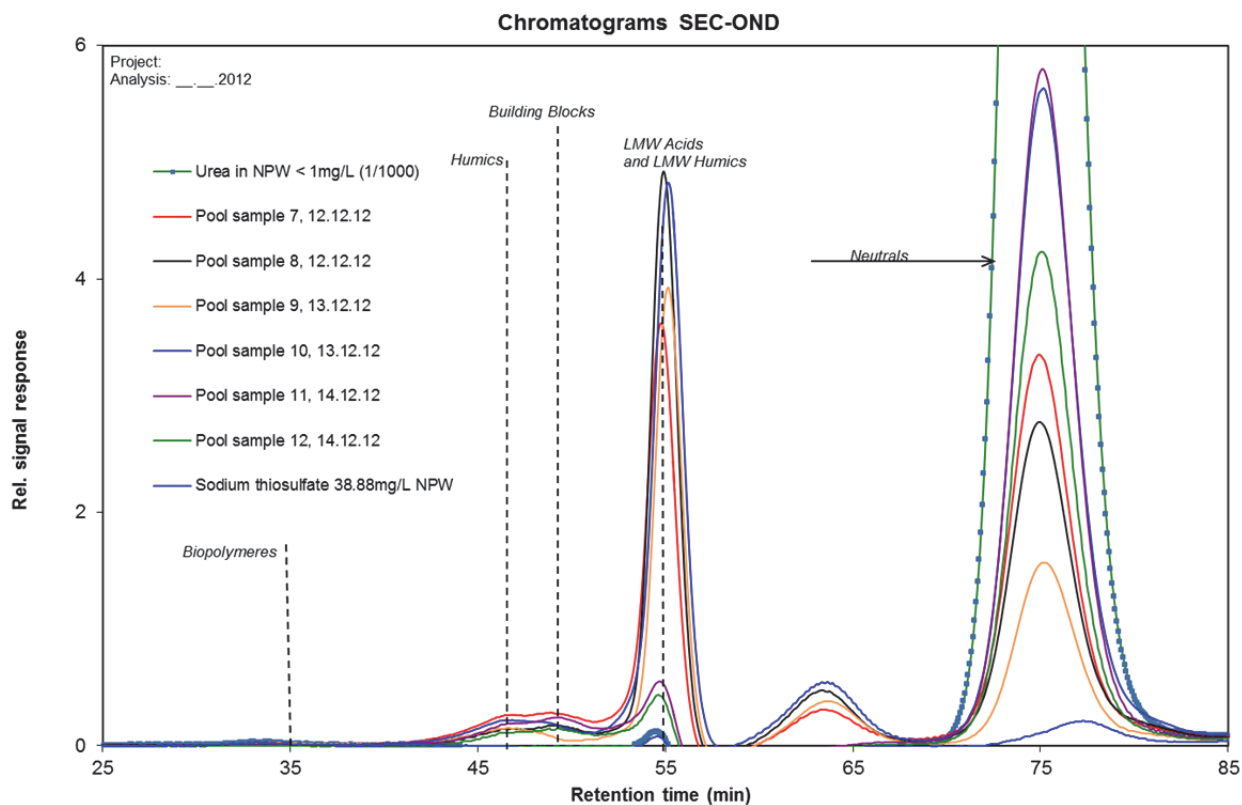


**Figure D.1.** SEC-OND chromatograms of 12 pool samples showing the different fractions (size) of the dissolved organic nitrogen in the swimming pool samples. The chromatograms of solutions of urea and sodium thiosulfate in pure water (NPW) are also shown for comparison.

**Table D.1.** Ratio of urea on the total dissolved organic nitrogen (DON) concentration for 12 pool samples, measured with SEC-OND. The concentrations of urea (ppb N) and DON (ppb N) were derived from the chromatograms in Figure D.1. The concentration of DON without urea as well as the fraction of urea relative to total DON (% N) are also given.

Pool sample	Urea (ppb N)	Total DON (ppb N)	Total DON - Urea (ppb N)	Fraction of urea (% N)
1	120	164	44	73%
2	313	678	365	46%
3	448	529	81	85%
4	598	810	212	74%
5	553	700	147	79%
6	360	501	141	72%
7	143	277	134	52%
8	123	266	143	46%
9	68	186	118	37%
10	246	414	168	59%
11	245	289	44	85%
12	180	212	32	85%

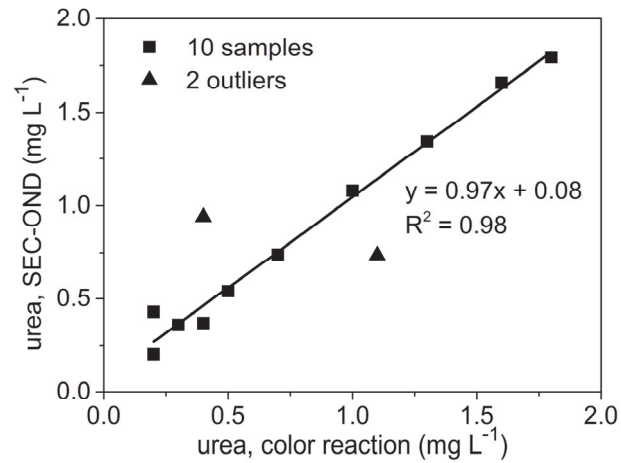


**Figure D.2.** Comparison of urea concentrations in 12 pool water samples measured with SEC-OND and the colorimetric method described in the main text. The two distinct analytical methods showed a very good correlation ( $R^2 = 0.98$ ) except for two outliers for unknown reasons.

## **E** Additional information on pool facility and on-site measurements

### **Text E.1.**

Further information on the pool facility and the conduction of the measurements with MIMS are given elsewhere (Soltermann et al., 2014). A summary of the essential information for this manuscript is given in the following.

#### ***Pool facility and water treatment part***

The pool facility in which the on-site measurements were conducted included three pools: a 50 m swimmer pool (1'580 m<sup>3</sup>), a diving well (370 m<sup>3</sup>) and a wading pool (56 m<sup>3</sup>). The turn-over times were estimated to be 1 h for the wading pool and 4.5 h for the swimming pool. The water from all pools was treated in a common treatment part including a collecting basin, a multilayer filter and a UV treatment for the swimming pool and one for the wading and diving pool. Free chlorine concentration and pH were controlled in each pool separately.

#### ***MIMS sampling ports***

The sampling ports in the wading pool and in the swimming pool were located 30–40 cm below the water surface in the middle of the longitudinal side of the pool. Samples flow was gravity-driven from the sampling ports to the control gauge (pH and free chlorine). An intersection right before the gauge lead a side stream to a 200 mL volumetric flask for MIMS analysis. The sample flow was constantly between 20–40 mL min<sup>-1</sup> resulting in an average residence time of 5–10 minutes in the volumetric flask. The sample was withdrawn by the MIMS from the bottom of the volumetric flask. Control measurement with pool water taken with a 2 L bottle directly from the wading pool revealed that there was no trichloramine outgassing or loss during the sampling procedure.

#### ***MIMS calibration***

According to the findings in the main text, trichloramine calibrations were performed every 2–4 days with trichloramine standard addition to pool water. During the sampling campaign a loss of sensitivity (1–2 % per day) and a temporal increase of the background of the MIMS was observed. Considering these facts, data were analysed by using interpolated values of the steepness and the intercept for the calibration line.

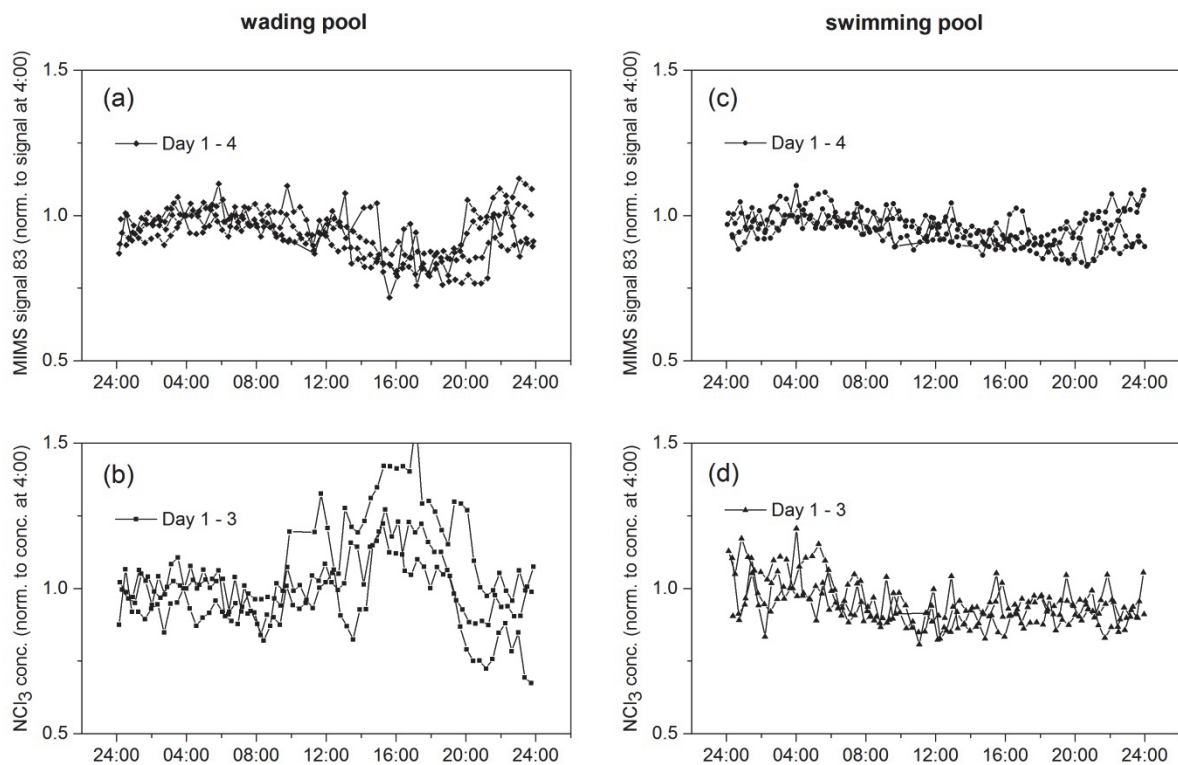


**Figure E.3.** Daily evolution of (a, c) signal 83 m/z and (b, d) the trichloramine concentration over a period of 3–4 days. The signals were normalized to the signal at 4:00 a.m. of the same day.

Trichloramine concentrations typically increased with bather presence in the afternoon while the contrary was the case for signal 83 m/z. This effect was more pronounced in the wading pool, where the bather density was clearly higher.



## References

- Chon, K., Y. Lee, J. Traber and U. von Gunten (2013). "Quantification and characterization of dissolved organic nitrogen in wastewater effluents by electro dialysis treatment followed by size-exclusion chromatography with nitrogen detection." *Water Research* 47(14): 5381-5391.
- Huber, S., A. Balz and M. Abert (2011a). "New method for urea analysis in surface and tap waters with LC-OCD-OND (liquid chromatography-organic carbon detection-organic nitrogen detection)." *Journal of Water Supply: Research and Technology—AQUA* 60(3): 159-166.
- Huber, S. A., A. Balz, M. Abert and W. Pronk (2011b). "Characterisation of aquatic humic and non-humic matter with size-exclusion chromatography – organic carbon detection – organic nitrogen detection (LC-OCD-OND)." *Water Research* 45(2): 879-885.
- Kumar, K., R. W. Shinness and D. W. Margerum (1987). "Kinetics and mechanisms of the base decomposition of nitrogen trichloride in aqueous-solution." *Inorganic Chemistry* 26(21): 3430-3434.
- Saguinsin, J. L. S. and J. C. Morris (1975). *The chemistry of aqueous nitrogen trichloride. Disinfection Water and Wastewater.* J. D. Johnson. Michigan, Ann Arbor Science: 277-299.
- Swiss society of engineers and architects (SIA) (2013). "Water and water treatment in public pools (German)."
- Soltermann, F., T. Widler, S. Canonica and U. von Gunten (2014). "Photolysis of inorganic chloramines and efficiency of trichloramine abatement by UV treatment of swimming pool water." *Water research* 56: 280-291.
- Team R Development Core (2013). "R: A language and environment for statistical computing." R Foundation for Statistical Computing. Vienna, Austria, 2013. ISBN 3-900051-07-0. <http://www.R-project.org>.



# **Chapter 5**

## **Photolysis of inorganic chloramines and efficiency of trichloramine abatement by UV treatment of swimming pool water**

Fabian Soltermann, Tobias Widler,

Silvio Canonica and Urs von Gunten (2014)

*Water Research*, 56, 280-291

## Abstract

Trichloramine, one of the three inorganic chloramines (mono-, di- and trichloramine), is a problematic disinfection by-product in recreational pool water since it causes skin and eye irritations as well as irritations of the respiratory tract. The most commonly used chloramine mitigation strategy in pool water is UV treatment. Experiments with membrane inlet mass spectrometry (MIMS) confirmed that inorganic chloramines are effectively degraded by UV irradiation with low-pressure (LP) and medium-pressure (MP) mercury lamps (apparent quantum yields (QY):  $\text{NH}_2\text{Cl} = 0.50$  (LP) and  $0.31$  (MP)  $\text{mol einstein}^{-1}$ ,  $\text{NHCl}_2$ :  $1.06$  (LP) and  $0.85$  (MP)  $\text{mol einstein}^{-1}$ ). Trichloramine showed the fastest depletion with a quantum yield slightly above  $2 \text{ mol einstein}^{-1}$  in purified (LP and MP) and pool water (MP). This high quantum yield can partly be explained by reactions involving  $\cdot\text{OH}$  radicals (purified water) and the reaction of trichloramine with moieties formed during UV irradiation of pool water. The presence of free chlorine affects trichloramine degradation (QY:  $\sim 1.5 \text{ mol einstein}^{-1}$ ) since it scavenges  $\cdot\text{OH}$  radicals and competes with trichloramine for reactive species (e.g. organic amines).

Measurements in a pool facility revealed that the installed UV reactors degraded trichloramine by 40–50 % as expected from laboratory experiments. However, trichloramine reduction in the pools was less pronounced than in the UV reactors. Model calculations combining pool hydraulics with formation/abatement of trichloramine showed that there was a fast trichloramine formation in the pool from the residual chlorine and nitrogenous precursors. The main factors influencing trichloramine concentrations in pool water are the free chlorine concentration and the UV treatment in combination with the recirculation rate through the water treatment system.

## 5.1 Introduction

Disinfection of recreational pool water is necessary for hygienic safety reasons. Since the turnover time of pool water is in the order of several hours, the presence of a residual disinfectant in the pool is statutory in most countries. Commonly, free chlorine is used for disinfection of pool water, with the consequence that numerous chlorinated disinfection by-products (DBP) are formed (Richardson et al., 2010). Inorganic chloramines (mono-, di- and trichloramine) belong to this group of undesired DBPs. Mono- and dichloramine are not known to have serious adverse health effects but to act as precursors for more potent DBPs such as nitrosamines (Schreiber and Mitch, 2006; Soltermann et al., 2013). In contrast, trichloramine can provoke skin and eye irritations and is suspected to cause inflammation of the respiratory tract and potentially also asthma (Bernard et al., 2003; Schmalz et al., 2011b; Parrat et al., 2012). Trichloramine is clearly more volatile than mono- and dichloramine, hence uptake via inhalation is the dominant pathway of exposure.

The legal threshold for inorganic chloramines, also referred to as combined chlorine, in Swiss and German pool water is  $0.2 \text{ mg L}^{-1}$  as  $\text{Cl}_2$  (DIN, 2012; SIA, 2013). In Switzerland a regulatory value for trichloramine exists only for indoor pool air ( $0.2 \text{ mg m}^{-3}$ ) but not for pool water (SIA, 2013). This standard was exceeded in 10–15 % of the pool facilities in two studies considering a total of more than 100 facilities with different pool types in Germany and Switzerland (DGUV, 2009; Parrat et al., 2012). Data on trichloramine levels in pool water is very limited due to the lack of adequate analytical methods. Measured trichloramine concentrations reported in literature were mostly between  $0.1$  and  $0.5 \text{ }\mu\text{M}$  ( $0.02$ – $0.1 \text{ mg L}^{-1}$  as  $\text{Cl}_2$ ) but reached up to  $\sim 1 \text{ }\mu\text{M}$  ( $0.2 \text{ mg L}^{-1}$  as  $\text{Cl}_2$ ) (Gérardin and Subra, 2004; Weaver et al., 2009; Soltermann et al., 2014).

A substantial fraction of trichloramine in pool water is assumed to originate from the pH-dependent reaction of free chlorine with urea (Blatchley and Cheng, 2010; Schmalz et al., 2011a; Hansen et al., 2012). However, the reaction of free chlorine with urea is very slow under swimming pool conditions and there is no kinetic data available on the trichloramine formation from other nitrogenous precursors than urea. Even if other precursors have lower concentrations than urea, they can significantly contribute to the trichloramine formation if they react quickly with free chlorine. Measurement of trichloramine concentrations in various pool waters and on-site measurements revealed that the trichloramine concentration is strongly linked to residual chlorine and quickly changes with bather load while pH variations (7–7.5) and urea concentration play a minor role (Soltermann et al., 2014).

Because combined chlorine is photosensitive, a common strategy for combined chlorine mitigation in pool water is UV treatment. This approach is based on various studies investigating the photolysis of combined chlorine with a focus on monochloramine (Cooper et al., 2007; Watts and Linden, 2007; Li and Blatchley, 2009; De Laat et al., 2010; Hansen et al., 2013). Li and Blatchley (2009) found that higher chlorinated chloramines are more photosensitive. The apparent photolysis rate constants depend on the irradiation wavelength due to the wavelength-dependence of the molar absorption coefficients and the quantum yields. Especially for di- and trichloramines, quantum yields  $> 1$  hinted at the reaction of these species with photolysis products. Field studies confirmed that UV treatment with low-pressure (LP) and medium-pressure (MP) lamps reduced combined chlorine concentration in pool water by about 50–70 % while no clear effect on trichloramine concentration could be observed (Gérardin et al., 2005; Cassan et al., 2006; Kristensen et al., 2009). Furthermore, a significant increase of trihalomethane concentrations was linked to UV treatment in some studies (Gérardin et al., 2005; Cassan et al., 2006).

In this study the photolysis (quantum yields, kinetics) of chloramines ( $\text{NH}_2\text{Cl}$ ,  $\text{NHCl}_2$ ,  $\text{NCl}_3$ ) with LP and MP irradiation was investigated. In addition, trichloramine photolysis was studied in different pool waters to elucidate matrix effects. Furthermore, on-site measurements of trichloramine and combined chlorine were conducted in a pool facility to investigate the performance of MP UV lamps and their effect on trichloramine and combined chlorine concentrations in pool water. Based on this a model was developed to test the influence of various operational parameters on trichloramine concentrations.

## 5.2 Materials and Methods

### 5.2.1 Reagents

All chemicals were analytical grade and used without further purification. Sodium hypochlorite (6–14 % active chlorine), dimethylamine (DMA), *tert*-butanol (t-BuOH), morpholine (Mor), ammonium chloride and ortho-phosphoric acid were obtained from Sigma-Aldrich. Sodium dihydrogenphosphate, sodium hydroxide pellets, hydrochloric acid and perchloric acid were purchased from Merck. Atrazine was obtained from Riedel-de Haën. Ultrapurified water was produced by a “barnstead nanopure” water purification system (Thermo Scientific). Ready-to-use DPD-, buffer- and KI-solutions for free and combined chlorine analysis were provided by SWAN Analytical Instruments AG (Hinwil, Switzerland). Chloramine stock solutions ( $\text{NH}_2\text{Cl}$ : 25 mM,  $\text{NHCl}_2$  and  $\text{NCl}_3$ : ~2 mM) were produced as described elsewhere (Soltermann et al., 2014).

### 5.2.2 Analytical methods

Chloramine analyses were performed with a membrane inlet mass spectrometer (MIMS 2000 from Microlab, Aarhus). The inlet temperature was fixed at 40 °C and the sample flow rate was about 8 mL min<sup>-1</sup>. In purified water, the signals of the ions (m/z)  $\text{NH}_2^{37}\text{Cl}^{37}\text{Cl}^{*+}$  (53),  $\text{NH}^{35}\text{Cl}^{37}\text{Cl}^{*+}$  (87) and  $\text{N}^{35}\text{Cl}^{37}\text{Cl}^{*+} / \text{N}^{37}\text{Cl}^{37}\text{Cl}^{*+}$  (86 / 88) were used to quantify mono-, di- and trichloramine, respectively. Trichloramine in pool water samples was measured by analysing the 88 m/z ion signal (Weaver et al., 2009). During the field study in the pool facility, signal 83 m/z was analysed, which presumably represents the trihalomethane concentration (ion  $\text{HC}^{35}\text{Cl}^{35}\text{Cl}^{*+}$  from chloroform and monobromodichloromethane) with potentially slight interferences from other substances. Since in Switzerland the filling water of the pools and the hypochlorite solution used for disinfection contain typically very small bromide concentrations, signal 83 m/z mainly represents chloroform (von Gunten and Salhi, 2003). Trichloramine calibrations were performed in purified water for laboratory experiments and with standard additions to pool water for on-site trichloramine measurements. It was demonstrated that the pool water matrix affects trichloramine measurement with MIMS (Soltermann et al., 2014). During the field campaign in the pool facility, MIMS calibrations (performed every 2–4 days) revealed a continuous loss of sensitivity. Therefore, trichloramine concentrations were calculated with an interpolated slope. Further information on MIMS analysis (interpolations of calibration slope and baseline) is given in the supporting information (SI, section E).

Free and combined chlorine measurements in the laboratory were performed with a DPD test kit (Chematest 20 S, SWAN Analytical Instruments AG, Hinwil, Switzerland). On-site measurements were conducted with both the test kit (Chematest 20 S) and an on-line measurement system (Analyzer AMI Codes II-CC, SWAN Analytical Instruments AG). Spectrophotometrical measurements were performed with a Cary 100 Scan (Varian), and pH was measured with a 632 pH-Meter (Metrohm). A high performance liquid chromatography (HPLC, Agilent 1100 series) coupled with a UV-visible diode array detector was used for atrazine analysis. Urea measurements were performed by the enzymatic hydrolysis of urea to ammonia with urease. Thereafter, ammonia was quantified according to the recommendations of the Federal Office of Public Health (FOPH) (FOPH, 2007) using a Beckman DU 640 spectrophotometer.

### 5.2.3 UV irradiation experiments

#### *Photoreactor and actinometry*

UV irradiation experiments were performed with a low-pressure (LP) (Heraeus Noblelight, TNN 15/32) and a medium-pressure (MP) mercury lamp (Heraeus Noblelight, TQ 150) in a temperature controlled ( $25 \pm 0.2^\circ \text{C}$ ) merry-go-round photoreactor. To lower the fluence rate of the MP lamp independently of the wavelength by about 75 %, two stainless-steel wire cloths were wrapped around the quartz cooling jacket. Atrazine (5  $\mu\text{M}$ , buffered at pH 7.0 with 2 mM phosphate buffer) was used as chemical actinometer to regularly determine the UV lamp intensity. Thereby, the fluence rate of the UV lamp was calculated using equation 5.1:

$$E_p^0(238 - 400 \text{ nm}) = \frac{k_{p,\text{atrazine}}}{2.303 \times \phi_{\text{atrazine}} \times \sum_{\lambda=238 \text{ nm}}^{400 \text{ nm}} (f_{p,\lambda} \times \epsilon_{\text{atrazine},\lambda})} \quad (5.1)$$

where the subscript  $\lambda$  indicates the wavelength of light,  $E_p^0$  (238–400 nm) is the photon fluence rate ( $\text{einstein m}^{-2} \text{ s}^{-1}$ ) in the wavelength range of 238–400 nm,  $k_{p,\text{atrazine}}$  is the pseudo first-order rate constant of atrazine photolysis ( $\text{s}^{-1}$ ),  $\phi_{\text{atrazine}}$  is the quantum yield of atrazine photolysis ( $0.046 \text{ mol einstein}^{-1}$  (Hessler et al., 1993), assumed to be  $\lambda$ -independent),  $f_{p,\lambda}$  is the emission spectrum of the UV lamp (according to the manufacturer) normalized to the wavelength interval of 238–400 nm and  $\epsilon_{\text{atrazine},\lambda}$  is the spectral molar absorption coefficient of atrazine ( $\text{m}^2 \text{ mol}^{-1}$ ). UV doses were calculated from  $E_p^0$  (238–400 nm) under consideration of the wavelength-dependent photon energy because the manufacturer did not quantitatively report a UV lamp emission for  $\lambda < 238 \text{ nm}$ . However, there seems to be a slight light emission at  $\lambda < 238 \text{ nm}$  according to the emission spectra of the lamp (SI, Figure A.1). This emission might be



partly eliminated by the absorption of the cooling jacket. Apparent quantum yields  $\phi_i$  (mol einstein<sup>-1</sup>) for mono-, di- and trichloramine were calculated using equation 5.2, in which the symbols are defined analogously as for equation 5.1, the subscript  $i$  indicating each one of the individual chloramines. The fluence-based rate constant  $k_{E^0}$  (cm<sup>2</sup> mJ<sup>-1</sup>) was calculated with equation 5.3 in which  $E^0$  (238–400 nm) is the fluence rate (mJ cm<sup>-2</sup> s<sup>-1</sup>).

$$\phi_i = \frac{k_{p,i}}{2.303 \times E_p^0(238-400 \text{ nm}) \times \sum_{\lambda=238 \text{ nm}}^{400 \text{ nm}} (f_{p,\lambda} \times \varepsilon_{i,\lambda})} \quad (5.2)$$

$$k_{E^0} = \frac{k_{p,i}}{E^0(238-400 \text{ nm})} \quad (5.3)$$

Information about the emission spectra of the MP UV lamp and the measured absorption spectra of the inorganic chloramines and atrazine is provided in the supplementary information (SI, section A). It must be considered that the quartz cooling jacket as well as the quartz tubes might have slightly shifted the spectra of the light reaching the sample in comparison to the emitted light. This would approximately increase the quantum yield by  $\leq 5\%$  and the fluence by  $\leq 20\%$ . Since this potential effect was a systematic error, relative comparisons are not affected. The photoreactor and the procedure of the actinometry are described in detail in Canonica et al. (2008).

### ***Apparent quantum yield experiments***

Immediately before irradiation, solutions of the target substance or pool samples (18 mL) were filled from a 2-liter bottle into quartz tubes (inner diameter: 14 mm) using a dispenser. Since about 60 mL of sample was needed to reach a steady-state signal for MIMS analysis, several tubes were measured in series for each irradiation step. To account for the slight decrease of the concentration in the stock solution (outgassing and decay), blank measurements for each irradiation step were performed with samples that experienced the same treatment but without UV irradiation. Sample analyses were completed within 10 minutes after the end of the irradiation. MIMS measurement gave constant signals during trichloramine analysis, indicating that trichloramine degradation was not significant except for pool samples containing  $< 0.1 \text{ mg L}^{-1}$  as Cl<sub>2</sub> free chlorine. A previous study showed that monochloramine photolysis depends on the presence of dissolved oxygen (De Laat et al., 2010). The present experiments were performed in aerated solutions, and the oxygen concentration, as measured by MIMS for several runs, was stable during the irradiation.

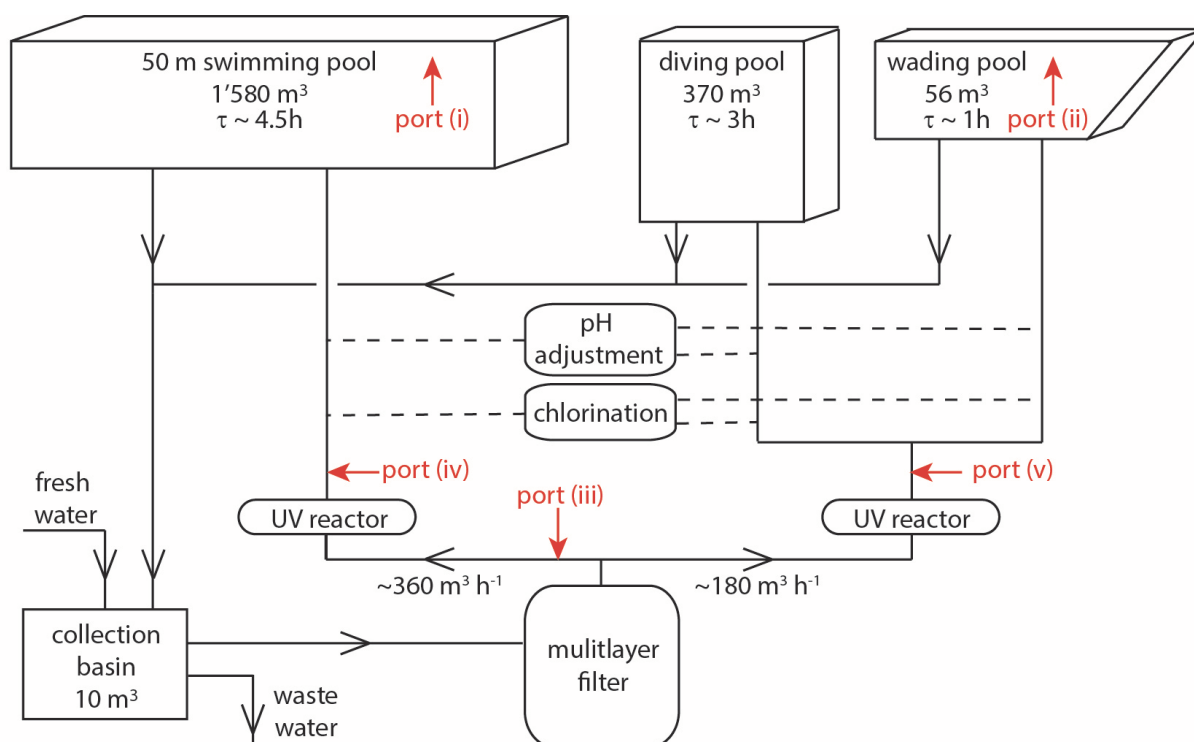
### 5.2.4 Experiments on trichloramine reactivity

Trichloramine (0.5–1  $\mu\text{M}$ ) in buffered solution (pH 7, 2 mM phosphate buffer) was measured with MIMS from the bottom of a completely filled, stirred 1-liter bottle. After reaching a steady-state signal, a reactant (secondary amine, chlorinated secondary amine or UV treated chlorinated secondary amine solution) was added in molar excess (10–100-fold) to create pseudo first-order conditions (at least with respect to the parent reactants). Depletion of trichloramine was analysed to determine a pseudo first-order rate constant. Because trichloramine washing out of the membrane (90 % washed out) took about 3-4 minutes, reactant concentrations were chosen to result in sufficiently high half-lives of trichloramine to minimize interference by this memory effect. Secondary amines were chlorinated by mixing them with free chlorine (1:1 molar ratio). UV-treated (up to about 2'000  $\text{mJ cm}^{-2}$ ) chlorinated secondary amines were produced to test their reactivity with trichloramine.

### 5.2.5 Pool facility for field study

#### *Pool dimensioning and water treatment*

The field study on trichloramine photolysis was performed in a pool facility with a swimming, a diving and a wading pool with volumes of 1'580  $\text{m}^3$ , 370  $\text{m}^3$  and 56  $\text{m}^3$ , respectively (Scheme 5.1). All pools had a shared water treatment which consisted of a collection basin and a multilayer filter. After the multilayer filter, the water was split into two streams leading (i) to the swimming pool (360  $\text{m}^3 \text{h}^{-1}$ ) and (ii) to the diving and the wading pool (180  $\text{m}^3 \text{h}^{-1}$ ). Each stream was equipped with a Barrier M900 (Siemens) or a Barrier M525 (Siemens) UV reactor for the swimmer or the diving/wading pool, respectively. According to the calibration performed by the supplier, the UV reactors (swimming pool and diving / wading pool) provided a UV dose of 55 and 50  $\text{mJ cm}^{-2}$ , respectively, considering the wavelength range of 200–300 nm. This UV dose corresponds to a dose of 110 and 100  $\text{mJ cm}^{-2}$  considering the emission spectra of the UV lamp used in the laboratory from 240 to 400 nm (SI, Table A.1), as it was done for the chloramine photolysis in this study. The reactors had an internal fluence measurement and control system. However, the actual UV dose can deviate from the theoretical values because the water flows were adjusted manually by throttle valves and not measured. Chlorination and pH regulation were performed separately for each pool, according to a continuous measurement of pool water with electrodes (AMI Trides 2, SWAN Analytical Instruments AG (Hinwil, Switzerland)). The water flow from the sampling ports (located 30–40 cm below the water surface in each pool) to the gauges for pH and free chlorine measurement (located in the treatment facility below the pools) was gravity driven with a tube length of about



**Scheme 5.1:** Pool size, water flow and sampling ports in the pool facility. Fluxes and hydraulic residence times ( $\tau$ ) are based on the dimensioning and were not measured in this study. Ports (i) and (ii) to measure free chlorine concentration and pH were located in each pool 30–40 cm below the water surface.

10–20 meters. Fresh water addition (on average  $\sim 10 \text{ m}^3$  per day) was adjusted according to the number of visitors, and after a weekly filter backwashing ( $20\text{--}40 \text{ m}^3$  per backwashing) (SI, Figure D.1). Fresh water addition and visitor frequency was quite constant during the time of the field study (SI, Figure D.2).

### ***Sampling ports for pool water analysis***

Water samples were taken from 5 ports (Scheme 5.1): (i) The swimming pool, (ii) the wading pool, (iii) the pipe leading to the UV reactors, after the UV reactors leading to (iv) the swimming pool and (v) the wading pool. The water flowed ( $10\text{--}40 \text{ mL min}^{-1}$ ) from the sampling ports to volumetric flasks ( $200 \text{ mL}$ ) which served as an overflow system (SI, Scheme E.1). For the connection of the ports (i) and (ii) with the sampling flasks, the already existing tubing to the chlorine and pH gauges was used. Because the water for MIMS analysis was withdrawn from the bottom of the flask, where the pool sample entered, it had only a short residence time of a few minutes before the analysis. Measurement of signal  $83 \text{ m/z}$ , acting as a proxy for the chloroform concentration, confirmed that there was no loss due to outgassing because signal  $83 \text{ m/z}$  was almost equal in samples from all ports. The signal from the wading pool was constantly slightly below the others, which might be explained by the higher

outgassing in the wading pool caused by an inlet via a fountain and by the high surface to volume ratio.

Although there was no trichloramine loss due to outgassing, trichloramine concentrations measured in the sampling flask of the swimming pool were only  $63\pm 6\%$  ( $n = 5$  on 4 different days) of the concentrations measured in samples taken directly from the pool. Additionally, free chlorine concentrations measured in the pool were usually  $0.40\text{--}0.50\text{ mg L}^{-1}$ , although free chlorine concentration measured at the regulation gauge was always about  $0.32\text{ mg L}^{-1}$ . This revealed that there was a constant free chlorine consumption in the tubing from the sampling port in the swimming pool to the sampling flask (flow time of a few minutes) which was similar to the observed trichloramine loss. Trichloramine and free chlorine concentrations measured in the sampling flask of the wading pool (port ii) corresponded to the concentrations measured directly in the pool ( $97\pm 4\%$ ,  $n = 5$ , measured on 3 different days).

### **5.2.6 Modelling of the swimming pool system with AQUASIM**

The software AQUASIM ([www.aquasim.eawag.ch](http://www.aquasim.eawag.ch)) is a model environment which supports the simulation of systems containing multiple, linked compartments (Reichert, 1994). The compartments can be modelled amongst others as plug-flow and mixed reactors, biofilm reactors, advective-diffusive reactors or stratified reactors. Various types of formation and degradation can be defined in a compartment and the compartments can be linked with an advective or diffusive flow. To model the trichloramine concentration in the pool system, for certain compartments (pools) formation and degradation rates were used while in other compartments (e.g. UV lamp) degradation was described as a relative loss in the compartment (loss = concentration output / concentration input).

## 5.3 Results and Discussion

### 5.3.1 Photolysis of inorganic chloramines in purified water with LP and MP lamps

#### *Fluence-based rate constants and quantum yields*

Monochloramine (12–15  $\mu\text{M}$ ), dichloramine (10–15  $\mu\text{M}$ ) and trichloramine (0.7–1.5  $\mu\text{M}$ ) solutions were irradiated with UV light from LP and MP lamps. Figure 5.1 illustrates the relative chloramine depletion as a function of the UV dose. No significant difference was observed between unbuffered chloramine solutions and solutions containing phosphate buffer (500  $\mu\text{M}$ , pH 7). Photodegradation rates of mono- and dichloramine were similar for irradiation with an LP lamp whereas the rate for trichloramine was higher. For MP irradiation, chloramine depletion rates increased in the order monochloramine < dichloramine < trichloramine. The required UV dose for chloramine abatement was higher with the MP lamp than with the LP lamp. This is reflected in the fluence-based rate constant ( $k_{E^0}$ ), which considers the quantum yield and the absorption at given wavelengths (Table 5.1, eq. 5.1). Measured apparent quantum yields for LP irradiation (Table 5.1) of monochloramine ( $0.50 \pm 0.04 \text{ mol einstein}^{-1}$ ) and trichloramine ( $2.11 \pm 0.13 \text{ mol einstein}^{-1}$ ) photolysis were in agreement with values from the literature ( $0.26\text{--}0.62$  and  $1.85 \pm 0.11 \text{ mol einstein}^{-1}$ , respectively) while the apparent quantum

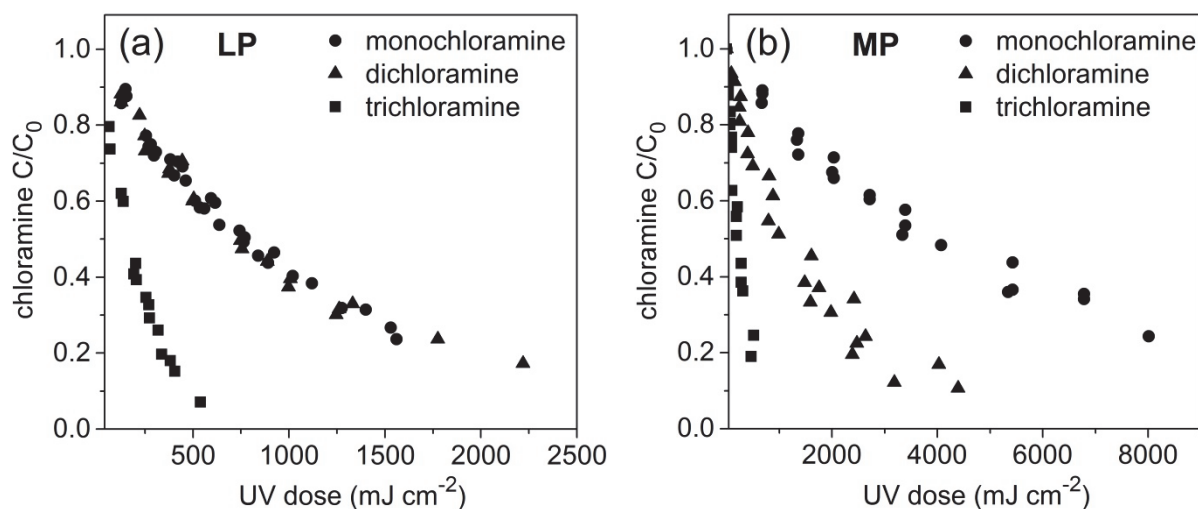


**Figure 5.1:** Photolysis of mono-, di- and trichloramine with (a) low-pressure and (b) medium-pressure lamps. Three series were measured and illustrated together for each species and lamp. Initial concentrations were 12–15  $\mu\text{M}$ , 10–15  $\mu\text{M}$  and 0.7–1.5  $\mu\text{M}$  for mono-, di- and trichloramine, respectively.

**Table 5.1:** Apparent quantum yields  $\phi$  of chloramine photolysis with LP and MP lamps in the absence and presence of t-BuOH (250  $\mu\text{M}$ ) or free chlorine (0.1–0.8  $\text{mg L}^{-1}$  as  $\text{Cl}_2$ ) and the fluence-based rate constant  $k_{E^0}$ .

Compounds	$\phi$ (mol einstein <sup>-1</sup> )		$k_{E^0}$ (cm <sup>2</sup> mJ <sup>-1</sup> )	
	LP lamp	MP lamp	LP lamp	MP lamp
Monochloramine	0.50 ± 0.04	0.31 ± 0.02	9.0 ± 0.7 × 10 <sup>-4</sup>	1.8 ± 0.1 × 10 <sup>-4</sup>
Dichloramine	1.06 ± 0.10	0.85 ± 0.10	9.1 ± 0.7 × 10 <sup>-4</sup>	6.5 ± 0.7 × 10 <sup>-4</sup>
Dichloramine + t-BuOH		0.73 ± 0.01		5.6 ± 0.1 × 10 <sup>-4</sup>
Trichloramine	2.11 ± 0.13	2.30 ± 0.20	4.5 ± 0.2 × 10 <sup>-3</sup>	3.2 ± 0.3 × 10 <sup>-3</sup>
Trichloramine + t-BuOH		1.39 ± 0.13		1.9 ± 0.2 × 10 <sup>-3</sup>
Trichloramine + HOCl		1.46 ± 0.12		2.0 ± 0.2 × 10 <sup>-3</sup>

yield for dichloramine (1.06 ± 0.1 mol einstein<sup>-1</sup>) was lower than reported in literature (1.80 ± 0.10 mol einstein<sup>-1</sup>) (Cooper et al., 2007; Watts and Linden, 2007; Li and Blatchley, 2009; De Laat et al., 2010). Monochloramine had a slightly lower apparent quantum yield (0.31 ± 0.02 mol einstein<sup>-1</sup>) for MP irradiation than for LP irradiation, while di- and trichloramine's apparent quantum yields remained almost constant (0.85 ± 0.10 and 2.30 ± 0.20 mol einstein<sup>-1</sup>, respectively).

Previous studies showed that quantum yields of chloramine photolysis are strongly wavelength-dependent, especially for mono- and trichloramine. An almost 20 times higher quantum yield for monochloramine at  $\lambda = 222$  nm than at  $\lambda = 282$  nm and the contrary for trichloramine was suggested (Li and Blatchley, 2009). Because UV light from MP lamps is composed of various wavelengths below and above  $\lambda = 254$  nm (SI, Figure A.2), different quantum yields were expected for mono- and trichloramine with LP and MP irradiation. However, quantum yields only differed slightly between LP and MP irradiation and the apparent quantum yield for trichloramine with MP irradiation (2.30 ± 0.20 mol einstein<sup>-1</sup>) was clearly lower than previously measured at 282 nm (9.5 ± 0.35 mol einstein<sup>-1</sup>) (Li and Blatchley, 2009). Although apparent quantum yields for di- and trichloramine measured in this study were lower than reported values, they still suggest that indirect processes are relevant.

### ***Impact of $\cdot\text{OH}$ radical scavenging on trichloramine photolysis***

It is hypothesized that irradiation of trichloramine cleaves the N–Cl bond in a first step, leading to a  $\text{Cl}\cdot$  and a  $\text{NCl}_2\cdot$  radical (Li and Blatchley, 2009). In aqueous solution,  $\text{Cl}\cdot$  can react with  $\text{H}_2\text{O}$  ( $k(\text{Cl}\cdot + \text{H}_2\text{O}) = 2.5 \times 10^5 \text{ s}^{-1}$ , Buxton et al. (1998)) to form  $\cdot\text{OH}$  or react as an oxidant with

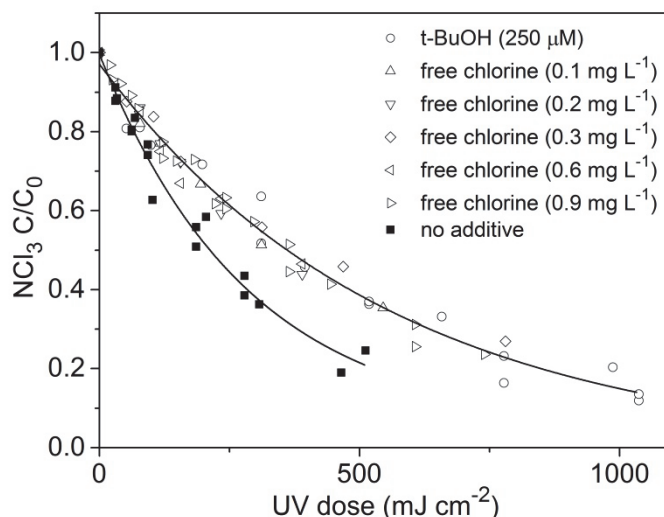


**Figure 5.2:** Trichloramine (0.7–1.5  $\mu\text{M}$ ) photolysis in absence and presence of t-BuOH ( $\sim 250$   $\mu\text{M}$ ) or free chlorine ( $C_{\text{initial}}$ : 0.1–0.9  $\text{mg L}^{-1}$  as  $\text{Cl}_2$ ) at pH 7.

other species. The further degradation pathway of  $\text{NCl}_2^\bullet$  is not fully understood yet but nitrate was shown to be the end product and NO and nitrite were assumed to be intermediates (Li and Blatchley, 2009).  $\text{NHCl}_2^\bullet$ ,  $\text{Cl}^\bullet$ ,  $^\bullet\text{OH}$  or further reaction products could cause apparent quantum yields  $> 1$  for trichloramine photolysis in pure solutions by their reaction with trichloramine. To investigate the role of  $^\bullet\text{OH}$  radicals or its reaction products in trichloramine photolysis, t-BuOH ( $\sim 250$   $\mu\text{M}$ ), an  $^\bullet\text{OH}$  radical scavenger ( $k(^\bullet\text{OH} + \text{t-BuOH}) = 6 \times 10^8 \text{ M}^{-1} \text{ s}^{-1}$ , Buxton et al. (1988)), was added to trichloramine solutions (0.7–1.5  $\mu\text{M}$ ) (Figure 5.2). The concentration of t-BuOH was set high enough to quench  $> 90\%$  of the  $^\bullet\text{OH}$  radicals (assuming a diffusion-controlled reaction of  $^\bullet\text{OH}$  with trichloramine ( $k(^\bullet\text{OH} + \text{NCl}_3) = 10^{10} \text{ M}^{-1} \text{ s}^{-1}$ )). Under these conditions,  $\text{Cl}^\bullet$  is partly ( $\sim 40\%$ ) scavenged by t-BuOH ( $k(\text{Cl}^\bullet + \text{tert-BuOH}) = 6.5 \times 10^8 \text{ M}^{-1} \text{ s}^{-1}$ ) before it can form  $^\bullet\text{OH}$  (Buxton et al., 1998). The presence of t-BuOH inhibited trichloramine photolysis significantly and the quantum yield decreased from  $2.30 \pm 0.20$  to  $1.39 \pm 0.13 \text{ mol einstein}^{-1}$ . Since  $\text{OCl}^\ominus$  is also known to act as an  $^\bullet\text{OH}$  radical scavenger ( $k(^\bullet\text{OH} + \text{OCl}^\ominus) = 9 \times 10^9 \text{ M}^{-1} \text{ s}^{-1}$  (Buxton and Subhani, 1972)), a similar effect was expected for the range of  $\text{OCl}^\ominus$  concentrations in pool water ( $\sim 0.1$ – $0.4 \text{ mg L}^{-1}$  as  $\text{Cl}_2$ , respectively  $1.5$ – $6 \mu\text{M}$ ). However, the lowest free chlorine concentration had a 50 times lower scavenging rate ( $2.9 \times 10^3 \text{ s}^{-1}$ ) than t-BuOH ( $1.5 \times 10^5 \text{ s}^{-1}$ ), and  $\text{HOCl}$  photolysis can also result in the formation of  $^\bullet\text{OH}$  radicals (Watts and Linden, 2007). The data in Figure 5.2 illustrate that the presence of free chlorine ( $C_{\text{initial}}$ : 0.1–0.9  $\text{mg L}^{-1}$  as  $\text{Cl}_2$ ) buffered at pH 7 caused a similar decrease in photodegradation as t-BuOH (250  $\mu\text{M}$ ). This suggests that in purified water even the lowest free chlorine concentration effectively quenched the  $^\bullet\text{OH}$  radicals and thereby decreased the apparent

quantum yield of trichloramine to  $1.46 \pm 0.12$  (Table 5.1). Another possible explanation for the decreased apparent quantum yield could be a fast trichloramine re-formation from the reaction of trichloramine photolysis products with chlorine. MIMS measurements revealed that there was no slow (10–20 minutes after the irradiation) trichloramine formation in the irradiated samples with free chlorine, but a fast re-formation during or shortly after the irradiation cannot be excluded.

### **5.3.2 UV-induced formation of trichloramine-reactive products in pool water**

In addition to the enhancement of trichloramine degradation by a photo-induced chain reaction, products from the photolysis of other substances in the pool may lead to a further consumption of trichloramine. To illustrate this effect, the stability of spiked trichloramine was investigated in (i) untreated pool water, (ii) irradiated pool water ( $1'060 \text{ mJ cm}^{-2}$ , MP lamp) and (iii) in irradiated plus re-chlorinated (to a level of  $0.23 \text{ mg L}^{-1}$  as  $\text{Cl}_2$ ) pool water (Figure 5.3a). Spiking and measurement of trichloramine occurred a few minutes after the treatment. Consequently, short-lived photolysis products were no longer present during this experiment on trichloramine stability. Pool water initially contained free chlorine ( $0.4 \text{ mg L}^{-1}$  as  $\text{Cl}_2$ ) which disappeared during the UV treatment ( $1'060 \text{ mJ cm}^{-2}$ ). The same procedure was performed with a sample in which free chlorine was initially quenched with ammonium to  $< 0.05 \text{ mg L}^{-1}$  as  $\text{Cl}_2$  (Figure 5.3b). Thereby, the monochloramine concentration in the pool water sample increased. Figure 5.3 illustrates that trichloramine decay was much faster in irradiated pool water (no treatment vs. UV). Trichloramine was less stable in the chlorine-free pool water, but the effect of UV irradiation remained considerable ( $\text{NH}_4^+$  vs.  $\text{NH}_4^+ + \text{UV}$ ). Conclusively, UV irradiation of pool water leads to the formation of  $\text{NCl}_3$ -reactive moieties. However, results in Figure 5.3 also reveal that this effect could be partially reversed by the addition of free chlorine (UV vs. UV + HOCl). Blank experiments (no trichloramine spiked) revealed that an addition of free chlorine after UV irradiation induced trichloramine formation. This is in agreement with a previous study showing that UV treatment increases the trichloramine formation from chlorination of chlorocreatinine (Weng et al., 2013). However, this increased trichloramine formation could only explain a minor part of the apparently regained trichloramine stability, which suggests that trichloramine and free chlorine compete for the same reactive sites and that their chlorination impedes the reaction with trichloramine.



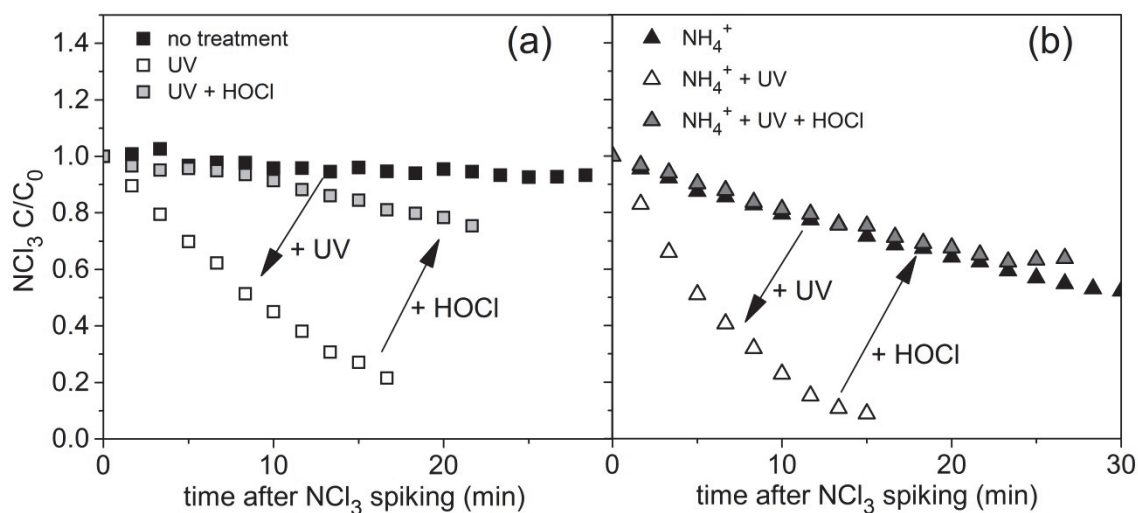


**Figure 5.3:** (a) Trichloramine decay after spiking it to pool water, UV treated pool water (UV) and UV treated re-chlorinated pool water (UV + HOCl). (b) The same experimental procedure was repeated with pool water in which free chlorine was quenched with ammonium prior to the different treatments.

The formation of nitrite and ammonium from chloramine irradiation is an example for a UV-induced formation of substances that act as a trichloramine sinks (Li and Blatchley, 2009). However, ammonium levels were only slightly increased after the irradiation of pool water ( $8.5 \mu\text{g N L}^{-1}$ ) (UV) and trichloramine stability was much higher in the  $\text{NH}_4^+$ -quenched sample with a high ammonium concentration ( $12 \mu\text{g N L}^{-1}$ ). Therefore, other mechanisms must be responsible for the reduced trichloramine stability after irradiation. To further elucidate this effect, trichloramine stability was tested in untreated and UV-treated solutions containing secondary amines (dimethylamine and morpholine) and their chlorinated forms (Table 5.2). Trichloramine ( $0.5\text{--}1 \mu\text{M}$ ) was quickly degraded by the reaction with dimethylamine ( $5\text{--}50 \mu\text{M}$ ) and morpholine ( $5\text{--}25 \mu\text{M}$ ) in buffered solution at pH 7 ( $k_{\text{app}} = 25 \pm 3$  and  $160 \pm 12 \text{ M}^{-1} \text{ s}^{-1}$  for dimethylamine and morpholine, respectively (SI, Figure B.1)). In pool water, secondary amines are mainly present in their chlorinated form, since they quickly undergo reactions with free chlorine ( $k_{\text{app}} = 350\text{--}61'000 \text{ M}^{-1} \text{ s}^{-1}$  at pH 7, Deborde and von Gunten (2008)). Chlorinated secondary amines have a lower reactivity with trichloramine (Table 5.2). It is likely that UV irradiation of chlorinated secondary amines breaks the N-Cl bond, which renders the products again accessible for a reaction with trichloramine. This could explain why trichloramine showed an increased reactivity with UV-treated chlorinated secondary amines (Table 5.2 and SI, Figure B.2)

**Table 5.2:** Apparent second-order rate constants  $k_{\text{app}}$  ( $\text{M}^{-1} \text{s}^{-1}$ ) at pH 7 for the reaction of trichloramine (0.5–1  $\mu\text{M}$ ) with secondary amines (dimethylamine (5–50  $\mu\text{M}$ ), morpholine ((5–25  $\mu\text{M}$ ), their chlorinated form ( $k_{\text{app, chlorine}}$ ) and their chlorinated form after UV treatment ( $k_{\text{app, chlorine+UV}}$ ) (MP lamp, ~2'200 and 1'700  $\text{mJ cm}^{-2}$  for dimethylamine and morpholine, respectively).

Compound	$k_{\text{app}}$	$k_{\text{app, chlorine}}$	$k_{\text{app, chlorine+UV}}$
DMA	25 ± 3	2.6 ± 1.8	9.6
Morpholine	160 ± 12	29 ± 8	65

Thus, the presence of free chlorine can reduce trichloramine photolysis in pool water by quenching  $\cdot\text{OH}$  radicals or by reacting with potential UV-induced reaction partners of trichloramine.

### 5.3.3 Quantum yields measured in pool water samples

Trichloramine (~1.5  $\mu\text{M}$ ) was spiked to 9 pool water samples and apparent quantum yields were measured analogously to pure trichloramine solutions by performing measurements of blanks and irradiated samples simultaneously (information on pool water samples, SI, Table C.1). Figure 5.4 shows the apparent quantum yields in relation to the corresponding free chlorine concentration (prior to irradiation) in pool water. Apparent quantum yields for trichloramine in pool water containing common free chlorine concentrations (0.2–0.5  $\text{mg L}^{-1}$  as  $\text{Cl}_2$ ) were between 2 and 3  $\text{mol einstein}^{-1}$  and thus comparable to pure solution ( $2.30 \pm 0.20 \text{ mol einstein}^{-1}$ ). The sample with an initial free chlorine concentration < 0.1  $\text{mg L}^{-1}$  as  $\text{Cl}_2$  had a clearly increased quantum yield of 4.3. A whirlpool sample containing a high free chlorine concentration (1  $\text{mg L}^{-1}$  as  $\text{Cl}_2$ ) had an apparent quantum yield of 1.5  $\text{mol einstein}^{-1}$  which was close to the value in the presence of t-BuOH or free chlorine (~1.4–1.5  $\text{mol einstein}^{-1}$ , see above). These results are in agreement with the effects described in the previous section which suggest a free chlorine dependence of the trichloramine photolysis. Low free chlorine levels are not sufficient to quench all the  $\text{NCl}_3$ -reactive moieties and  $\cdot\text{OH}$  radicals formed by UV-irradiation while high free chlorine levels can effectively consume both. Apparent quantum yields in pool water treatment are assumed to be in the range of 2–3  $\text{mol einstein}^{-1}$  since pool water commonly contains sufficient residual chlorine after the filtration step.

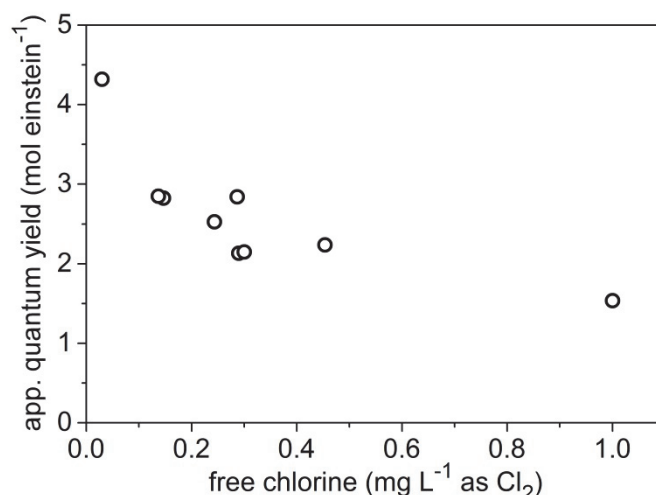


**Figure 5.4:** Apparent quantum yields of spiked trichloramine ( $\sim 1.5 \mu\text{M}$ ) in pool water samples as a function of the initial free chlorine concentration ( $\text{mg L}^{-1}$  as  $\text{Cl}_2$ ).

### 5.3.4 Full-scale study

#### *Effect of MP UV treatment on trichloramine concentrations in an indoor swimming pool*

##### UV reactor

Results in Figure 5.1 reveal that typical UV doses applied in Swiss pool water treatment ( $60\text{--}100 \text{ mJ cm}^{-2}$  for LP and  $120\text{--}200 \text{ mJ cm}^{-2}$  for MP ( $\lambda = 238\text{--}400 \text{ nm}$ )) would barely affect mono- and dichloramine concentrations while trichloramine would be decreased by about 20–50 % in one treatment cycle. To evaluate these findings, water samples were analysed for trichloramine before and after the UV reactors in a pool facility. Since MIMS analyses took about 15 minutes for each sample, fast changes in trichloramine concentration, as occurring in the wading pool, affected the accuracy of the calculated trichloramine reduction by the UV reactor ( $[\text{NCl}_3]$  after /  $[\text{NCl}_3]$  before). The trichloramine reduction was calculated exclusively with night time values (00:00 – 06:00), since trichloramine concentrations were relatively stable during the night. The impact of UV irradiation on trichloramine concentration was assessed during two periods of 8 days, each with a treatment sequence of “UV on” / “UV off” / “UV on”. Results in Figure 5.5 show that 40–50 % of trichloramine was degraded in the UV reactor when the UV lamps were turned on. The trichloramine elimination was slightly higher than expected ( $\sim 30\%$ ) from the applied UV dose. This deviation might be explained by (i) the uncertainty of the UV dose, (ii) a different spectral distribution of radiation of the pool and laboratory MP lamps and (iii) the fact that the free chlorine concentration passing the sand filter was lower than in the pools, which may slightly increase the apparent quantum yield.

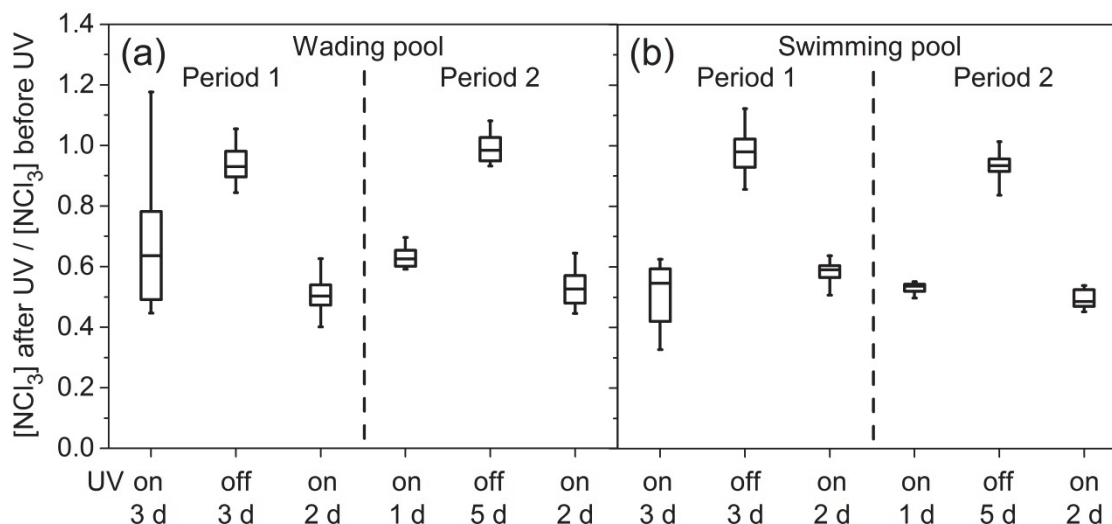


**Figure 5.5:** Relative reduction of the trichloramine concentration upon UV treatment ( $[\text{NCl}_3]$  after /  $[\text{NCl}_3]$  before) for (a) the wading pool and (b) the swimming pool during two measurement periods of 8 days (x-axis: 3d = 3 days). UV treatment was switched off and on for several days during each period (x-axis). The high variation in the efficiency of the UV reactor of the wading pool in the first period was due to a malfunction of the UV reactor which switched the UV lamps on and off frequently.

### Trichloramine in swimming pools

To investigate the effect of UV treatment on the concentration of trichloramine in pool water, trichloramine was measured at the inlets and within the swimming and wading pools (Figure 5.6). UV treatment ran for 3 days, was switched off for 3 days and was then turned on for another 2 days. The free chlorine concentration was maintained at a constant concentration of 0.32 and 0.35  $\text{mg L}^{-1}$  as  $\text{Cl}_2$  for the swimming and the wading pool, respectively. Due to the aforementioned free chlorine consumption before the regulation gauge of the swimming pool (section 5.2.4), this resulted in a mean free chlorine concentration of  $\sim 0.45$  and  $0.35 \text{ mg L}^{-1}$  as  $\text{Cl}_2$  in the swimming and the wading pool, respectively. Similarly, the shown trichloramine concentration of the swimming pool (Figure 5.6) was only about 60% of the effective concentration in the swimming pool due to the loss in the tubing between the sampling port and the sampling flask (section 5.2.4). The urea concentration increased in the wading pool during the day ( $\sim 1 \text{ mg L}^{-1}$ ) for short periods but dropped to lower levels ( $0.55\text{--}0.70 \text{ mg L}^{-1}$ ) each night.

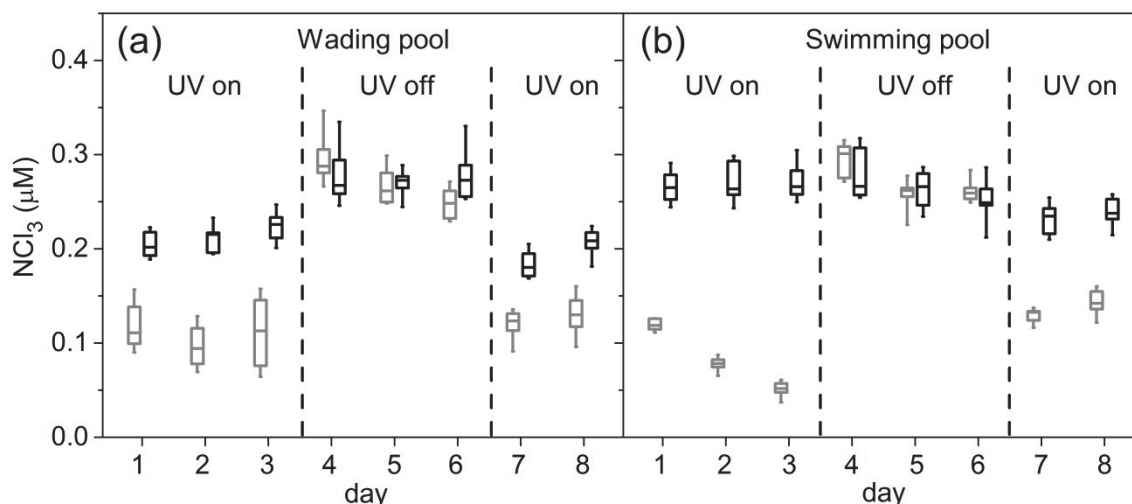


**Figure 5.6:** Trichloramine concentration in the pools (black) and their inlets (gray) for (a) the wading pool and (b) the swimming pool as a function of the UV treatment.

Trichloramine concentrations at the pool inlets were significantly lower during the period with UV treatment than without UV treatment. However, the trichloramine concentration in the wading pool was only slightly affected by UV treatment (~20 % decrease) while the trichloramine concentration within the swimming pool remained almost unchanged after switching off the UV light and slightly decreased (~10 %) after switching on the UV light. Changes in UV treatment affected trichloramine concentrations quickly (within one day) and no cumulative long-term effect was observed for the 3 day period. The UV treatment was more effective in the wading pool with a shorter turn-over time of about 1 h. Even for this short residence time, the trichloramine concentration increased from the concentration at the inlet to a higher steady-state concentration in the pool. This suggests that trichloramine formation is a rather fast process and that UV treatment does not considerably affect trichloramine concentrations in pools with turn-over times of several hours and similar chemical conditions and UV doses as in the investigated pool. This is in agreement with other studies and will be discussed in more detail with model calculations in section 5.3.4 (Gérardin et al., 2005; Soltermann et al., 2014).

In another campaign, the evolution of the trichloramine concentration was measured in the swimming and the wading pools during one day and the UV reactors were turned off at 22.30 when trichloramine concentrations were stable and not influenced by changing bather loads (Figure 5.7). Trichloramine concentrations showed typical evolutions with little variations in the swimming pool and a clear increase in the wading pool during periods of heavy use (morning, afternoon). The slight increase of the trichloramine concentrations in both pools

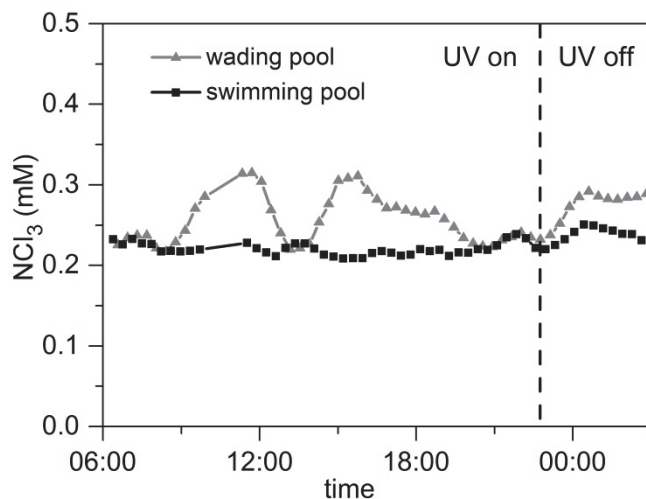


**Figure 5.7:** Trichloramine evolution in the wading and the swimming pool from 6:00–3:00. UV treatment was stopped at 22:30 (dashed line). The trichloramine concentration was smoothed by plotting the moving average of 3 measurements.

around 21:00 might have been caused by the cleaning of the pool facility, during which the circulation through the water treatment was interrupted. After turning off the UV reactors, trichloramine concentrations increased in both pools, more pronounced in the wading pool (~20 %) than in the swimming pool (~10 %). Hence, UV treatment clearly affected trichloramine concentrations in the wading pool which had a shorter turn-over time.

Simultaneously to trichloramine, combined chlorine was measured on-line in either the swimming pool or the wading pool. The obtained results suggest that combined chlorine concentrations respond much slower to changing UV treatment (SI, section F). According to the applied UV dose and the monochloramine photolysis in pure solution (section 5.3.1), combined chlorine is only marginally degraded in one treatment cycle. However, combined chlorine concentrations seemed to increase for several days after ceasing UV treatment and decreased accordingly after switching on the treatment. This suggests a cumulative, long-term effect of UV treatment on the combined chlorine concentration.

Signal 83  $m/z$  remained on the same level before and after the UV reactor which implies that chloroform was not degraded during UV treatment. At first glance, signal 83  $m/z$  seemed to decrease in pool water when the UV lamp was turned off and increased after switching it on (SI, section F.2). However, further measurements revealed that mainly backwashing the filter – and not switching off the UV lamps – was causing the chloroform decrease. Therefore, no clear assessment of the effect of UV treatment on trihalomethanes is possible at this point.

### ***Modeling of trichloramine formation, decay and photodegradation in an indoor swimming pool***

To estimate the trichloramine formation rate in pool water and to investigate the influence of pool water treatment parameters (e.g. UV treatment, residence time, fresh water addition) on the trichloramine concentration in pools, a simplified model of the pool facility in Scheme 5.1 was developed. The model was set up with the software AQUASIM (Reichert, 1994) as follows:

- Pools were modelled as completely mixed reactors with the volumes and the approximated fluxes according to Scheme 5.1. Previous literature suggests that this scenario is not always met and that some swimming pools might be stratified during the day (Weng and Blatchley, 2011).
- The free chlorine concentration was kept constant at 0.45, 0.35 and 0.30 mg L<sup>-1</sup> as Cl<sub>2</sub> for the swimming, wading and diving pool, respectively, at pH 7.2.
- Three processes reducing trichloramine concentration were implemented in the model:
  - (1) Trichloramine degradation in the UV reactor was estimated to be 40 % (Figure 5).
  - (2) The trichloramine decay rate in pool water was estimated to be  $7 \times 10^{-5} \text{ s}^{-1}$ . This value was deduced from fitting the model to measured changes in trichloramine concentrations after turning off the UV treatment. This rate is within the range of measured decay rates of trichloramine in pool water ( $\sim 2\text{--}8 \times 10^{-5} \text{ s}^{-1}$ , (Soltermann et al., 2014)). Previous studies measured trichloramine decay rates of  $3.4 \times 10^{-5} \text{ s}^{-1}$  and  $7.5 \times 10^{-6} \text{ s}^{-1}$  in pure and phosphate buffered solutions, respectively (Saguinsin and Morris, 1975; Kumar et al., 1987) or estimated a decay rate of  $2.9 \times 10^{-5} \text{ s}^{-1}$  at temperatures slightly lower than in indoor swimming pools (McKay et al., 2013).
  - (3) A trichloramine loss of 40 % was implemented in the model between the pool effluent and the UV reactors. Measured concentrations in the sampling flasks of the swimming pool and before the UV lamp were similar. While there was no loss in the tubing from sampling port (iii) before the UV lamp to the mass flask, trichloramine decreased by about 40 % in the tubing from port (i) in the swimming pool to the sampling flask (section 5.2.4, Figure 5.6 and SI, section E). Based on this, it can be concluded that the trichloramine concentration in the swimming pool was constantly about 40 % higher than before the UV lamp. The decrease in trichloramine concentration between the swimming pool and the UV treatment might be caused by trichloramine outgassing at the pool surface and the spillway or by degradation in the multilayer filter. Trichloramine outgassing at the pool surface was not implemented in

the model since Schmalz et al. (2011a) showed that the mass balance of trichloramine in the pool water is hardly affected by the outgassing at the pool surface of a competition swimming pool.

- Trichloramine was assumed to be formed by the reaction of HOCl with a nitrogen-containing precursors (N-precursor) (eq. 5.4). Assuming a constant precursor concentration, an effective rate constant  $k_{\text{eff}}$  ( $k_{\text{eff}} = k \times [\text{N-precursor}]$ ) for the trichloramine formation can be estimated by fitting model results to the measured concentrations in the pool facility.

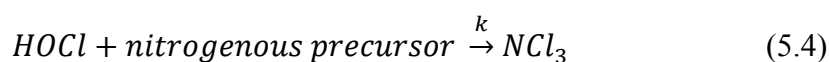
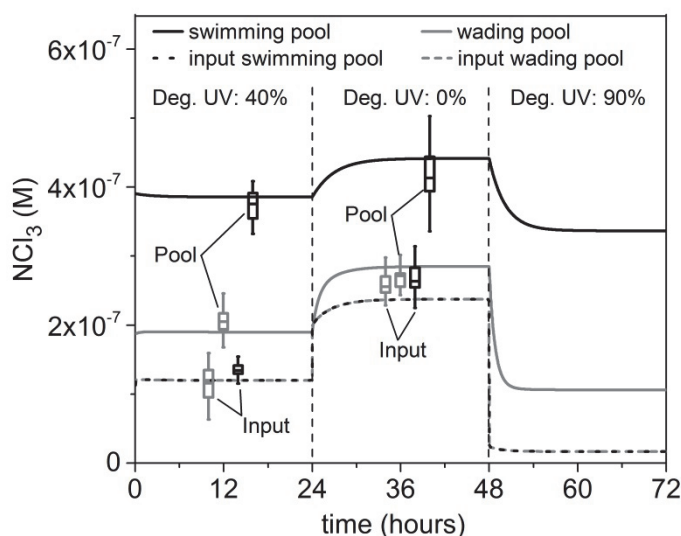


Figure 5.8 shows modelled trichloramine concentrations in the swimming and the wading pool over a period of three days by modelling a hypothetical trichloramine degradation in the UV reactor of 40 %, 0 % and 90 % for the first, second and third day, which represent a common, no and a very high UV degradation, respectively. To match model results with the measured concentrations in Figure 5.6 and 5.7, trichloramine formation was fitted ( $k_{\text{eff}} = 10^5 \text{ s}^{-1}$ ). The resulting trichloramine formation rate is much higher than expected given the rate limiting step of the reaction of free chlorine with urea ( $k = 2.35 \times 10^4 \text{ M}^{-1} \text{ s}^{-1}$  at pH 2, Blatchley and Cheng (2010)). Based on this value and neglecting subsequent chlorination steps, the modelled trichloramine was  $\sim 2\text{--}5 \times 10^{-9} \text{ M}$  which is 100 times lower than the measurements (SI, Figure G.1). Trichloramine was also modelled with the chlorine depletion ( $k = 4.58 \times 10^{-6} \text{ s}^{-1}$ ) in excess of urea ( $3.3 \times 10^{-5} \text{ M} \sim 1 \text{ mg L}^{-1}$ ) and a 1:1 reaction to trichloramine (Schmalz et al., 2011a). The resulting trichloramine concentration ( $0.5\text{--}2 \times 10^{-8} \text{ M}$ ) was about 20 times lower than the measured concentration in the pools (SI, Figure G.2). It is hypothesized that urea is not the main trichloramine precursor, which is in agreement with another study (Soltermann et al., 2014).





**Figure 5.8:** Modelled (lines) and measured (boxplots) trichloramine concentrations in the swimming (black) and the wading pool (grey) during periods with a hypothetical trichloramine degradation of 40 %, 0 % and 90 % in the UV reactors. The measured concentrations were averages from Figure 5.6 (excluding days 1–3 for the swimming pool) which were corrected by a factor of 0.63 for the swimming pool as described in section 5.2.4.

Setting a trichloramine reduction of 40 % in the UV reactors lowered the trichloramine concentration in the swimming pool by 13 % and in the wading pool by 33 % (Figure 5.8). Since the effect of UV treatment was less pronounced in the field study and the new equilibrium concentrations were reached even faster, trichloramine formation and decay must have been slightly faster in the field than in our model. The effect of a trichloramine reduction of 90 % in the UV reactor, which would require a 5 times higher UV dose than for a reduction of 40 %, lowered the trichloramine concentration only by 23 % and 63 % in the swimming and the wading pool, respectively (Figure 5.8). Thus, mitigation of trichloramine in pool water by increasing the UV dose is limited. Doubling the flow through the water treatment would halve the UV dose per cycle because of the shorter residence time in the UV reactor. Due to the additional trichloramine mitigation on the spillway and in the multilayer filter, trichloramine concentrations in the pools would drop (to a level of 79 % and 88 % for the swimming and wading pool, respectively) with an increased treatment flow even if the UV degradation was reduced by 50 % (SI, Figure G.4). An increase in the water flow with a constant UV dose in the UV reactors would lower trichloramine concentrations even more significantly (72 % and 68 % for the swimming and wading pool, respectively) (SI, Figure G.5). However, it must be considered that a constant trichloramine elimination by outgassing on the pool water surface,

the spillway and the inlet in the collection basin or by the degradation in the multilayer filter was assumed. It was not confirmed by on-site measurements that this elimination is constant at high flow rates and this elimination can be different in other pool facilities. Nevertheless, increasing the flow rate improves the effectiveness of the UV treatment since more water is treated and the reduced residence time does not allow for the same trichloramine formation.

Further runs with the model showed that changes in free chlorine or precursor concentration resulted in a fast and linear change of the trichloramine concentration and therefore represent an effective tool for trichloramine mitigation (SI, Figure G.6 and G.7). An increase of the fresh water addition by a factor of 10 did not greatly affect trichloramine concentrations in the pool since the dilution was still only 6 % per day (SI, Figure G.8). Conclusively, the most effective strategy to lower trichloramine concentration in pool water is to increase the recirculation flow while keeping the UV dose at the same level, which implies a proportional increase of the fluence rate. After considering all of the factors including UV dose, recirculation rate, free chlorine concentration, fresh water addition and bather load, lowering of the free chlorine concentration might be the most viable option to decrease trichloramine concentrations.

## 5.4 Conclusions

Trichloramine, a hazardous disinfection by-product of pool water chlorination, is formed by reactions of free chlorine with nitrogenous precursors. Because inorganic chloramines are susceptible to UV irradiation, an increasing number of pool facilities augment their treatment with this technology to abate chloramines. Experiments in pure aqueous solutions revealed that the apparent rate constants of chloramine photolysis increased with the number of N-Cl bonds for medium-pressure (MP) UV irradiation while mono- and dichloramine were equally degraded by low-pressure (LP) UV irradiation. For trichloramine phototransformation apparent quantum yields  $> 1 \text{ mol einstein}^{-1}$  for LP and MP irradiation were found, indicating that secondary processes, probably involving  $\cdot\text{OH}$  radicals, are important for trichloramine degradation. Trichloramine quantum yields in pool water samples increased for decreasing free chlorine concentrations. Pre-treatment of the pool water matrix with UV enhanced its reactivity with trichloramine, whereas chlorine addition after UV irradiation increased trichloramine stability.

UV reactors in this pool study mitigated about 40–50 % of trichloramine in the recycled water. Although this is quite considerable, the effect of UV treatment on trichloramine concentration in pools depends on the pool size and the recirculation rate. For pools with a fast turn-over ( $\sim 1$  hour), trichloramine elimination by UV at the inlet clearly affected the concentration in the pool whereas for a turn-over of 4–5 hours, trichloramine concentrations were not lowered considerably.

Consequently a high recirculation rate is required to lower the trichloramine concentration. Otherwise trichloramine will quickly reach a steady-state concentration similar to the one without UV treatment. A model combining hydraulics with trichloramine formation and abatement kinetics confirmed that an increase of the recirculation rate through the treatment part could effectively lower trichloramine concentrations in the pools. However, most pool operators might abandon this option because of limitations in the infrastructure and additional energy costs. The model allowed for an assessment of other trichloramine mitigation strategies (e.g. increased fresh water addition or lower free chlorine levels). Based on our results, lower trichloramine concentrations in pool waters can be most effectively achieved by lowering the free chlorine concentration. However, this strategy might be restricted due to hygienic reasons.

## **Acknowledgements**

This work was supported by the Swiss Federal Office of Public Health (FOPH). The authors thank Elisabeth Salhi (Eawag) for laboratory support, Rene Schittli (Kantonales Labor Zürich) for collaboration in pool water sampling and analysis and Gérard Donzé (FOPH) for the fruitful discussions.

---

## References

- Bernard, A., S. Carbonnelle, O. Michel, S. Higuët, C. de Burbure, J. P. Buchet, C. Hermans, X. Dumont and I. Doyle (2003). "Lung hyperpermeability and asthma prevalence in schoolchildren: unexpected associations with the attendance at indoor chlorinated swimming pools." *Occupational and Environmental Medicine* 60(6): 385-394.
- Blatchley, E. R. and M. Cheng (2010). "Reaction Mechanism for Chlorination of Urea." *Environmental Science & Technology* 44(22): 8529-8534.
- Buxton, G. V., M. Bydder and G. A. Salmon (1998). "Reactivity of chlorine atoms in aqueous solution - Part 1 The equilibrium  $\text{Cl} \cdot + \text{Cl}^- \rightleftharpoons \text{Cl}_2^{\cdot -}$ ." *Journal of the Chemical Society-Faraday Transactions* 94(5): 653-657.
- Buxton, G. V., C. L. Greenstock, W. P. Helman and A. B. Ross (1988). "Critical review of rate constants for reactions of hydrated electrons, hydrogen atoms and hydroxyl radicals." *Phys. Chem. Ref. Data* 17: 513-886.
- Buxton, G. V. and M. S. Subhani (1972). "Radiation chemistry and photochemistry of oxychlorine ions. Part 2.-Photodecomposition of aqueous solutions of hypochlorite ions." *Journal of the Chemical Society, Faraday Transactions 1: Physical Chemistry in Condensed Phases* 68(0): 958-969.
- Canonica, S., L. Meunier and U. Von Gunten (2008). "Phototransformation of selected pharmaceuticals during UV treatment of drinking water." *Water Research* 42(1-2): 121-128.
- Cassan, D., B. Mercier, F. Castex and A. Rambaud (2006). "Effects of medium-pressure UV lamps radiation on water quality in a chlorinated indoor swimming pool." *Chemosphere* 62(9): 1507-1513.
- Cooper, W. J., A. C. Jones, R. F. Whitehead and R. G. Zika (2007). "Sunlight-Induced Photochemical Decay of Oxidants in Natural Waters: Implications in Ballast Water Treatment." *Environmental Science & Technology* 41(10): 3728-3733.
- De Laat, J., N. Boudiaf and F. Dossier-Berne (2010). "Effect of dissolved oxygen on the photodecomposition of monochloramine and dichloramine in aqueous solution by UV irradiation at 253.7 nm." *Water Research* 44(10): 3261-3269.
- Deborde, M. and U. von Gunten (2008). "Reactions of chlorine with inorganic and organic compounds during water treatment--Kinetics and mechanisms: A critical review." *Water Research* 42(1-2): 13-51.
- Deutsche gesetzliche Unfallversicherung (DGUV) (2009). "Trichloramine in swimming pools (German)."
- Deutsches Institut für Normung (DIN) (2012). "Treatment of water of swimming pools and baths — Part 1: General requirements (German)."
- Federal Office of Public Health (FOPH), Switzerland (2007). "Determination of ammonia in drinking water, photometrically (German)."
- Gérardin, F., G. Hecht, G. Huber-Pelle and I. Subra (2005). "Traitement UV: Suivi de l'évolution des concentrations en chloroforme et en trichlorure d'azote dans les eaux de baignade d'un centre aquatique." *Hygiène et sécurité du travail - Cahiers de notes documentaires* 201: 19-30.
- Gérardin, F. and I. Subra (2004). "Development of a sampling and analysis method for trichloramine in water (French)." *Hygiène et sécurité du travail - Cahiers de notes documentaires* 194: 39-49.

Hansen, K. M. S., S. Willach, M. G. Antoniou, H. Mosbaek, H. J. Albrechtsen and H. R. Andersen (2012). "Effect of pH on the formation of disinfection byproducts in swimming pool water - Is less THM better?" *Water Research* 46(19): 6399-6409.

Hansen, K. M. S., R. Zortea, A. Piketty, S. R. Vega and H. R. Andersen (2013). "Photolytic removal of DBPs by Medium pressure UV in swimming pool water." *Science of the Total Environment* 443: 850-856.

Hessler, D. P., V. Gorenflo and F. H. Frimmel (1993). "Degradation of aqueous atrazine and metazachlor solutions by UV and UV/H<sub>2</sub>O<sub>2</sub> - Influence of pH and herbicide concentration." *Acta Hydrochimica Et Hydrobiologica* 21(4): 209-214.

Kristensen, G. H., M. M. Klausen, H. R. Andersen, L. Erdinger, F. Lauritsen, E. Arvin and H. J. Albrechtsen (2009). Full scale test of UV-based water treatment technologies at Gladsaxe Sport Centre— with and without advanced oxidation mechanisms. *Swimming Pool and Spa International Conference*.

Kumar, K., R. W. Shinness and D. W. Margerum (1987). "Kinetics and mechanisms of the base decomposition of nitrogen trichloride in aqueous-solution." *Inorganic Chemistry* 26(21): 3430-3434.

Li, J. and E. R. Blatchley (2009). "UV Photodegradation of Inorganic Chloramines." *Environmental Science & Technology* 43(1): 60-65.

McKay, G., B. Sjelín, M. Chagnon, K. P. Ishida and S. P. Mezyk (2013). "Kinetic study of the reactions between chloramine disinfectants and hydrogen peroxide: Temperature dependence and reaction mechanism." *Chemosphere* 92(11): 1417-1422.

Parrat, J., G. Donze, C. Iseli, D. Perret, C. Tomicic and O. Schenk (2012). "Assessment of Occupational and Public Exposure to Trichloramine in Swiss Indoor Swimming Pools: A Proposal for an Occupational Exposure Limit." *Annals of Occupational Hygiene* 56(3): 264-277.

Reichert, P. (1994). "AQUASIM - a tool for simulation and data analysis of aquatic systems." *Water Science & Technology* 30(2).

Richardson, S. D., D. M. DeMarini, M. Kogevinas, P. Fernandez, E. Marco, C. Lourencetti, C. Balleste, D. Heederik, K. Meliefste, A. B. McKague, R. Marcos, L. Font-Ribera, J. O. Grimalt and C. M. Villanueva (2010). "What's in the Pool? A Comprehensive Identification of Disinfection By-products and Assessment of Mutagenicity of Chlorinated and Brominated Swimming Pool Water." *Environmental Health Perspectives* 118(11): 1523-1530.

Saguinsin, J. L. S. and J. C. Morris (1975). The chemistry of aqueous nitrogen trichloride. *Disinfection Water and Wastewater*. J. D. Johnson. Michigan, Ann Arbor Science: 277-299.

Schmalz, C., F. H. Frimmel and C. Zwiener (2011a). "Trichloramine in swimming pools - Formation and mass transfer." *Water Research* 45(8): 2681-2690.

Schmalz, C., H. Wunderlich, R. Heinze, F. Frimmel, C. Zwiener and T. Grummt (2011b). "Application of an optimized system for the well-defined exposure of human lung cells to trichloramine and indoor pool air." *Journal of water and health* 9(3): 586-596.

Schreiber, I. M. and W. A. Mitch (2006). "Nitrosamine Formation Pathway Revisited: The Importance of Chloramine Speciation and Dissolved Oxygen." *Environmental Science & Technology* 40(19): 6007-6014.

Swiss society of engineers and architects (SIA) (2013). "Water and water treatment in public pools (German)."

---

Soltermann, F., M. Lee, S. Canonica and U. von Gunten (2013). "Enhanced N-nitrosamine formation in pool water by UV irradiation of chlorinated secondary amines in the presence of monochloramine." *Water Research* 47(1): 79-90.

Soltermann, F., T. Widler, S. Canonica and U. von Gunten (2014). "Comparison of a novel extraction-based colorimetric (ABTS) method with membrane introduction mass spectrometry (MIMS): Trichloramine dynamics in pool water." *Water Research* 58: 258-268.

von Gunten, U. and E. Salhi (2003). "Bromate in drinking water a problem in Switzerland?" *Ozone science & engineering* 25(3): 159-166.

Watts, M. J. and K. G. Linden (2007). "Chlorine photolysis and subsequent OH radical production during UV treatment of chlorinated water." *Water Research* 41(13): 2871-2878.

Weaver, W. A., J. Li, Y. L. Wen, J. Johnston, M. R. Blatchley and E. R. Blatchley (2009). "Volatile disinfection by-product analysis from chlorinated indoor swimming pools." *Water Research* 43(13): 3308-3318.

Weng, S. C. and E. R. Blatchley (2011). "Disinfection by-product dynamics in a chlorinated, indoor swimming pool under conditions of heavy use: National swimming competition." *Water Research* 45(16): 5241-5248.

Weng, S. C., J. Li, K. V. Wood, H. I. Kenttämä, P. E. Williams, L. M. Amundson and E. R. Blatchley III (2013). "UV-induced effects on chlorination of creatinine." *Water Research* 47(14): 4948-4956.





# **Supporting Information for Chapter 5**

## **Photolysis of inorganic chloramines and efficiency of trichloramine abatement by UV treatment of swimming pool water**

Fabian Soltermann, Tobias Widler,

Silvio Canonica and Urs von Gunten (2014)

*Water Research*, 56, 280-291

## A Additional information on actinometry and quantum yield calculations

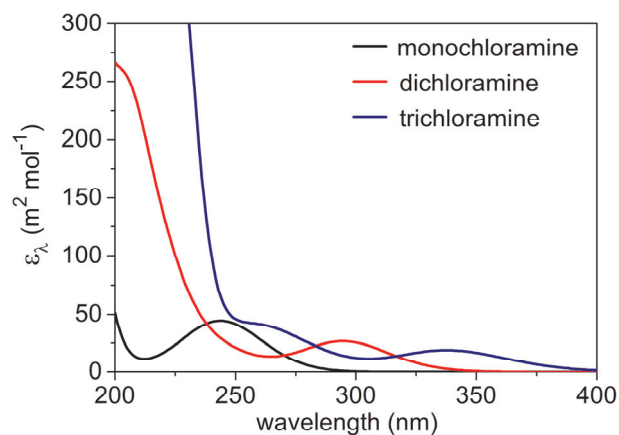


**Figure A.1.** Measured molar absorption coefficients ( $\epsilon_\lambda$ ) for mono-, di- and trichloramine.

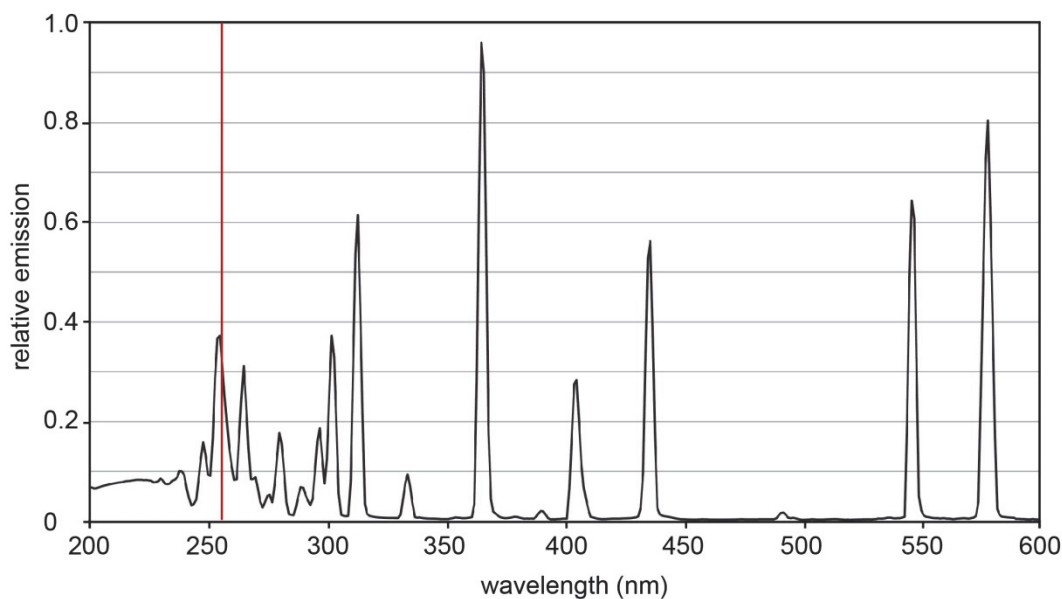


**Figure A.2.** Emission spectra of the medium-pressure (MP) mercury lamp (black line) according to the supplier (Peschl Ultraviolet, online catalogue 2013, [www.peschl-ultraviolet.com](http://www.peschl-ultraviolet.com)). The red line corresponds to the emission of a low-pressure (LP) lamp. Values for wavelength-dependent light emission can be found in Table A.1.

**Text A.1.** The spectral molar absorption coefficients ( $\epsilon$ ) for mono-, di-, trichloramine and atrazine were calibrated using the molar absorption coefficients for specific wavelengths given in the literature. Mono- and dichloramine concentrations derived from the given molar absorption coefficients at 243 and 294 nm ( $\text{NH}_2\text{Cl}$ :  $\epsilon_{243\text{nm}} = 44.5 \text{ m}^2 \text{ mol}^{-1}$ ,  $\epsilon_{294\text{nm}} = 2.7 \text{ m}^2 \text{ mol}^{-1}$ ,  $\text{NH}_2\text{Cl}$ :  $\epsilon_{243\text{nm}} = 24.5 \text{ m}^2 \text{ mol}^{-1}$ ,  $\epsilon_{243\text{nm}} = 27.6 \text{ m}^2 \text{ mol}^{-1}$ ). Trichloramine was quantified using literature values for the molar absorption coefficient at 336 and 360 nm ( $\text{NCl}_3$ :  $\epsilon_{336\text{nm}} = 19.0 \text{ m}^2 \text{ mol}^{-1}$ ,  $\epsilon_{360\text{nm}} = 12.6 \text{ m}^2 \text{ mol}^{-1}$ ) and atrazine with the molar absorption coefficient at 254 nm (atrazine:  $\epsilon_{254\text{nm}} = 386 \text{ m}^2 \text{ mol}^{-1}$ ) (Hand and Margerum, 1983; Nick et al., 1992; Schurter et al., 1995).

**Table A.1.** Wavelengths with corresponding emission intensities of the medium-pressure (MP) lamp, normalized distribution function of the lamp emission, the wavelength-dependent energy of a photon and normalized energy distribution of the MP lamp.

Peaks MP lamp (nm)	Light emission <sup>1)</sup> (mmol quanta h <sup>-1</sup> )	Normalized spectrum $f_{p,\lambda}$ , normalized 238-390 nm (-)	Energy per photon at $\lambda$ (J photon <sup>-1</sup> )	Normalized energy distribution $f_{\lambda}$ normalized 238-390 nm (-)	$f_{p,\lambda}$ * Energy per photon (J photon <sup>-1</sup> )
238-240	8	0.037	8.3E-19	0.048	3.1E-20
248	5	0.023	8.0E-19	0.029	1.9E-20
254	30	0.140	7.8E-19	0.168	1.1E-19
265	11	0.051	7.5E-19	0.059	3.8E-20
270	5	0.023	7.4E-19	0.026	1.7E-20
275	2	0.009	7.2E-19	0.010	6.7E-21
280	6	0.028	7.1E-19	0.030	2.0E-20
289	4	0.019	6.9E-19	0.020	1.3E-20
297	9	0.042	6.7E-19	0.043	2.8E-20
302	17	0.079	6.6E-19	0.080	5.2E-20
313	41	0.191	6.3E-19	0.186	1.2E-19
334	5	0.023	5.9E-19	0.021	1.4E-20
366	71	0.330	5.4E-19	0.276	1.8E-19
390	1	0.005	5.1E-19	0.004	2.4E-21
Total	215	1	9.6E-18	1	6.5E-19

<sup>1)</sup> Source: Peschl Ultraviolet (online-catalogue, 2013)

**Table A.2.** Molar absorption coefficients ( $\epsilon$ ) of mono-, di-, trichloramine and atrazine used for calculation of the quantum yields.

Peaks MP lamp (nm)	$\epsilon_{\lambda}$ NH <sub>2</sub> Cl m <sup>2</sup> mol <sup>-1</sup>	$\epsilon_{\lambda}$ NHCl <sub>2</sub> m <sup>2</sup> mol <sup>-1</sup>	$\epsilon_{\lambda}$ NCl <sub>3</sub> m <sup>2</sup> mol <sup>-1</sup>	$\epsilon_{\lambda}$ atrazine m <sup>2</sup> mol <sup>-1</sup>
238-240	42.8	39.3	114.7	976.5
248	43.1	23.4	49.2	433.5
254	37.1	17.5	43.2	386.0
265	21.2	13.4	39.1	415.2
270	14.7	14.4	35.4	365.1
275	9.6	16.9	30.7	266.2
280	5.8	20.4	25.7	152.2
289	2.0	25.7	17.7	27.2
297	0.7	26.6	13.1	6.8
302	0.3	24.8	11.8	4.5
313	0.0	16.7	12.6	3.0
334	0.0	3.7	18.8	2.7
366	0.0	0.0	10.1	2.1
390	0.0	0.0	2.6	1.7

## B Reactivity of trichloramine

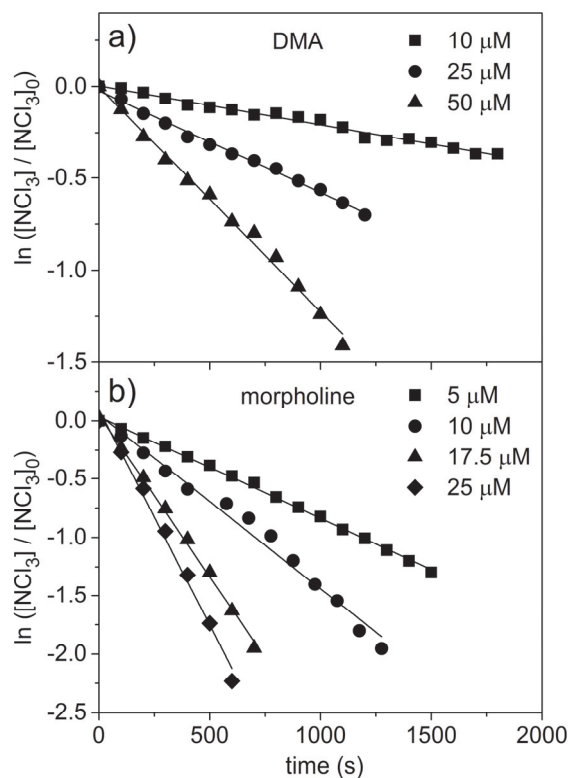


**Figure B.1.** Reaction of trichloramine (0.5–1  $\mu\text{M}$ ) with (a) DMA (10–50  $\mu\text{M}$ ) and (b) morpholine (5–25  $\mu\text{M}$ ) at pH 7.

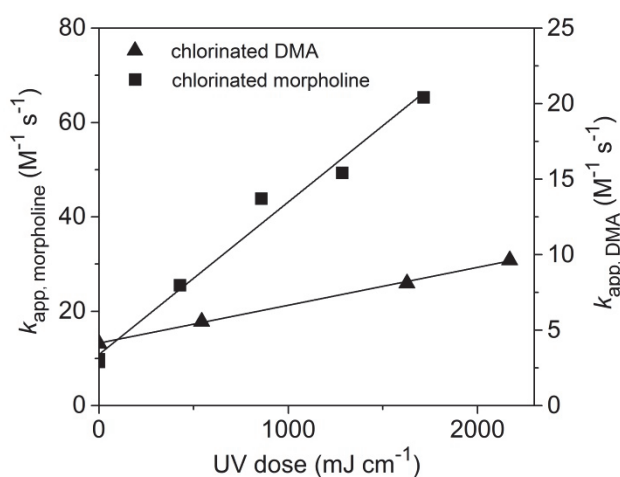


**Figure B.2.** Apparent second-order rate constants for the reaction of trichloramine with chlorinated DMA (25  $\mu\text{M}$ ) and chlorinated morpholine (25  $\mu\text{M}$ ) at pH 7 in dependence of UV treatment of the chlorinated amine prior to the reaction with trichloramine (0.5–1  $\mu\text{M}$ ).

## C Information on pool water samples used for quantum yield experiments

**Table C.1.** Characteristics of pool water samples used for quantum yield experiments.

Sample nr.	quantum yield mol einstein <sup>-1</sup>	pH (-)	NCl <sub>3</sub> before spiking (μM)	free chlorine (mg L <sup>-1</sup> as Cl <sub>2</sub> )	combined chlorine (mg L <sup>-1</sup> as Cl <sub>2</sub> )	urea (mg L <sup>-1</sup> )	conductivity (uS cm <sup>-1</sup> )	TOC mg C L <sup>-1</sup>
1	2.8	7.09	0.32	0.29	0.14	1.3	466	2.0
2	4.3	7.48	0.03	0.03	0.16	1.8	930	1.6
3	2.8	7.33	0.19	0.15	0.14	1.6	760	1.9
4	2.2	7.32	0.38	0.45	0.11	1	810	1.6
5	2.5	7.12	0.23	0.24	0.11	0.4	873	1.1
6	2.1	7.36	0.20	0.29	0.09	0.2	894	0.9
7	2.1	7.4	0.32	0.30	0.12	0.7	854	1.4
8	2.9	7.29	0.17	0.14	0.16	1.1	609	1.2
9	1.5	7.54	0.48	1.00	0.16	0.5	621	1.0

## D Additional information on the swimming pool facility

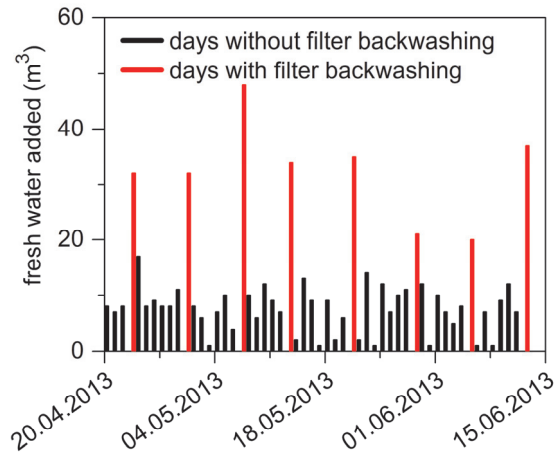


**Figure D.1.** Fresh water addition to the three pools over the period of the field study.

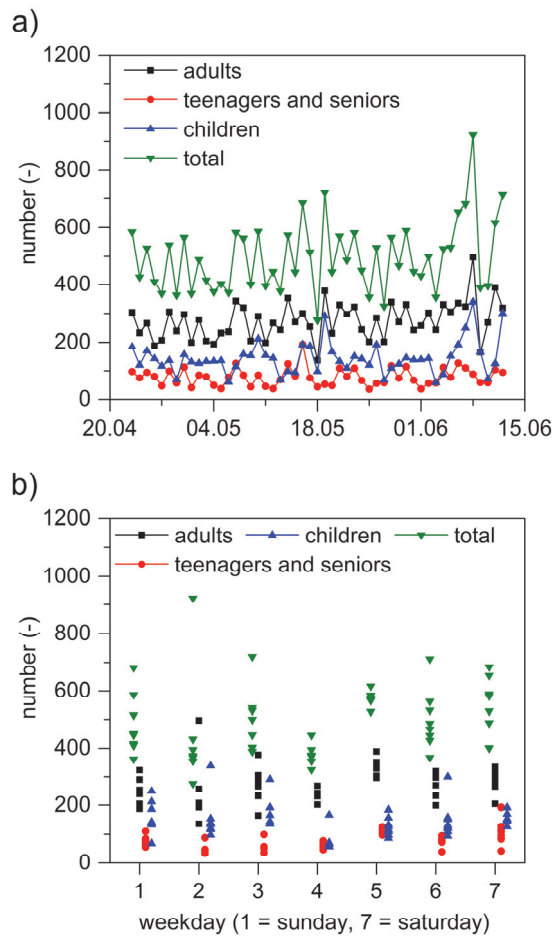
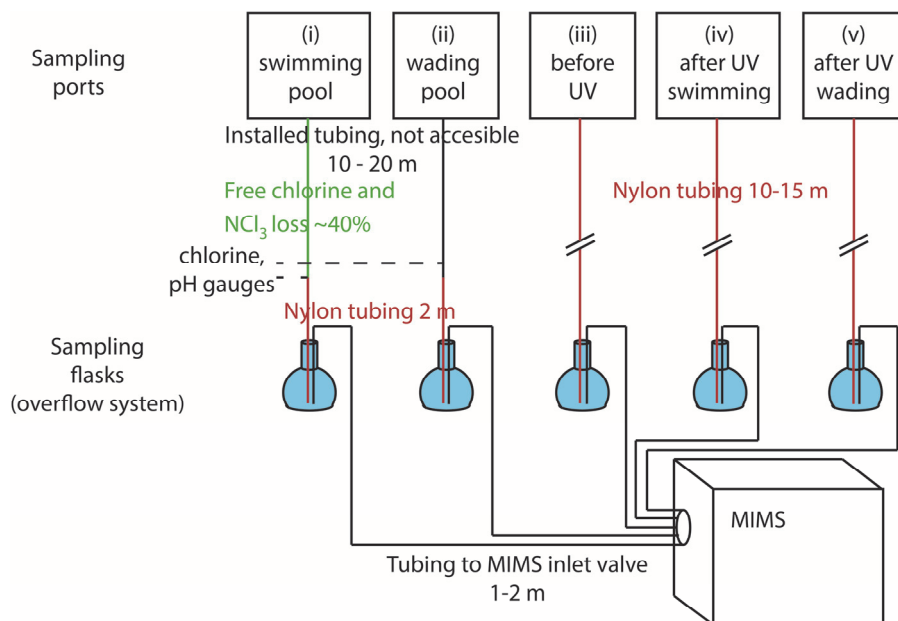


**Figure D.2.** (a) Visitor's frequency of the pool facility over the period of the field study and (b) sorted by weekdays.

## E Information on MIMS measurements on-site.



**Scheme E.1** Overview of the sampling system for trichloramine analysis. The water flow from the sampling ports to the sampling flasks was controlled to be  $10\text{--}40\text{ mL min}^{-1}$ . The tubing from the ports (i) and (ii) to the chlorine and pH gauges was a permanent installation. A free chlorine and trichloramine loss of about 40 % was observed between the sampling port and the sampling flask of the swimming pool (green line). All other connections between the ports and the sampling flasks were of nylon tubing (diameter 1.9 mm, Palle Knudsen, Denmark) and free of losses.

### Text E.2

#### MIMS calibration

MIMS calibration for trichloramine measurements was performed every 2–4 days. The baseline for signal 88  $m/z$  was determined every 1–3 days. The MIMS was installed at the pool facility for more than one month. The instrument lost about 1–2 % of sensitivity per day. After using a new filament for ionisation, the background increased during the first 2–3 days. Results were not analysed during that period. A similar increase of the background was observed at the end of the sampling campaign for unknown reasons. Figure E.1 and E.2 show the changes of sensitivity and background with time. Data were analysed by using the interpolated slope of the calibration (Figure E.1) and the interpolated background at the end of the sampling campaign (Figure E.2). The increase of the background for signal 88  $m/z$  was compared to the constant measurement of signal 171  $m/z$ . This signal was assumed to represent the evolution of the



background of the instrument since no substance in pool water was expected to give this signal. Trichloramine concentration was calculated using the interpolated baseline during the phase of increasing baseline.

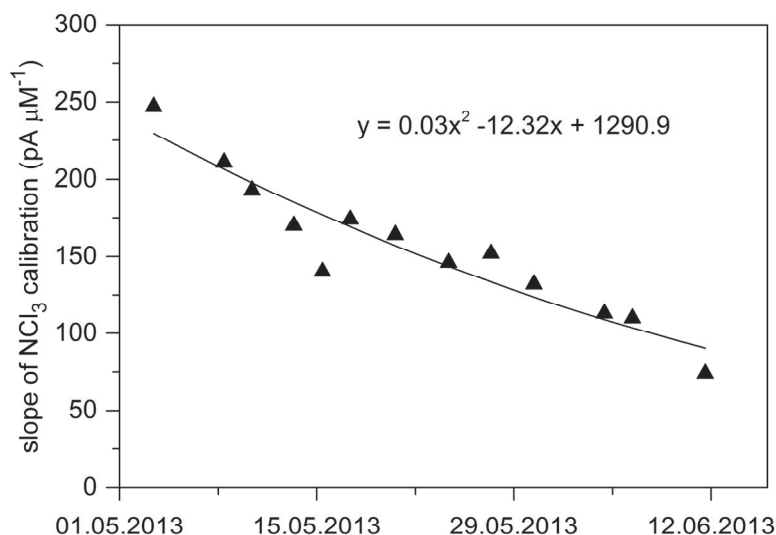


**Figure E.1** Evolution and interpolation of the slope of the trichloramine calibration used for the calculation of the trichloramine concentrations.

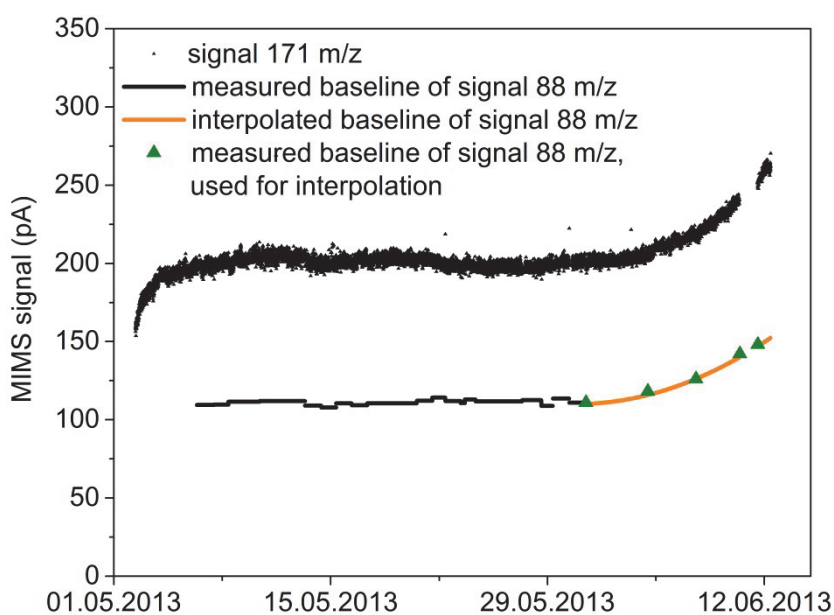


**Figure E.2** Evolution of the signal 171 m/z and the measured and interpolated baseline for signal 88 m/z.

## F Effect of UV treatment on combined chlorine concentration and on signal 83 m/z

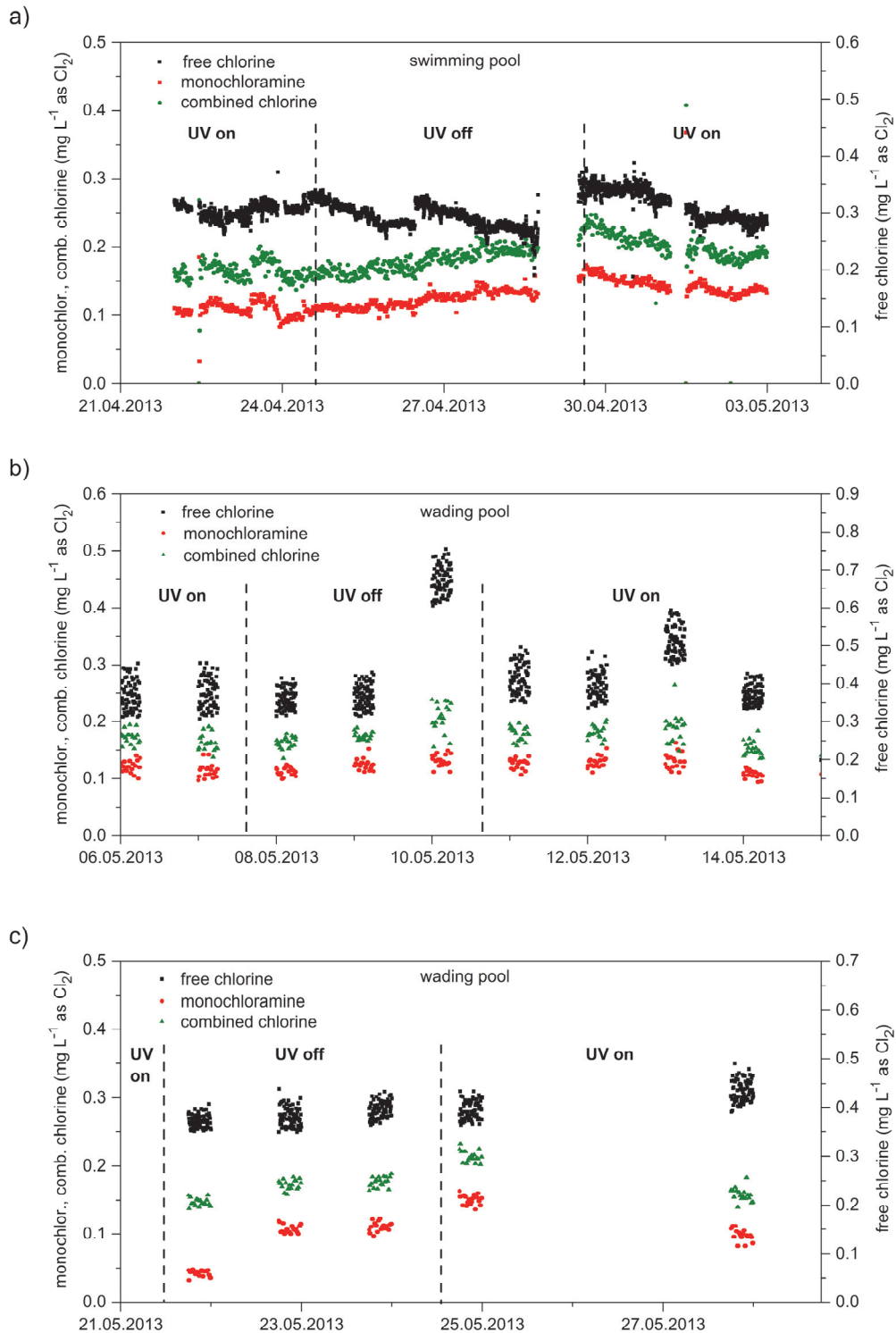


**Figure F.1** Evolution of free chlorine, combined chlorine and monochloramine in (a) the swimming pool and (b,c) the wading pool after switching the UV reactor on and off. For the wading pool, only data between 0:00 and 06:00 were plotted to reduce the impact of changing bather load.

**Text F.1.** Data in Figure F.1 on the combined chlorine concentration in the swimming pool (a) show a slight but steady increase of the combined chlorine concentration after the UV reactor was switched off and a decrease after it was turned on. Data on the wading pool (b and c) was less clear. Generally, it seemed that combined chlorine and monochloramine concentrations responded slowly to UV treatment and that 3 days were not enough to reach a new steady-state condition (Figure F.1a). Therefore, it is assumed that combined chlorine stability in pool water is high, leading to a cumulative effect of the UV treatment since pool water was treated every 4–5 hours on average.

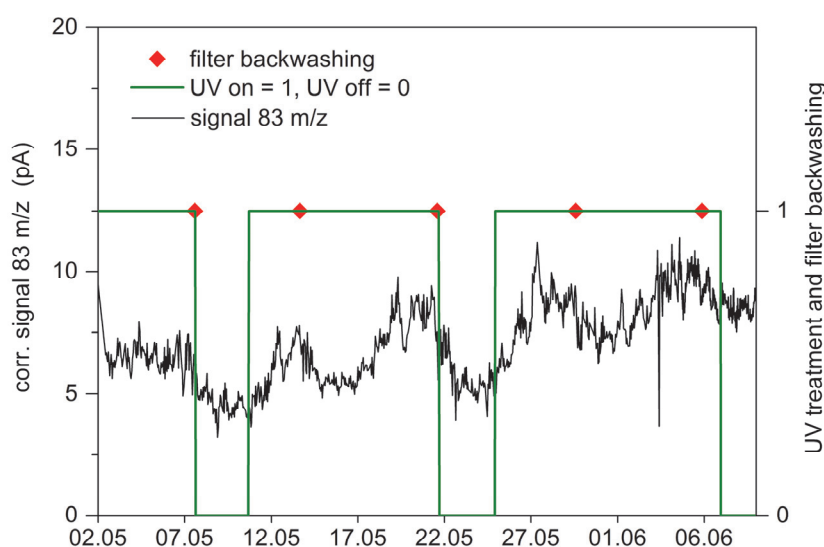


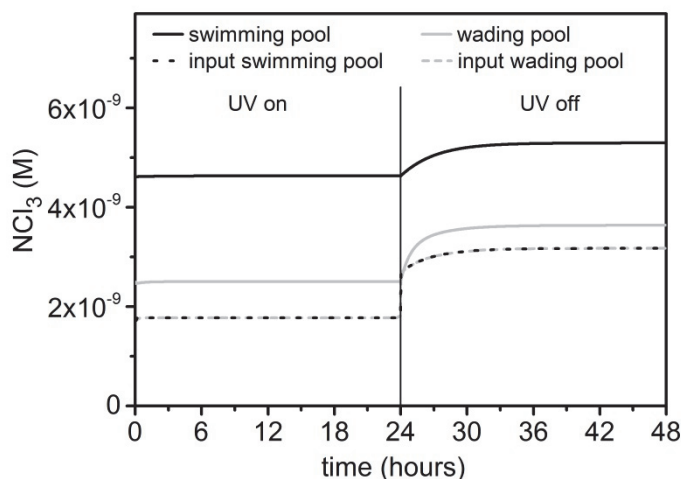
**Figure F.2.** Evolution of signal 83 m/z (which is assumed to represent chloroform) of the swimming pool in relation to UV treatment and filter backwashing. Signal 83 m/z was corrected with the trichloramine calibration (signal 83 m/z / slope of the trichloramine calibration) to consider the loss of sensitivity of the MIMS.

**Text F.2.** The results in Figure F.2 show that signal 83 m/z dropped after each filter backwashing for 2–3 days before it increased again. It seemed that a steady-state concentration was reached shortly before the weekly filter backwashing. Thus, backwashing of the filter diminished chloroform formation in the pool water. This might either be due to the improved filter capacity after the backwashing (less precursor in the pool water) or due to the cleaned filter (less precursors present in the filter).

A previous study reported an increased trihalomethane formation when pool water was treated with UV for one week (Cassan et al., 2006). The effect of UV treatment on signal 83 m/z cannot be assessed conclusively. No change in signal 83 m/z was observed over the UV

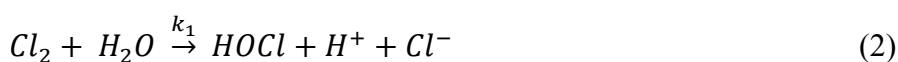
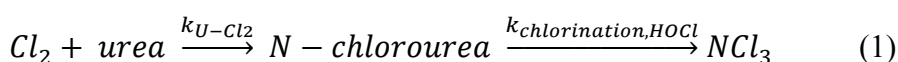
reactors. An interpretation of the long-term effect of the UV treatment on signal 83 m/z is not possible since UV treatment was always stopped shortly before or after the filter was backwashed. Since the filter backwashing caused a clear decrease of signal 83 m/z even when the UV treatment was not switched off, it can be assumed that this, and not the UV treatment, was the predominant reason for the signal drop when UV treatment was switched off simultaneously to the filter backwashing.

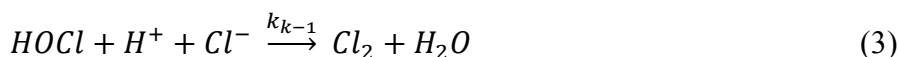
## G Information on the pool facility model



**Figure G.1.** Evolution of trichloramine concentration after switching on the UV treatment (40 % degradation in the UV reactors) and turning it off 24 hours later. Trichloramine formation was calculated using data from Blatchley and Cheng (2010).

**Text G.1.** Trichloramine concentration was modeled for two days with a trichloramine degradation of 40 % in the UV reactors on the first day and no degradation in the UV reactors on the second day. Trichloramine formation was calculated by assuming that the first chlorination step of urea by Cl<sub>2</sub> is the rate limiting step ( $k_{U-Cl_2} = 2.34 \times 10^{-4} \text{ M}^{-1} \text{ s}^{-1}$ ) in the trichloramine formation as suggested by Blatchley and Cheng (2010). Further chlorination with HOCl was assumed to be fast and to result in a stoichiometric formation of one trichloramine per urea (eq. 1). The Cl<sub>2</sub> concentration was derived at pH 7.2 with the free chlorine concentration (0.45 mg L<sup>-1</sup>, 0.35 mg L<sup>-1</sup> and 0.3 mg L<sup>-1</sup> for the swimming, wading and diving pool, respectively) and the chloride concentration according to the equations 2 + 3 from Deborde and von Gunten (2008) with  $k_1 = 22.3 \text{ s}^{-1}$  and  $k_{-1} = 4.3 \times 10^4 \text{ M}^{-2} \text{ s}^{-1}$ . The chloride concentration was measured daily during one week (several weeks after the sampling campaign) and showed almost no variation (156 ± 6 mg L<sup>-1</sup>). Urea concentration was set to a constant concentration of 0.6 mg L<sup>-1</sup> for all pools.





The calculated trichloramine concentration was 100 times lower than the measured concentration on-site. This suggests that either the reaction rate (which was measured at pH 2) was significantly higher in pool water or trichloramine in pool water mainly originated from other nitrogenous precursors than urea.

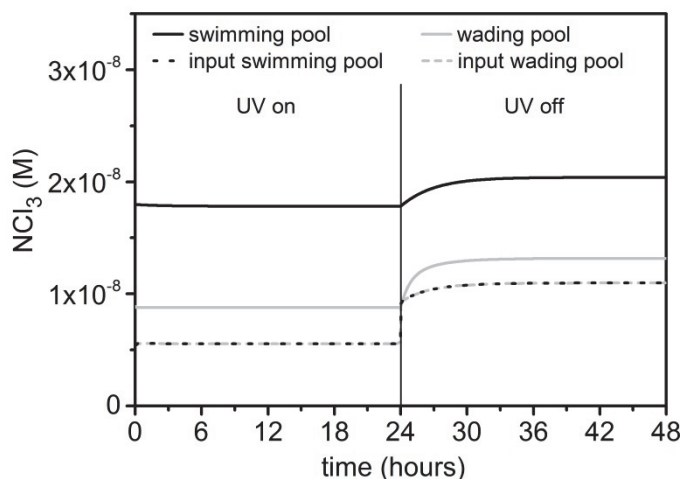
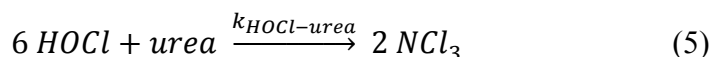
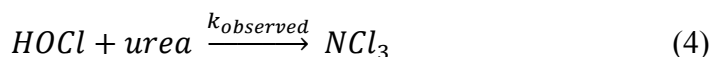


**Figure G.2.** Evolution of trichloramine concentration after switching on the UV treatment (40 % degradation in the UV reactors) and turning it off 24 hours later. Trichloramine formation was calculated using data from Schmalz et al. (2011).

**Text G.2.** A model was run with trichloramine degradation of 40 % in the UV reactors on the first day and no degradation in the UV reactors on the second day. Trichloramine formation was modeled using data from Schmalz et al. (2011) (eq. 4). Schmalz et al. (2011) deduced the reaction rate from the free chlorine depletion in excess of urea ( $3.3 \times 10^{-5} \text{ M}$ ) which allows to calculate the second order rate constant for the reaction of HOCl with urea ( $k_{\text{HOCl-urea}} = k_{\text{observed}} / [\text{urea}] = 4.58 \times 10^{-6} \text{ s}^{-1} / 3.3 \times 10^{-5} \text{ M} = 0.14 \text{ M}^{-1} \text{ s}^{-1}$ ). Schmalz et al. (2011) found that at pH 7.1 about 76 % of the nitrogen in urea was converted to trichloramine. In the model, a complete conversion of urea-nitrogen to trichloramine was assumed which would consume 3 HOCl molecules per trichloramine formed (eq. 5).



The resulting trichloramine concentration was about 20 times lower than the measured concentration on-site. This suggests that trichloramine formation from urea accounts only for about 5 % of the total trichloramine formation. To reach the measured trichloramine concentrations,  $k_{\text{HOCl-urea}}$  needs to be  $\sim 3.2 \text{ M}^{-1} \text{ s}^{-1}$ , a factor 20 higher than derived from literature data.

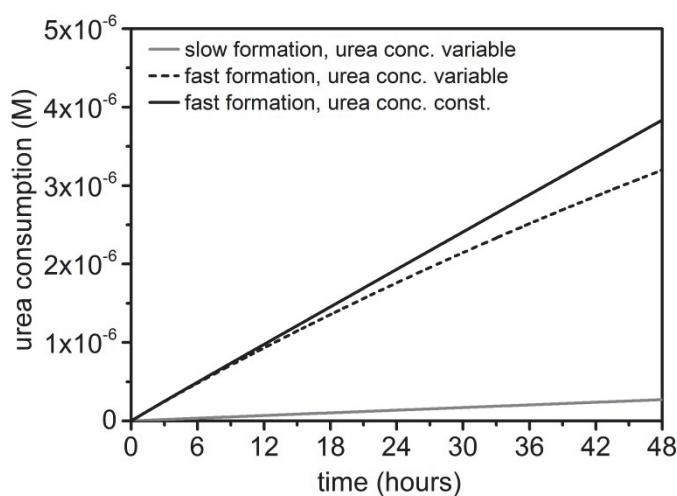


**Figure G.3** The hypothetical urea consumption as a function of time in a model with a slow reaction of urea with free chlorine (according to Schmalz et al. (2011)), or a fast reaction of urea with free chlorine (fitted value (Text G.2)) with a constant and variable urea concentration, respectively.

**Text G.3.** Three model runs were performed to quantify the urea consumption in the swimming pool. In the first two runs, the initial urea concentration was set to  $10^{-5} \text{ M}$  in the whole system without further urea addition. Trichloramine formation was modeled according to Schmalz et al. (2011) (i) with  $k_{\text{HOCl-urea}} = 0.14 \text{ M}^{-1} \text{ s}^{-1}$  (slow formation) and (ii) with  $k_{\text{HOCl-urea}} = 3.2 \text{ M}^{-1} \text{ s}^{-1}$  (fast formation, see Text G.2). In a third run, the urea concentration was kept constant at  $10^{-5} \text{ M}$  and trichloramine formation was modeled with  $k_{\text{HOCl-urea}} = 3.2 \text{ M}^{-1} \text{ s}^{-1}$  (fast formation). The results in Figure G.3. show that the urea consumption was about 1 % and 18 % of the initial concentration within 24 h in the runs without urea addition for slow and fast trichloramine formation, respectively. The moderate urea decrease is in good agreement with the slow trichloramine decrease over night, which was observed in the same pool facility (Soltermann et al., 2014). A urea depletion of 18 % of  $0.6 \text{ mg L}^{-1}$  ( $10^{-5} \text{ M}$ ) urea in the total water volume of

about  $2 \times 10^6$  L implies a urea introduction of 200 g per day to maintain a constant urea level in the pool facility. This results in an average urea introduction per visitor of 0.4 g since the average number of visitors was about 500 per day. This urea input is in agreement with Weng and Blatchley (2011) who calculated a urea input of 0.56–1.2 g per bather.

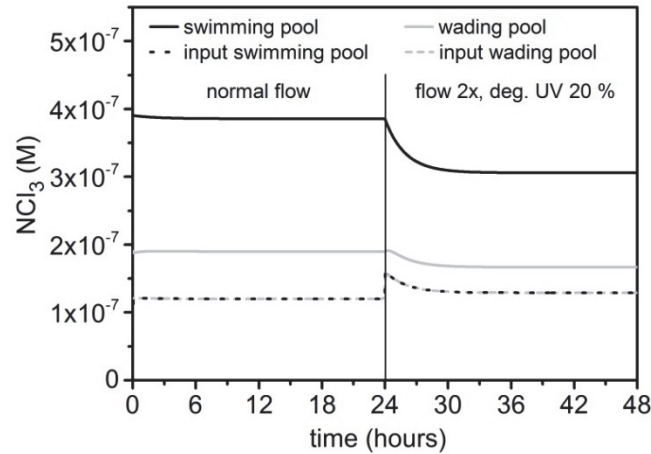


**Figure G.4.** Modeled evolution of the trichloramine concentration after doubling the recirculation rate through the water treatment system. The UV degradation was adjusted to the higher flow through the UV reactor (degradation in the UV reactor: 20 %).

**Text G.4.** Water flow through the water treatment was doubled after 24 hours. Trichloramine elimination in the UV reactors was assumed to be inversely proportional to the water flow (resulting in a 20 % degradation of trichloramine in the UV reactors) because of the diminished residence time of the pool water in the UV reactor. This assumption is an approximation which is not true for all ranges of UV intensities. The results in Figure G.4. show that the trichloramine concentration significantly decreased in the swimming pool due to the shorter residence time and the trichloramine degradation in the spillway / multilayer filter.



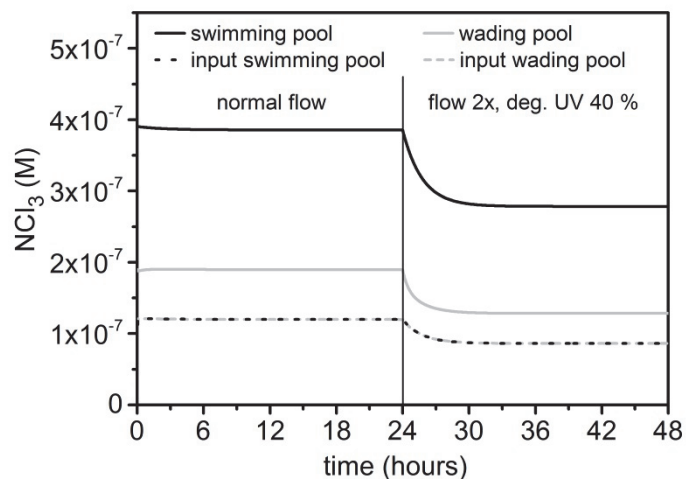


**Figure G.5.** Modeled evolution of the trichloramine concentration after an increase of the recirculation rate through water treatment by a factor of two. Trichloramine degradation in the UV reactor was set to 40 %.

**Text G.5.** The recirculation rate through the water treatment system was doubled after 24 hours. Trichloramine reduction in the UV reactors was kept constant at 40 %. Especially trichloramine concentration in the wading pool dropped more than in Figure G.4 where the UV degradation was adjusted to 20 %.

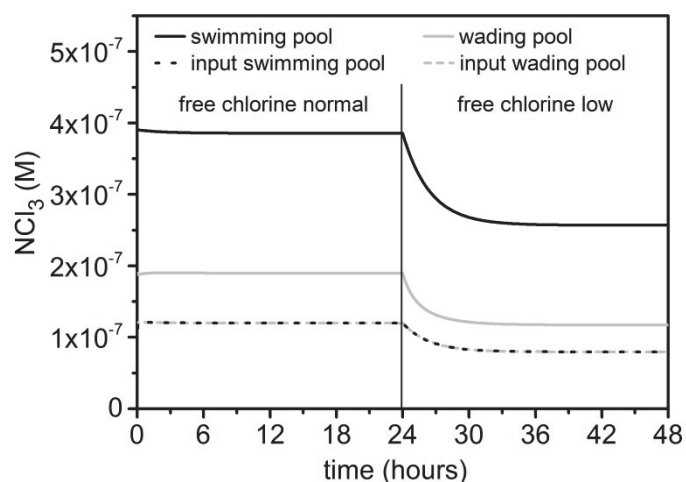


**Figure G.6.** Modeled evolution of the trichloramine concentration in a model run in which the free chlorine concentration was lowered after 24 hours from 0.45 and 0.35 mg L<sup>-1</sup> to 0.3 and 0.2 mg L<sup>-1</sup> in the swimming and wading pool, respectively.

**Text G.6.** A free chlorine reduction of about 33 % resulted in trichloramine reduction similar to the free chlorine reduction. This is in a good agreement with other measurements in the same pool facility and with samples from other swimming pools in which a linear correlation between the free chlorine and the trichloramine concentration was found (Soltermann et al., 2014).

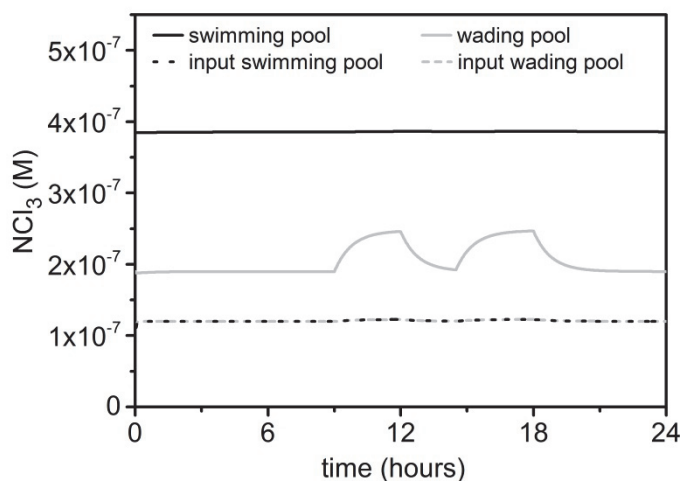
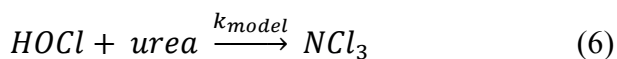


**Figure G.7.** Modeled evolution of the trichloramine concentration within two periods (9:00–12:00 and 14:30–18:00) of high urea concentration ( $1 \text{ mg L}^{-1}$ ) in the wading pool and the swimming pool.

**Text G.7.** Trichloramine concentrations in the wading and the swimming pool were modeled for changing urea concentrations as they typically occurred in the pool facility: Urea was assumed to be the only trichloramine precursor and to be at a constant level in all pools ( $0.6 \text{ mg L}^{-1}$ ) except for the wading pool ( $1 \text{ mg L}^{-1}$ ) during the time of heavy use (9:00–12:00 and 14:30–18:00). A similar increase was observed during heavy use of the wading pool (Soltermann et al., 2014). Trichloramine formation was calculated using eq. 6, in which  $k_{\text{model}}$  resulted from  $k_{\text{eff}}$  ( $10^5 \text{ s}^{-1}$ , see main text) from previous models and a constant urea concentration ( $0.6 \text{ mg L}^{-1}$ ).



The modeled trichloramine increase was less pronounced than the measured increase of the trichloramine concentration shown in Figure 7 (main text). This indicates that there was an even stronger increase of other trichloramine precursors than urea. Trichloramine concentration in the swimming pool remained unchanged by the higher trichloramine concentration in the wading pool since the volume of the wading pool ( $56 \text{ m}^3$ ) represents only a small fraction of the total water volume in the three pools ( $\sim 2'000 \text{ m}^3$ ).

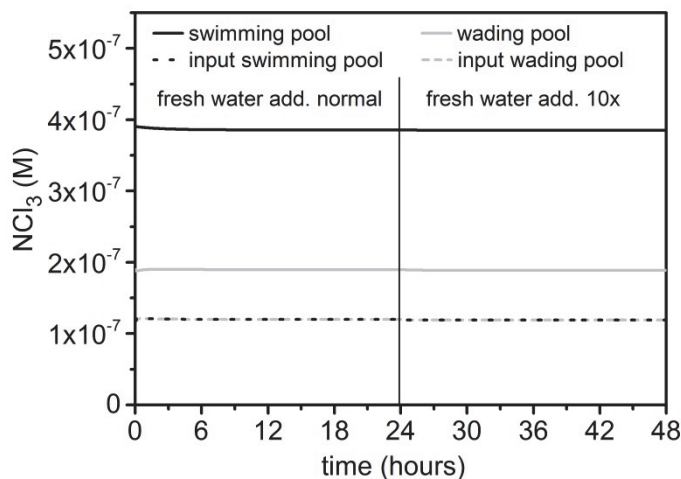


**Figure G.8.** Modeled evolution of the trichloramine concentration after increase of the fresh water addition by a factor of 10 after 24 hours.

**Text G.8.** Fresh water addition was increased from  $0.13$  to  $1.3 \text{ L s}^{-1}$  after 24 hours. Trichloramine concentrations in the swimming and the wading pool remained unchanged. The model only reflects the dilution of the trichloramine concentration and not the dilution of the nitrogenous precursors. The total volume of the system is around  $2'000 \text{ m}^3$  wherefore a dilution of  $0.5 \%$  and  $5.6 \%$  per day resulted for the fresh water addition of  $0.13$  and  $1.3 \text{ L s}^{-1}$ , respectively. This dilution might be important for stable, slowly reacting substances but has little effect on substances with a short half-life in pool water. An example of such moieties would be precursors for trihalomethanes (THM) which are rather slowly reacting substances. However, these substances were mainly introduced by the filling water and not by the bather load. Therefore, an increased fresh water addition would not lower the THM precursor concentrations in pool water.

## References

- Blatchley, E. R. and M. Cheng (2010). "Reaction Mechanism for Chlorination of Urea." *Environmental Science & Technology* 44(22): 8529-8534.
- Cassan, D., B. Mercier, F. Castex and A. Rambaud (2006). "Effects of medium-pressure UV lamps radiation on water quality in a chlorinated indoor swimming pool." *Chemosphere* 62(9): 1507-1513.
- Deborde, M. and U. von Gunten (2008). "Reactions of chlorine with inorganic and organic compounds during water treatment--Kinetics and mechanisms: A critical review." *Water Research* 42(1-2): 13-51.
- Hand, V. C. and D. W. Margerum (1983). "Kinetics and mechanisms of the decomposition of dichloramine in aqueous-solution." *Inorganic Chemistry* 22(10): 1449-1456.
- Nick, K., H. Schöler, G. Mark, T. Söylemez, M. Akhlaq, H. Schuchmann and C. von Sonntag (1992). "Degradation of some triazine herbicides by UV radiation such as used in the UV disinfection of drinking water." *Aqua- Journal of Water Supply: Research and Technology* 41(2): 82-87.
- Schmalz, C., F. H. Frimmel and C. Zwiener (2011). "Trichloramine in swimming pools - Formation and mass transfer." *Water Research* 45(8): 2681-2690.
- Schurter, L. M., P. P. Bachelor and D. W. Margerum (1995). "Nonmetal redox kinetics - monochloramine, dichloramine, and trichloramine reactions with cyanide ion." *Environmental Science & Technology* 29(4): 1127-1134.
- Soltermann, F., T. Widler, S. Canonica and U. von Gunten (2014). "Comparison of a novel extraction-based colorimetric (ABTS) method with membrane introduction mass spectrometry (MIMS): Trichloramine dynamics in pool water." *Water Research* 58: 258-268.
- Weng, S. C. and E. R. Blatchley (2011). "Disinfection by-product dynamics in a chlorinated, indoor swimming pool under conditions of heavy use: National swimming competition." *Water Research* 45(16): 5241-5248.

# Chapter 6

## **Enhanced *N*-nitrosamine formation in pool water by UV irradiation of chlorinated secondary amines in the presence of monochloramine**

Fabian Soltermann, Minju Lee,

Silvio Canonica and Urs von Gunten (2013)

*Water Research*, 47(1), 79-90

## Abstract

*N*-Nitrosamines, in particular *N*-nitrosodimethylamine (NDMA), are carcinogens which occur as chlorine disinfection by-products (DBPs) in swimming pools and hot tubs. UV treatment is a commonly used technique in swimming pools for disinfection and DBP attenuation. UV irradiation is known to efficiently degrade *N*-nitrosamines. However, UV irradiation (at  $\lambda = 254$  nm) of chlorinated dimethylamine (CDMA) and monochloramine, two NDMA precursors present in swimming pool water, resulted in a substantial UV-induced NDMA formation (~1–2 % yield based on initial CDMA concentration) simultaneously to NDMA photolysis. Maximum NDMA concentrations were found at UV doses in the range used for advanced oxidation (350–850 mJ cm<sup>-2</sup>). Very similar behavior was found for other chlorinated secondary amines, namely diethylamine and morpholine. Effectiveness of UV irradiation for *N*-nitrosamine abatement depends on initial *N*-nitrosamine and precursor concentrations and the applied UV dose. *N*-Nitrosamine formation is hypothesized to occur via the reaction of nitric oxide or peroxyxynitrite with the secondary aminyl radical, which are products from the photolysis of monochloramine and chlorinated secondary amines, respectively. Experiments with pool water showed that similar trends were observed under pool water conditions. UV treatment (UV dose: ~360 mJ cm<sup>-2</sup>) slightly increased NDMA concentration in pool water instead of the anticipated 50 % abatement in the absence of NDMA precursors.

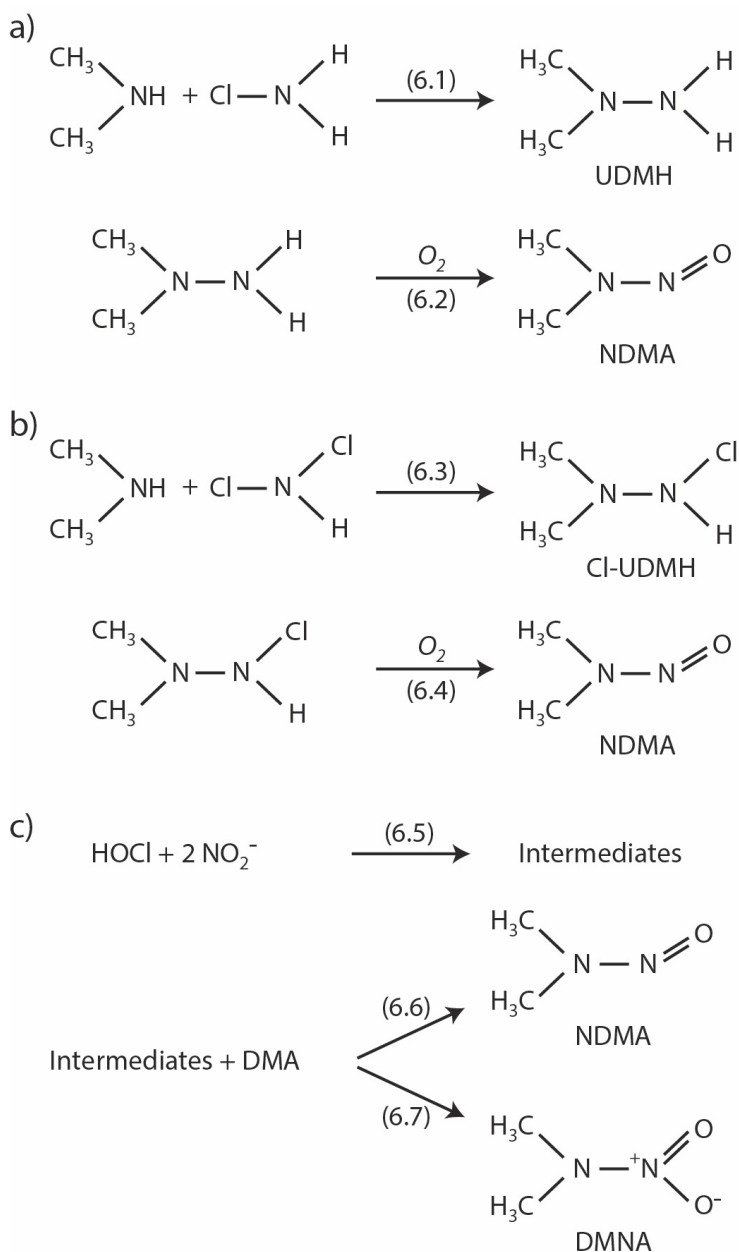
## 6.1 Introduction

Due to their carcinogenic properties, *N*-nitrosamines are of high concern in food products, drinking water and every day products (e.g. cigarettes and cosmetics) (Ketola et al., 2002; Huber et al., 2011). Although the main *N*-nitrosamine exposure occurs via food, nitrosamine uptake via drinking water can be relevant (Kristensen et al., 2009). The most studied *N*-nitrosamine is *N*-nitrosodimethylamine (NDMA) which is mutagenic with a life time cancer risk of  $10^{-6}$  for a concentration of  $0.7 \text{ ng L}^{-1}$  in drinking water (Buxton and Subhani, 1972; WHO, 2008; 2012). Nevertheless, only few regulatory agencies have established standards for NDMA in drinking water of around  $10 \text{ ng L}^{-1}$  (2013; 2013). The World Health Organisation (WHO) sets a guideline value of  $100 \text{ ng L}^{-1}$  which was adopted as target value by Japan (Canonica et al., 1995; WHO, 2008).

*N*-Nitrosamines were measured in drinking water, surface waters, and waste water effluent at concentration levels of  $\leq 100 \text{ ng L}^{-1}$ ,  $\leq 60 \text{ ng L}^{-1}$ , and  $8\text{--}400 \text{ ng L}^{-1}$ , respectively (INRS, 2007; Krauss et al., 2009; Bessonneau et al., 2011; SIA, 2011). Recently, concerns have arisen about *N*-nitrosamine concentrations in swimming pool water. NDMA was measured in swimming pools and hot tubs with concentrations of up to  $450 \text{ ng L}^{-1}$  (Walse and Mitch, 2008; Jurado-Sanchez et al., 2010). These findings were linked to epidemiological studies which showed a correlation between swimming in pool water and risk of developing bladder cancer (Walse and Mitch, 2008; Garcia et al., 2012).

NDMA is a disinfection by-product (DBP) in chlorinated and chloraminated water (Mitch and Sedlak, 2002; Schreiber and Mitch, 2006; Schreiber and Mitch, 2007; Hansen et al., 2013). Its formation in swimming pools is assumed to occur mainly through the slow reaction of monochloramine with dimethylamine (DMA) via the formation of unsymmetrical dimethylhydrazine (UDMH) as an intermediate (Scheme 6.1a, eqs. 6.1, 6.2) or through the faster reaction of dichloramine with DMA via the chlorinated UDMH (Scheme 6.1b, eqs. 6.3, 6.4) (Schreiber and Mitch, 2006). Schreiber and Mitch (2006a) suggest that the major NDMA formation in pool water occurs via the dichloramine pathway, which includes the oxidation of chlorinated UDMH to NDMA by the incorporation of dissolved oxygen (Scheme 6.1b, eq. 6.4). A much faster NDMA formation, with a parallel dimethylnitramine (DMNA) formation, occurs at breakpoint chlorination involving nitrite, free chlorine and DMA as precursors (Scheme 6.1c) (Schreiber and Mitch, 2007). Schreiber and Mitch (2007) did not reveal the exact reaction mechanism, but assumed that the formation involves peroxyxynitrite and hydroxyl radicals ( $\cdot\text{OH}$ ) rather than dinitrogen tetroxide as described in previous studies (Choi and Valentine, 2003).

Other *N*-nitrosamine formation pathways were reported from the reaction of secondary amines (e.g. morpholine) with nitrosating agents such as nitric oxide or peroxyxynitrite (APHA, 2005; Canonica et al., 2008; Kinani et al., 2012). The formation via peroxyxynitrite was reported to generate the corresponding *N*-nitramines as a side product to the *N*-nitrosamines (Scheme 6.1c, eqs. 6.6, 6.7) (Kinani et al., 2012). For morpholine, the ratio of *N*-nitramine and *N*-nitrosamine formation depends on various factors such as pH or carbonate concentration (APHA, 2005).



**Scheme 6.1:** NDMA formation from (a) the slow reaction of  $\text{NH}_2\text{Cl}$  and DMA via UDMH, (b) the faster reaction of  $\text{NHCl}_2$  and DMA via Cl-UDMH and (c) the very fast formation at breakpoint chlorination from HOCl, nitrite and DMA via peroxyxynitrite or other reactive nitrogen oxides (adapted from Schreiber and Mitch (2006) and Schreiber and Mitch (2007)).



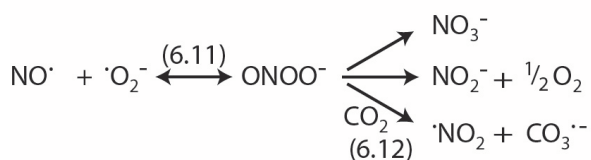
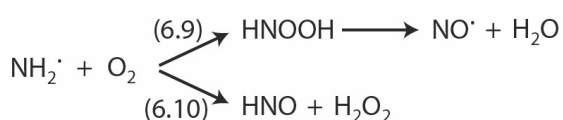
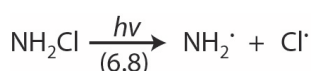
While there are numerous *N*-nitrosamine formation pathways, only a few *N*-nitrosamine mitigation strategies are considered to be effective (Davey et al., 2011). Various studies suggest to prevent *N*-nitrosamine formation by precursor oxidation with O<sub>3</sub>, ClO<sub>2</sub>, Fe(VI) and Cl<sub>2</sub> (Bogatu et al.; Yiin and Margerum, 1990; Hansen et al., 2013; Weng et al., 2013). After their formation, photolysis is the most effective *N*-nitrosamine mitigation strategy, especially for NDMA (Gérardin and Subra, 2004; Nawrocki and Andrzejewski, 2011; Weng et al., 2012; Wang et al., 2013). Plumlee and Reinhard (2007) reported that many *N*-nitrosamines have similar absorption spectra and quantum yields. The UV fluence-based rate constant of NDMA hardly differs for low- and medium-pressure lamps but changes with pH and initial concentration (Sharpless and Linden, 2003; Gérardin and Subra, 2004; Parrat et al., 2012).

In addition to disinfection, UV treatment in swimming pools is used to diminish the chloramine concentration to reach regulatory standards and to prevent DBP formation. The required UV dose for a 50 %-degradation of monochloramine, the dominant chloramine in pool water, is reported to be about 700 mJ cm<sup>-2</sup> ( $\lambda = 254$  nm) (Plewa et al., 2008). This is at the lower end of typical UV doses for pre-oxidation (~750–1500 mJ cm<sup>-2</sup>) and above the ones for disinfection (40–100 mJ cm<sup>-2</sup>) (Shah et al., 2011; Hansen et al., 2013). In Switzerland, pool water is recirculated through the treatment system and it is commonly irradiated with a UV dose of 40–100 mJ cm<sup>-2</sup> per treatment cycle. The average number of treatment cycles that pool water experiences can be calculated from the average residence time in the system and the hydraulic residence time in the pool.

It has been demonstrated that UV treatment of chlorinated pool waters may also enhance the concentration of other DBPs (e.g. THM, dichloromethylamine, dichloroacetonitrile, cyanogen chloride) (Reichert, 1994; Cassan et al., 2006). Other studies showed that UV irradiation can induce NDMA formation, for instance the irradiation of nitrate or nitrite in the presence of dimethylamine (DMA) (Ohta et al., 1982; Lee and Yoon, 2007). However, the *N*-nitrosamine yields in these studies were low and only relevant under extreme conditions. The fact that NDMA photolysis forms its own precursors again (e.g. DMA and nitrite) is not problematic since the NDMA yield from these substances is very low (0.2 % after 24 h in the presence of free chlorine) (Sharpless and Linden, 2003; Xu et al., 2009). Nevertheless, photolysis of chloramines leads to a number of reactive nitrogen species such as aminyl radicals, nitric oxide, peroxyxynitrite, and nitrite (Scheme 6.2) which may lead to *N*-nitrosamines in combination with secondary amines (Li and Blatchley, 2009; De Laat et al., 2010; Kinani et al., 2012). Nitric oxide can react to peroxyxynitrite in the presence of superoxide ( $\cdot\text{O}_2^-$ ) (Scheme 6.2, eq. 6.11, Lobachev and Rudakov (2012));  $\cdot\text{O}_2^-$  may be formed over numerous pathways during

photolytic processes in natural waters (Liviak et al., 2010). Since the concentrations of chloramines and secondary amines are significant in swimming pools, it can be hypothesized that UV treatment may induce simultaneously the degradation of *N*-nitrosamines, which are already in solution, and the formation of new *N*-nitrosamines.

The objective of this study was to investigate UV treatment as a mitigation option for *N*-nitrosamines in chloraminated pool water. The UV-induced formation and abatement of NDMA, a general model compound for *N*-nitrosamines was investigated in waters containing monochloramine and chlorinated dimethylamine. Furthermore, the kinetics of the main UV-induced NDMA formation pathway in pool water were elucidated and its validity for the formation of other *N*-nitrosamines (*N*-nitrosodiethylamine, *N*-nitrosomorpholine) was assessed. The relevance of the UV-induced *N*-nitrosamine formation was also investigated in pool water samples.



**Scheme 6.2:** Potential *N*-nitrosamine and *N*-nitramine precursors derived from monochloramine photolysis (adapted from Li and Blatchley (2009), Lobachev and Rudakov (2012) and Uppu et al. (2005)).

## 6.2 Materials and Methods

### 6.2.1 Reagents

All chemicals were analytical grade and used without further purification. Dimethylamine (DMA), ammonium chloride, *tert*-butanol (t-BuOH), morpholine (Mor), diethylamine (DEA), sodium hypochlorite (6–14 % active chlorine), and sodium nitrate were obtained from Sigma-Aldrich. *N*-Nitrosodimethylamine (NDMA), *N*-nitrosodiethylamine (NDEA), and the *N*-nitrosamine mix (EPA 8270 Appendix IX) including *N*-nitrosomorpholine (NMor) were purchased from Supelco. Sodium sulfate, disodium carbonate, ascorbic acid, sodium dihydrogenphosphate and disodium hydrogenphosphate were obtained from Merck. *N*-Nitrodimethylamine (also known as dimethylnitramine (DMNA)) was purchased from Cambridge Isotope Laboratories. Ultrapurified water was produced by the “barnstead nanopure” water purification system from Thermo Scientific.

The concentration of the hypochlorite stock solution was quantified spectrophotometrically at  $\lambda = 292$  nm (molar absorption coefficient =  $350 \text{ M}^{-1} \text{ cm}^{-1}$ ) (Soulard et al., 1981). Stock solutions of chlorinated secondary amines (chlorinated dimethylamine (CDMA), chlorinated diethylamine (CDEA) and chlorinated morpholine (CMor)) were produced just before the experiments by vigorously mixing the secondary amine with hypochlorite (molar ratio N/Cl 1:1) for a few seconds. Solutions were kept in closed bottles with little headspace to prevent the loss by evaporation.

Monochloramine ( $\text{NH}_2\text{Cl}$ ) stock solutions were freshly prepared daily with a slightly modified method of Shang and Blatchley (1999) by mixing ammonium chloride and hypochlorite (molar ratio N/Cl 1:1) with a dual syringe pump with a T-mixing system at pH 9.5. The  $\text{NH}_2\text{Cl}$  concentration was quantified using the method by Schreiber and Mitch (2005) considering the absorption of  $\text{NH}_2\text{Cl}$  and dichloramine ( $\text{NHCl}_2$ ) at  $\lambda = 245$  and 295 nm ( $\text{NH}_2\text{Cl}$ :  $\epsilon_{245\text{nm}} = 445 \text{ M}^{-1} \text{ cm}^{-1}$ ,  $\epsilon_{295\text{nm}} = 14 \text{ M}^{-1} \text{ cm}^{-1}$ ;  $\text{NHCl}_2$ :  $\epsilon_{245\text{nm}} = 208 \text{ M}^{-1} \text{ cm}^{-1}$ ,  $\epsilon_{295\text{nm}} = 267 \text{ M}^{-1} \text{ cm}^{-1}$ ). To check for the presence of trichloramine, the absorbance at 360 nm was analysed ( $\epsilon_{360\text{nm}} = 126 \text{ M}^{-1} \text{ cm}^{-1}$ ) (Schurter et al., 1995).  $\text{NH}_2\text{Cl}$  dissociation might be considerable if experiments are conducted at neutral or acidic pH with high  $\text{NH}_2\text{Cl}$  and phosphate buffer concentrations (Jafvert and Valentine, 1992). Therefore,  $\text{NH}_2\text{Cl}$  stability was kinetically modelled with data from Jafvert and Valentine (1992) to verify that  $\text{NH}_2\text{Cl}$  did not dissociate under the experimental conditions (data not shown).

## 6.2.2 Analytical methods

### *N-Nitrosamines and dimethylnitramine (experiments in ultrapurified water)*

Concentrations of *N*-nitrosamines and dimethylnitramine (DMNA) in experiments with ultrapurified water and atrazine samples for actinometry were analysed with a high performance liquid chromatography (HPLC) coupled with a UV-visible absorbance diode array detector (Agilent 1100 series and UltiMate 3000). *N*-Nitrosamine and atrazine separation were conducted with a TSKgel G2500PWXL (Tosoh Bioscience) and a Nucleosil 100-5 C18 (Macherey-Nagel) column, respectively. *N*-Nitrosamines and atrazine were detected at 228 nm and 254 nm, respectively. The limits of quantification were around 0.25  $\mu\text{M}$  for the *N*-nitrosamines and DMNA with a precision of about 5 %. *N*-Nitrosomorpholine (NMor) calibration experienced interferences from the neighbouring peak in the *N*-nitrosamine mix. Therefore, quantification was less precise than for the other two nitrosamines. However, NMor peaks from experiments in ultrapurified water were free of interferences.

### *N-Nitrosodimethylamine in pool water*

The analyses of pool water samples were conducted with an HPLC (UltiMate 3000) equipped with a post-column Griess reagent system. Solid phase extraction (SPE) of *N*-nitrosamines was performed before the analysis. The SPE procedure and the analytical system is described in detail elsewhere (Bessonneau et al., 2011). For the method, limits of detection ( $3.4 \times \text{stdv.}$ ) and of quantification ( $10 \times \text{stdv.}$ ) of *N*-nitrosodimethylamine are 0.08 nM and 0.22 nM, respectively (Bessonneau et al., 2011). All samples in this study had a signal to noise ratio (S/N) > 3 (only one sample with  $2 < \text{S/N} < 3$ ) and were in a range where the calibration showed a good linearity.

### *NH<sub>2</sub>Cl and CDMA*

Measurements of pure  $\text{NH}_2\text{Cl}$  and CDMA solutions were performed on a Varian Cary 1E UV/VIS spectrophotometer.  $\text{NH}_2\text{Cl}$  was analysed as described above. CDMA depletion was measured by monitoring the absorbance at  $\lambda_{\text{max}} = 265 \text{ nm}$  ( $\epsilon_{265\text{nm}} = 297 \pm 16 \text{ M}^{-1}\text{cm}^{-1}$ ). Since the absorption spectra of  $\text{NH}_2\text{Cl}$  and CDMA interfere, they could not be measured when present in the same solution.

### *pH*

Measurements of pH were conducted with a pH electrode (Ross SemiMicro pH, Thermo Scientific). Calibration was performed with buffer solutions of pH 7 and 9 (CertiPUR, Merck).

### 6.2.3 Pool water samples

Pool water samples were collected from two different public indoor swimming pools (Table 6.1). In both pools, water treatment includes filtration and chlorination. Free chlorine and combined chlorine were measured with a colorimetric, DPD-based test kit (Chemotest 25, SWAN) on site. The pH was measured on site with a pH electrode and remained stable ( $\pm 0.1$ ) from sampling until the end of the experiment.

**Table 6.1:** Characteristics of swimming pools and their waters.

	volume (m <sup>3</sup> )	hydraulic residence time in pool (h)	average residence time in system <sup>1</sup> (h)	pH (-)	combined chlorine (mg L <sup>-1</sup> as Cl <sub>2</sub> )	free chlorine (mg L <sup>-1</sup> as Cl <sub>2</sub> )
Pool A	650	4.5	26	7.7	0.15	0.25
Pool B	750	4.7	42	7.4	0.1	0.4

<sup>1</sup> based on fresh water addition

#### *Sample preparation*

Solid phase extraction was needed to quantify *N*-nitrosamines in pool waters (1 L). Irradiation time of selected samples was 7.5 minutes ( $\sim 360$  mJ cm<sup>-2</sup>). Since only about 150 mL of the sample could be irradiated in the UV reactor in one turn, stepwise irradiation of the sample lasted for almost two hours. Blank samples (without UV irradiation) were kept at room temperature ( $23 \pm 1$  °C) in the laboratory and quenched at the same time as the irradiated sample. All pool water experiments were conducted within 12 hours after pool water sampling.

### 6.2.4 UV experiments

UV experiments were conducted with a low-pressure lamp emitting monochromatic light at  $\lambda = 254$  nm. All experiments were performed at  $25 \pm 0.2$  °C. The UV dose was regularly measured. Details about the UV reactor and the performed chemical actinometry with atrazine can be found elsewhere (Plewa et al., 2011).

Blank samples (without UV irradiation) were kept in stoppered volumetric flasks on the laboratory bench at room temperature ( $23 \pm 1$  °C) during the experiment. All samples (irradiated and blanks) were quenched after irradiation with an excess of ascorbic acid to prevent further *N*-nitrosamine formation. Thiosulfate was used in several previous studies to quench *N*-nitrosamine formation (Kovacic et al., 1965; Xiao et al., 2012). However, experiments showed that thiosulfate is not an appropriate quenching agent for *N*-nitrosamine formation in the presence of nitrite and DMA since a significant thiosulfate-induced NDMA formation was observed in such solutions (SI, section H).

## 6.3 Results and Discussion

### 6.3.1 NDMA formation during UV irradiation

To investigate the UV-induced NDMA formation, the model precursors monochloramine ( $\text{NH}_2\text{Cl}$ ) and chlorinated dimethylamine (CDMA) were irradiated. CDMA was chosen instead of DMA because DMA chlorination is a fast process in pool waters treated with chlorine ( $k_{\text{app}}$  at pH 7  $\sim 10^4 \text{ M}^{-1}\text{s}^{-1}$ ) (Deborde and von Gunten, 2008). Thus, it is likely that chlorinated amines such as CDMA and not free amines such as DMA will be present under realistic conditions in pool water. Rate constants for chlorination of other secondary amines also suggest that the chlorinated forms will predominate for most secondary amines (Deborde and von Gunten, 2008). Hence, most commonly found secondary amines in swimming pools such as creatinine, L-arginine or L-histidine are most likely present in their chlorinated form (Reichert, 1994).

UV irradiation of solutions containing CDMA and  $\text{NH}_2\text{Cl}$  resulted in a temporarily high, UV-dose dependent NDMA formation (Figure 6.1). NDMA concentration increased in a first phase (UV dose  $< 350 \text{ mJ cm}^{-2}$ ) and remained on a high level ( $350 \text{ mJ cm}^{-2} < \text{UV dose} < 700 \text{ mJ cm}^{-2}$ ) before it decreased. This evolution of NDMA is due to NDMA formation from products of CDMA and  $\text{NH}_2\text{Cl}$  photolysis. At the same time, NDMA is also photolysed under the applied UV conditions. Therefore, the NDMA concentration increased at low UV doses when the NDMA formation was dominant. A peak was observed when the rate of NDMA formation and NDMA degradation were equal. Thereafter, the NDMA concentration decreased because NDMA formation from the photolysis of the precursors diminished due to their depletion and only its photolytic degradation occurred (see also section 6.3.5 for modelling results).

To investigate the impact of pH on NDMA formation, irradiation experiments were conducted at a single initial concentration of both  $\text{NH}_2\text{Cl}$  and CDMA (2.5 mM) and different pH values (6.5, 7, 7.5 and 8) (Figure 6.2). NDMA concentrations in irradiated samples showed almost no pH-dependence, except for a slightly increased NDMA formation at pH 8 for UV doses below  $500 \text{ mJ cm}^{-2}$ . This suggests that neither the UV-induced NDMA formation nor the NDMA degradation is strongly influenced by pH changes in the range of 6.5–8. Previous studies reported an influence of pH on NDMA photolysis for more extreme pH values (pH 3 and 9.4) (Gérardin and Subra, 2004; Parrat et al., 2012).

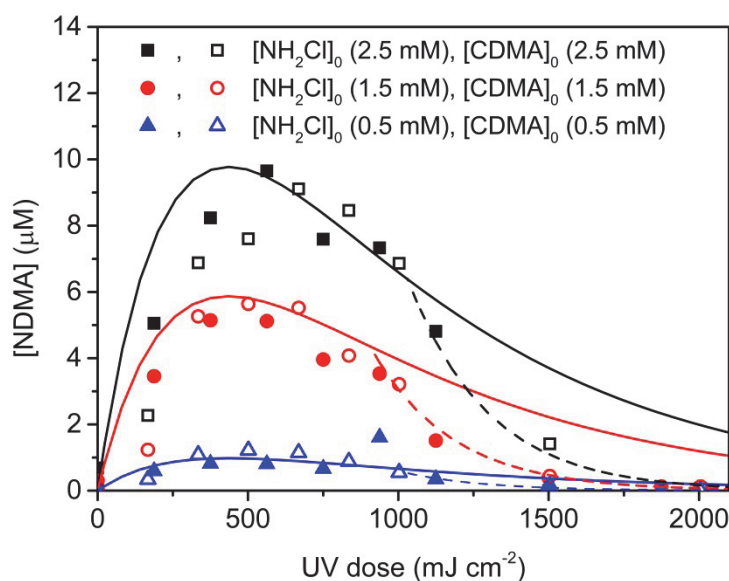


**Figure 6.1:** Evolution of NDMA as a function of the UV dose for  $\text{NH}_2\text{Cl}$ - and CDMA-containing waters (pH 7.5 (filled symbols); pH 7.2 (open symbols)). Lines and dashed lines represent model calculation (see section 6.3.5 for details).

However, pH-dependence of the NDMA formation in the blank (without UV irradiation) was much more pronounced in the pH range 6.5–8, with a maximum at pH 7.5. This observation is in agreement with previous studies (Mitch and Sedlak, 2002; Schreiber and Mitch, 2006). The blank formation without UV irradiation depends on precursor concentrations and on the reaction time, NDMA formation is slowed down at low concentrations. The UV-induced formation depends on precursor concentrations and on the UV dose. Additionally, the NDMA yield in the UV-induced NDMA formation might be slightly influenced by precursor concentrations due to potential competitive reactions. In conclusion, it is assumed that UV-induced NDMA formation gains importance at low precursor concentrations due to the slower formation without UV irradiation.

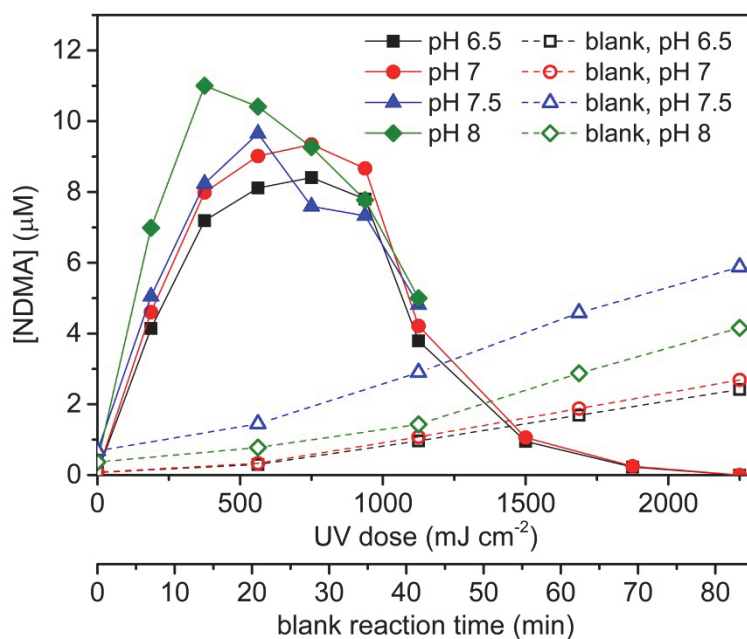


**Figure 6.2:** NDMA formation in irradiated samples containing  $[\text{CDMA}]_0 = 2.5 \text{ mM}$  and  $[\text{NH}_2\text{Cl}]_0 = 2.5 \text{ mM}$  in dependence of pH (6.5–8). Blank samples were controls of the same solutions without UV irradiation. NDMA concentration in irradiated samples for pH 7.5 and 8 could not be analysed for irradiation times higher than  $1'200 \text{ mJ cm}^{-2}$  due to a significantly interfering peak in the chromatogram.

### 6.3.2 NDMA formation as a function of precursor concentrations

The influence of precursor concentrations on NDMA formation at a UV dose of  $830 \text{ mJ cm}^{-2}$  was investigated by varying the initial concentration of one precursor (0–5 mM) and keeping the initial concentration of the second precursor constant (0.5 and 2.5 mM) (Figure 6.3). The NDMA concentration increased linearly with the initial CDMA and  $\text{NH}_2\text{Cl}$  concentration for stoichiometric ratios  $< 1$ . For monochloramine in excess, NDMA almost reached a plateau. However, increasing CDMA concentrations in excess resulted in a continuous but reduced increase of NDMA concentrations. The difference in the behaviour between  $\text{NH}_2\text{Cl}$  and CDMA might be explained by the fact that  $\text{NH}_2\text{Cl}$  photolysis is slower than CDMA photolysis (SI, section B). Therefore, CDMA availability might still be the limiting factor even if it is initially present in a slight excess. Additionally, irradiation of pure CDMA generates NDMA while this is not the case for monochloramine.



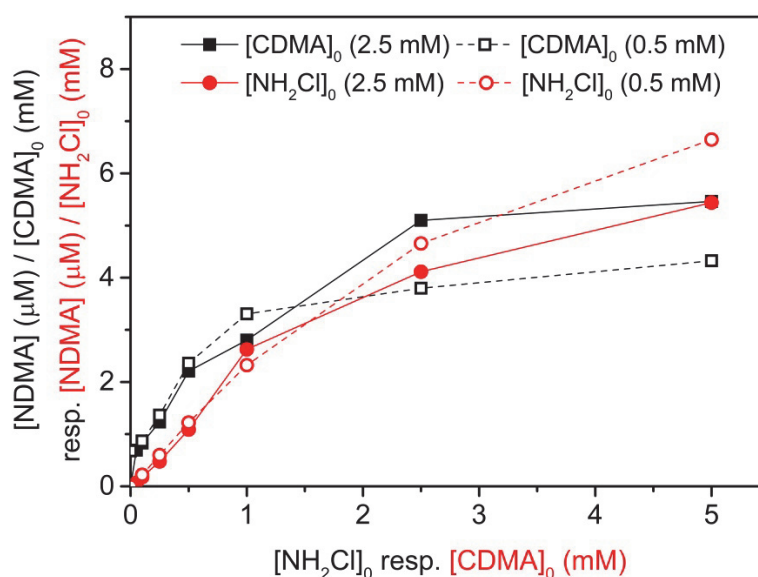


**Figure 6.3:** Dependence of NDMA concentration on initial  $\text{NH}_2\text{Cl}$  and CDMA concentrations ( $\text{pH} = 7.2$ , UV dose =  $830 \text{ mJ cm}^{-2}$ ). Squares: CDMA concentration constant (0.5 and 2.5 mM), variation of  $\text{NH}_2\text{Cl}$  concentration (0–5 mM). Circles:  $\text{NH}_2\text{Cl}$  concentration constant (0.5 and 2.5 mM), variation of CDMA concentration (0–5 mM).

### 6.3.3 UV-induced NDMA formation pathway in chloraminated water

#### *Initial step in $\text{NH}_2\text{Cl}$ and CDMA photolysis*

The breakage of the N-Cl bond is assumed to be the initial step in  $\text{NH}_2\text{Cl}$  photolysis (Li and Blatchley, 2009; De Laat et al., 2010). The similar nature of the N-Cl bond in CDMA and the similar absorption spectrum of CDMA suggests an analogous behaviour. The products of these N-Cl bond cleavages are  $\cdot\text{Cl}$  atoms and the aminyl and dimethylaminyl radicals, respectively (Schemes 6.2 and 6.3a, eqs. 6.8, 6.14). This hypothesis was supported by experiments measuring indirectly the  $\cdot\text{Cl}$  atoms formation.  $\cdot\text{Cl}$  atoms are in equilibrium with hydroxyl radicals ( $\cdot\text{OH}$ ) in aqueous solutions by reaction with  $\text{H}_2\text{O}$  (eq. 6.13) (Buxton et al., 1998).



At circumneutral pH the equilibrium shown in eq. 6.13 is strongly on the right.  $\cdot\text{OH}$  can be scavenged with dimethylsulfoxide (DMSO) (Buxton et al., 2000) and the reaction products, namely methansulfinatate, methansulfonate and sulfatate, can be used for their quantification (Lee et al., 2004). This method does not allow an exact quantification since conversion of  $\cdot\text{Cl}$  atoms to  $\cdot\text{OH}$  might not be complete (due to side reactions with DMSO or with CDMA /  $\text{NH}_2\text{Cl}$  and their degradation products) or additional  $\cdot\text{OH}$  might be formed from other degradation products. However, experimental results (SI, section D) suggest a substantial formation of  $\cdot\text{Cl}$  atoms and

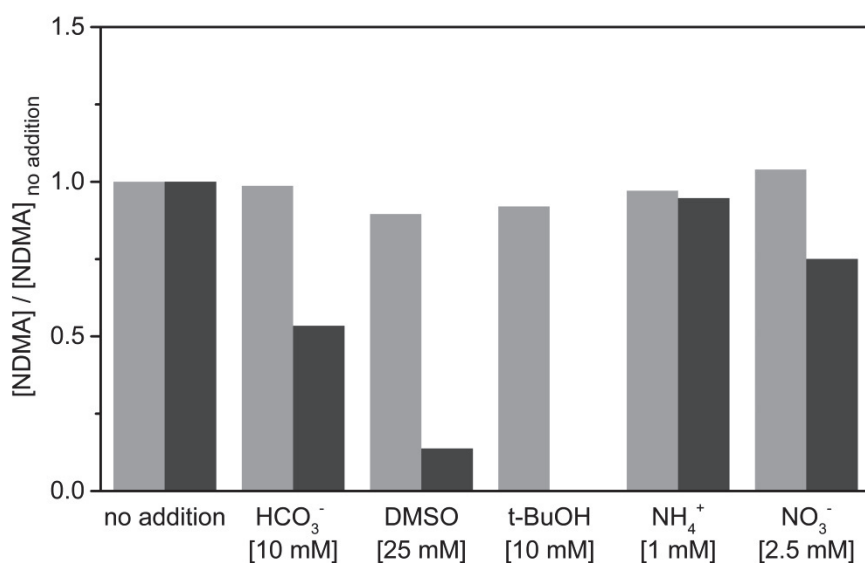


**Figure 6.4:** Effect of various solutes ( $\cdot\text{OH}$  scavengers ( $\text{HCO}_3^-$ , DMSO, and t-BuOH) and nitrogen species ( $\text{NH}_4^+$  and  $\text{NO}_3^-$ )) on NDMA formation with UV irradiation (grey bars) and without UV irradiation (black bars) ( $[\text{CDMA}]_0 = 2.5 \text{ mM}$ ,  $[\text{NH}_2\text{Cl}]_0 = 2.5 \text{ mM}$ ,  $\text{pH} = 7.2$ , UV dose  $\sim 800 \text{ mJ cm}^{-2}$  or  $\sim 30 \text{ min}$  of reaction time for the control without UV irradiation). Solute effects are always set in relation to the control without addition. NDMA concentration in the control was  $9.06 \pm 0.32 \text{ }\mu\text{M}$  for irradiated samples and  $0.36 \pm 0.16 \text{ }\mu\text{M}$  for non-irradiated samples.

hence  $\cdot\text{OH}$  by the cleavage of the N-Cl bond (50–100 %). An alternative degradation pathway of  $\text{NH}_2\text{Cl}$  and CDMA might be the reaction with  $\cdot\text{OH}$ . It is suggested that the reaction of  $\text{NH}_2\text{Cl}$  with  $\cdot\text{OH}$  forms  $\cdot\text{NHCl}$  radicals without being the main pathway (Li and Blatchley, 2009). The  $\cdot\text{NHCl}$  radical is assumed to follow a similar reaction pathway as the aminyl radical, including the formation of nitric oxide.

To investigate the role of  $\cdot\text{OH}$  in the UV-induced NDMA formation, we irradiated samples containing CDMA and  $\text{NH}_2\text{Cl}$  in the presence/absence of  $\cdot\text{OH}$  scavengers (Figure 6.4). Additionally, we tested the influence of ammonia and nitrate on NDMA formation. Ammonia and nitrate did not substantially influence UV-induced NDMA formation. Only DMSO and t-BuOH slightly decreased NDMA formation in the irradiated samples by about 10 %. This points to a minor role of  $\cdot\text{OH}$  radicals in the NDMA formation pathway. However, DMSO and t-BuOH hindered NDMA formation very efficiently in the sample without UV irradiation. Hence,  $\cdot\text{OH}$  radicals or other radical intermediates scavenged by DMSO and t-BuOH seemed to play an important role in the NDMA formation pathway without UV irradiation. Schreiber and

Mitch (2006a) observed only a slight inhibition of NDMA formation in the reaction of dichloramine with DMA by the addition of t-BuOH. However, they suggest that  $\cdot\text{OH}$  radicals play an important role in the enhanced NDMA formation at breakpoint chlorination (Schreiber and Mitch, 2007).

### ***NDMA formation pathway***

In the case of CMDA, it is likely that the dimethylaminy radical is the first intermediate in CDMA photolysis (Scheme 6.3a, eq. 6.14) and at the same time a direct NDMA precursor.  $\text{NH}_2\text{Cl}$  photolysis results in various potential NDMA precursors (Scheme 6.2, eqs. 6.8–6.11). Therefore, various formation pathways must be envisaged (Scheme 6.3).

1. The reaction of the dimethylaminy radical with the aminyl radical would result in the formation of unsymmetrical dimethylhydrazine (UDMH). UDMH, or in presence of free chlorine potentially the chlorinated form, react with  $\text{O}_2$  to NDMA (Scheme 6.3b, eq. 6.16). Irradiation of UDMH and chlorinated UDMH showed low yields of NDMA and the observed kinetics are too slow to be responsible for the observed NDMA formation in Figure 6.1 (SI, section E).

2. The reaction of the dimethylaminy radical with nitric oxide (Scheme 6.3c) is assumed to be a very fast reaction which does not lead to other products than NDMA (Kinani et al., 2012).

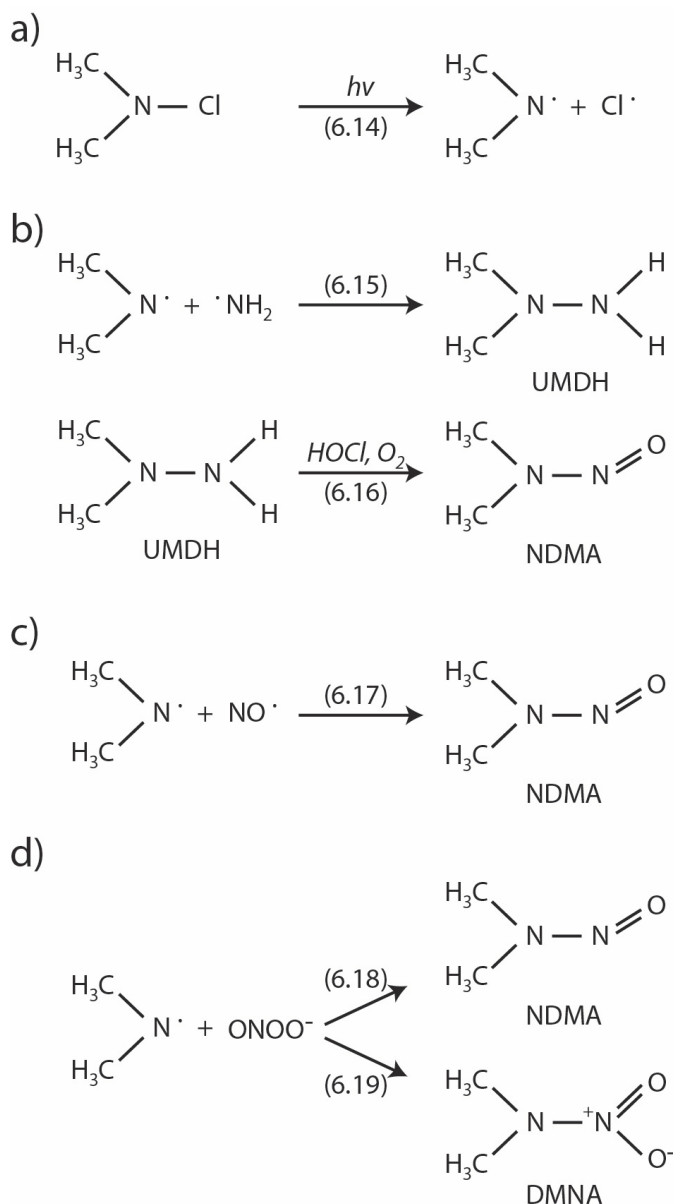
3. *N*-nitrosamine formation from peroxyxynitrite and secondary amines (Scheme 6.3d) is described in detail by Kirsch et al. (2012). They found a pH-dependence of *N*-nitrosamine formation due to peroxyxynitrite stability. However, results in Figure 6.2 show no significant pH-dependence. Furthermore, *N*-nitrosamine formation via peroxyxynitrite is known to go along with *N*-nitramine formation (Scheme 6.3d, eqs. 6.18, 6.19). Peroxyxynitrite decays to nitric oxide or  $\cdot\text{NO}_2$  radicals which form *N*-nitrosamine and *N*-nitramine, respectively (Scheme 6.2, eqs. 6.11 (reverse reaction), 6.12) (APHA, 2005). However, dimethylnitramine (DMNA) was not detected under our experimental conditions.

4. Other products of  $\text{NH}_2\text{Cl}$  photolysis are dinitrogen tetroxide ( $\text{N}_2\text{O}_4$ ) and nitrite. DMNA is assumed to be a by-product in the NDMA formation from these precursors and NDMA formation yields are thought to be low (Schreiber and Mitch, 2007; Hansen et al., 2013).

In conclusion, it is very likely that *N*-nitrosamine formation in UV irradiated water samples containing chlorinated secondary amines and  $\text{NH}_2\text{Cl}$  occurs via pathway 2, the reaction of secondary aminyl-radicals with nitric oxide (Scheme 6.3c). However, the occurrence of potential *N*-nitramine peaks in experiments with diethylamine and morpholine (see section 6.3.4) and of DMNA in irradiated pool samples (see section 6.3.6) suggests that a formation via

peroxynitrite might also be possible in real water samples (Scheme 6.3d, eqs. 6.18, 6.19). The peroxynitrite precursor  $O_2^{\cdot-}$  (Scheme 6.2, eq. 6.11) can be formed by various photo-induced processes in natural waters (Liviak et al., 2010).

Nevertheless, both *N*-nitrosamine formation pathways suggest that *N*-nitrosamine formation proceeds via the secondary aminyl radical with limited influence of the structure of the secondary amines.



**Scheme 6.3:** Potential NDMA formation pathways during photolysis of CMDA- and  $\text{NH}_2\text{Cl}$ -containing waters. (a) Formation of the dimethylaminyl radical from CMDA photolysis; reaction of the dimethylaminyl radical with (b) the aminyl radical, (c) nitric oxide, and (d) peroxynitrite.

### 6.3.4 N-Nitrosamine formation by UV irradiation of solutions containing selected chlorinated secondary amines and monochloramine

*N*-Nitrosamines have similar absorption spectra ( $200 \text{ nm} < \lambda < 360 \text{ nm}$ ) and their UV degradation is similar under artificial sunlight conditions (Dickenson et al., 2008; Wang et al., 2013). Furthermore, it can be hypothesized that *N*-nitrosamine formation by UV treatment of a chloraminated solution in presence of chlorinated secondary amines should be similar to the NDMA formation from irradiation of CDMA- and chloramine-containing solutions (see section 6.3.3). Chlorinated diethylamine (CDEA) and chlorinated morpholine (CMor) were chosen as model compounds to verify this hypothesis. CDMA, CDEA and CMor were irradiated in the presence of  $\text{NH}_2\text{Cl}$  at pH 7.2. Figure 6.5 shows that the evolution of *N*-nitrosodiethylamine (NDEA) and *N*-nitrosomorpholine (NMor) concentrations, as a function of the UV dose, followed a similar pattern as NDMA. The slower NMor decrease at high UV doses might have been due to an interfering peak in the HPLC analysis. While *N*-nitrosamine formation in the irradiated sample did not differ much among the three model compounds, NDMA formation clearly outcompeted NMor and NDEA formation in the blank sample (Figure 6.5, dashed lines). Simultaneously to *N*-nitrosamine formation in the irradiated CDEA and CMor sample, a second peak of an unknown compound appeared in the HPLC chromatogram (SI, section G). The simultaneous increase and decrease with the *N*-nitroso-peaks might be a hint that these peaks refer to the corresponding *N*-nitramines. *N*-Nitro-compounds are generally slightly less photodegradable and their formation would occur in parallel to the *N*-nitrosamine formation in the formation pathway via peroxyxynitrite (Konermann et al., 2008).

Hence, it can be hypothesized that UV irradiation of chloraminated solutions with any chlorinated secondary amine enhances the formation of the corresponding *N*-nitrosamine. For the selected amines, the formation rates and yields were quite similar. Thus, UV treatment is assumed to increase *N*-nitrosamine formation for any chlorinated secondary amine with the net contribution being higher for those *N*-nitrosamines with a slow formation without UV irradiation.

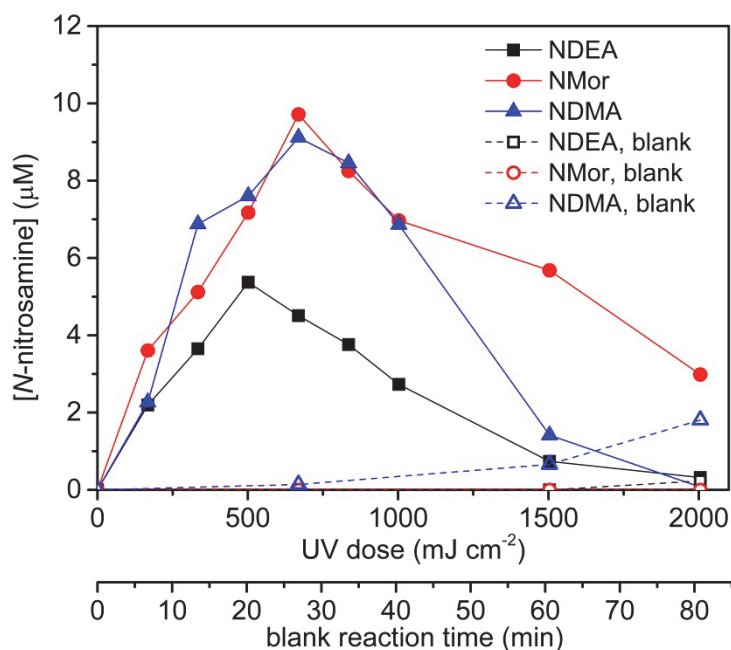


**Figure 6.5:** *N*-Nitrosodiethylamine (NDEA), *N*-nitrosomorpholine (NMor), and *N*-nitrosodimethylamine (NDMA) formation in UV irradiated samples containing  $[\text{NH}_2\text{Cl}]_0 = 2.5$  mM and  $[\text{Cl-diethylamine}]_0 = 2.5$  mM,  $[\text{Cl-morpholine}]_0 = 2.5$  mM, and  $[\text{Cl-dimethylamine}]_0 = 2.5$  mM. Blank samples: control of the same solution without UV irradiation. All samples were at pH 7.2.

### 6.3.5 Modelling UV dose-dependent NDMA formation

Taking into account the findings from the previous sections, a simplified model was established to assess the NDMA formation yields in Figure 6.1. A complete kinetic model should include the NDMA-, CDMA- and  $\text{NH}_2\text{Cl}$ -photolysis with intermediates and the NDMA formation from these intermediates. Furthermore, the model should consider UV filter effects of  $\text{NH}_2\text{Cl}$  and CDMA in solution (see below and SI, section A). Since this leads to a complex model with many unknown reactions, a simplified model was used to roughly estimate the NDMA yields from CDMA and to test the plausibility of the suggested mechanism.

#### *Model parameters*

(i) Quantum yields. NDMA, CDMA and  $\text{NH}_2\text{Cl}$  quantum yields were measured and used in the model (SI, section B and C). NDMA and CDMA quantum yields in pure solutions were  $0.43 \pm 0.03$  and  $0.68 \pm 0.04$  mol einstein<sup>-1</sup>, respectively. In the case of NDMA, lower quantum yields of 0.3–0.4 mol einstein<sup>-1</sup> were reported previously (Sharpless and Linden, 2003; Hansen et al., 2012; Wang et al., 2013). These quantum yields were partly measured under different conditions (solar irradiation, acidic or alkaline pH) (SI, section C). Pseudo-first-order rate constants for NDMA photolysis showed no significant dependence on the initial concentration

(5 and 25  $\mu\text{M}$ ). The measured  $\text{NH}_2\text{Cl}$  quantum yields ( $0.38 \pm 0.1 \text{ mol einstein}^{-1}$ ) were in agreement with previously reported values ( $0.26\text{--}0.62 \text{ mol einstein}^{-1}$ ) (Cooper et al., 2007; Watts and Linden, 2007; Dickenson et al., 2008; Li and Blatchley, 2009; De Laat et al., 2010). Li and Blatchley (2009) explained the variation in measured quantum yield by the varying excess of ammonia in the  $\text{NH}_2\text{Cl}$  production. De Laat et al. (2010) did not see any influence of the initial ammonia excess but mentioned an impact of the dissolved oxygen concentration on the  $\text{NH}_2\text{Cl}$  quantum yield.

(ii) Filter effects. The presence of  $\text{NH}_2\text{Cl}$  and CDMA at a mM concentration inhibited NDMA photolysis (SI, section C). Calculations of the Morowitz factor gave evidence that this was mainly due to the filter effect of  $\text{NH}_2\text{Cl}$  and CDMA which have relevant molar absorption coefficients at  $\lambda = 254 \text{ nm}$  (SI, section A and C).

This filter effect might also explain why the maximum of the NDMA concentration in an irradiated CDMA and  $\text{NH}_2\text{Cl}$  solution was shifted towards higher UV doses for higher initial  $\text{NH}_2\text{Cl}$  and CDMA concentrations (maximum at  $\sim 600 \text{ mJ cm}^{-2}$  for  $c_0 = 2.5 \text{ mM}$  and at  $\sim 450 \text{ mJ cm}^{-2}$  for  $c_0 = 1.5 \text{ mM}$ ) (Figure 6.1). The shift was in agreement with the initial Morowitz factors of 0.23 and 0.35 for  $c_0 = 2.5 \text{ mM}$  and  $c_0 = 1.5 \text{ mM}$  of each  $\text{NH}_2\text{Cl}$  and CDMA, respectively (SI, Table A1). However,  $\text{NH}_2\text{Cl}$  and CDMA filter effects decreased with increasing UV dose since the  $\text{NH}_2\text{Cl}$  and CDMA concentrations decreased.

The influence of the changing Morowitz factor was not considered in our simplified model and the pseudo first-order rate constants of CDMA and NDMA in pure solutions were used. Thereby, NDMA photolysis is overestimated in the first phase when  $\text{NH}_2\text{Cl}$  and CDMA concentrations are still high. Conclusively, the NDMA formation yields were slightly overestimated.

(iii) Role of  $\text{NH}_2\text{Cl}$ . Experiments with varying initial CDMA and  $\text{NH}_2\text{Cl}$  concentrations (Figure 6.3) revealed that NDMA formation depended slightly on  $\text{NH}_2\text{Cl}$  concentrations if the ratio of the initial concentrations of  $\text{NH}_2\text{Cl}$  and CDMA was  $\leq 1$  (Figure 6.3). The simplified model neglected the effect of  $\text{NH}_2\text{Cl}$  concentration since the initial  $\text{NH}_2\text{Cl}$  to CDMA ratio was 1:1 in the modelled experiments (Figure 6.1).

### **Model results**

A description of the simplified conceptual model is presented in SI, section F. Model results given in Figure 6.1 suggested that the simplified model provides a reasonable fit for the measured data. The lines in Figure 6.1 represent model results while the dashed lines show modelled NDMA concentrations if no NDMA formation is considered at high UV doses. The

slightly delayed increase of the measured data as well as the delayed peak for high CDMA and  $\text{NH}_2\text{Cl}$  concentrations might be due to the disregarded filter effect. The steep decrease of NDMA concentration at high UV doses followed the NDMA depletion in pure NDMA solution (dashed lines). This indicates that at this stage of the process NDMA formation ceased. Thus, either precursor depletion was faster than predicted from pure solutions or NDMA formation was inhibited by another process.

Overall, the model results revealed that NDMA yields were about 2 % at  $[\text{CDMA}]_0 = 1.5 \text{ mM}$  and 2.5 mM and 1 % at  $[\text{CDMA}]_0 = 0.5 \text{ mM}$  (best fit for fraction of dimethylaminy radicals leading to NDMA (SI, section F)). The NDMA peak concentration was about 0.4 % of the initial CDMA concentration resulting from a simultaneous formation and photolysis of NDMA.  $\text{NH}_2\text{Cl}$  and CDMA concentrations at the NDMA peak concentration were calculated to be about 70 % and 40 % of the initial concentrations, respectively. The model results confirm our previous assumptions that NDMA formation is a fast process involving photolytic degradation products from  $\text{NH}_2\text{Cl}$  and CDMA.

### **6.3.6 NDMA formation versus degradation during UV treatment of chloraminated water**

The efficiency of nitrosamine mitigation by UV treatment in chloraminated water depends basically on two factors: the applied UV dose and the ratio of the initial NDMA and precursor concentrations. This is illustrated by the results in Figure 6.6 which show the measured depletion of NDMA (25  $\mu\text{M}$ ) in pure water, in presence of  $\text{NH}_2\text{Cl}$  (2.5 mM) and in presence of each  $\text{NH}_2\text{Cl}$  (2.5 mM) and CDMA (2.5 mM) at pH 7.2. The presence of  $\text{NH}_2\text{Cl}$  slowed down the NDMA photolysis due to the UV-filter effect of  $\text{NH}_2\text{Cl}$  and not because of an additional NDMA formation (SI, section C). The effect of additional NDMA formation was observed in the sample containing NDMA, CDMA and  $\text{NH}_2\text{Cl}$ . In this case, the NDMA concentration even increased slightly at the beginning of the irradiation. Thus, the effectiveness of UV treatment for NDMA mitigation is overestimated if only the NDMA degradation in pure solutions is considered. The net NDMA formation from  $\text{NH}_2\text{Cl}$  (2.5 mM) and CDMA (2.5 mM) can be approximated by the subtraction of the NDMA concentration in the sample containing NDMA (25  $\mu\text{M}$ ) and  $\text{NH}_2\text{Cl}$  (2.5 mM) from the sample containing NDMA (25  $\mu\text{M}$ ),  $\text{NH}_2\text{Cl}$  (2.5 mM) and CDMA (2.5 mM) (Figure 6.6, dashed line (line I – line II)). This approximated net NDMA formation is very similar to NDMA in an irradiated sample with initial  $\text{NH}_2\text{Cl}$  and CDMA concentrations of 2.5 mM each (Figure 6.1). The difference might be explained by the additional UV filter effect by CDMA on the NDMA degradation (which is not considered in



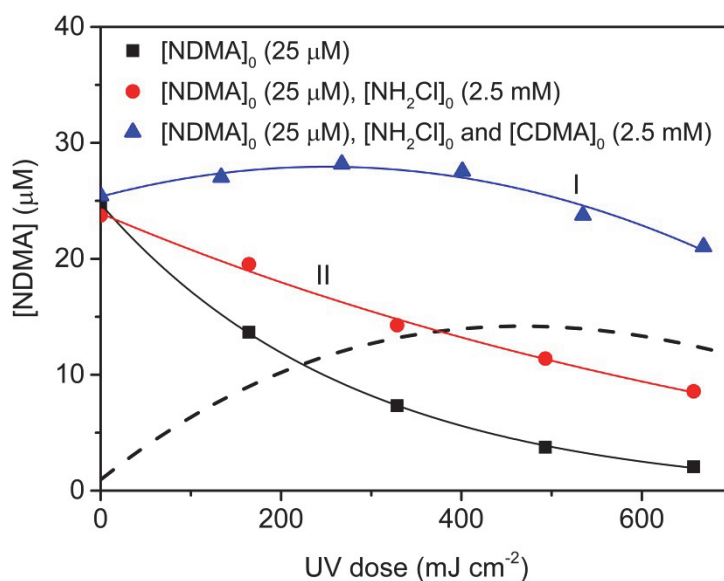


**Figure 6.6:** NDMA evolution in UV irradiated samples containing NDMA, NDMA /  $\text{NH}_2\text{Cl}$  and NDMA /  $\text{NH}_2\text{Cl}$  / CDMA at pH 7.2. Trend lines to guide the eye. The dashed line represents the calculated net NDMA concentration by subtracting trend lines I – II.

line II) and a possible NDMA reformation from NDMA photolysis products in the presence of products from  $\text{NH}_2\text{Cl}$  and CDMA photolysis.

### 6.3.7 NDMA formation in irradiated pool water samples

Irradiation experiments with pool water were performed at low NDMA, CDMA and  $\text{NH}_2\text{Cl}$  concentrations and with typical UV doses for pool water treatment ( $360 \text{ mJ cm}^{-2}$ ) to test our mechanistic hypotheses under realistic conditions.

First, it was investigated whether in pool water (i) the NDMA photolysis and (ii) the UV-induced NDMA formation from  $\text{NH}_2\text{Cl}$  and CDMA were similar to the formation observed in Figure 6.1 (Figure 6.7a):

(i) Untreated pool water (pool B), which contained  $\text{NH}_2\text{Cl}$  ( $\sim 1 \mu\text{M}$ ), was spiked with NDMA (20 nM) (Figure 6.7a, I). NDMA concentration in the blank sample (without UV, 2 hours reaction time) corresponded to the spiked NDMA concentration. UV treatment reduced the NDMA concentration to about 50 % which was in agreement with the expected NDMA degradation of about 75 % from previous experiments in purified water without filter effect and higher NDMA concentrations.

(ii) To test NDMA formation yield at low concentration, untreated pool water (pool B) was spiked with CDMA [ $10 \mu\text{M}$ ] and  $\text{NH}_2\text{Cl}$  [ $10 \mu\text{M}$ ] (Figure 6.7a, II). Only a small NDMA

formation was observed in the blank sample (without UV). UV treatment of the sample resulted in a NDMA concentration of about 10 nM. This corresponds to a net NDMA yield of 0.2 % (based on the estimated photodegraded CDMA concentration (~50 % of the initial concentration)) which corresponded to about half of the yield at 100 times higher concentrations and the same UV dose.

Secondly, the relevance of the UV-induced NDMA formation in pool water was investigated (Figure 6.7b). Consequently, (iii) untreated pool water and (iv) pool water spiked with  $\text{NH}_2\text{Cl}$  was irradiated (UV dose:  $360 \text{ mJ cm}^{-2}$ ):

(iii) Irradiation of untreated pool water A (Figure 6.7b, III) was expected to result in a 50 % degradation of NDMA according to the previous experiments (see above, (i)). However, results in Figure 6.7b show that UV treatment slightly increased the NDMA concentration. This increase was not observed in the blank sample without irradiation. Hence, even if NDMA concentrations in the pool samples were close to the detection limit, it can be concluded that there must have been a significant UV-induced NDMA formation which outcompeted its degradation.

(iv) To investigate the effect of UV-induced NDMA formation in pool water with higher chloramine concentrations, pool water samples from pool A (IV) and B (V) were spiked with  $10 \mu\text{M}$  of  $\text{NH}_2\text{Cl}$  (~3 times higher than pool water regulation for combined chloramines in Switzerland) (Figure 6.7b). Spiked pool water samples showed an increased NDMA concentration in the irradiated sample as well as in the control without UV irradiation (2 hours of reaction time). However, the NDMA formation was significantly enhanced by UV irradiation and more pronounced than in the untreated pool water sample. Thus, the net NDMA formation by UV irradiation can easily exceed NDMA formation in samples without UV irradiation for a reaction time of several hours.

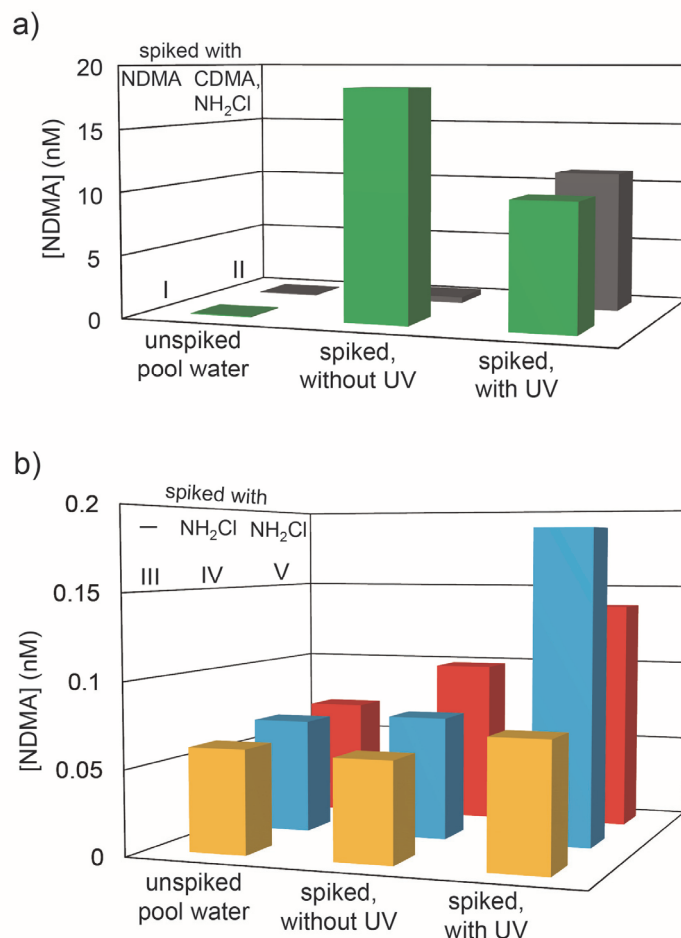


**Figure 6.7:** Irradiation experiments with pool water A and B (Table 6.1) (pH: pool A = 7.7, pool B = 7.4). Irradiated (UV dose:  $360 \text{ mJ cm}^{-2}$ ) and blank samples (without UV irradiation) were quenched directly after the UV treatment ( $\sim 2$  hours). a) I: pool B,  $[\text{NDMA}]_0 = 20 \text{ nM}$  added; II: pool B,  $[\text{NH}_2\text{Cl}]_0 = 10 \text{ }\mu\text{M}$  and  $[\text{CDMA}]_0 = 10 \text{ }\mu\text{M}$  added. b) III: pool A, no additions; IV: pool A,  $[\text{NH}_2\text{Cl}]_0 = 10 \text{ }\mu\text{M}$  added; V: pool B,  $[\text{NH}_2\text{Cl}]_0 = 10 \text{ }\mu\text{M}$  added. The unspiked pool water samples were quenched directly before each experiment.

## 6.4 Conclusions

Chlorination in combination with UV treatment is a commonly used technique for pool water treatment. The chlorination of pool water, with consequent chloramine formation, induces the formation of various hazardous disinfection by-products. For example, the reaction of secondary amines with chloramines present in pool water leads to a slow formation of *N*-nitrosamines. This formation becomes relevant due to the long hydraulic residence time of pool water (20–40 d). Hydraulic residence time can be much longer in other systems, where they do not have any regulations on fresh water addition.

UV treatment is assumed to be an appropriate process for *N*-nitrosamine mitigation because of the high photolability of *N*-nitrosamines. Furthermore, potential precursors for *N*-nitrosamine formation (e.g.  $\text{NH}_2\text{Cl}$  and chlorinated secondary amines in chlorinated pool waters) are degraded by photolysis. However, the products of  $\text{NH}_2\text{Cl}$  and chlorinated dimethylamine photolysis quickly form NDMA with yields of 1–2 %. This formation is assumed to occur by the reaction of nitric oxide or peroxyxynitrite with the secondary aminyl radical. The UV-induced *N*-nitrosamine formation was also observed to a very similar extent for chlorinated morpholine and chlorinated diethylamine. Thus, this *N*-nitrosamine formation can play an important role in all chloraminated waters containing secondary amines (e.g. pool water and water reuse systems).

The effectiveness of UV treatment for *N*-nitrosamine degradation in pool water depends on the applied UV dose and the ratio of NDMA and its precursors. UV treatment of waters containing chloramines and chlorinated secondary amines can result in a net *N*-nitrosamine formation despite of the photolability of *N*-nitrosamines. However, it is difficult to assess the overall effect of the UV treatment since swimming pools are a complex system with many parameters influencing the UV-independent and the UV-induced NDMA formation and degradation (precursor concentrations, hydraulic residence time in pool and residence time in the system, UV dose per treatment cycle, temporal pattern of bather load, pH, temperature and spatial differences in conditions). The results of this study show that only UV doses above 2'000  $\text{mJ cm}^{-2}$  (about 30 times the typical disinfection dose) can provide a complete *N*-nitrosamine degradation in one treatment cycle, though such high UV doses can increase the formation of various other disinfection by-products.

Conclusively, UV treatment can be an appropriate means for *N*-nitrosamine degradation if the water contains relatively high *N*-nitrosamine concentrations compared to chloramines and chlorinated secondary amines. This is more likely the case in waters where precursors have

long contact time. However, there is a substantial risk to induce a net *N*-nitrosamine formation by UV treatment of pool water.

## **Acknowledgements**

This work was supported by the Swiss Federal Office of Public Health (FOPH). Minju Lee gratefully acknowledges financial support from the Federal Commission for Scholarships for Foreign Students (FCS), Switzerland. The authors thank Hans-Ulrich Laubscher and Lisa Salhi for technical support, and Rene Schittli (Kantonales Labor Zürich) for collaboration in pool water sampling.

## References

- American Public Health Association (APHA) (2005). "Standard methods for the examination of water & wastewater."
- Bessonneau, V., M. Derbez, M. Clément and O. Thomas (2011). "Determinants of chlorination by-products in indoor swimming pools." *International Journal of Hygiene and Environmental Health* 215(1): 76-85.
- Bogatu, C., D. Leszczynska, L. Beqa, G. Mosoarca, L. Coheci, E. Derwich, Z. Benziane, R. Taouil, V. Srilalitha and A. R. G. Prasad "1. Trichloramine Formation and Decay during Breakpoint Process."
- Buxton, G. V., M. Bydder and G. A. Salmon (1998). "Reactivity of chlorine atoms in aqueous solution - Part 1 The equilibrium Cl-center dot+Cl-reversible arrow Cl-2(center dot-)." *Journal of the Chemical Society-Faraday Transactions* 94(5): 653-657.
- Buxton, G. V., M. Bydder, G. A. Salmon and J. E. Williams (2000). "The reactivity of chlorine atoms in aqueous solution. Part III. The reactions of Cl-center dot with solutes." *Physical Chemistry Chemical Physics* 2(2): 237-245.
- Buxton, G. V. and M. S. Subhani (1972). "Radiation chemistry and photochemistry of oxychlorine ions. Part 2.-Photodecomposition of aqueous solutions of hypochlorite ions." *Journal of the Chemical Society, Faraday Transactions 1: Physical Chemistry in Condensed Phases* 68(0): 958-969.
- Canonica, S., U. Jans, K. Stemmler and J. Hoigne (1995). "Transformation kinetics of phenols in water - photosensitization by dissolved natural organic material and aromatic ketones." *Environmental Science & Technology* 29(7): 1822-1831.
- Canonica, S., L. Meunier and U. Von Gunten (2008). "Phototransformation of selected pharmaceuticals during UV treatment of drinking water." *Water Research* 42(1-2): 121-128.
- Cassan, D., B. Mercier, F. Castex and A. Rambaud (2006). "Effects of medium-pressure UV lamps radiation on water quality in a chlorinated indoor swimming pool." *Chemosphere* 62(9): 1507-1513.
- Choi, J. H. and R. L. Valentine (2003). "N-nitrosodimethylamine formation by free-chlorine-enhanced nitrosation of dimethylamine." *Environmental Science & Technology* 37(21): 4871-4876.
- Chon, K., Y. Lee, J. Traber and U. von Gunten (2013). "Quantification and characterization of dissolved organic nitrogen in wastewater effluents by electro dialysis treatment followed by size-exclusion chromatography with nitrogen detection." *Water Research* 47(14): 5381-5391.
- Cooper, W. J., A. C. Jones, R. F. Whitehead and R. G. Zika (2007). "Sunlight-Induced Photochemical Decay of Oxidants in Natural Waters: Implications in Ballast Water Treatment." *Environmental Science & Technology* 41(10): 3728-3733.
- Davey, N. G., E. T. Krogh and C. G. Gill (2011). "Membrane-introduction mass spectrometry (MIMS)." *TrAC Trends in Analytical Chemistry* 30(9): 1477-1485.
- De Laat, J., N. Boudiaf and F. Dossier-Berne (2010). "Effect of dissolved oxygen on the photodecomposition of monochloramine and dichloramine in aqueous solution by UV irradiation at 253.7 nm." *Water Research* 44(10): 3261-3269.
- Deborde, M. and U. von Gunten (2008). "Reactions of chlorine with inorganic and organic compounds during water treatment--Kinetics and mechanisms: A critical review." *Water Research* 42(1-2): 13-51.

Dickenson, E. R. V., R. S. Summers, J.-P. Croué and H. Gallard (2008). "Haloacetic acid and Trihalomethane Formation from the Chlorination and Bromination of Aliphatic  $\beta$ -Dicarbonyl Acid Model Compounds." *Environmental Science & Technology* 42(9): 3226-3233.

Deutsches Institut für Normung (DIN) (2012). "Treatment of water of swimming pools and baths — Part 1: General requirements (German)."

Garcia, J., T.-D. Nguyen, T.-H. Tran-Thi, T.-H. Nguyen, A.-M. Laurent and C. Beaubestre (2012). "P2. 3.7 Innovative Colorimetric Sensors for the Detection of Nitrogen Trichloride at ppb Level." *Tagungsband*: 1467-1469.

Gérardin, F. and I. Subra (2004). "Development of a sampling and analysis method for trichloramine in water (French)." *Hygiène et sécurité du travail - Cahiers de notes documentaires* 194: 39-49.

Hansen, K. M., H.-J. Albrechtsen and H. R. Andersen (2013). "Optimal pH in chlorinated swimming pools—balancing formation of by-products." *Journal of water and health* 11(3): 465-472.

Hansen, K. M. S., S. Willach, M. G. Antoniou, H. Mosbaek, H. J. Albrechtsen and H. R. Andersen (2012). "Effect of pH on the formation of disinfection byproducts in swimming pool water - Is less THM better?" *Water Research* 46(19): 6399-6409.

Huber, S., A. Balz and M. Abert (2011). "New method for urea analysis in surface and tap waters with LC-OCD-OND (liquid chromatography-organic carbon detection-organic nitrogen detection)." *Journal of Water Supply: Research and Technology—AQUA* 60(3): 159-166.

National Institute for Research and Security (INRS) (2007). "Trichloramine and other chlorinated products (French)."

Jafvert, C. T. and R. L. Valentine (1992). "Reaction Scheme for the chlorination of ammoniacal water." *Environmental Science & Technology* 26(3): 577-586.

Jurado-Sanchez, B., E. Ballesteros and M. Gallego (2010). "Screening of N-nitrosamines in tap and swimming pool waters using fast gas chromatography." *Journal of Separation Science* 33(4-5): 610-616.

Ketola, R. A., T. Kotiaho, M. E. Cisper and T. M. Allen (2002). "Environmental applications of membrane introduction mass spectrometry." *Journal of mass spectrometry* 37(5): 457-476.

Kinani, S., B. Richard, Y. Souissi and S. Bouchonnet (2012). "Analysis of inorganic chloramines in water." *TrAC Trends in Analytical Chemistry* 33(0): 55-67.

Konermann, L., J. Messinger and W. Hillier (2008). *Mass spectrometry-based methods for studying kinetics and dynamics in biological systems. Biophysical Techniques in Photosynthesis*, Springer: 167-190.

Kovacic, P., C. T. Goralski, J. J. Hiller Jr, J. A. Levisky and R. M. Lange (1965). "Amination of Toluene with Trichloramine-Lewis Acid Catalyst<sup>1</sup>." *Journal of the American Chemical Society* 87(6): 1262-1266.

Krauss, M., P. Longrée, F. Dorusch, C. Ort and J. Hollender (2009). "Occurrence and removal of N-nitrosamines in wastewater treatment plants." *Water Research* 43(17): 4381-4391.

Kristensen, G. H., M. M. Klausen, H. R. Andersen, L. Erdinger, F. Lauritsen, E. Arvin and H. J. Albrechtsen (2009). "Full scale test of UV-based water treatment technologies at Gladsaxe Sport Centre—with and without advanced oxidation mechanisms." *Swimming Pool and Spa International Conference*.



- Lee, C. and J. Yoon (2007). "UV-A induced photochemical formation of N-nitrosodimethylamine (NDMA) in the presence of nitrite and dimethylamine." *Journal of Photochemistry and Photobiology a-Chemistry* 189(1): 128-134.
- Lee, Y., C. Lee and J. Yoon (2004). "Kinetics and mechanisms of DMSO (dimethylsulfoxide) degradation by UV/H<sub>2</sub>O<sub>2</sub> process." *Water Research* 38(10): 2579-2588.
- Li, J. and E. R. Blatchley (2009). "UV Photodegradation of Inorganic Chloramines." *Environmental Science & Technology* 43(1): 60-65.
- Liviac, D., E. D. Wagner, W. A. Mitch, M. J. Altonji and M. J. Plewa (2010). "Genotoxicity of Water Concentrates from Recreational Pools after Various Disinfection Methods." *Environmental Science & Technology* 44(9): 3527-3532.
- Mitch, W. A. and D. L. Sedlak (2002). "Formation of N-nitrosodimethylamine (NDMA) from dimethylamine during chlorination." *Environmental Science & Technology* 36(4): 588-595.
- Nawrocki, J. and P. Andrzejewski (2011). "Nitrosamines and water." *Journal of Hazardous Materials* 189(1-2): 1-18.
- Ohta, T., J. Suzuki, Y. Iwano and S. Suzuki (1982). "Photochemical nitrosation of dimethylamine in aqueous-solution containing nitrite." *Chemosphere* 11(8): 797-801.
- Parrat, J., G. Donze, C. Iseli, D. Perret, C. Tomicic and O. Schenk (2012). "Assessment of Occupational and Public Exposure to Trichloramine in Swiss Indoor Swimming Pools: A Proposal for an Occupational Exposure Limit." *Annals of Occupational Hygiene* 56(3): 264-277.
- Plewa, M. J., E. D. Wagner and W. A. Mitch (2011). "Comparative Mammalian Cell Cytotoxicity of Water Concentrates from Disinfected Recreational Pools." *Environmental Science & Technology* 45(9): 4159-4165.
- Plewa, M. J., E. D. Wagner, M. G. Muellner, K.-M. Hsu and S. D. Richardson (2008). "Comparative mammalian cell toxicity of N-DBPs and C-DBPs." *Urbana* 51: 61801.
- Reichert, P. (1994). "AQUASIM - a tool for simulation and data analysis of aquatic systems." *Water Science & Technology* 30(2).
- Schreiber, I. M. and W. A. Mitch (2005). "Influence of the order of reagent addition on NDMA formation during chloramination." *Environmental Science & Technology* 39(10): 3811-3818.
- Schreiber, I. M. and W. A. Mitch (2006). "Nitrosamine Formation Pathway Revisited: The Importance of Chloramine Speciation and Dissolved Oxygen." *Environmental Science & Technology* 40(19): 6007-6014.
- Schreiber, I. M. and W. A. Mitch (2007). "Enhanced nitrogenous disinfection byproduct formation near the breakpoint: Implications for nitrification control." *Environmental Science & Technology* 41(20): 7039-7046.
- Schurter, L. M., P. P. Bachelor and D. W. Margerum (1995). "Nonmetal redox kinetics - monochloramine, dichloramine, and trichloramine reactions with cyanide ion." *Environmental Science & Technology* 29(4): 1127-1134.
- Shah, A. D., A. D. Dotson, K. G. Linden and W. A. Mitch (2011). "Impact of UV Disinfection Combined with Chlorination/Chloramination on the Formation of Halonitromethanes and Haloacetonitriles in Drinking Water." *Environmental Science & Technology* 45(8): 3657-3664.

Shang, C. and E. R. Blatchley (1999). "Differentiation and quantification of free chlorine and inorganic chloramines in aqueous solution by MIMS." *Environmental Science & Technology* 33(13): 2218-2223.

Sharpless, C. M. and K. G. Linden (2003). "Experimental and model comparisons of low- and medium-pressure Hg lamps for the direct and H<sub>2</sub>O<sub>2</sub> assisted UV photodegradation of N-nitrosodimethylamine in simulated drinking water." *Environmental Science & Technology* 37(9): 1933-1940.

SIA (2011). "Wasser und Wasseraufbereitungsanlagen in Gemeinschaftsbädern." Schweizerischer Ingenieur- und Architektenverein.

Soulard, M., F. Bloc and A. Hatterer (1981). "Diagrams of existence of chloramines and bromamines in aqueous solution." *Journal of the Chemical Society, Dalton Transactions*(12): 2300-2310.

Team R Development Core (2013). "R: A language and environment for statistical computing." R Foundation for Statistical Computing. Vienna, Austria, 2013. ISBN 3-900051-07-0. <http://www.R-project.org>.

Walse, S. S. and W. A. Mitch (2008). "Nitrosamine carcinogens also swim in chlorinated pools." *Environmental Science & Technology* 42(4): 1032-1037.

Wang, W., Y. C. Qian, J. M. Boyd, M. H. Wu, S. E. Hrudey and X. F. Li (2013). "Halobenzoquinones in Swimming Pool Waters and Their Formation from Personal Care Products." *Environmental Science & Technology* 47(7): 3275-3282.

Watts, M. J. and K. G. Linden (2007). "Chlorine photolysis and subsequent OH radical production during UV treatment of chlorinated water." *Water Research* 41(13): 2871-2878.

Weng, S. C., J. Li and E. R. Blatchley (2012). "Effects of UV254 irradiation on residual chlorine and DBPs in chlorination of model organic-N precursors in swimming pools." *Water Research* 46(8): 2674-2682.

Weng, S. C., J. Li, K. V. Wood, H. I. Kenttämä, P. E. Williams, L. M. Amundson and E. R. Blatchley (2013). "UV-induced effects on chlorination of creatinine." *Water Research* 47(14): 4948-4956.

WHO (2008). N-Nitrosodimethylamine in Drinking-water. Background Document for Development for of WHO Guidelines for Drinking-water Quality. World Health Organisation.

Xiao, F., X. R. Zhang, H. Y. Zhai, I. M. C. Lo, G. L. Tipoe, M. T. Yang, Y. Pan and G. H. Chen (2012). "New Halogenated Disinfection Byproducts in Swimming Pool Water and Their Permeability across Skin." *Environmental Science & Technology* 46(13): 7112-7119.

Xu, B. B., Z. L. Chen, F. Qi, J. Ma and F. C. Wu (2009). "Inhibiting the regeneration of N-nitrosodimethylamine in drinking water by UV photolysis combined with ozonation." *Journal of Hazardous Materials* 168(1): 108-114.

Yiin, B. S. and D. W. Margerum (1990). "Nonmetal redox kinetics: reactions of sulfite with dichloramines and trichloramine." *Inorganic Chemistry* 29(10): 1942-1948.

# **Supporting Information for Chapter 6**

## **Enhanced *N*-nitrosamine formation in pool water by UV irradiation of chlorinated secondary amines in the presence of monochloramine**

Fabian Soltermann, Minju Lee,

Silvio Canonica and Urs von Gunten (2013)

*Water Research*, 47(1), 79-90

## A NH<sub>2</sub>Cl and CDMA absorption spectra and calculation of Morowitz factor

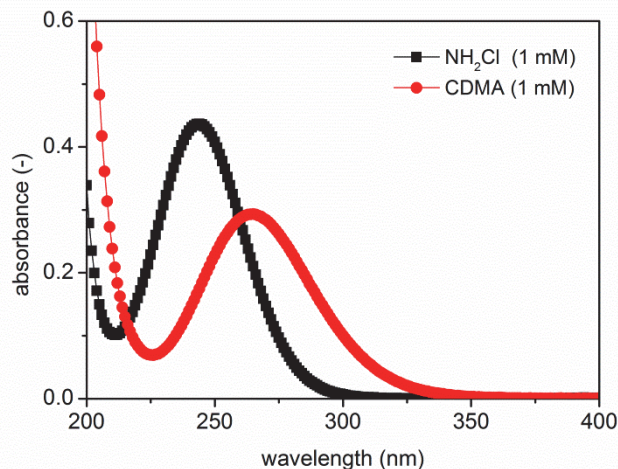


**Figure A.1.** Absorption spectra of NH<sub>2</sub>Cl (1 mM) and CDMA (1 mM), optical path length = 1 cm. Local maximum at 245 nm and 265 nm for NH<sub>2</sub>Cl and CDMA, respectively. Molar absorption coefficients ( $\epsilon$ ) at  $\lambda = 254$  nm were  $372 \text{ M}^{-1}\text{cm}^{-1}$  and  $293 \text{ M}^{-1}\text{cm}^{-1}$  for NH<sub>2</sub>Cl and CDMA, respectively.

### Text A.1.

The photolysis of a compound can be inhibited by the presence of another light absorbing species. In such a case, a light filter effect of the additional species can be considered in the general equation for photolysis (eq. A.1) by including the Morowitz factor ( $S$ ) calculated with equation A.2.

$$k_{p,i,\lambda}^0 = \frac{k_{p,obs,i,\lambda}}{S_\lambda} = \frac{2.3 \times \epsilon_{i,\lambda} \times \Phi_{i,\lambda} \times E'}{S_\lambda} \quad (\text{A.1})$$

Equation A.1 includes the following parameters:

$k_{p,i,\lambda}^0$  = photolytic rate constant for substance  $i$  at wavelength  $\lambda$  in a solution of zero optical density

( $\text{s}^{-1}$ ).

$k_{p,obs,i,\lambda}$  = observed photolytic rate constant for substance  $i$  at wavelength  $\lambda$  in a solution with filter effect ( $\text{s}^{-1}$ ).

$S_\lambda$  = Morowitz factor of the solution at wavelength  $\lambda$  (-).

$\epsilon_{\lambda,i}$  = molar absorption coefficient of substance  $i$  at wavelength  $\lambda$  ( $\text{m}^2 \text{ mol}^{-1}$ ).

$\Phi_{i,\lambda}$  = quantum yield of substance  $i$  at wavelength  $\lambda$  ( $\text{mol einstein}^{-1}$ ).

$E'$  = photon fluence rate ( $\text{einstein m}^{-2} \text{ s}^{-1}$ ).

$$S_{\lambda,CDMA,NH_2Cl} ([CDMA], [NH_2Cl]) = \frac{1 - e^{-2.303(\varepsilon_{\lambda,CDMA} [CDMA] + \varepsilon_{\lambda,NH_2Cl} [NH_2Cl]) b}}{2.303 (\varepsilon_{\lambda,CDMA} [CDMA] + \varepsilon_{\lambda,NH_2Cl} [NH_2Cl]) b} \quad (\text{A.2})$$

Equation A.2 includes the following parameters:

$b$  = path length of the light through the sample (cm),

$\varepsilon_{\lambda,i}$  = molar absorption coefficient of substance  $i$  at the wavelength  $\lambda$  ( $M^{-1} \text{ cm}^{-1}$ ),

[substance  $i$ ] = concentration of the substance  $i$  (M).

**Table A.1.** Morowitz factors were calculated with an approach based on eq. A.2 and are explained in detail elsewhere (Wenk et al., 2011). Molar absorption coefficients at  $\lambda = 254$  nm were obtained from data in Figure A.1. The inner radius of the tubes used for the UV experiments was 7.1 mm.

Substance	Concentration (mM)	Absorbance (-)	Morowitz factor (-)
NH <sub>2</sub> Cl	2.5	0.94	0.37
NH <sub>2</sub> Cl	2.3	0.86	0.39
NH <sub>2</sub> Cl	0.5	0.19	0.78
NH <sub>2</sub> Cl	0.46	0.17	0.80
CDMA	2.5	0.70	0.43
CDMA	0.5	0.14	0.82
NH <sub>2</sub> Cl + CDMA	each 2.5	1.64	0.23
NH <sub>2</sub> Cl + CDMA	each 1.5	0.98	0.35
NH <sub>2</sub> Cl + CDMA	each 0.5	0.33	0.66

## B NH<sub>2</sub>Cl and CDMA photolysis and quantum yields

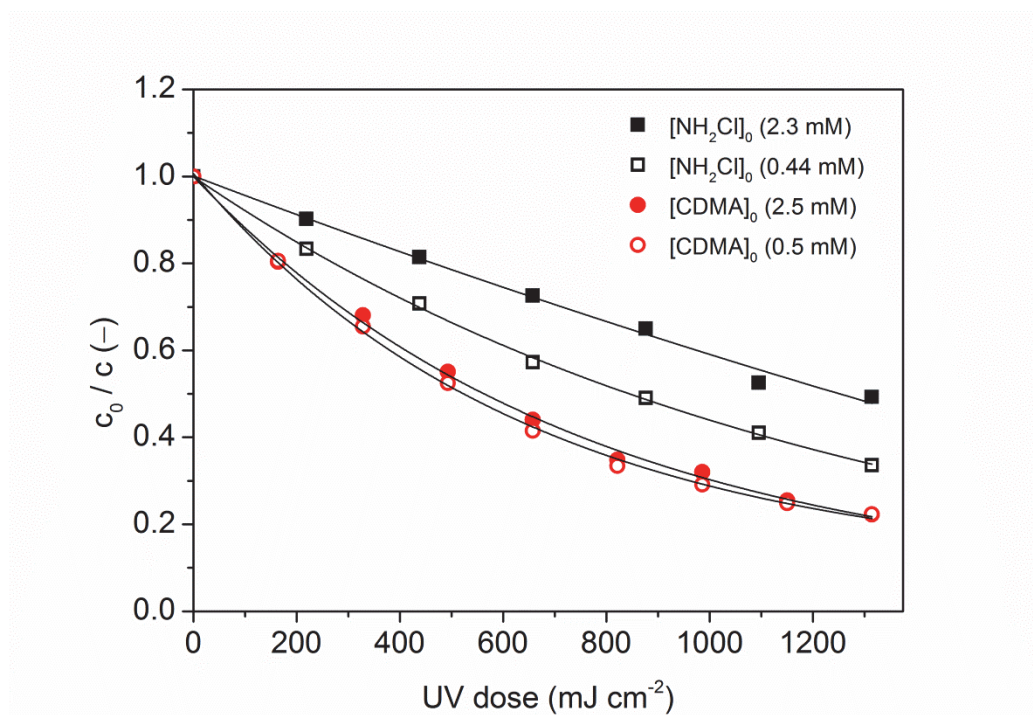


**Figure B.1.** Photolytic decay of NH<sub>2</sub>Cl and CDMA with UV irradiation. Photolytic rate constants and quantum yields are given in Table B.1, further information in Text B.1.

**Table B.1.** Photolytic degradation rates for NH<sub>2</sub>Cl and CDMA irradiation at different concentrations.

Substance	$k_{E', \text{obs}}$ ( $\text{cm}^2 \text{mJ}^{-1}$ )	$k_{p, \text{obs}}$ ( $\text{s}^{-1}$ )	$R^2$ (-)	$\Phi$ ( $\text{mol einstein}^{-1}$ )
[CDMA] <sub>0</sub> (2.5 mM)	1.16E-03	1.06E-03	0.995	0.64
[CDMA] <sub>0</sub> (0.5 mM)	1.18E-03	1.07E-03	0.990	0.65
[CDMA] <sub>0</sub> (2.5 mM)*	1.23E-03	1.12E-03	0.995	0.68
[CDMA] <sub>0</sub> (0.5 mM)*	1.33E-03	1.22E-03	0.990	0.73
[NH <sub>2</sub> Cl] <sub>0</sub> (2.3 mM)	5.59E-04	5.10E-04	0.987	0.31
[NH <sub>2</sub> Cl] <sub>0</sub> (0.44 mM)	8.25E-04	7.53E-04	0.999	0.45

\* Only values with UV dose < 700 mJ cm<sup>-2</sup> considered

**Text B.1.**

Measured quantum yield for  $\text{NH}_2\text{Cl}$  in this study (0.31 and 0.46 for  $c_0 = 2.3$  mM and  $c_0 = 0.44$  mM, respectively) are in good agreement with recently published values ranging from 0.26 to 0.62 mol einstein<sup>-1</sup> (Cooper et al., 2007; Watts and Linden, 2007; Li and Blatchley, 2009; De Laat et al., 2010). Quantum yields determined by Cooper et al. (2007) and by Watts and Linden (2007), namely 0.26 and 0.3 mol einstein<sup>-1</sup>, are below those from Li and Blatchley (2009) and de Laat et al. (2010), namely 0.62 and 0.54 mol einstein<sup>-1</sup>. Li and Blatchley (2009) explained the lower quantum yield by the fact that monochloramine was produced with an excess of ammonia. De Laat et al. (2010) found no influence of the N/Cl ratio in  $\text{NH}_2\text{Cl}$  preparation on the quantum yield for  $1.25 < \text{N/Cl} < 20$ . However, de Laat et al. (2010) reports a lower quantum yield of 0.28 mol einstein<sup>-1</sup> for oxygen-saturated conditions while the higher quantum yield of 0.54 mol einstein<sup>-1</sup> was measured under oxygen-free conditions.

## C NDMA photolysis and quantum yield

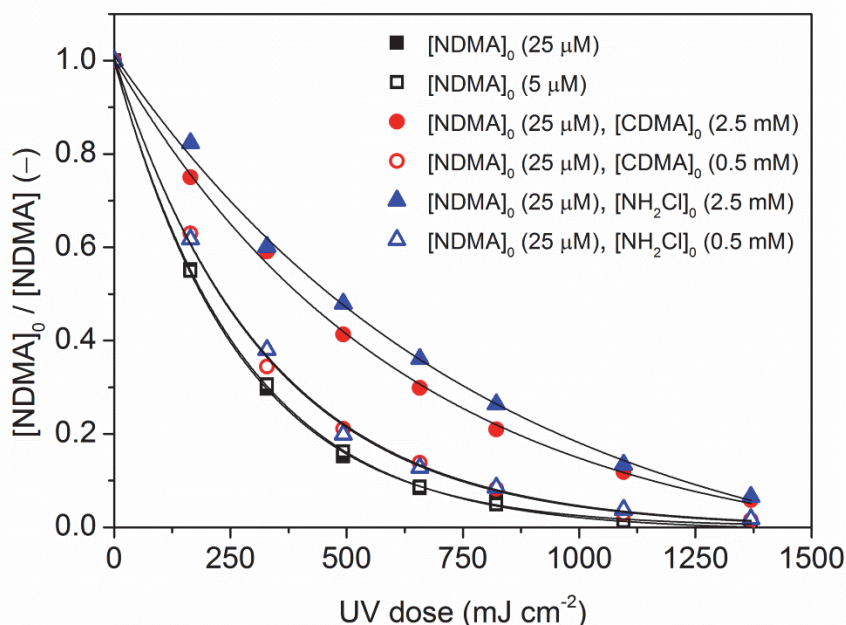


**Figure C.1.** Photolytic decay of NDMA in the presence  $\text{NH}_2\text{Cl}$  or CDMA. Photolytic rate constants and quantum yields are given in Table C.1, further information in Text C.1.

**Table C.1.** Photolytic degradation rates for NDMA in presence and absence of  $\text{NH}_2\text{Cl}$  and CDMA at different concentrations. Degradation rates were corrected with the corresponding Morowitz factor.

Substances	$k_{E'}^{\text{obs}}$ ( $\text{cm}^2 \text{mJ}^{-1}$ )	$k_p^{\text{obs}}$ ( $\text{s}^{-1}$ )	$R^2$ (-)	Morowitz factor (-)	$k_{E'}$ ( $\text{cm}^2 \text{mJ}^{-1}$ )	$k_p$ ( $\text{sec}^{-1}$ )	$\Phi$ ( $\text{mol einstein}^{-1}$ )
NDMA (5 $\mu\text{M}$ )	3.92E-03	3.59E-03	0.996	1.00	3.92E-03	3.59E-03	0.45
NDMA (25 $\mu\text{M}$ )	3.60E-03	3.29E-03	0.999	1.00	3.60E-03	3.29E-03	0.41
NDMA (25 $\mu\text{M}$ ) + $\text{NH}_2\text{Cl}$ (0.46 mM)	2.95E-03	2.70E-03	0.998	0.80	3.68E-03	3.37E-03	0.42
NDMA (25 $\mu\text{M}$ ) + $\text{NH}_2\text{Cl}$ (2.3 mM)*	1.57E-03	1.43E-03	0.996	0.39	4.04E-03	3.69E-03	0.47
NDMA (25 $\mu\text{M}$ ) + CDMA (0.5 mM)	3.01E-03	2.83E-03	0.977	0.82	3.67E-03	3.45E-03	0.44
NDMA (25 $\mu\text{M}$ ) + CDMA (2.5 mM)*	1.83E-03	1.68E-03	0.995	0.43	4.26E-03	3.90E-03	0.49
						average:	0.45
						std. dev.:	0.03

\* Only values with UV dose < 660  $\text{mJ cm}^{-2}$  considered



**Text C.1.**

NDMA followed an exponential decay which was inhibited by the presence of  $\text{NH}_2\text{Cl}$  and CDMA. Results show that the consideration of the UV filter effect (by including the Morowitz factor) of  $\text{NH}_2\text{Cl}$  and CDMA explained the measured differences in NDMA degradation. Thus, it is assumed that the inhibition of the NDMA degradation at high  $\text{NH}_2\text{Cl}$  and CDMA concentrations is primarily caused by the filter effect and not by renewed NDMA formation.

Quantum yields for NDMA photolysis under similar conditions were measured previously and ranged from 0.3 to 0.41 mol einstein<sup>-1</sup> (Sharpless and Linden, 2003; Lee et al., 2005; Plumlee and Reinhard, 2007; Williams et al., 2011). Plumlee and Reinhard (2007) additionally showed that UV absorbance of various nitrosamines is very similar and that their quantum yields were between 0.41 and 0.61 mol einstein<sup>-1</sup> for irradiation experiments with a solar spectra ( $290 \text{ nm} < \lambda < 800 \text{ nm}$ ). Williams et al. (2011) found slightly lower quantum yields under the same conditions, namely 0.32, 0.31 and 0.23 mol einstein<sup>-1</sup> for *N*-nitrosodimethylamine (NDMA), *N*-nitrosodimethylamine (NDEA) and *N*-nitrosomorpholine (NMor), respectively. Quantum yields for NDMA by Lee et al. (2005) ranged from 0.26 mol einstein<sup>-1</sup> in  $\text{N}_2$ -saturated solutions to 0.31 mol einstein<sup>-1</sup> in  $\text{O}_2$ -saturated solutions at irradiation with a low pressure lamp. Sharpless and Linden (2003) found NDMA quantum yields to be similar for low pressure- and medium pressure lamps. Other studies suggest that NDMA photolysis is influenced by many factors such as pH, initial concentration, dissolved oxygen concentration and humic acid concentration (Stefan and Bolton, 2002; Xu et al., 2009).

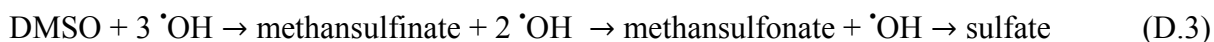
NDMA quantum yields were calculated with the molar absorption coefficient of  $1'650 \text{ M}^{-1} \text{ cm}^{-1}$  from Lee et al. (2005). The resulting quantum yield of  $\sim 0.43 \text{ mol einstein}^{-1}$  for NDMA in pure solution in this study is slightly higher than the above mentioned quantum yields from literature. However, degradation rates given by Xu et al. (2009) for similar pH values and initial concentrations were twice as high. The differences in the quantum yield can only partly be explained by different initial NDMA concentrations, since Lee et al. (2005) did their experiments at rather high concentrations while the other quantum yields were measured under similar conditions.

## D $\cdot\text{Cl}$ atom formation from $\text{NH}_2\text{Cl}$ and CDMA photolysis

### Text D.1

#### Experimental setup

The aim of the experiment was to confirm that the first step in  $\text{NH}_2\text{Cl}$  and CDMA photolysis is the cleavage of the N-Cl bond. This would result in the formation of a  $\cdot\text{Cl}$  atom. The  $\cdot\text{Cl}$  atom further reacts to a hydroxyl radical ( $\cdot\text{OH}$ ) in aqueous solutions (Buxton et al., 2000). The reverse reaction is possible but using dimethylsulfoxide (DMSO) as an  $\cdot\text{OH}$  scavenger prevents the reverse reaction. Therefore, each  $\cdot\text{Cl}$  atom is converted into an  $\cdot\text{OH}$  which further reacts with DMSO. Quantification of  $\cdot\text{OH}$  with DMSO was studied previously (Lee et al., 2004). Conclusively, one  $\cdot\text{OH}$  is consumed to form methansulfinate from DMSO, two  $\cdot\text{OH}$  to form methansulfonate and three  $\cdot\text{OH}$  to sulfate (eq. D.3).



#### Methods

All chemicals were purchased or produced as described in the main text. The additionally used chemicals sodium methanesulfonate, and sodium methanesulfinate were obtained at analytical grade from Sigma-Aldrich.  $\text{NH}_2\text{Cl}$  and CDMA production as well as UV irradiation was conducted as described in the main text. Sulfonate, sulfinate and sulfate were analysed with ion chromatography (Dionex ICS3000; column: AS9HC 4\*250mm with guard column; mobile phase:  $\text{Na}_2\text{CO}_3$  (9 mM) /  $\text{NaOH}$  (2 mM) with 1 ml min<sup>-1</sup>; detection: suppressed conductivity). Peak identification occurred by retention time and standard addition.

#### Results

Methansulfinate and sulfate formation was not observed in the irradiated samples. Experiments in Figures D.1a–d show that the course of the methansulfonate formation corresponds perfectly to the  $\text{NH}_2\text{Cl}$  and CDMA depletion. This is true for the entire time frame of the experiment. However, the  $\cdot\text{OH}$  yields (= potential  $\cdot\text{OH}$  from  $\text{NH}_2\text{Cl}$  degradation /  $\cdot\text{OH}$  formation measured with methansulfonate) were  $\sim 0.4$  and  $\sim 0.8$  for  $[\text{NH}_2\text{Cl}]_0 = 2.34$  mM and  $[\text{NH}_2\text{Cl}]_0 = 0.46$  mM, respectively. Even lower yields of  $\sim 0.16$  and  $\sim 0.25$  were observed for  $[\text{CDMA}]_0 = 2.5$  mM and  $[\text{CDMA}]_0 = 0.5$  mM, respectively.

Since  $\cdot\text{OH}$  yields increased with higher excess of DMSO, an experiment with increasing DMSO excess was conducted (Figure D.2). A high UV dose ( $\sim 2'700$  mJ cm<sup>-2</sup>) was applied to ensure the complete photolysis of  $\text{NH}_2\text{Cl}$  and CDMA. Increasing DMSO excess resulted in higher  $\cdot\text{OH}$  yields. In the case of  $\text{NH}_2\text{Cl}$ , the yield was even higher than one. This implies that there is either a second source of  $\cdot\text{OH}$  or DMSO is degraded to methansulfonate by another

species than  $\cdot\text{OH}$ . Thus, this method is not accurate for the exact quantification of  $\cdot\text{Cl}$  atoms in our system. However, it suggests that the  $\cdot\text{Cl}$  atom is one of the major products from the irradiation of  $\text{NH}_2\text{Cl}$  and CDMA.

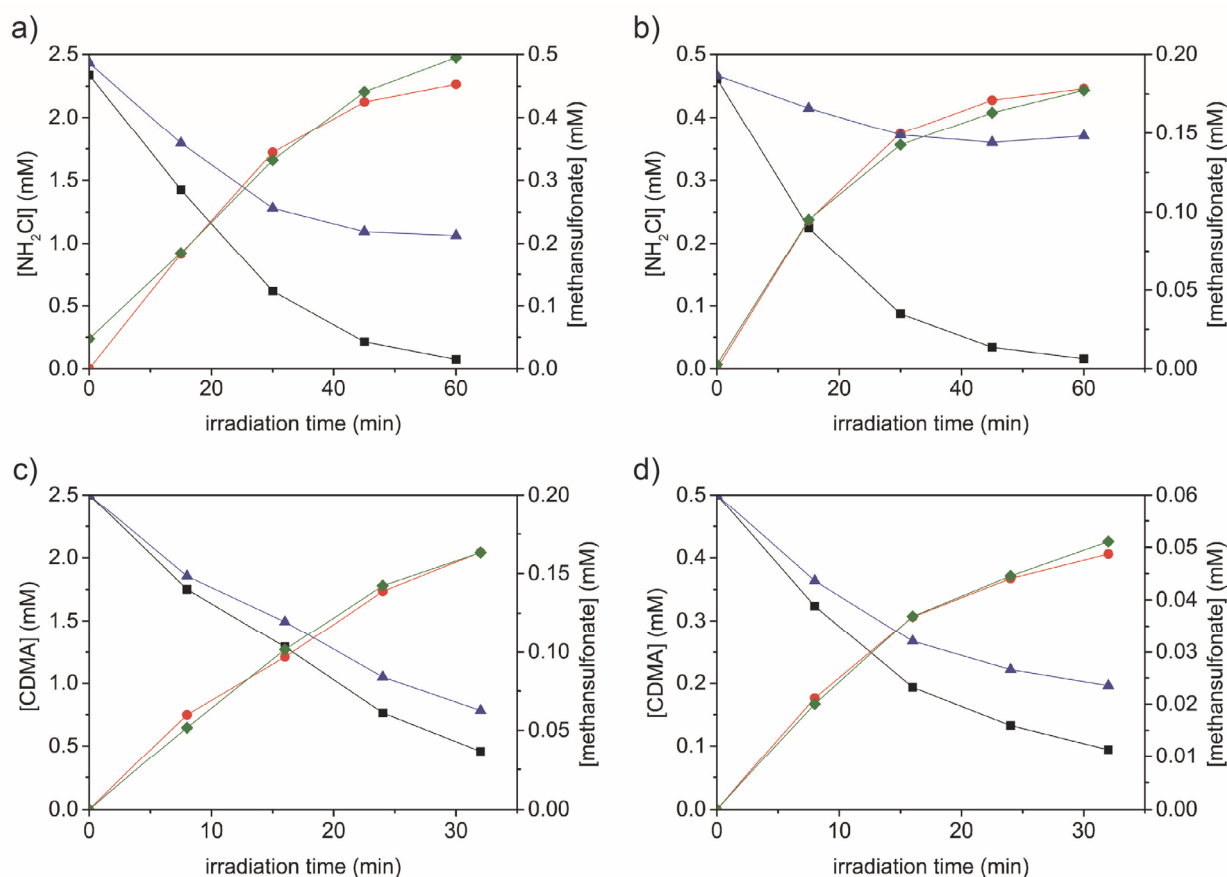


**Figure D.1 a–d.** Methansulfonate formation from CDMA and  $\text{NH}_2\text{Cl}$  irradiation ( $I \sim 0.9 \pm 0.05 \text{ mJ cm}^{-2} \text{ s}^{-1}$ ) with DMSO (25 mM) ( $\blacksquare$  = CDMA or  $\text{NH}_2\text{Cl}$  concentration;  $\bullet$  = degraded CDMA or  $\text{NH}_2\text{Cl}$ ;  $\blacklozenge$  = methansulfonate concentration;  $\blacktriangle$  = “ $\cdot\text{OH}$  formation potential” + “ $\cdot\text{OH}$  formation” ( $[\text{NH}_2\text{Cl}]_t + 2 \times [\text{methansulfonate}]_t$ )).

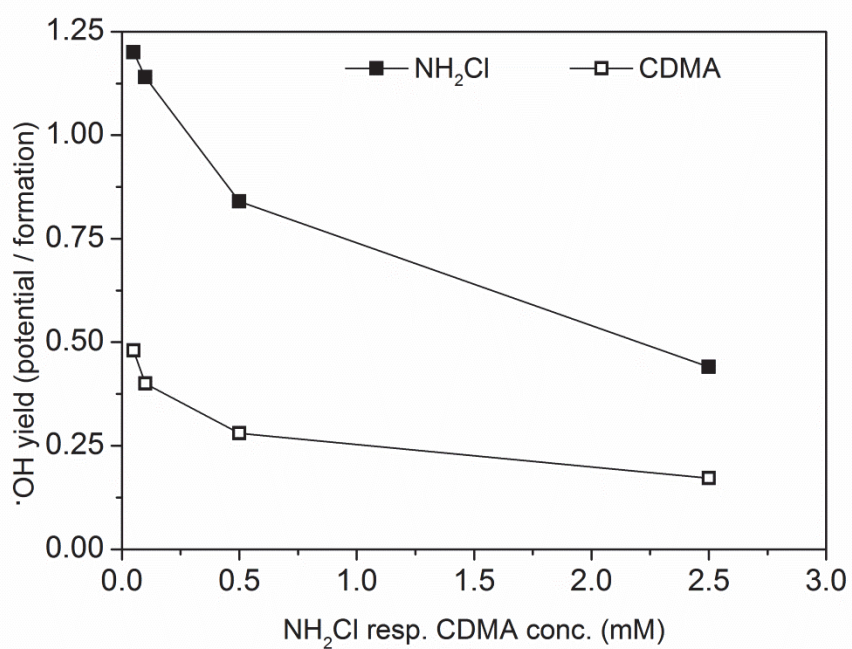


**Figure D.2.**  $\cdot\text{OH}$  yield ( $\cdot\text{OH}$  radical formation potential:  $[\text{NH}_2\text{Cl}]_0$  or  $[\text{CDMA}]_0$  / ( $\cdot\text{OH}$  formation =  $2 \times [\text{methansulfonate}]$ ) in UV irradiation (irradiation time: 1 h  $\sim 2700 \text{ mJ cm}^{-2}$ ) of  $\text{NH}_2\text{Cl}$  and CDMA with DMSO (25 mM).

## E NDMA formation from UDMH irradiation in presence of free chlorine

### Text E.1.

Unsymmetrical dimethylhydrazine was obtained from Merck. All chemicals were purchased as described in the main text. Irradiation was conducted as described in the main text.

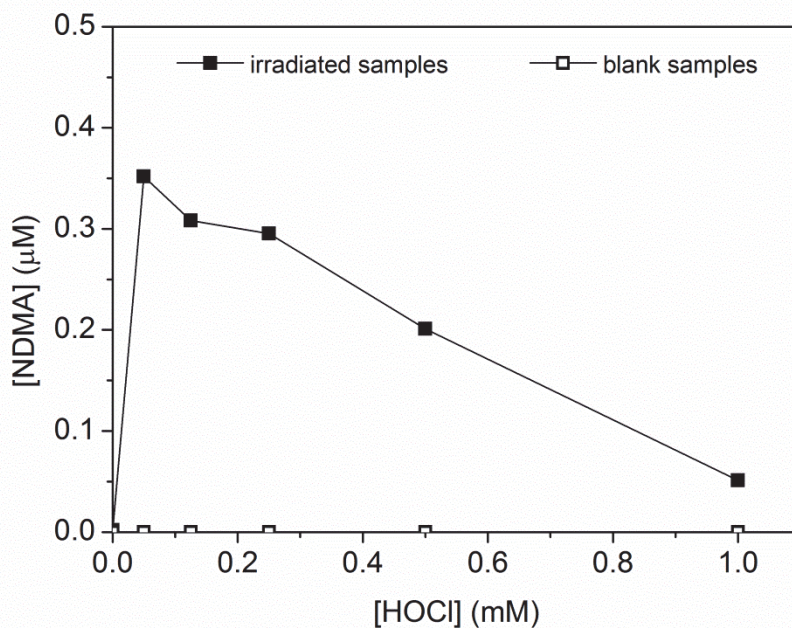


**Figure E.1.** NDMA formation from UV irradiation (applied UV dose  $\sim 800 \text{ mJ cm}^{-2}$ ) of unsymmetrical dimethylhydrazine (UDMH) (0.5 mM) in presence and absence of HOCl at pH 7.2. Blank samples were kept without UV irradiation during the duration of the experiments.

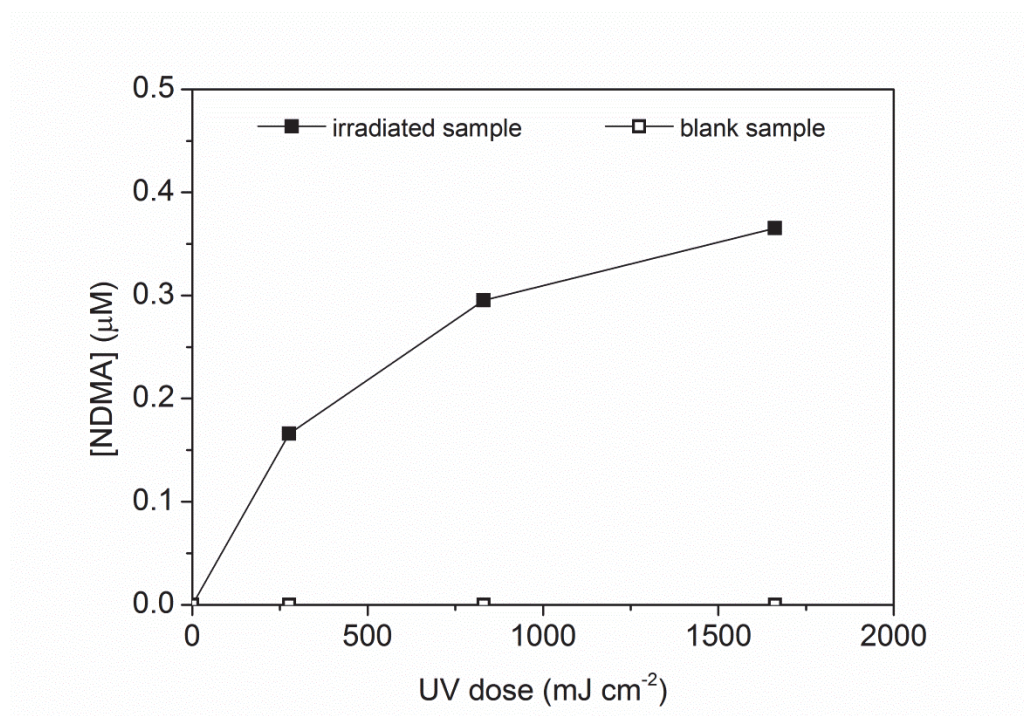


**Figure E.2.** NDMA formation from UV irradiation of UDMH (0.5 mM) in presence of HOCl (0.25 mM) at pH 7.2. Blank samples without UV irradiation were quenched simultaneously.

## F Simplified model for NDMA formation

**Table F.1.** Input parameters for the simplified NDMA formation model. Model calculations were done with Kintecus (Iannis, 2002). Rate constants for NDMA and CDMA photolysis were obtained from irradiation experiments reported in Section B and C. Modelling was done on a UV-dose scale and not on a time scale. Reaction rate constant “a” simulates the lifetime of the dimethylaminyl radicals. This constant is unknown and probably not UV-dose dependent. Model results remained unchanged for  $a > 10^{-1} \text{ cm}^2 \text{ mJ}^{-1}$ , which corresponds to a reaction rate constant of  $a > 0.9 \times 10^{-1} \text{ s}^{-1}$  since the irradiation experiments were performed with UV intensities around  $0.9 \text{ mJ cm}^{-2} \text{ s}^{-1}$ . The model data was fitted to the measured data by varying factor “b” which represents the fraction of dimethylaminyl radicals converted to NDMA (e.g.  $b = 0.02$  results in a 2 % yield for NDMA formation from dimethylaminyl radicals). Product 4 was introduced as a dummy to represent the cumulative NDMA formation (hypothetical NDMA concentration that would be reached without NDMA degradation). The concentration of product 1 corresponds to the amount of degraded NDMA. Figure F.1 shows model results for an initial CDMA concentration of 2.5 mM and values of  $1 \times 10^4$  and 0.02 for a and b, respectively.

<b>k (cm<sup>2</sup> mJ<sup>-1</sup>)</b>	<b>reactions</b>
3.75E-03	NDMA ==> product 1
1.28E-03	CDMA ==> DMA_rad
a x b	DMA_rad ==> NDMA + product 4
a x (1-b)	DMA_rad ==> product 3



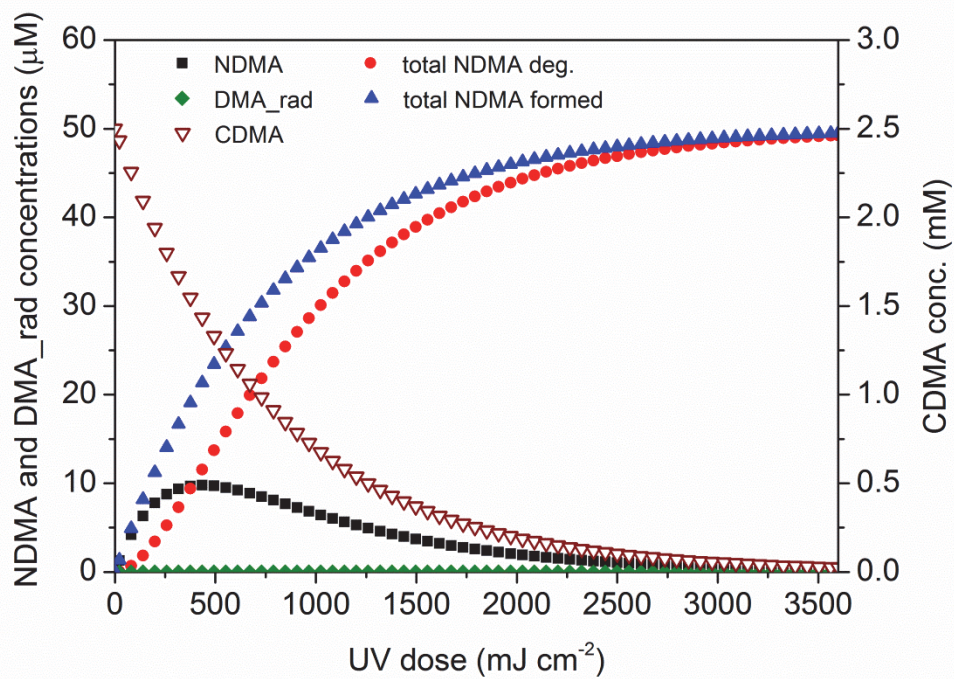


**Figure F.1.** Evolution of NDMA, DMA<sub>rad</sub>, “total NDMA degraded” (= product 1) and “total NDMA formed” (= product 4) concentrations (μM) in the simplified model with CDMA<sub>0</sub> = 2.5 mM, a = 10'000 and b = 0.02 as starting conditions.



## G Formation of the unknown compound during the irradiation of $\text{NH}_2\text{Cl}$ and chlorinated secondary amines

### Text G.1.

In UV irradiated samples containing  $\text{NH}_2\text{Cl}$  and chlorinated secondary amines, other peaks than the corresponding *N*-nitrosamine peak were detected as well (Figure G.1 and G.2). One of the peaks in the irradiated chlorinated diethylamine (CDEA) and chlorinated morpholine (CMor) samples showed a similar behaviour to the *N*-nitrosamine peak having a maximal concentration after about  $1'250 \text{ mJ cm}^{-2}$ . This behavior supports the hypothesis that the unknown peak might be the corresponding *N*-nitro-compound. The maximal peak area was 30 % and 200 % of the corresponding *N*-nitrosamine peak for CDEA and CMor, respectively. The retention times were 19 minutes in the sample with CDEA and 33 minutes in the sample with CMor. The peak was not observed in the sample without UV irradiation (blank).

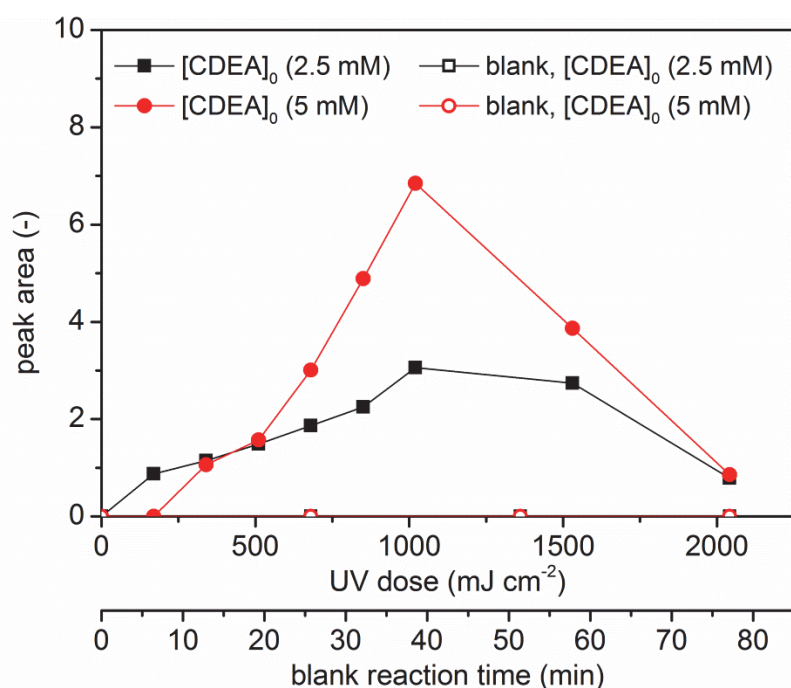


**Figure G.1.** HPLC peak area evolution of an unknown compound during the irradiation of CDEA and  $[\text{NH}_2\text{Cl}]_0 = 2.5 \text{ mM}$ . Blank samples were without UV irradiation.

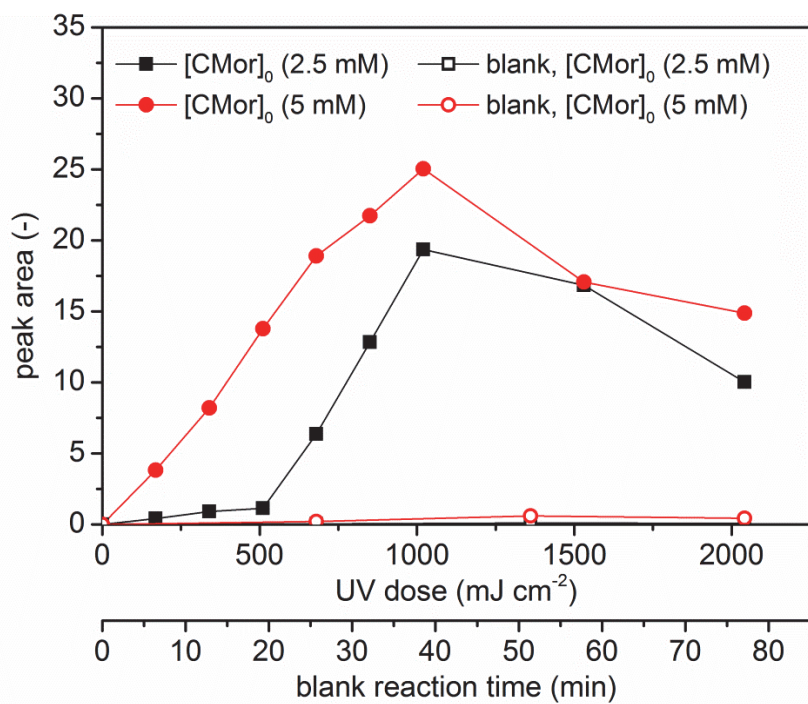


**Figure G.2.** HPLC peak area evolution of an unknown compound during the irradiation of CMor and  $[\text{NH}_2\text{Cl}]_0 = 2.5 \text{ mM}$ . Blank samples were without UV irradiation.

## **H NDMA formation induced by the quenching agent thiosulfate**

### **Text H.1.**

Three quenching agents (ascorbic acid, thiosulfate and sodium sulfite) were tested if they do not induce a NDMA formation in the presence of dimethylamine and nitrogenous species ( $\text{NO}_2^-$ ,  $\text{NO}_3^-$  and  $\text{NH}_4^+$ ). Therefore, DMA (5 mM) and one of the nitrogenous specie (5 mM) was mixed at pH 7 (phosphate buffer, 10 mM). The quenching agent was added immediately after mixing. The samples were stored in the dark at 5 °C. NDMA formation was controlled after 30, 40 and 60 hours. In none of the samples NDMA could be detected, except for the samples containing dimethylamine (5 mM), nitrite (5 mM) and thiosulfate (10 mM). This sample had a NDMA concentration of 0.25  $\mu\text{M}$ , 0.42  $\mu\text{M}$  and 0.82  $\mu\text{M}$  after a reaction time of 30, 40 and 60 hours, respectively.

## References

- Buxton, G. V., M. Bydder, G. A. Salmon and J. E. Williams, 2000. The reactivity of chlorine atoms in aqueous solution. Part III. The reactions of Cl-center dot with solutes. *Physical Chemistry Chemical Physics* 2 (2), 237-245.
- Cooper, W. J., A. C. Jones, R. F. Whitehead and R. G. Zika, 2007. Sunlight-Induced Photochemical Decay of Oxidants in Natural Waters: Implications in Ballast Water Treatment. *Environmental Science & Technology* 41 (10), 3728-3733.
- De Laat, J., N. Boudiaf and F. Dossier-Berne, 2010. Effect of dissolved oxygen on the photodecomposition of monochloramine and dichloramine in aqueous solution by UV irradiation at 253.7 nm. *Water Research* 44 (10), 3261-3269.
- Iannis, J. C., 2002. Kintekus, downloaded from [www.kintekus.com](http://www.kintekus.com) in september 2010.
- Lee, C., W. Choi and J. Yoon, 2005. UV photolytic mechanism of N-nitrosodimethylamine in water: Roles of dissolved oxygen and solution pH. *Environmental Science & Technology* 39 (24), 9702-9709.
- Lee, Y., C. Lee and J. Yoon, 2004. Kinetics and mechanisms of DMSO (dimethylsulfoxide) degradation by UV/H<sub>2</sub>O<sub>2</sub> process. *Water Research* 38 (10), 2579-2588.
- Li, J. and E. R. Blatchley, 2009. UV Photodegradation of Inorganic Chloramines. *Environmental Science & Technology* 43 (1), 60-65.
- Plumlee, M. H. and M. Reinhard, 2007. Photochemical Attenuation of N-Nitrosodimethylamine (NDMA) and other Nitrosamines in Surface Water. *Environmental Science & Technology* 41 (17), 6170-6176.
- Sharpless, C. M. and K. G. Linden, 2003. Experimental and model comparisons of low- and medium-pressure Hg lamps for the direct and H<sub>2</sub>O<sub>2</sub> assisted UV photodegradation of N-nitrosodimethylamine in simulated drinking water. *Environmental Science & Technology* 37 (9), 1933-1940.
- Stefan, M. I. and J. R. Bolton, 2002. UV direct photolysis of N-nitrosodimethylamine (NDMA): Kinetic and product study. *Helvetica Chimica Acta* 85 (5), 1416-1426.
- Watts, M. J. and K. G. Linden, 2007. Chlorine photolysis and subsequent OH radical production during UV treatment of chlorinated water. *Water Research* 41 (13), 2871-2878.
- Wenk, J., U. von Gunten and S. Canonica, 2011. Effect of Dissolved Organic Matter on the Transformation of Contaminants Induced by Excited Triplet States and the Hydroxyl Radical. *Environmental Science & Technology* 45 (4), 1334-1340.
- Williams, M., J. Du, R. Kookana and M. Azzi, 2011. Biodegradation, Hydrolysis and Photolysis Testing of Nitrosamines in Aquatic Systems. CO<sub>2</sub> Technology Centre Mongstad. Commonwealth Scientific and Industrial Research Organisation (CSIRO), Advanced Coal Technology Portfolio.
- Xu, B. B., Z. L. Chen, F. Qi, J. M. Shen and F. C. Wu, 2009. Factors influencing the photodegradation of N-nitrosodimethylamine in drinking water. *Frontiers of Environmental Science & Engineering in China* 3 (1), 91-97.

# **Chapter 7**

## **General Conclusions**

Trichloramine is a disinfection by-product that is assumed to cause severe adverse health effects. However, it has rarely been measured in pool water because an appropriate method was lacking so far. As outlined in chapter 4, a fast, reliable, easy-applicable and low-cost colorimetric method (extraction-based ABTS method) for trichloramine analysis was developed in this thesis. A comparison with membrane introduction mass spectrometry (MIMS) measurements, a more sophisticated and expensive method, revealed that both methods do not suffer from interferences and are in good agreement, with the only restriction that MIMS calibration must be performed by standard addition to pool water samples. The extraction-based ABTS method is a suitable method for pool attendants who perform single measurements at irregular time intervals. The MIMS is a good option for continuous and long-term measurements of trichloramine at several points in the pool water cycle as shown in chapter 4 and 5. The collection and the analysis of such big data sets requires an adequate software (chapter 3). The software engineered in this thesis facilitates an automated data acquisition and handling for multiple samples over a long time frame. It further allows for efficiently analyzing the data with automated algorithms for continuous, steady-state and flow-injection measurements.

The extraction-based ABTS method and the MIMS enabled the measurement of trichloramine in 30 pool water samples. Trichloramine concentrations ranged up to 0.5  $\mu\text{M}$  and correlated clearly with the free chlorine and the HOCl concentrations ( $R^2 = 0.64$  and  $0.79$ , respectively). The correlations with pH and the combined chlorine concentrations were weak while no correlation was observed with the urea concentrations. This highlights the important role of free chlorine for trichloramine concentration in pool water and also indicates that urea is probably not the main source for the trichloramine formation as shown by model calculations in chapter 5. These results also indicate that an increased fresh water addition does not significantly lower the trichloramine concentration because trichloramine formation/decay are fast processes compared to dilution by fresh water addition.

Free chlorine influences the trichloramine concentration by its reaction with precursors leading to trichloramine formation as well as by its competition with trichloramine for reactive moieties, thereby stabilizing trichloramine. In chapter 2, the reactivity of trichloramine with various model compounds (e.g. primary and secondary amines, amides, hydroxylated phenolic compounds and fulvic acids) is compared to the reactivity of free chlorine. Most compounds react faster with free chlorine than with trichloramine except for some phenolic compounds. Since all investigated compounds have a decreased reactivity with trichloramine after chlorination, the presence of free chlorine is likely to inhibit the degradation of trichloramine.

Additional evidence for such a trichloramine stabilization mechanism is provided in chapters 2 and 5, in which the stability of trichloramine in the presence of chlorinated fulvic acids and in chlorinated, irradiated pool water matrices were studied. In both cases, chlorination reduced the reactivity of the target moieties with trichloramine. The decay rate of trichloramine in pool water in the presence of residual free chlorine was only slightly higher than the trichloramine self-decay in pure water at the same pH. Therefore, increasing the free chlorine concentration in a swimming pool with residual free chlorine mainly affects the trichloramine concentration by an increased trichloramine formation. A strong correlation between the free chlorine and the trichloramine concentration was also found during on-site experiments in which the free chlorine concentration was varied in a wading pool (chapter 4). Furthermore, trichloramine and chlorine reacting with various substrates yielded similar reaction products. At pH 7 the apparent second order rate constant for the reaction of trichloramine with amides is very low ( $k_{\text{app}} = 10^{-2} - 10^{-1} \text{ M}^{-1} \text{ s}^{-1}$ ), slightly higher for primary amines ( $k_{\text{app}} = 10^{-1} - 10^0 \text{ M}^{-1} \text{ s}^{-1}$ ) and rather high for secondary amines ( $k_{\text{app}} = 5 \times 10^1 - 5 \times 10^2 \text{ M}^{-1} \text{ s}^{-1}$ ). Trichloramine is able to perform chlorine addition as well as electron transfer reactions. Hence, it has a similar potential to produce disinfection by-products as free chlorine.

In chapter 5, UV treatment of chloramines is discussed, which is probably the most used trichloramine mitigation strategy. As known from literature, inorganic chloramines are photodegraded by UV irradiation with low- and medium-pressure mercury lamps. Among the inorganic chloramines, trichloramine is the most efficiently degraded by photolysis. The UV dose that is commonly applied in pool water treatment eliminates about 30–50% of the trichloramine per treatment cycle. On-site measurements confirmed that this is not only the case for batch experiments of pure solutions irradiated in the laboratory, but also for pool water samples treated in a commercial flow-through UV reactor equipped with a medium-pressure mercury lamp. Hence, the commonly applied UV doses in public pools appears to be in a reasonable range for trichloramine degradation. For public health it is less relevant how much trichloramine is degraded in the treatment system, the effective trichloramine concentration in the pool is the decisive factor here. Despite the significant degradation in the UV reactor, trichloramine concentrations decreased only insignificantly in a competition and a wading pool (~10 % and ~20 %, respectively). This suggests that there is a fast trichloramine formation in the pool, which leads to almost the same steady-state concentration as without UV treatment. The effect of UV treatment was less pronounced in a competition pool than in a wading pool since the residence time of the water in the competition pool was higher (~4.5 h) than in the wading pool (~1 h). Trichloramine mitigation seems to be only efficient in swimming pools

with short residence times and even a higher UV dose could not reduce the trichloramine concentration in pool water significantly.

UV treatment also mitigates other disinfection by-products. The results presented in chapter 5 suggest that the level of total inorganic chloramines decreases with UV treatment. No effect was observed on trihalomethanes. To verify these observations, the impact of UV treatment should be studied over a longer period than it was done in this thesis because these disinfection by-products are stable in pool water but might be photodegraded at much higher UV doses. Chapter 6 elucidates the effect of UV treatment on nitrosamines, a carcinogenic disinfection by-product in pool water. As demonstrated in previous studies, *N*-nitrosodimethylamine is slowly formed in pool water and sensitive to UV irradiation. However, UV irradiation of the pool water matrix enhances the formation of *N*-nitrosodimethylamine since the irradiation of aqueous solutions containing both monochloramine and chlorinated dimethylamine results in the formation of intermediate products (such as nitric oxide) which can lead to a fast formation of *N*-nitrosodimethylamine. The same formation pathway is valid for other nitrosamines. Whether this formation outcompetes the photodegradation of nitrosamines depends on the initial precursor and nitrosamine concentrations and on the applied UV dose.

In conclusion, it is possible to accurately measure trichloramine in pool water. The extraction-based ABTS method allows pool attendants to routinely measure trichloramine concentrations in pool water. Such periodic measurements in different swimming pools could improve the understanding of which conditions/treatments are favorable to lower trichloramine levels. According to our results, it is important to lower the free chlorine concentration as much as possible. An elimination of trichloramine in the treatment part by UV irradiation or potentially also by stripping can only partly reduce the trichloramine concentration in pool water due to the trichloramine formation in the pool. Hence, trichloramine formation in the pool itself must be reduced either by lowering the free chlorine concentration or by reducing the nitrogenous precursors (probably many more than just urea) by a better hygiene. However, for more stable substances such as trihalomethanes, elimination in the treatment part (e.g. by stripping) might be a good option although it is related to a higher energy demand.

In spite of the findings of this doctoral thesis, there are numerous questions about the optimization of pool water treatment that still need to be addressed. Further research should aim to maximize the safety of swimming in public pools with regard to both, microbiological risks and risks from disinfection by-products for a short term (acute) and long term (chronic) perspective. This optimization requires disinfection methods and conditions leading to only low



by-product formation while still guaranteeing a proper disinfection. To better assess the acceptable levels of disinfection by-products in pool water, the adverse health effects of swimming in and visiting an indoor pool facility should be studied in more detail. Currently, there is a lack of clear evidence for various health effects such as asthma and blood cancer. However, it is highly challenging to evaluate the impact of swimming on the risk of chronic diseases. Therefore, measures can also be justified based on the precautionary principle, especially because many of the pool visitors belong to high risk groups such as children or elderly people. In the overall evaluation of swimming, it is important that the benefits of swimming for health and recreation are also considered.

To understand the adverse health effect of swimming, the identification and quantification of disinfection by-products constitute the first step. Then, a risk assessment of the disinfection by-products is necessary considering their concentrations, their toxicity and the exposure of the swimmer/bather. Cumulative effects of various disinfection by-products in the complex pool water mixture should be implemented in the risk assessment. One option to do this is to study the cell toxicity of pool water as it has already been done in other studies. However, disinfection by-products have various pathways for their uptake and represent thereby various risks to humans. The goal of research should be to understand the fate of disinfection by-products in pool water, to understand their uptake by and their effects on the human body. If necessary, mitigation strategies should be developed to a stage, in which they can be implemented. Currently, there are a few disinfection by-products such as trihalomethanes, haloacetic acids, nitrosamines and halogenated phenols for which research has just started to tackle these goals.

With regard to trichloramine, this doctoral thesis established the option to measure trichloramine in pool water and provided insights on the reactivity of trichloramine. This facilitates to further study trichloramine formation and to potentially identify the main precursors. Up to date, only the trichloramine yield from the chlorination of various precursors at different pH values has been studied. Data about the kinetics of these reactions are not available and data about the precursor concentration in pool water are very scarce. This lack of information hampers the prevention of trichloramine formation. According to the results of this study, UV treatment is not an efficient trichloramine mitigation strategy since it cannot compensate for the fast trichloramine formation occurring in the swimming pool. Further research should focus on the prevention of trichloramine formation by e.g. precursor mitigation or on the elimination of trichloramine in pool water. Furthermore, the role of trichloramine in

the formation of other hazardous disinfection by-products in pool water should not be neglected in future investigations on disinfection by-product formation.





---

## Curriculum Vitae

**Fabian Soltermann**      born on November 24, 1981 in Baden, Switzerland  
citizen of Vechigen (BE), Switzerland

### Education

1997 – 2001      Matura Typus C, Kantonsschule Baden

2001 – 2007      Master studies in Environmental Sciences  
ETH Zurich, Switzerland  
Master thesis: „*Modelling the global fate of polybrominated diphenyl ethers (PBDEs): Does debromination of higher brominated PBDEs significantly contribute to the presence of lowly brominated PBDEs in the environment?*“

9/2010 – 1/2015      Doctoral thesis  
Eawag, Department of Water Resources and Drinking Water, Switzerland  
ETH Zurich, Institute of Biogeochemistry and Pollutant Dynamics, Switzerland

### Professional experiences

6/2008 – 7/2010      Project manager  
Huber Energietechnik AG, Zürich

2/2008 – 4/2008      Research assistant  
Safty & Environmental Technology Group, ETH Zurich

11/2011 – 1/2008      Civilian service  
Eidg. Forschungsanstalt für Wald, Schnee und Landschaft (WSL), Bellinzona

11/2005 – 2/2006      Practical training  
Givaudan Schweiz AG, Dübendorf

4/2004 – 10/2004      Civilian service  
Fundación Sembres, Quito, Ecuador

2002 – 2003      Teaching assistant “Chemistry I/II”  
ETH Zürich

6/2001 – 9/2001      Civilian service  
Fondacion “Les Cerlatez”, Saignelégier